UNIVERSITAT DE BARCELONA

Advancing induced pluripotent stem cell (iPSC) technology by assessing genetic instability and immune response

Jordi Requena Osete

UNIVERSITY OF BARCELONA
FACULTY OF FARMACY AND FOOD SCIENCES
CAMPUS DIAGONAL, AV. JOAN XXIII, 27-31, 08028

ADVANCING INDUCED PLURIPOTENT STEM CELL (IPSC) TECHNOLOGY BY ASSESSING GENETIC INSTABILITY AND IMMUNE RESPONSE

BIOMEDICINE PHD PROGRAM

BARCELONA, 14th OF JULY, 2017

ADVANCING INDUCED PLURIPOTENT STEM CELL (IPSC) TECHNOLOGY BY ASSESSING GENETIC INSTABILITY AND IMMUNE RESPONSE

Memoria presentada por Jordi Requena Osete, Licenciado en Biología (2008-2012), para optar al Título de Doctor por la Universidad de Barcelona. Programa de Doctorado en Biomedicina (2013-2017).

Tesis Doctoral realizada en la Facultad de Medicina de la Universidad Barcelona bajo la dirección del Dr. Michael John Edel y bajo la tutoría del Dr. JosepMª Canals Coll.

TO OBTAIN
BIOMEDICINE PHD

PRESENTED BY
JORDI REQUENA OSETE

DIRECTOR
MICHAEL JOHN EDEL

TUTOR
JOSEP Mª CANALS COLL

BARCELONA, 14th OF JULY, 2017

“Que tot està per fer, i tot és possible...”

(Miquel Martí Pol)

ACKNOWLEDGMENTS

In the first place, I would like to acknowledge and to express my gratitude to my thesis director Dr. Michael John Edel, who gave me the opportunity to join his team to do this project, for his guidance and counsel. I am very thankful for his patience with my mistakes and for reminding me to stay focused at all time. Thank you for sharing your experience and knowledge as mentor.

Secondly, I would like to express special thanks to Dra. Belén Álvarez Palomo. Without her hard work it would not be possible to finish this research. I have learnt so much from her insightful observations. Thank you for assisting me and teaching me so many different research techniques.

I am really thankful and want to acknowledge as well Dra. Jovita Mezquita Pla, for her expert advice in molecular genetics techniques. Thank you for your encouragement and motivation during this intense period of research.

I have been able to count with you all three, Mike, Belén and Jovita, since the very first day and all along the 4 years of this PhD and previous master. Thank you to you all for leading me during these first steps in the scientific world while working and designing experiments together.

My sincere thanks also goes to my tutor Dr. JosepMª Canals Coll, for his assistance and help. I also would like to acknowledge to all my other fellow labmates from the Pluripotency laboratory in the Faculty of Medicine: Helena Sarret, Carme Grau, Adrià Martínez, Martí Sal, David, Isart Roca and Dra. Cristina Menchón. Thank you for the stimulating lab-meeting discussions and for all the fun we have had in the last four years.

This thesis would not have been possible without the excellent facilities the University of Barcelona provides to researchers and the people who run them such professionally, whose wise advice has been of huge value. In special to the Flow Cytometry unit: Isabel Crespo, Cristina Xufré, Cristina López and Sara Ozcoz; to Fluorescence Microscopy unit: Maria Calvo, Elisenda Coll and Anna Bosch and to the Animal House personal: JosepMª Marimón and Garikoitz Azkona.

I want to acknowledge all the collaborators that have contributed to this work in other research centers: to Dr. Manel Esteller, Dr. Raúl Delgado and Dr. Sebastian Moran from the Cancer Epigenetics group in IDIBELL; to Dr. Alejandro Vaquero and Dra. Irene Santos from the Chromatin Biology group in IDIBELL and to Dra. Antonella Consiglio from the Stem Cells and Neuroplasticity laboratory at IBUB.

I also would like to acknowledge all the scientists from other Groups and Departments of the Medicine Faculty and Hospital Clinic that have contributed and helped in the development of this thesis. In special to Dra. Carmen Barrot from the Forensic Anatomy Department for RT-PCR analysis; to Dr. Manel Joan and Dra. Anna Boronat from the Immunology Department; to Montse Pau and Dr. Xavier Gassull from Neurofisiology; Rafael Oliva and his group for the proteomic analysis from the Molecular Genetics group and to the Cytogenetic Unit: Dolors Costa, Joan and Candi.

During my short but intense stays in other laboratories I have been warmly received and treated with nice hospitality; I would like to acknowledge to Dra. Victoria Moreno from

the Research Center Principe Felipe in Valencia, as well as to Eric López Mocholi and Ana Alastrue Agudo for animal surgery and technical support; to Dra. María Blasco and Dra. Agueda Tejera from CNIO, in Madrid; to Dr. Rodney Dilley from the Harry Perkins Research Institute in Perth, Western Australia and to Dr. Jordi Calderó and Dra. Ana Casanovas from the Biomedical Research Center in Lleida.

Last, but not the least, I also want to acknowledge my family, to my father Antonio and my mother Ramona and to my brother JosepMª and sister MªJesús, for all their unforgettable support and for their continuous back-up. As well to my flatmate, uncle Fernando, for his company while I was living in Barcelona.

Finally, to the grants that have given financial support to enable this research project: FBG project 307900 and MINECO project BFU2011–26596 and BFU2014-54467-P.

INDEX

Index

Index

GLOSSARY

ATM: Ataxia Telangiectasia Mutated
bFGF: Basic fibroblast growth factor
BIN1: Bridging Integrator 1
BMP: Bone Morphogenetic Protein
BRCA2: Breast Cancer Type 2 susceptibility protein
CCD1: Cyclin D1
CCL2: Chemokine (C-C motif) ligand 2
CDK: Cyclin Dependent Kinase
CM: Cardiomyocytes
CML: Chronic myelogenous leukemia
CNS: Central Nervous System
CNV: Copy Number Variation
CTLs: Cytotoxic T Lymphocytes
DH iPSC: Cyclin D1 made human iPSC
DHFR: Dihidroxifolate reductase
DNA-PKcs: DNA dependent protein kinases
DSB: Double Strand Break
ENDO: Endoderm cells
ESC: Embryonic Stem Cells
FGF2: Fibroblast Growth Factor 2
GFP: Green Fluorescent Protein
hESC: human embryonic Stem Cells
HFFs: Human Foreskin Fibroblasts
HLA: human leukocyte antigen
HR: Homologous Recombination
ICM: inner cell mass
IL-10: Interleukin 10
IL-15: Interleukin 15
IL-6: Interleukin 6
IPSC: induced Pluripotent Stem Cells
KLF4: Krupple-Like Factor 4
LIF: Leukaemia inhibitory factor
LIG3: Ligase 3
LPS: Lypopolysaccharides
MCP1: Monocyte Chemotactic Protein 1
MEFs: Mouse Embryonic Fibroblasts
mESC: mouse Embryonic Stem Cells
MH iPSC: C-Myc made human iPSC
MHC: Major Histocompatibility Complex
MN: Motor Neuron
MRN: Mre11-Rad50-NBS1
mRNA: messenger RNA
MSC: Mesenchymal Stem Cells
NBS1: Nijmegen Breakage Syndrome 1
NHEJ: Non-Homologous End Joining
NSC: Neural Stem Cells
OCT4: Octamer-binding Transcription Factor 4
OSKM: Oct4, Sox2, Klf4 and c-Myc

PAMP: Pathogen Associated Molecular Pattern
PARP1: Poly (ADP-ribose) polymerase-1
PI3K: Phosphoinositide 3-kinase
Pol μ: Polimerase μ
Pol λ: Polimerase λ
POLQ or Pol θ: Polymerase θ
Poly(I:C): Polyinosinic:polycytidylic acid
ROS: Reactive Oxigen Species
RPA: Replication Protein A
RPE: Retinal Pigmented Epithelial
SCI: Spinal Cord Injury
SNP: Single Nucleotide Polymorphism
SIRT1: Silent mating-type information regulation 2 homologue 1
SMA: Spinal Muscle Atrophy
SNP: Single Nucleotide Polymorphism
SOX2: SRY (sex determining region Y)-Box 2
TCR: T Cell Receptor
TGFβ: Transforming Growth Factor β
TLRs: Toll-Like Receptors
TLR3: Toll-Like Receptor 3
TLR4: Toll-Like Receptor 4
TSS: Transcription Start Site
VPA: Valproic Acid
XRCC4: X-ray Repair Cross Complementing 4

ABSTRACT

Induced pluripotent stem cells (iPSC) can be made from adult somatic cells by reprogramming them with Oct4, Sox2, Klf4 and c-Myc. IPSC have given rise to a new technology to study and treat human disease (Takahashi *et al*., 2007). However, before iPSC clinical application, we need to step back and address two main challenges:

(i) Genetic stability of iPSC.
(ii) Immune response of iPSC-derived cells.

To address these key issues, the overall mission of this PhD thesis is to advance iPSC technology by addressing two objectives. First, is to replace c-Myc with Cyclin D1 in the reprogramming cocktail (Oct4, Sox2, Klf4 and c-Myc or Cyclin D1) and second, to study the immune response of iPSC-derived cells.

The quality of the starting iPSC determines the quality of the differentiated cells to be transplanted for clinical applications. In terms of genetic stability, aberrant cell reprogramming leads to genetic and epigenetic modifications that are the most significant barriers to clinical applications of patient iPSC derivatives (Gore *et al.*, 2011). Such aberrations can result from the cellular stress that accompanies reprogramming or from the reprogramming factors themselves (Lee et al., 2012a). IPSC made with c-Myc are neoplastic in mouse models and have a higher tumorigenic potential than embryonic stem cells, prompting a search for new pluripotency factors that can replace the oncogenic factors Klf4 and c-Myc (Huangfu *et al*., 2008; Miura *et al*., 2009; Okita *et al.*, 2007). We chose Cyclin D1 to replace c-Myc because of previous observation it can be used to reprogram cells to iPSC (Edel *et al*., 2010) and because of its DNA repair function (Chalermrujinanant et al., 2016). In this thesis we adopt a synthetic mRNA method to demonstrate that Cyclin D1 and c-Myc made iPSC have equal pluripotency using standard methods of characterisation. Moreover, no significant changes in copy number variation were found between starting skin cells and iPSC highlighting it is the method of choice for generating high quality iPSC. Further in-depth analysis revealed that Cyclin D1 made iPSC have reduced genetic instability assessed by: (i) reduced DNA double strand breaks (DSB), (ii) higher nuclear amount of the homologous recombination key protein Rad51, (iii) reduced multitelomeric signals (MTS) and (iv) reduced teratoma growth kinetics in vivo, compared to c-Myc made iPSC. Moreover, we demonstrate that Cyclin D1 iPSC derived neural stem cells engraft successfully, survive long term and differentiate into mature neuron cell types with high efficiency, with no evidence of pathology in a spinal cord injury rat model.

As we move towards the clinic with iPSC-derived cells for cell transplantation, the immunogenic response is thought to be one of the main advantages of iPSC technology for clinical application, because of its perceived lack of immune rejection of autologous cell therapy. We hypothesize that iPSC derived cells are unlikely to provoke an immune response. Here we have performed an analysis of the innate and adaptive immune response of human skin cells (termed F1) reprogramed to iPSC and then compared to iPSC-derived cells (termed F2) using proteomic and methylome arrays. We found little differences between MHCI expression and function; however, we discovered a short isoform of the Toll-like receptor 3 (TLR3), essential for viral dsRNA innate immune recognition, which is predominantly upregulated in all iPSC derived cells analysed and not seen in normal endogenous cells. High levels of the TLR3 isoform is associated with unresponsiveness to viral stimulation measured by lack of IL6 secretion in iPSC derived neural stem cells. We propose a new model that TLR3 short isoform competes with the full length *wild type* isoform destabilizing the essentially required TLR3

dimerization process. These differences could result in supressed inflammatory effects for transplanted human iPSC-derived cells in response to viral or bacterial insult. Further work to determine the *in vivo* effects is warranted and calls for screening of iPSC lines for TLR3 isoform expression levels before clinical use. In conclusion, this thesis has advanced iPSC technology by defining a new *method* that is a significant advance with novel insights that has immediate impact on current methods to generate iPSC for clinical application and more accurate disease modelling.

INTRODUCTION

1. STEM CELLS

Stem cells are cells with self-renewing capability and the ability to differentiate into various cell types. They can be classified according to their capacity to differentiate and their origin.

Depending on their capacity to differentiate into other cell types stem cells are classified as:

Totipotent:

Stem cells with the ability to differentiate into all possible cell types. They have a self-organizing ability to generate a whole organism (Niwa et al., 2007). Only the zygote and early blastomere are totipotent in mammals.

Pluripotent:

Stem cells that can give rise to cell types from the three germ layers: ectoderm, mesoderm and endoderm. They differ from totipotent cells as pluripotent cells cannot give rise to the trophectoderm, which will form the placenta in a developing embryo. For instance, inner cell mass (ICM) cells that are specific to the early embryo are pluripotent (Pera et al, 2010).

Multipotent:

Stem cells that can give rise to all cell types within a particular lineage. For instance, mesenchymal stem cells can give rise to bone, muscle or adipose cells. Neural stem cells and Hematopoietic stem cells are other examples.

Unipotent:

Stem cells that can only generate one type of cell. For example spermatogonial stem cells can only form sperm (Jaenisch et al., 2008).

Depending on their origin, stem cells are classified into:

Embryonic:

Embryonic Stem Cells (ESC) are derived from the epiblast of the blastocyst and can be expanded indefinitely under proper culture conditions in vitro (Evans et al., 1981; Thomson et al., 1998). In embryos in vivo, pluripotent cells are transiently present before differentiating into somatic cells. ESC can give rise to all cell types of the three germ layers of the foetus: ectoderm, mesoderm and endoderm. When ESCs are injected into adult mice they produce teratomas, which contain tissues comprising the three germ layers. When taken from the blastocyst and cultured in vitro, cells keep their pluripotent

potential even after prolonged culture. It was first shown with mouse Embryonic Stem Cells (mESC) after being reintroduced into a blastocyst by their complete integration into the developing embryo (Beddington et al., 1989). Unlike mESC, human Embryonic Stem Cells (hESC) cannot contribute to the germ line after introduction into a host blastocyst (Yu et al., 2008).

Germinal:

Germinal stem cells or embryonic germ cells (EGC) are the cells that give rise to the gametes (sperm and eggs) in adults. They can be derived from primordial germ cells in vitro. Mouse EGS are also pluripotent and are undistinguishable from mESC morphologically, also expressing typical mESC markers. Furthermore, they can contribute to chimaeric mice upon blastocyst injection (Yu et al., 2008).

Somatic:

Somatic stem cells are undifferentiated cells found in adult or fetal somatic differentiated tissues. They have limited self-renewal capability and generally can differentiate only into cell types associated with the organ system in which they reside. Many tissues have niches of somatic stem cells, like: pancreas, brain, bone marrow, mammary gland, liver, skeletal muscle, the gastrointestinal tract, skin, dental pulp, blood and the eye.

2. EMBRYONIC STEM CELLS (ESC)

Mouse embryonic stem cells (mESC) were the first embryonic stem cells to be isolated from the inner cell mass (ICM) of mouse blastocysts and successfully cultured in vitro (Evans et al., 1981; Martin et al., 1981). They were initially cultured on top of a feeder layer of mitotically inactivated mouse embryonic fibroblasts (MEFs). Posterior analysis with filtered feeder layer produced conditioned medium led to the identification of leukaemia inhibitory factor (LIF). However, in serum-free medium, LIF alone was not able to prevent mESC differentiation, although with bone morphogenetic protein (BMP) pluripotency was sustained (Yu et al., 2008).

Later in 1998, human Embryonic Stem Cells (hESC) were also isolated from embryos (Thomson et al., 1998). Initially it was achieved with a suboptimal culture media conditions using a feeder layer and serum-containing medium. This time however, LIF and other related cytokines failed to support human and non-human primate ESC. Instead, Basic fibroblast growth factor (bFGF) and transforming growth factor β (TGFβ)/Activin/Nodal signalling were reported to be of high importance for the culture of undifferentiated hESC (Yu et al., 2008). Because of the critical requirement of hESC on bFGF, they are thought to be derived from a later stage of the inner cell mass development than mESC.

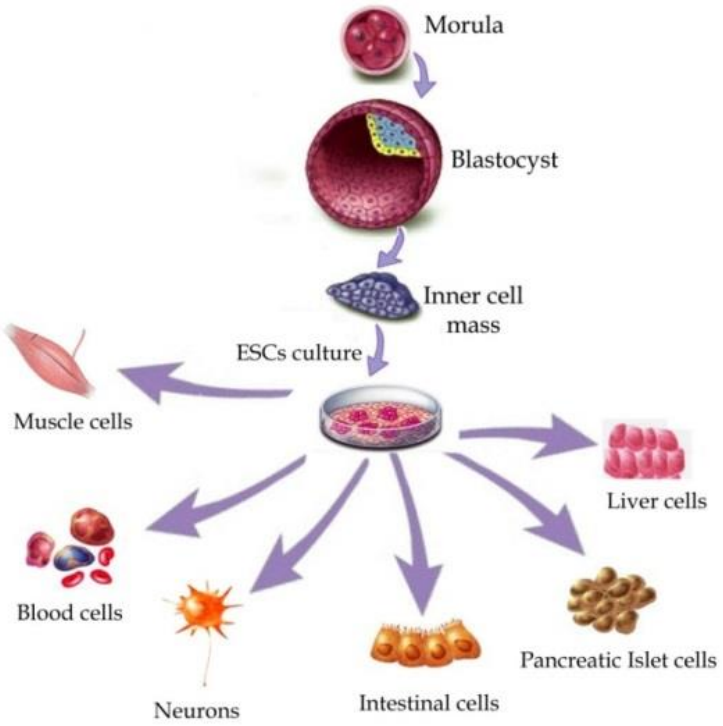

Introduction figure 1. Embryonic stem cells (ESC). ESC are isolated from the inner cell mass of the blastocyst. In vitro they can self-renew indefinitely and differentiate into cell types from the three germ layers: mesoderm, endoderm and ectoderm. Therefore ESC can be expanded in high numbers in vitro, differentiated into specific cell lineages such as: liver, pancreatic islet cells, intestinal cells, neurons, blood cells or muscle cells, and then transplanted to patients with damaged target tissues.

3. INDUCED PLURIPOTENT STEM CELLS (IPSC)

Due to the difficulty of finding a stable source of hESCs and the ethical issues associated to work with human embryos to isolate them, there was an urgency to find an alternative method to isolate pluripotent cells for the regenerative medicine field. Hence, in 2006 the discovery of induced pluripotent stem cells (iPSCs) signified a great leap in the field, which was awarded with the Nobel Prize later in 2012. IPSC avoid the ethical concerns of ESC, since they come from somatic cells of an adult organism.

Induced pluripotent stem cells (iPSCs) are originated from adult somatic cells that have been reprogrammed, through ectopic expression of four defined factors: Oct4, Sox2, Klf4 and c-Myc (OSKM) (Takahashi *et al*., 2007) to cells with similar characteristics to embryonic stem cells (ESCs), meaning they can self-renew and differentiate to tissues of the three germ layers: mesoderm, endoderm and ectoderm. It was first discovered in 2006 by Dr. Shinya Yamanaka with mouse cells (Takahashi et al., 2006), and was confirmed later in human cells (Takahashi et al., 2007). Previously, reprogramming only had been possible by transfer of nuclear contents into oocytes (Gourdon *et al*, 1962, Wilmut *et al*, 1997) or by cell fusion with ES cells (Cowan *et al*, 2005).

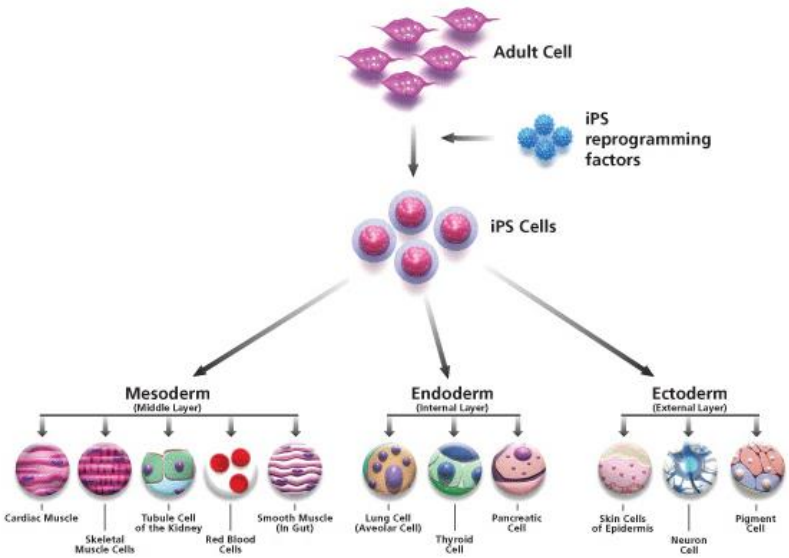

Introduction figure 2. Induced pluripotent stem cells (iPSC) are reprogrammed from adult cells using defined factors: OCT4, SOX2, KLF4 and C-MYC (Takahashi et al., 2006). They can self-renew indefinitely and can differentiate into cell types from the three germ layers: mesoderm, endoderm and ectoderm.

Human iPSC can be established from various tissues: adult and embryonic fibroblasts (Takahashi et al., 2007; Yu et al., 2007), keratinocytes (Aasen *et al*., 2008), adipose tissue (Sun *et al*., 2009), peripheral blood (Loh *et al*., 2009), cord blood (Giorgetti *et al*., 2009), amniotic fluid-derived cells (Ye *et al*., 2009), neural precursor cells (Kim *et al*., 2009), among others.

Human iPSCs express marker genes, growth properties and morphology similar to human ESCs, however, they are not identical. Thus, it has been of interest the investigation to optimize the reprogramming method to yield iPSCs fully equivalent to

ES cells. The assays used for establishing pluripotency equivalence between ESC and iPSC are four criteria (Lujan *et al*., 2010):

1) By subcutaneously injecting iPSC into mice it results in teratoma formation, containing tissues from the three germ layers: ectoderm, mesoderm and endoderm.

2) Injecting iPSC into blastocysts develops into contribution to chimera animal formation.

3) Germline transmission: progeny is able to display transgene expression.

4) Full embryo contribution (ability to generate more live-births "all-iPS cell embryos") by tetraploid (4N) embryo complementation.

Human ESC and iPSC present differences in important aspects like global gene expression, epigenetic landscape and genomic imprinting. However, iPSC acquire ESC cell cycle properties during reprogramming (Ghule *et al*., 2010). But, although extended culture of iPSC makes them transcriptionally closer to ESC (Chin *et al*., 2009), it as well triggers chromosomal aberrations (Mayshar *et al*., 2010). It has also to be taken into account that iPSC derived from adult cells harbor residual DNA methylation signatures from their tissue of origin, retaining a specific epigenetic memory that influence differentiation propensity. Thus the forming potential of iPSCs depends on the differentiation status of the donor cell. For instance, blood-derived iPSC yielded more hematopoietic colonies than fibroblast-derived iPSC (Kim *et al.*, 2010).

3.1 REPROGRAMMING METHODS:

Several methods have been established for reprogramming cells to a pluripotent state. The first method to make human iPSCs used a retroviral vector delivery system, carrying the risk of transgene reactivation and insertional mutagenesis (Takahashi *et al*., 2006; Takahashi et al., 2007). Since then many other groups have used the same methods to reprogram cells to pluripotency (Aasen *et al*., 2008; Stadtfeld et al., 2008; Okita et al., 2007; Yu et al., 2007; Woltjen et al., 2009Edel *et al*., 2010; McLenachan *et al*., 2012). Research efforts thus focused on searching different ways to induce pluripotency with non-viral methods to prevent transgene reactivation and avoid the risk of genomic recombination or insertional mutagenesis (Fusaki *et al*., 2009; Zhou *et al.*, 2009; Warren *et al.*, 2010; Masuda *et al.*, 2013; Yoshioka *et al.*, 2013). Hence, currently only three non-integrative methods appear to be appropriate for reprogramming patient cells for clinically safe cellular therapy: Sendai virus, mRNA transfections and episomal vectors (Introduction Fig. 3).

3.1.1 Transfection of synthetic modified mRNA:

Consists on the administration of messenger RNA (mRNA) modified to overcome innate antiviral immune responses. Although a daily transfection regime is required to maintain a sustained expression, mRNA reprogramming allows a higher reprogramming

efficiency (Warren *et al*., 2010). It offers the best option for future clinical applications as expression is transient over 48 hours and you can control the dose. In this thesis we have focused on reprogramming to iPSC by mRNA transfections as a substitute to retroviral transduction.

3.1.2 Sendai virus:

Non-integrative Sendai virus have the advantages of wide host specificity and low pathogenicity, and the disadvantage of strong immunogenic response (Fusaki *et al*., 2009), triggering the applicability of this method to firstly require the development of less antigenic vectors.

3.1.3 Episomal vectors:

Consist on introducing episomal genes that are ectopically expressed in the cells. Afterwards, the episome is naturally withdrawn by dilution while the iPSC divide (Yu *et al*., 2009). Furthermore, in the case of episomal vectors and Sendai virus, final clones have to be shown to be free of the original vector or virus.

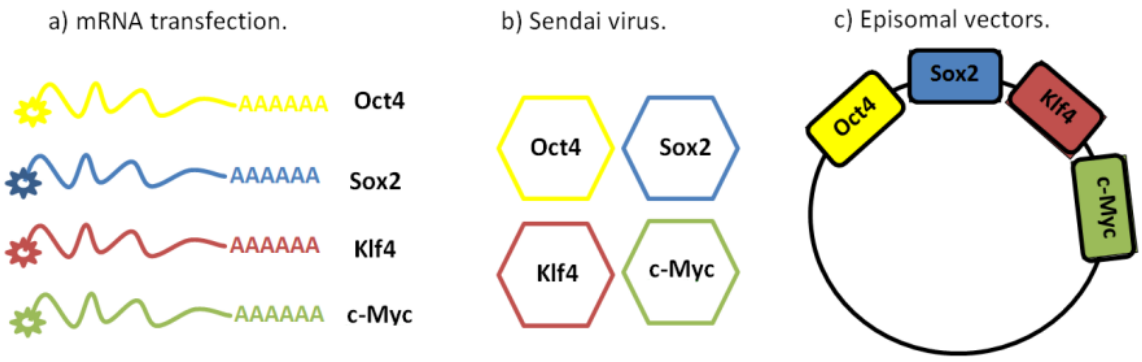

Introduction figure 3. Three main non-integrative methods for reprogramming adult cells to iPSCs in a clinical grade way in order to avoid insertional mutagenesis or transgene reactivation: a) Direct transfection of synthetic modified mRNA (Warren *et al*., 2010), b) Sendai virus (Fusaki *et al*., 2009) and c) Episomal vectors: (Yu *et al*., 2009). Diagram has been made by the author.

However, regardless the method used, cell reprogramming always led to chromosome abnormalities and genomic instability (Gore et al., 2011), which is one of the main barriers to clinical application. Indeed, about half of the human adult derived iPSC clones exhibit genetic and epigenetic variations, thought to result from incomplete reprogramming, mutation in somatic cells and cellular stress during reprogramming (Koyanagi-Aoi *et al*., 2013).

Futhermore, an extensive comparison of all the non-integrating reprogramming methods has reported that, although having a lower successful rate and having a higher workload, mRNA transfections is more efficient, colonies emerge earlier and has a lower rate of aneurploidy than Sendai virus and episomal vectors (Schlaeger et al., 2015).

3.2 REPROGRAMMING FACTORS

In order to discover the cocktail combination of reprogramming factors, Dr. Yamanaka screened 24 candidate factors: Ecat1, Dppa5, Fbxo15, Nanog, ERas, Dnmt3l, Ecat8, Gdf3, Sox15, Dppa4, Dppa2, Fthl17, Sall4, Oct3/4, Sox2, Rex1, Utf1, Tcl1, Dppa3, Klf4, β-catenin, c-Myc, Stat3 and Grb2 (Takahashi et al., 2006). Finding the most suitable reprogramming factors cocktail combination is important to obtain high quality iPSCs carrying few or no genetic aberrations to become less tumorigenic. Accordingly, other transcription factors alternative to classic Oct4, Sox2, Klf4 and c-Myc (OSKM) have been evaluated as potential reprogramming factors, such as the orphan nuclear receptor Esrrb, which was used as a substitute of Klf4 together with Oct4 and Sox2 (Feng *et al*., 2009), or Glis1 that was able to substitute c-Myc reducing the number of partially reprogramed cells (Maekawa *et al*., 2011). Similarly, it was observed reprogramming by removing c-Myc and only using Oct4, Sox2 and Klf4 (Yamanaka *et al*., 2006), although it was highly inefficient and most clones had issues to get expanded. Even, it has been explored cell lines that can be reprogrammed with just Oct4 and Sox2 (Giorgetti et al., 2009; Giorgetti *et al.*, 2010; Montserrat *et al*., 2013) and even only with Oct4 in adult neural stem cells (Kim *et al.*, 2009). However, they were only successful starting from specific cell origins like cord blood (CB) cells or neural stem cells, which are not easily available, and using lentiviral vectors instead of clinical grade methods. Yet, the main transcription factors used for reprogramming are Oct4, Sox2, Klf4 and c-Myc, described below:

OCT4:

The main transcription factors to maintain pluripotency are Oct4, Sox2 and Nanog. Octamer-binding transcription factor 3/4, also known as Oct4 or Pou5f1, is a POU domain containing core transcription factor that binds specific target loci for maintaining pluripotency (Boyer *et al*., 2005). Oct4 expression is necessary to develop the inner cell mass in vivo. It is therefore highly expressed in ESC and iPSC and when its expression diminishes cells differentiate and lose pluripotency. Actually, the main classical four reprogramming transcriptional factors: Oct4, Sox2, Klf4 and c-Myc must have a specific stoichiometry: OSKM in a proportion of 3:1:1:1 (Kawamura *et al*, 2009). Hence, a critical amount of Oct4 is required to sustain pluripotency since only a 50% increase or decrease of Oct4 can lead to ESC differentiation (Yamanaka, 2008; Niwa et al., 2000).

SOX2:

Sex-determining region Y (SRY)-related HMG-box 2 (Sox2) transcription factor is part of a large family of 20 proteins sharing the DNA-binding motif HMG box. Sox2 is expressed in ESC, iPSC, extra-embryonic ectoderm, trophoblast stem cells and neural stem cells (Avilion et al., 2003). Similarly to Oct4, Sox2 dysregulation results in rapid differentiation (Fong et al., 2008; Yamanaka et al., 2008). Sox2 dimerizes with Oct4 (Yuan et al., 1995) being involved in the self-renewal of ESC and iPSC. Indeed, half of Oct4 bound genes are also bound by Sox2 and 87% of these are also co-occupied with Nanog (Boyer et al., 2005)

KLF4:

Kruppel-like factor 4 (Klf4) was first considered a candidate in the Reprogramming factors cocktail since it had been shown to contribute to the long-term maintenance of the ES cell phenotype and the rapid proliferation of ES cells in culture (Li et al., 2005a). Later, it has been shown that Klf4 induces epithelial properties by up-regulating E-cadherin directly (Li et al., 2010). Therefore, Klf4 mainly acts at the initial phase of reprogramming to initiate mesenchymal-to-epithelial transition (Chen et al., 2011). On the other hand, Klf4 had previously been reported to suppres proliferation as well through activating p21 (Zhang et al., 2000), to inhibit apoptosis induced by c-Myc (Zindy et al., 1998) and to repress p53 (Rowland *et al*., 2005).

C-MYC:

Myc genes are key regulators of cell proliferation, and their deregulation contributes to the origin of most tumours in humans. Specifically, c-Myc is a proto-oncogene that can give raise to tumor formation (Okita et al., 2007). It has many targets that enhance proliferation and transformation (Adhikary et al., 2005), many of which may have roles in the generation of iPSC. In ESC, c-Myc has been shown to maintain pluripotency and self-renewal (Varlakhanova et al., 2010). On the other hand, c-Myc role in iPSC reprogramming is not only in cell proliferation increase but also through the control of histone acetylation (Fernandez et al., 2003; Araki et al., 2011), since it associates with histone acetyltransferase (HAT) complexes and induces global histone acetylation allowing Oct3/4 and Sox2 to bind to their specific target loci. Therefore, in the absence of c-Myc, the overall efficiency of reprogramming is drastically reduced and the reprogramming time is increased (Habib et al., 2013).

The first part of the thesis is based on a previous observation that c-Myc oncogene, one of the four reprogramming factors, can be replaced by cell cycle gene Cyclin D1 in the reprogramming cocktail (Edel *et al*., 2010). With this replacement we pursue to reduce iPSCs cancer threat and genetic instability.

3.3 REPROGRAMMING EFFICIENCY

The issue of low efficiency in reprogramming still remains one of the main challenges to solve in the iPSC field. Reprogramming efficiency is determined by counting the number of iPSC colonies formed after reprogramming and dividing it by the total number of infected cells seeded. However, efficiency can be increased by modulating key components, like hypoxic condition (5% O2) (Yoshida *et al*., 2009) during reprogramming or by activation of enhancers or inhibition of barriers.

For example, a manner to increase efficiency is to modulate certain genes such as: downregulation of p53-p21 pathway (Kawamura *et al*., 2009), overexpression of Lin28 that inhibits Let7 induced differentiation (Heo *et al*., 2009), overexpression of Nanog (Han *et al*., 2010) or depletion of the structural component Mbd3, which promoted near 100% induction of somatic cells reprogrammed to pluripotency through suppressing the formation of the Nucleosome Remodelling and deacetylases (NuRD) complex (Rais et al., 2013), among others.

Other approaches to increase efficiency are based on chemicals that are added during the reprogramming process. For instance the addition of vitamin C (Esteban *et al*., 2009); cytokines like tamoxifen (Yang et al., 2010b); the histone deacetylase inhibitor Valproic acid (VPA[1]) (Huangfu D. *et al*., 2008); the inhibitor of DNA methyltransferases 5-azacytidine (5-AZA) (Shi *et al*., 2008); inhibitor of MAPK (Yang. *et al*., 2010) or the inhibitor of GSK3 to suppress differentiation (Ying *et al*., 2008).

Also, depending on the reprogramming method used efficiency is going to be different. It has been reported that viral reprogramming efficiency (0.04%) is lower than modified mRNA efficiency (1.4%) (Warren *et al*, 2010). This is another reason why in this thesis we wanted to reprogram cells using mRNA transfections.

[1] The lack of chromatin silencing caused by VPA demethylation also renders the activation of the Dlk1-Dio3 gene cluster, involved in the development of the wholly reprogramming process (Stadtfeld *et al*., 2010).

3.4 THERAPEUTIC POTENTIAL OF IPSC

Human iPSC technology holds great promise in the regenerative medicine field because of their capability to differentiate into any cell type of the three germ layers. Even elderly patient cells also have the ability to be reprogrammed into iPSCs (Dimos *et al.*, 2008). Potential clinical applications range from drug screening, disease modelling and autologous cell therapies.

Drug screening in iPSC derived cells is advantageous because of the possibility to do the screening on specific cell types that without iPSC differentiation are difficult to find a source to obtain. Furthermore iPSC can be easily expanded to produce higher number of differentiated cells to work with.

Disease modelling using iPSC derived cells is advantageous to unveil the mechanism of specific diseases since scientists can work with iPSC containing the specific mutation that confers the illness. For example, iPSC technology has been used for setting cellular models for studding human diseases and performing drug screening tests. For instance, in 2010, Rett syndrome (RTT) patient-iPSC-derived neurons were produced as a model to study the disease. These cells were reported to exhibit fewer glutaminergic synapses formation, reduced neuritis spines density, smaller soma size, electrophysiological defects and altered calcium signalling; showing thus a neural network maturity deficiency (Marchetto *et al.*, 2010). Thus, there is still a need to improve the differentiation methods employed not only for being more suitable for transplants but to reach an acceptable cellular platform for clinical drug screening research as well.

3.4.1 IPSC Cell Therapy

Regarding cell therapy, the potential application of iPSCs-derived cells offers a source for therapeutic treatment, either autologous or allogeneic, of a wide range of diseases, like neurodegenerative disorders, spinal cord injury, anaemia or diabetes among others. Correspondingly, numerous studies have been conducted since iPSC discovery to prove iPSCs derived cells therapeutic potential in animal models, aiming engraftment potential and illness recovery.

The first graft trial of iPSC-derived tissue in animal models was done in 2007 to treat sickle cell anaemic mice (Hanna et al., 2007). Hematopoietic progenitors (HP) were derived from iPSCs reprogrammed from mouse fibroblasts. In those iPSCs, genetic defects responsible for the anaemia were repaired through homologous recombination. The transplantation of those HPs reconstituted the haematopoietic system of sickle mice correcting the disease phenotype (Hanna *et al.*, 2007).

Afterwards, in 2008 it was reported that loss of motor neurons from spinal cord and the motor cortex could be replaced with patient specific iPSCS-derived motor neurons in mice with amyotrophic lateral sclerosis (ALS) (Dimos *et al.*, 2008). Even elderly patients cells were able to be reprogrammed into iPSCs.

Later on, engraftment of iPSC-derived myocites was successfully viable in dystrophic mice suffering from Duchenne muscular dystrophy (MD), in which regeneration and functional improvement was observed by transplanting satellite cells into dystrophin-

deficient mice (Darabi *et al*., 2012). Moreover, the amount of stem or progenitor cells needed to be appropriate to succeed in graft transplantation (Darabi *et al*., 2012).

IPSC-transplantation therapy research has also focus on ischemic stroke of infarcted brains. Formerly sensorimotor function in rat brain was significantly improved after transplanted iPSCs migrated to injured areas, and differentiated into neuron-like cells successfully (Jiang *et al.*, 2011). And most recently iPSC-derived neurons and astrocytes were transplanted into brain damaged areas after ischemic stroke injury in a rat model in which function recovery was significantly improved in comparison with control groups (Yuan *et al*., 2013).

In another disease model, human iPSC derived from fibroblasts of patient with spinal muscle atrophy, were genetically corrected. Afterwards, iPSC were derived into motor neurons and were transplanted into a spinal muscle atrophy mouse model. A significant recovery was shown in the cells injected group compared with the control sham group (Corti et al., 2012).

These previously described approaches in neurodegenerative disorders demonstrate the potential viability of transplantation therapy of human iPSCs-derived neuron. This new biomedical tool also offers the promises of potential treatment for Parkinson and Diabetes for example, as it has been reported the generation of functional human pancreatic β cells in vitro (Pagliuca et al., 2014), among other diseases.

Early this year, it has been published the first human clinical trial for iPSC transplantation therapies has been finished in the RIKEN institute, Japan (Mandai et al., 2017). It has consisted on iPSC derived retinal pigmented epithelial (RPE) cells transplantation in two age-related macular degeneration (AMD) patients. In the second patient however, the experiment was suspended since it were found genetic instabilities in that patient iPSC. The trial has demonstrated the viability and safety of the procedure and that although there has not been reported any improvement in patients sight, at least the degeneration did not worsen but was maintained. Authors insisted though, in the fact that only one patient was not enough to claim any conclusion. However, the first clinical trial of iPSC in human has been overall satisfactory.

In this thesis, we have assessed iPSC derived Neural Stem Cells (NSC) survival, engraftment and differentiation potential in a spinal cord injury (SCI) rat model and iPSC derived Motor Neurons (MN) in a Spinal Muscle Atrophy (SMA) mouse model.

3.4.1.1 Spinal Cord Injury (SCI)

According to the world Health Organization, every year between 250.000 and 500.000 people worldwide suffer a spinal cord injury (SCI) (WHO webpage, 2017). In the last decades, progress had been made in surgical and rehabilitation treatments for SCI, however these approaches are only palliative. Transection of the spinal cord typically creates limited repair and poor functional recovery after the loss in motor and sensory function below the injury site. The accumulative death of neurons, astroglia, and oligodendroglia in and around the lesion site leads to neural circuitry disruption and dysfunction (Beattie et al., 2000). After the lesion, because of the scar formation,

injured axons are unable to grow, regenerate or reconnect, triggering a permanent interruption of the injured nervous route (Beattie et al., 2000; Blight et al., 1992; Grossman et al., 2001). Over the following hours after the traumatic insult, by-products of cell necrosis (DNA, ATP, glutamate) are released into the microenvironment leading to a rapid and progressive secondary injury cascade which generates further cell death and activation of pro-inflammatory microglia (Choo et al., 2007; LaPlaca et al., 2007). Macrophages and microglia infiltrate and generate ROS while phagocyting debris. Neutrophils and later lymphocytes also infiltrate the immune-privileged blood-spinal cord barrier and contribute to inflammatory response (Waxman, 1989; Ulndreaj et al., 2016).

During the following days, neurons are hampered to regenerate by an interlaced network of hyperproliferative astrocytes forming the glial scar around the lesion. The extracellular matrix also contains chondroitin sulfate proteoglycan (CSPGs) deposits which form a formidable barrier to neuronal growth. Therefore, inability to remyelinate spared axons and failure of axons to build again the signal conduction because of the astrocyte scar contribute to the incurability of SCI (Deumens et al., 2006; Dietz et al., 2006; Harel et al., 2006).

A number of interventions transplanting cell types derived from the adult Central Nervous System (CNS), have shown therapeutic efficacy in various animal models of SCI (Ogawa et al., 2002). However, there were still some barriers to clinical translation like the issues of isolation and expansion of large numbers of cells in a uniform manner and patient immunosuppression after transplant. In this sense, numerous pluripotent and multipotent cell types have been investigated for treating SCI (Tobias et al., 2003; Erceg et al., 2010; Tetzlaff et al., 2011; Vawda et al., 2012; Lopez-Serrano et al., 2016). Therefore, since the discovery of induced pluripotent stem cells (Takahashi et al., 2006), iPSC derived cells have held great promise for the regenerative medicine field. IPSC provide an autologous cell source and avoid the ethical and moral concerns of other stem cell sources. These pluripotent cells can be expanded indefinitely in vitro and can provide a large quantity of differentiated cells for transplantation, including specific cells of neuronal or glial fates (Benzing et al., 2006; Gerrard et al., 2005; Itsykson et al., 2005; Keirstead et al., 2005; Lee et al, 2007; Li et al., 2005b; Ludwig et al., 2006; Erceg et al., 2008).

IPSC technology tool offers the promises of potential treatment for a wide range of diseases described above. However, autologous iPSC-derived cellular transplantations still bargain the hurdle of tumorigenic threat.

3.5 TUMORIGENIC THREAT OF IPSC

One of the main concerns of iPSC is the potential tumorigenic threat of iPSC-derived cells after transplantation into patients, since stem cells and cancer cells share some characteristics. Some shared features are: rapid proliferation rate, lack of contact inhibition, propensity for genomic instability, high activity of telomerase, high expression of oncogenes, miRNA signatures and epigenetic status (Ben-David et al., 2011b). Self-renewal capacity and pluripotency are double-edged swords that prompt ESC and iPSC tumorigenic as well as cancer cells. Spontaneous transformation of ESC in culture increases the risk of formation of teratocarcinomas (Werbowetski-Ogilvi et al., 2009) on transplantation of differentiated cells derived from ESC. However, iPSC-derived teratomas develop faster, more efficiently and more aggressively than ESC-derived teratomas (Moriguchi et al., 2010). Even the formation of benign teratomas is also unacceptable regarding transplantation therapy. There is a need to understand the carcinogenic aspects of iPSC. Therefore, ESCs and iPSC tumorigenicity is a big hurdle hindering clinical application nowadays.

IPSC cancer risk has been studied widely in mouse models (Alvarez *et al*., 2013; Mc Lenachan *et al.*, 2012; Kiuru *et al*., 2009; Miura *et al.*, 2009; Okita *et al*., 2007). Interestingly, the tumorigenicity of virally derived iPSC and transgene-free iPSC showed no significant differences (Moriguchi et al., 2010). Thus, regardless the method used in reprogramming there is a genotoxic stress response that can lead to aneuploidy with aberrant iPSC karyotypes (Mayshar et al., 2010). Also iPSC derived from mature somatic cells that have lived longer enough to acquire mutation that randomly confer anti-apoptotic advantages, are more prone to be selected during culture (Mayshar et al., 2010). Regarding reprogramming factors, c-Myc is a well-established oncogene involved in tumor development (Albihn et al., 2010); however, Oct4, Sox2 and Klf4 are also known to be associated with cancer progression in specific tumours (Wang *et al*., 2010; Ji *et al*., 2010; Tian *et al*., 2010).

Tumorigenesis in ESC and iPSC has been proposed to be Nanog-related, because regardless of the reprogramming genes used, its pre-transduction treatment activated the carcinogenic program (Grad et al 2011). Also, during reprogramming, inactivation of p53-p21 antitumor system either yields iPSC generation or renders cancer (Hussein et al., 2011). Hence, downregulation of p53 pathway during reprogramming can lead to high levels of DNA damage, therefore compromising genomic integrity. Damage can be noted as a rise in the CNV levels, found higher in early-passaged iPSCs. However, most of these changes are lost by the selection pressure of the culture (Hussein et al., 2011).

Several strategies have been proposed to cope with tumorigenicity and improve safety. As only few several hundreds of pluripotent cells are enough to generate tumours, it is required a 100% pure population of differentiated cells to safely apply ESC and iPSC derived treatments. Eliminating the remaining pluripotent cells by cytotoxic antibodies (Choo *et al*., 2008) or even separating ESC using MACS or FACS (Fong *et al*., 2009) don't result in 100% pure cultures of only differentiated cells. Or even introduction of suicide genes to attack the tumour (Schuldiner *et al*., 2003).

3.5.1 Ki67

Once iPSC pluripotency capabilities are assessed in vivo with teratoma formation assays[2] to corroborate differentiation into the three germ layer tissues in vivo, assessment of proliferation rate of teratomas can be measured with Ki67 staining.

Ki67 (or MIB1) is a nuclear protein that is a cellular marker for proliferation (Scholzen et al., 2000). Furthermore, it is associated with ribosomal RNA transcription (Bullwinkel et al., 2006). Through interphase, Ki67 antigen can be solely detected in the cell nucleus. However, in mitosis most of the protein is relocated to the surface of the chromosomes. During all active phases of cell cycle (G_1, S, G_2, and mitosis) Ki67 is present, but is lacking in resting cells (G_0) (Bruno et al., 1992).

Ki67 is an excellent marker to define the growth portion of a population of cells. Interestingly, the fraction of Ki67 positive tumour cells, also called Ki67 labelling index, is very often correlated with the clinical course of cancer. The main examples for this marker are carcinomas of the prostate, brain, breast and nephroblastoma. Prognostic values for survival and tumour reappearance has repeatedly been proven in uni- and multivariate analysis for these types of tumours.

[2] By injecting iPSC subcutaneously into nude mice.

4. C-MYC AND CYCLIN D1

Since the aim of this first part of the thesis is to remove the oncogenic threat of c-Myc from the reprogramming cocktail and replace it with Cyclin D1, here these two genes are introduced and an overview is given.

4.1 C-MYC

Identified three decades ago, c-Myc is a well-established oncogene, associated with many human cancers, involved in tumour development (Dang, 2010; Wasylishen and Penn, 2010; Albihn et al., 2010). All Myc family proteins (C-Myc, N-Myc and L-Myc) regulate processes involved in many if not all aspects of cell fate. Indeed, in vitro and in vivo DNA-binding studies, have designated an increasing number of genes as Myc targets (Ji et al., 2011; Margolin et al., 2009; Shaffer et al., 2006; Wasylishen and Penn, 2010). Likewise, numerous transcription factors and chromatin regulating factors interact with Myc (Cheng et al., 1999; Cowling and Cole, 2006; Eilers and Eisenma, 2008; Rahl et al., 2010; Wasylishen and Penn, 2010).

Regarding genetic aberrations, Myc dysregulation is directly linked with gene amplification. Myc overexpression elevated DHFR gene copy number within 3 weeks by 10 fold (Denis et al., 1991) or even just within 72h after overexpression (Mai et al., 1994; Mai et al., 1996). Indeed, every single cell expressing the conditional Myc gene showed DHFR[3] amplification (Mai et al., 1994). Other genes found amplified after 72h of c-myc overexpression are: ribonucleotide reductase R2 (R2) (Kuschak et al., 1999), the carbamyl-P synthetase, aspartate transcarbamylase, dihydro-orotase (CAD) enzyme conding gene (Miltenberger et al., 1995; Fukasawa et al., 1997; Chernova et al., 1998; Eberhardy and Farnham 2001), ornithine decarboxylase (George et al., 1996; Rounbehler et al., 2009), Cyclin B1 and Cyclin D2 (Mai et al., 1999, 2005).

4.1.1 C-Myc pleiotropic effects

Myc carry out important cellular functions by targeting regulator genes involved in proliferation, differentiation, metabolism, apoptosis, translation, stromal remodelling, inflammation, angiogenesis and invasion (reviewed in Sodir et al., 2009). Accordingly, Myc acts as a master regulator of tumor development by activating or repressing genes related with all this pathways. Therefore, Myc dysregulation initiates a dynamic process of genomic instability that is linked to tumor initiation.

[3] DHFR gene encodes a protein that provides methotrexate (MTX) drug resistance.

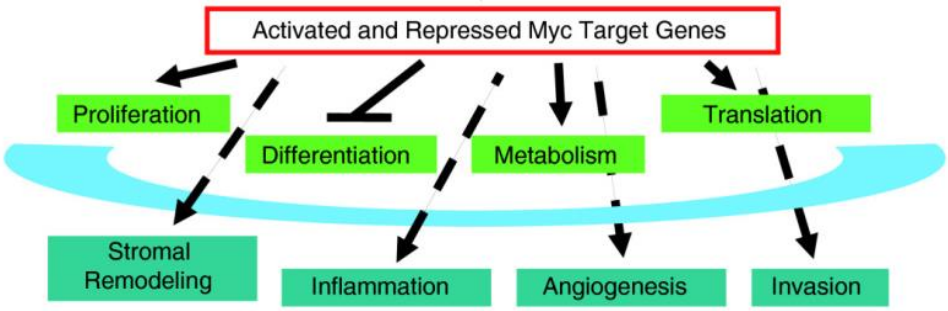

Introduction figure 4. C-Myc pleiotropic effects. C-Myc target genes involved in a great diversity of pathways, such as enhancement of proliferation, inflammation, angiogenesis, metabolism and invasion and inhibition of differentiation. Image from Sodir et al., 2009.

4.1.2 C-Myc in cancer

MYC genes are dysregulated in numerous human neoplasias. Indeed, more than 70% of all tumours have some form of c-Myc gene dysregulation (Nesbit et al., 1999). Therefore, Myc pathology has been studied in neoplasms including Burkitt lymphoma (Lombardi et al., 1987), B and T cell lymphoma (Slack et al., 2011), multiple myeloma (Anguiano et al., 2009; Chng et al., 2011), plasmacytoma (Shen-Ong et al., 1982), hepatocarcinoma (Kawate et al., 1995), lung carcinoma (Little et al., 1983), breast carcinoma (Lavialle et al., 1989), pancreatic cancer (Hessmann et al., 2016) , among others.

Myc genes are induced as response upon almost every signal transduction pathways known to be altered in cancer, comprising, for instance, those ruled by tyrosine kinase growth factor receptors, NF-κB and β-catenin (Kelly *et al.*, 1983; Renan, 1989; Duyao *et al.*, 1990; Marcu *et al.*, 1997; Zou *et al.*, 1997; He *et al.*, 1998). In turn, Myc proteins have a role as master transcriptional regulators of a wide range of target genes that execute a cellular response. As a matter of fact, 11% of all cellular loci are candidates to be bound by Myc (Fernandez et al., 2003; Orian et al.,2003; Hulf et al., 2005). Actually, MYC/MAX heterodimer are estimated to occupy more than 45% of all replication origins in human cells carrying Myc-binding E-box motifs (Swarnalatha et al., 2012). At the karyotype level, Myc overexpression cause chromosomal changes such as formation of extrachromosomal elements, centromere and telomere fusions, chromosome and chromatid breaks, ring chromosomes, translocations, deletions and inversions, aneuploidy, and the formation of Robertsonian chromosomes (Mai et al., 1996; Felsher and Bishop 1999; Rockwood et al., 2002; Guffei et al., 2007; Goncalves Dos Santos Silva et al., 2008; Silva et al., 2010; Chen et al., 2011).

Dysregulated Myc also modifies the nuclear architecture of cells, affecting therefore the positional organization of telomeres and chromosomes, which initiate a dynamic process of ongoing genomic instability (Chuang et al., 2004; Louis et al., 2005; Mai and Garini 2005; 2006; Vermolen et al., 2005). Myc dysregulation, even for as short as 2-12h, resulted in nuclear remodelling of the 3D organization and position of telomeres and chromosomes (Louis et al., 2005; Mai and Garini 2005). Therefore, by affecting nuclear organization, Myc drives dynamic remodelling of chromosomes, genes and their structural order. This is particularly relevant as gene activation, function and

nuclear space are functionally linked (Solovei et al., 2009). Furthermore, nuclear remodelling occurs during early malignancy and set the stage for neoplastic transformation (Mai and Garini 2005, 2006; Gadji et al., 2011, 2012).

4.2 CYCLIN D1

Cyclin D1 is a well-known cell cycle gene responsible for enabling the progress of the cell cycle from G2 to S phase. Its classical role is to interact with CDK4 and form a complex that phosphorylates the retinoblastoma (Rb) (Connell-Crowley et al., 1997). Then, phosphorylated retinoblastoma derepresses E2F, which internalizes to the nucleus and acts as a transcription factor to activate the synthesis of genes involved in cell cycle progression.
On the other hand, Cyclin D1 also carries out important non-canonical roles apart from cell cycle progression, in other cellular processes recently reviewed (Hydbring et al., 2016), such as: DNA damage repair, control of cell death, differentiation, migration, immune response and metabolism.

Here we want to seize both the capability of Cyclin D1 to facilitate the cell cycle progression, bypassing the limiting step of speeding the cell cycle during early reprogramming stages, and its advantageous role in DNA damage repair to propose Cyclin D1 as a safer candidate to replace c-Myc in the reprogramming cocktail.

4.2.1 CELL CYCLE

Cell cycle is a sequence of events that eventually leads to division and duplication of a cell. Multiple checkpoints are present within the cell cycle to regulate progression through various stages. These mechanisms are controlled by a family of cyclins and cyclin-dependent kinases (CDKs), where CDK functionality is dependent on their association with an active cyclin. Eukaryotic cells have some CDK-cyclin complexes that play defined roles at different phases of the cell cycle. These complexes comprise ten cyclins belonging to four different types (A, B, D, and E type), three interphase CDKs (CDK2, CDK4, and CDK6) and a mitotic CDK1 (Schwartz et al., 2009) (introduction figure 5).

Somatic cells are generally dependent on receiving specific mitogen signals, such as growth factors, to divide and proliferate (Evan et al., 2001). Once cells have received enough mitogen exposure, DNA damage has been checked and cells have confirmed they have all required machinery proteins needed for successful division, then they enter the cell cycle. On the contrary, ESC and iPSC do not require mitogenic factors since they express Oct4, Sox2 and Nanog and are cultured in medium with FGF2 and TGFβ1 that maintain pluripotency and continuous self-renewal of the cells (reviewed in Huang et al., 2015).

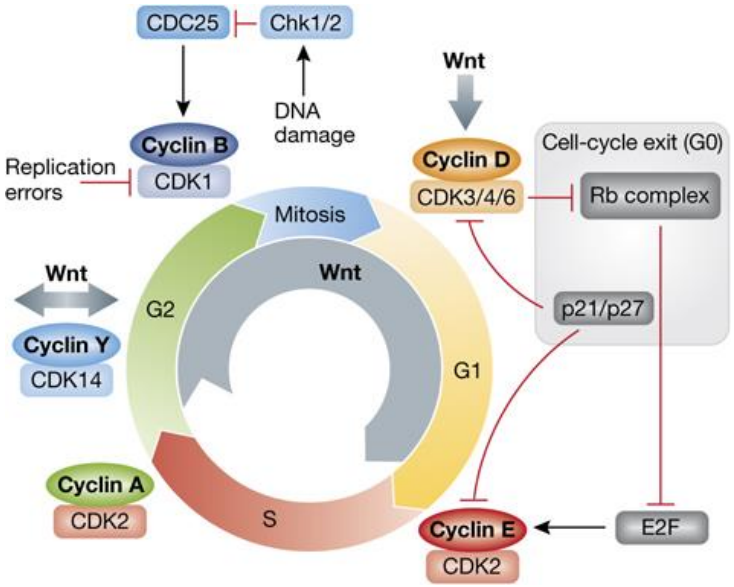

Introduction figure 5. Cell Cycle phases and Cyclins. Overview of the cell cycle phases: G_1, S, G_2 and M (mitosis). Cell-cycle progress is controlled by cyclins and their CDKs. In the G1 phase, Cyclin D-CDK4 complex phosphorylates Rb protein, which derepresses E2F inducing Cyclin E transcription. On the other hand, p21 and p27 oppose these effects and can result in the exit of the cell-cycle finishing in G_0. To ensure the integrity of the DNA there are several checkpoints in S phase after DNA replication. For example, chromosome abnormalities and DNA damage are reported to cyclin B/CDK1 complex via diverse pathways to delay or stop progression into mitosis. Image from Niehrs et al., 2012.

These cyclins activate CDKs by binding to them depending on their presence and levels. For example, Cyclin D complexes with CDK4 and CDK6 to stimulate the initiation of G1 phase and the start of the cell cycle, when the cell prepares for DNA synthesis (Schwartz et al., 2009). In normal cells, CDK activity is regulated by two types of inhibitors: INK4 proteins (A-D) and Cip/Kip family proteins (p21, p27, and p57) (Schwartz et al., 2009).

In cancer, cell cycle defects are frequently generated by changes in CDK activity as a result of accumulated mutations (Evan et al., 2001; Schwartz et al., 2009). These mutations lead to hyperactive CDKs that trigger unscheduled proliferation, such as CDK4 in melanoma (Schwartz et al., 2009), CDK6 in pro-B acute lymphocytic leukemia (Kuo et al., 2011), CDK5 in pancreatic adenocarcinomas (Eggers et al., 2011) or CDK1 and CDK2 in colon adenomas (Vermeulen et al., 2003).

4.2.2 Cyclin D1 in cancer

Cyclin D is involved in various types of cancers, however, it is not the only cyclin dysregulated. Cyclin E has also been reported to be overexpressed in breast and colon cancer (Vermeulen et al., 2003) and cyclin A and E are amplified in certain lung carcinomas. D type Cyclins function as growth sensors, which connect mitogen stimuli with the cell cycle progression (Choi et al., 2014a). Therefore, Cyclin D translocations, amplifications, missense mutations, and elevated protein levels are potential causes of cancer. Mutations and abnormities may increase cyclin D activity, resulting in enhanced cell cycle progression to S-phase and cell proliferation (Ashgar et al., 2015). Elevated levels of cyclin D proteins in cancer have been attributed to defective mechanisms of

degradation as well (Lahne et al., 2006). For example, overexpression of cyclin D1 linked to gene amplification has been studied in breast, esophageal, bladder, lung, and squamous cell carcinomas (Vermeulen et al., 2003). In B-cell lymphoma, overexpression of cyclin D1 has been observed due to gene translocation (Vermeulen et al., 2003). In prostate cancer however, low levels of cyclin D1 and D3 have been observed (Olshavsky et al., 2008).

In a ChiP promoter array assay, Cyclin D1 associated with approximately 900 genes in close proximity to the transcriptional start site (Fu et al., 2005). A large number of gene sets were associated with cell division (most involved in G2/M phase and cellular mitosis); other genes were found to regulate chromosomal stability. Hence, Cyclin D1 overexpression contributes to chromosomal instability by directly regulating a transcriptional program that governs it (Casimiro et al., 2012). Indeed, transient expression of Cyclin D1 over 7 days in the mammary gland induced chromosomal instability (Casimiro et al., 2012). Its overexpression also correlated with aneuploidy, supernumerary centrosomes, and spindle defects in mouse hepatocytes (Nelsen et al., 2005), and with aneuploidy and polyploidy in lymphoid tumors (Aggarwal et al., 2007). Still the number of genes targeted by Cyclin D1 is lower than c-Myc.

5. IPSC GENETIC STABILITY

Genetic instability refers to a series of chromosomal changes that enables cells to develop new and aggressive phenotypes to adapt to the changing selection pressures (Bayani et al., 2007). It is generally classified into two major types: DNA base changes that occur due to defects in the DNA repair processes including base excision repair, mismatch repair and nucleotide excision repair (Kolodner et al., 1995; Modrich et al., 1997; Rajagopalan et al., 2003) and abnormal karyotypes with structural and numerical chromosome alterations (Lengauer et al., 1997).

Human Pluripotent Stem Cells genomic instability was first documented in 2004 reporting karyotype abnormalities in ESCs, such as trisomy of chromosome 12 (Cowan *et al*., 2004; Draper *et al*., 2004). Since then and up to date, an emerging number of publications have aimed this issue, focusing on ESCs and iPSCs genetic and epigenetic instability (reviewed in Martins-Taylor et al., 2012; Peterson et al., 2013; Steinemann et al., 2013). Aberrant cell reprogramming lead to genetic and epigenetic modifications (Gore *et al.*, 2011), which are one of the most significant barriers to personalized clinical applications of patient iPSC derivatives. Such genetic aberrations are an important factor for assessing the quality of iPSC and can result from the cellular stress that accompanies reprogramming (Lee et al., 2012b). Therefore, it is crucial to define ways to reduce replicative stress induced by reprogramming (Ruiz et al., 2015). In Introduction Figure 6 it is schematized how during reprogramming process some but not all iPSCs acquire aberrations.

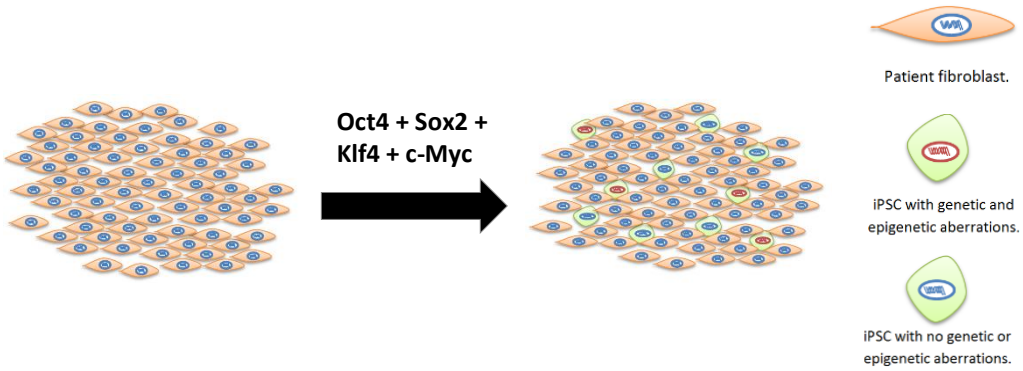

Introduction figure 6. Reprogramming of patient fibroblast using a clinical therapy viable method introducing the four Yamanaka genes: Oct4, Sox2, Klf4 and c-Myc. After reprogramming the resulting mosaic cell population contain a mixture of not reprogrammed cells (patient fibroblasts), cells reprogrammed carrying no genetic or epigenetic aberrations (green cells with blue nucleus) and cells reprogrammed carrying genetic and epigenetic defects (green cells with red nucleus). The proportion of cells carrying genetic and epigenetic aberrations is not actually known, but depends on reprogramming factors used and cell culture conditions. Diagram has been made by the author.

5.1 CELL STRESS

Oxidative and replicative cell stresses are the main causing agents of genetic instabilities. In normal situations DNA damage cause an immediate and p53-independent G1 arrest, caused by rapid proteolysis of Cyclin D1. This degradation is an essential component of cellular response to genotoxic stress (Agami et al., 2000). Accordingly, lowering replication stress during reprogramming by eliminating Myc, provides a simple strategy to reduce genomic instability on mouse and human iPSCs (Ruiz et al., 2015). Indeed, replication stress may result from metabolic starvation of nucleotides or from RNA polymerase transcription and DNA replication machinery clash causing replication fork collapse. Additionally, Myc expression also causes an accumulation of reactive oxygen species (ROS), which generates DNA breaks by oxidative stress (Khanna and Jackson 2001). ROS increases as a result of a biochemical imbalance caused by the sudden increase in gene products via Myc transcriptional activation (Vafa et al., 2002). Myc also alteres a mitochondrial gene, TFAM, which encodes a protein essential for mitochondrial function and biogenesis, and may lead to increased ROS (Dang et al., 2005).

5.1.1 Sirtuin 1

Sirtuins are an enzymatic type of NAD-dependent histone deacetylases found in prokaryotes and eukaryotes that regulate the expression of certain genes to help organisms to respond to metabolic and genotoxic stress through diverse pathways, such as metabolic homeostasis, cell survival pathways and cell-cycle control. Descriptions of knockout models for each of the seven mammalian Sirtuins suggest that during stress response Sirtuins protect genomic stability, triggering integrity through a variety of mechanisms, the main involved in chromatin-related functions (reviewed in Bosch-Presegué et al., 2014).

Sirtuin 1 (Silent mating-type information regulation 2 homologue 1 or Sirt1), a member of the class III histone deacetylase (HDAC) family, plays key roles in a variety of physiological processes such as genomic stability, metabolism, neurogenesis and cell survival.

It has also been reported to be necessary for proficient telomere elongation and genomic stability of iPSC (De Bonis et al., 2014). Also, Sirtuin 1 contributes to telomere maintenance and increases global homologous recombination. Sirtuin 1 null mouse embryonic fibroblasts (Sirt1-/-MEFs) were shown to express a higher number of multitelomeric signals per chromosome (Palacios et al., 2010). In addition, in human embryonic stem cells (hESC) Oct4 maintain the pluripotency through inactivation of p53 by Sirtuin 1 mediated deacetylation (Zhang et al., 2014). Furthermore, sirt1 has been reported to be necessary for proficient telomere elongation and genomic stability of induced pluripotent stem cells (De Bonis et al., 2014).

5.1.2 Apoptosis

In response of mammalian cells to stress, the tumour suppressor p53, often cited as the guardian of the genome, is a key mediator of cell-cycle arrest and/or apoptosis. At all times p53 protein is expressed in cells at low levels and is raised in response to stress. The regulatory loop ARF–Mdm2–p53 controls the protein level of p53. Mdm2 negatively regulates p53, causing its degradation by the proteasome, similarly ARF inhibits Mdm2 function (reviewed in Nag et al., 2013).

C-MYC has been shown to participate in the apoptotic response, either by inducing or sensitizing cells to apoptosis. Apoptosis generated or sensitized by c-MYC can be either p53-dependent or independent, determined by the cell type and apoptotic trigger (Askew *et al.*, 1991; Evan *et al.*, 1992; Shi *et al.*, 1992). For instance, dysregulated c-Myc induced apoptosis in Rat-1 fibroblast and in primary rat fibroblasts deprived of serum (Evan *et al.*, 1992). Mechanistically, Myc activation leads to increased ARF expression (Zindy et al., 1998), causing increased p53 protein, which triggers apoptosis. FoxO transcription factors have also been shown to facilitate Myc-induced ARF expression, binding to the *Ink4a/Arf* locus and activating its expression (Bouchard *et al.*, 2007).

On the other hand, many researches have also linked Cyclin D1 with anti-apoptotic properties. For example, Cyclin D1 has been reported to bind and sequester pro-apoptotic protein BAX, inhibiting therefore apoptosis (Beltran et al., 2011). Also, D-type cyclins have been shown to have overlapping roles in controlling Fas mediated apoptosis by repressing the expression of death receptors FAS and its ligand FASL (Choi et al., 2014b). Likewise, in prostate cancer cell lines, cyclin D1 was claimed to inhibit anoikis by binding to FOXO1 and FOXO3A in a CDK-independent manner (Gan et al., 2009).

5.2 EPIGENETIC STABILITY

Reprogramming to iPSC from somatic cells can be incomplete or can induce epigenetic anomalies which may alter the developmental potential of cells and may predispose to malignancies or rejection potential. Regarding ESC, during early development a massive epigenetic reprogramming of ESC chromatin is required, comprising changes in both DNA methylation and histone modifications (Ferguson, 2011; Meissner, 2010). Is in this delicate phase when alterations in cells epigenome are induced. Essentially, the main epigenetic alterations of pluripotent stem cells are: pattern alterations in imprinting, DNA methylations and histone modification.

Imprinting is the epigenetic silencing of some alleles of specific genes depending on a parent-of-origin specific manner. Alterations in imprinting provide growth advantages for pluripotent cells maintained in culture, since many imprinted genes are known to regulate growth during embryonic development (Piedrahita *et al.*, 2011). A large-scale comparison of hESCs, hiPSCs, somatic tissues and primary cell lines showed that

pluripotent cells are characterized by a high level of variation in the methylation status of a subset of imprinted genes (Nazor *et al.*, 2012).

Alterations in DNA methylation patterns can be either losses or gains of methylations that have been reported to be unchanging at different passages (Allegrucci *et al*., 2007), and can affect as well the developmental potential of PSCs lines (Bock *et al.*, 2011). These alterations in methylation patterns can be inherited by differentiated cells. Among pluripotent cells DNA methylation is particularly typical for a subset of imprinted developmental genes, for instance the alteration in methylation of the tumour suppressor RAS association domain family member 1 (RASSF1) gene has been observed several times suggesting a positive selection pressure. Human iPSC have been reported to have increased levels of DNA methylations, which are aberrant and different from ESCs during early passages. However, during prolonged culturing they gradually become even (Nishino *et al*., 2011).

Some studies revising histone trimethylation modifications reported iPSC to have increased levels of H3K27me3 (Doi *et al*., 2009; Guenther *et al*., 2010; Deng *et al*., 2009). However, in other studies lysine 9 (H3K9me3) rather than lysine 27 (H3K27me3) has been reported to be highly modified (Hawkins *et al*., 2010).

5.3 GENETIC STABILITY

Possible genetic alterations range from single nucleotide polymorphism, deficient mismatch repair, whole chromosome aneuploidies and subchromosomal aberrations, including gene duplications and deletions (Copy number variation or CNV) (Amps *et al*., 2011; Lauren *et al*., 2011; Peterson *et al*., 2011; Taapken *et al*., 2011). Aberrations can occur during reprogramming and long term culture of iPSCs or during differentiation.

Reprogramming can cause or select for alterations in iPSC as well. However, genetic alterations occur mostly during long-term culture of PSC, as late passage PSC are twice as likely to have genomic changes than early passage cells (33% compared with 14%), as reported in a large-scale study of more than 100 PSC lines (Amps et al., 2011). These results point to the fact that selective pressure may play an important role not in the acquisition but in a favoured accumulation of genomic alterations.

5.3.1 Aneuploidy

Karyotype abnormalities frequently accumulate in PSC during *in vitro* culture maintenance. Culture-induced genomic aberrations in PSC are unpredictable, variable between lines and can occur at any stage (Taapken *et al*., 2011; Martins-Taylor *et al.*, 2011; Hussein *et al.*, 2011; Amps *et al.*, 2011; Laurent *et al*., 2011). Therefore, it is difficult to develop specific culture conditions to maintain homogeneous genomically stable populations and a save passage number threshold cannot be determined.

Most frequent aneuploidy chromosome duplications in pluripotent cells have been observed on chromosomes 1, 12, 17 and X and amplifications of 20q have been detected in a 34% of PSC lines examined (Amps *et al.*, 2011; Taapken *et al.*, 2011; Mayshar et al., 2010). Specifically, trisomy of chromosome 12 is the most recurrent abnormality in both ESC (42.6%) and iPSC (32.9%) (Mayshar *et al.*, 2010; Taapken *et al.*, 2011). Genetic and epigenetic instability in pluripotent stem cells is associated with tumorigenic concerns (Peterson *et al.*, 2013) as the most common genetic alterations in PSC, such as the gains in chromosomes 1, 12, 17 and X, are also found in embryonal carcinomas (Atkin *et al.*, 1982; Rodriguez *et al.*, 1993; Skotheim *et al.*, 2002; Wang *et al.*, 1980).

Many chromosomal abnormalities found in ESC are also found in hiPSCs. While chromosome 8 gains are more likely to be found in iPSC, chromosome 17 gains are more likely in ESC (Taapken et al., 2011; Ben-David et al., 2011b; Martins-Taylor et al., 2011).

5.3.2 Single Nucleotide Polymorphism (SNP)

A single-nucleotide polymorphism is a variation in a single nucleotide that occurs at a specific position in the genome. Regarding pluripotent stem cells point mutations, 74% of mutations detected in iPSC are generated during reprogramming, 19% pre-existed in parental fibroblasts, and only 7% are caused by *in vitro* maintenance (Ji *et al.*, 2012).

Recently it has been described that by using a high-density DNA methylation array with the same sensitivity of SNP platforms, it can also be profiled copy number variation (CNV). This new method provided a robust and economic platform for detecting CNV and SNP in a single experiment (Feber *et al.*, 2014).

5.3.3 DNA double strand breaks (DSBs)

One of the most dangerous sources of cell instability is the formation of DNA double strand breaks (DSB). DSB are generated when both strands of DNA's phosphor-sugar backbones are broken at the same position or in sufficient closeness to enable physical separation of the double helix into two separate molecules. It is estimated that up to 10^5 spontaneous DNA lesions occur to a cell per day (Hoeijmakers et al., 2009), among which, around 10 are thought to be DSBs (Lieber et al., 2010).

DSB can be produced by endogenous and exogenous causes. Endogenous origins are reactive oxygen species (ROS) generated by the cellular metabolism and also replicative errors generated by replicative stress. Exogenous reasons are ionizing radiation (IR) and chemotherapeutic agents. Replication of DNA is believed to be the main cause of DSBs in proliferating cells as the DNA intermediates at replication forks are delicate and vulnerable to breakage.

DSBs are repaired by three different pathways: homologous recombination (HR), non-homologous end joining (NHEJ) and alternative non-homologous end joining or also called microhomology-mediated end joining (MMEJ). These pathways are schematized at the molecular level in introduction figure 7. DSB elimination is crucial for cell

survival. While homologous recombination gives rise to a precise recombination, non-homologous end joining triggers a low fidelity recombination that can lead to 1-4 nt deletions. Furthermore, alternative NHEJ leads to a highly error prone recombination that can lead to chromosomal translocations, insertions, deletions (CNV) and telomere fusions. Therefore, unsuccessful DSB repair potentially induces genetic instability, oncogenic chromosome translocations and therefore cancer.

5.3.3.1 Histone H2AX

In eukaryotes, DNA is organized into chromatin, a structure necessary for solving the problem of spatial accommodation and for restricting the functional transcription of DNA (Groth et al., 2007; Li et al., 2007). Nucleosomes are the monomeric blocks that build chromatin (Andrews et al., 2011; Zlatanova et al., 2009). They contain around 150bp of DNA enveloped around a histone octamer that consists of the core histones H2A, H2B, H3 and H4 in duplicate each (Luger et al., 1997). These histones can be replaced by variants as a mechanism of chromatin regulation (Talbert et al., 2010). Indeed, the H2A family contains plenty of variants, some of which are universally found in human and other eukaryotes, such as H2AX, H2AZ, H2A.F/Z, H2ABbd, macroH2A1 and macroH2A2. C-terminal usually contains the highest grade of divergence among H2A (Millar et al., 2013). Specifically, H2AX histone variant was first described in 1980 (West et al., 1980) and constitutes about 2.5-25% of the total H2A histone in the mammalian genome (Rogakou et al., 1998) and contains a hydrophobic Φ motif (SQ) in the C-terminus. H2AX serine 139 is phosphorylated (γH2AX) by ATM[4] (Burma et al., 2001), which forms a docking site for the accumulation of DNA repair proteins that triggers genome integrity preservation through HR, NHEJ and MMEJ repairing mechanisms.

5.3.3.2 DSBs repair molecular pathways

After DNA double strand break damage, histone variant H2AX binds to the broken strand ends. ATM then phosphorylates it at Ser139 (γH2AX) (Burma et al., 2001), which recruits damage-response factors in order to initiate the repair response to DSBs. The three main DSB repair mechanisms are schematized in introduction figure 3 and are explained in detail in the following paragraphs.

[4] Ataxia telangiectasia mutated (ATM) is a PIKK (phosphatidylinositol 3-kinase related kinase).

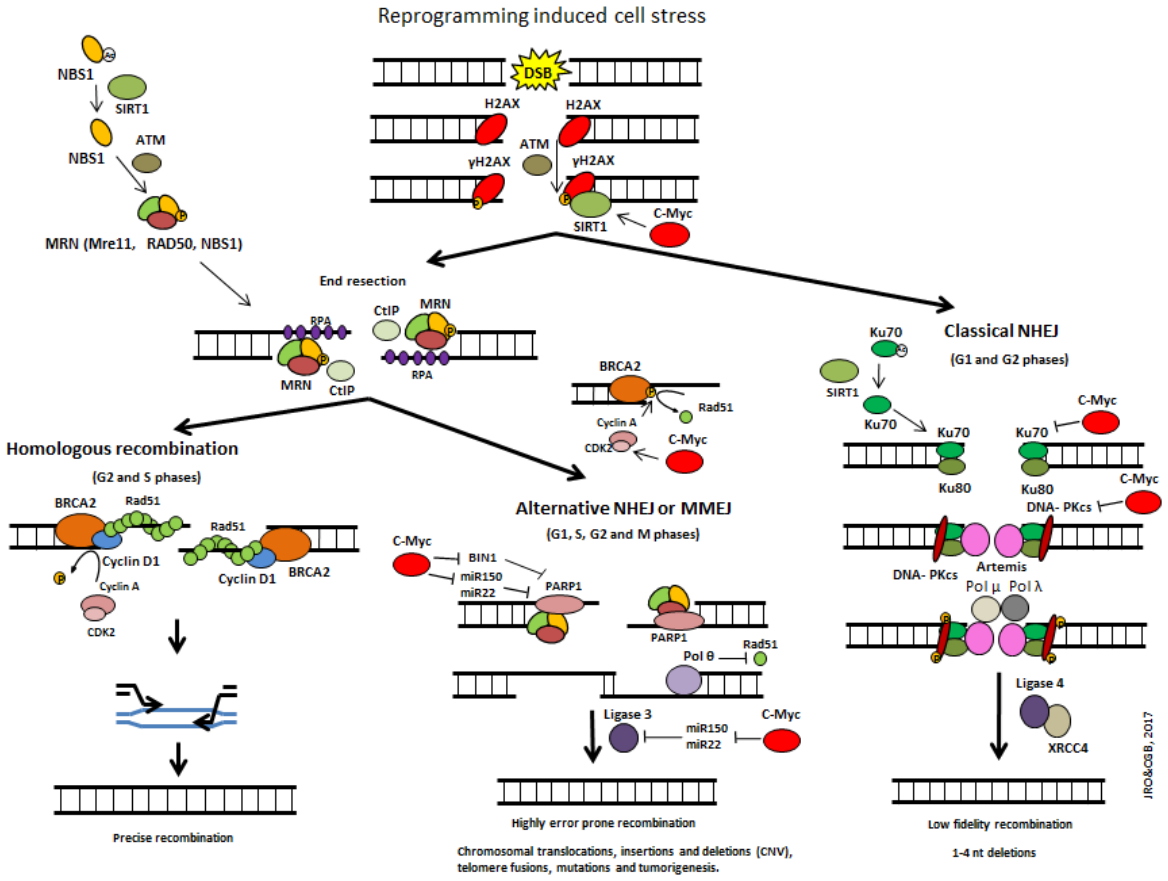

Introduction figure 7. Schematic diagram drawn by the PhD student about all different molecules involved in the main three repair pathways for DNA double strand breaks (DSB). It is represented how DSB caused by cell reprogramming induced stress can be repaired by homologous recombination (HR), non-homologous end joining (NHEJ) and alternative non-homologous end joining of microhomology-mediated end joining (MMEJ). Diagram authors: JRO: Jordi Requena Osete and CGB: Carme Grau Bové.

There is a dynamic interplay between several molecules that fluctuate depending on the cell cycle phase the cell is in that determines the repair pathway the cell is going to choose (reviewed in Frit et al., 2014 and Aparicio et al., 2014; Ceccaldi et al., 2016). Thus, depending on the cell cycle phase the cell is in, one pathway or another is going to be preferentially chosen to repair the DSB. Therefore, DSBs can be repaired in a Ku70/80 dependent manner through NHEJ or in an end resection mediated repair manner that can be conducted through homologous recombination or alternative NHEJ (Truong et al., 2013). NHEJ takes place during G1 and G2 phases. HR occurs during G2 and S phases, as Cyclin D1 is required to bind to BRCA2 to prevent Cyclin A/CDK2 phosphorylation. Alternative homologous recombination however, can occur at any phase of the cell cycle (G1, G2, S and M) (Aparicio et al., 2014).

If the cell enters the classical non-homologous end joining (NHEJ), Ku70-Ku80 heterodimer recognizes and binds the DSB site. To be able to form the heterodimer, Ku70 has to be deacetylated by Sirtuin 1 (Jeong et al., 2007). Ku70/80 proteins have 3 domains, 2 involved in the dimerization and one in DNA binding. Once Ku70-Ku80 has bound to the damaged DNA ends with high affinity, it acts as a scaffold to other factors to render the NHEJ repair (reviewed in Davis et al., 2013). Afterwards, Ser/Thr kinase

DNA-PKc[5] binds to Ku70/80, self-phosphorylates and phosphorylates Artemis nuclease protein, which is important for the stabilization of the DSB site. Artemis then cleaves the DNA blunt ends to allow the binding of X polymerases (Pol μ, Pol λ) (Franco et al., 2008; Davis et al., 2013). Then, although Polymerase μ has template-dependent activity (Moon et al., 2015), it also polymerizes along a discontinuous template in the presence of Ku, XRCC4 and Ligase 4 (Mahajan et al., 2002). Polymerase λ also polymerizes in a template-independent manner (García-Díaz et al., 2002). NHEJ finishes when Ligase 4 (LIG4) and the scaffold protein XRCC4 directly bind Ku70-Ku80 and catalyses the ligation and repair of the DNA ends.

If cells enter an end resection dependent repair mechanism, MRN complex, CtIP and RPA proteins are going to be recruited to the damaged site. The MRN complex is formed of: Meiotic recombination 11 (MRE11), RAD50 and Nijmegen breakage syndrome 1 (NBS1) proteins. Beforehand, sirtuin1 is responsible for NBS1 deacetylation (Yuan et al., 2007), which enables ATM to phosphorylate it (Lim et al., 2000; Wu et al., 2000; Zhao et al., 2000) to facilitate the assembly of the MRN complex at the DSB. Then, MRN nuclease with CtIP exonuclease together resect the double strand into a single strand ssDNA ends, where Replication protein A (RPA) is rapidly bound to protect them and facilitate the recruitment of Rad51 (Ruff et al., 2016).

After the strands have been resected, if the cell is in G2 or S phases the cell is preferentially going to enter homologous recombination (HR). In order to enter this mechanism, BRCA2 (breast cancer 2) has to bind ssDNA and is essential to mediate Rad51 monomer filaments binding to the strands (Davies et al., 2001; Davies et al., 2007). Rad51 recombinase monomers replace RPA and polymerize around the ssDNA ends forming a helical nucleoprotein (Holloman, 2011) that is essential to catalyse the exchange of strands with the homologous sister chromatid. Correspondingly, mutations in BRCA2 gene cause a loss of tumor suppressive function which correlates with an increased risk of breast cancer (O'Donovan et al., 2010). However, when BRCA2 is phosphorylated at the C-terminal domain at Serine 3291 by Cyclin A-CDK2, Rad51 cannot bind and homologous recombination is repressed (Chalermrujinanant et al., 2016; Esashi et al., 2005).

It has recently been reported a non-canonical function of the cell cycle gene Cyclin D1 in the homologous recombination pathway mechanism. Cyclin D1 directly interacts with the C-terminal domain of BRCA2 and with Rad51 and enhances Rad51 recruitment to BRCA2-bound DSB sites by blocking Cyclin A-CDK2 phosphorylation and inactivation of BRCA2 (Chalermrujinanant et al., 2016; Jirawatnotai et al., 2016).

If BRCA2 is phosphorylated at the Serine 3291, Rad51 is not recruited and HR is inhibited. Then, the cell engages the alternative non-homologous end joining (Alt-NHEJ) or micro-homology mediated end joining (MMEJ) mechanism to repair the damage. Alt-NHEJ, which is most active in the S and G2 phases of the cell cycle, is dependent on PARP1[6] signalling and relies on resection of the DNA by MRN and CtIP. First, PARP1 enzyme promotes poly(ADPribosyl)ation of the c- and n-terminus tail residues of the histones H1 and H2B, which induces relaxation of the chromatin and

[5] DNA-PKcs is a member of the phosphatidylinositol-3 (PI-3) kinase-like kinase family (PIKK).

[6] Poly (ADP-ribose) polymerase-1 (PARP1).

also acts as a signal for alternative NHEJ scaffold proteins to join and recruit the molecular machinery (Schreiber et al., 2006). Then, microhomologous base pairs at the resected ends drives the annealing of opposite ends of a DSB. Finally, annealed ends are subject to fill-in synthesis by the low-fidelity DNA polymerase θ (Pol θ), a specific polymerase of the alternative NHEJ pathway, which stabilizes the annealed intermediates and promotes end joining, primarily by LIG3[7].

Due to the high risk of mispairing during the microhomology base pairing, this process is highly promiscuous and leads to low-fidelity DNA synthesis. Therefore, alt-NHEJ introduces deletions and insertions that mark the break sites following repair. The deletions are produced by extended nucleolytic processing, whereas insertions are caused by Pol θ activity (Ceccaldi et al., 2015; Kent et al., 2015). Furthermore, Pol θ blocks HR by impeding the formation of the Rad51 nucleoproteins filaments (Mateos-Gomez et al, 2015).

As a consequence of DSB repair malfunction or the usage of the alternative NHEJ, cells can accumulate genetic instabilities such as chromosomal rearrangements (insertions, deletions or translocations) that can trigger CNV.

5.3.3.3 Myc and Cyclin D1 in DSB pathways

During reprogramming to iPSC using the classical cocktail of factors (Oct4, Sox2, Klf4 and c-Myc), c-Myc forced overexpression in the cells is going to produce a direct effect on the cell's choice of repairing mechanism. Correspondingly, it has been reported that c-Myc overexpression disrupts c-NHEJ because it directly interacts with Ku70 through its Myc box II (MBII) domain and inhibits therefore the DNA-PKcs activity (Li et al., 2012). It is also well established that c-Myc overexpression stimulates CDK2 activity (Rudolph et al., 1996; Pusch et al., 1997). Since CDK2, together with Cyclin A1, are responsible for phosphorylating BRCA2 impeding Rad51 binding, this might imply that Myc does not benefit HR. Likewise, in leukaemia cells, it has been reported that c-Myc overexpression downregulates microRNAs miR-150 and miR-22, two microRNA that inhibit ligase 3 and PARP1 transcription (Muvarak et al., 2015); thus, c-Myc tend to lead to an increase of LIG3 and PARP1 transcription. Furthermore, in cancer cells, c-Myc overexpression restores PARP1 expression by suppressing PAPR1 inhibitor BIN1 (Ganesan et al., 2011; Pyndiah et al., 2011). C-Myc overexpression therefore, has been reported through several lines to lead the repairing machinery towards the error-prone MMEJ repairing mechanism, promoting it rather than the other two more precise methods; contrarily to Cyclin D1 that is essential for conducting homologous recombination, rather than promoting the other two low fidelity repairing methods.

5.3.4 Copy Number Variation (CNV)

Copy Number Variation (CNV) occur when sections of the genome are repeated and the number of repeats in the genome varies between individuals in the human population (McCarroll et al., 2007). Long-term culture positively selects for amplifications but negatively select for deletions (Laurent *et al.*, 2011). This phenomenon can be explained by the strong culture dish selective pressure favouring best adapted cells (Hussein *et al.*,

[7] Ligase 3 (LIG3) acts in Alt-NHEJ and recognises single-stranded blunt ends with homology.

2011), resulting in enrichment of chromosomal trisomies and copy number gains, contributing to genomic variation detected in iPSC (Gore *et al.*, 2011; Ji *et al.*, 2012).

There are three technological platforms for copy number variation detections: array-based technology (including array comparative genomic hybridization (aCGH), as well as many other variants such as oligonucleotide array), SNP genotyping technology (Carter et al., 2007), and next-generation sequencing technology (Chiang et al., 2009). Various algorithms have been proposed for different data in recent years. The primary goal of all such studies is to identify and localize the copy number changes. One important commonality in data from different platforms is the spatial correlation among clones/probes/sequences.

The most recurrent Copy Number Variation (CNV) hotspot is the culture-induced amplification of the gene-rich locus at the long arm 20q11.21, has been estimated to be present in approximately 14.5% of PSC lines in independent experiments (Matins-Taylor *et al*., 2011; Maitra *et al*., 2005; Lefort *et al*., 2008; Spits *et al*., 2008; Wu *et al*., 2008; Werbowetski-Ogilvie *et al*., 2009; Narva *et al*., 2010; Amps *et al*., 2011, Laurent *et al*., 2011; Elliott *et al.*, 2010; Lund *et al.*, 2012). Common subchromosomal duplications in chromosome 20q were found in genes conferring cell growth or survival advantage, such as BCL2L1 (20Q11.21), which enhances ESC survival (Bai *et al.*, 2012) giving a selective advantage by attenuation of apoptosis; or also mir1825, which has over 400 predicted targets, rendering suppression of apoptosis as well or cell growth enhancement.

In order to promote transformation and tumour progression, amplified and rearranged loci must provide a selective survival advantage. For example, amplification of genes involved in DNA synthesis and cell-cycle progression provide a proliferative advantage to cells that harbor it (Kuschak et al., 2002). Therefore, CNV have been reported to be implicated in the growth and progress of many human malignancies, including cancers in breast, prostate and bladder (Feber *et al*., 2004; Holcomb *et al.*, 2009; Hammerman *et al*., 2012). It has been noted that iPSC may have higher numbers of subchromosomal CNV than ESC (Laurent et al., 2011; Martins-Taylor et al., 2011; Hussein et al., 2011), therefore making iPSC more prone to become tumorigenic than ESC. Early-passage iPSC are characterized by a huge incidence of CNV compared with parental fibroblasts. These alterations, especially copy number losses, are usually negatively selected in culture (Hussein et al., 2011).

CNV are not randomly distributed in the human genome, but tend to be clustered in regions of complex genomic architecture, consisting of complex patterns of direct and inverted LCRs (low copy repeats). For instance, CNVs preferentially occur in regions of heterochromatin near telomeres (Shao et al., 2008; Yatsenko et al., 2009) and centromeres (She et al., 2004; Nguyen et al., 2006).

5.3.5 TELOMERE LENGTH IN IPSC

Another source of instability in cells comes from the malfunction of cell chromosomes telomere maintenance. Telomeres consist of (TTAGGG)n palindromic repeats and associated proteins at the end of chromosomes. Mammalian telomeres contain a specific protein complex, shelterin, that functions to protect chromosome ends from all aspects of DNA damage to maintain genomic stability by protecting the chromosomes from

degradation and end-to-end fusion (Blackburn, 2001; Palm et al., 2008). It has been proposed that telomeres are fragile sites and shelterins are essential for preventing telomere breakage associated with replication fork stalling at telomeres (Martínez et al., 2009; Sfeir et al., 2009). Specifically, TRF1 shelterin is required for proper telomere replication preventing fork stalling. TRF1 deletion activates ATR signalling pathway causing fragile phenotype at telomeres and leading to end-to-end fusions and to a high incidence of telomere breakage causing multitelomeric signals (Sfeir et al., 2009).

5.3.5.1 Multitelomeric Signal (MTS)

Multitelomeric signals (MTS) consists on a telomere doublet signal in the chromosome arm (introduction figure 8, B). MTS have been proposed to reflect increased breakage at chromosome termini and subsequent repair by homologous recombination mechanisms (Lydeard et al., 2007). Therefore multitelomeric signals are regarded as a type of genetic instability (Meeker et al., 2004; Muñoz et al., 2005; Blanco et al., 2007; Martinez et al., 2009; Sfeir et al., 2009; Tejera et al., 2010). Cell tumorigenicity is fuelled by the accumulation of cellular damages, however, it remains to be established whether or not MTS are associated to cancer in humans. Furthermore, Sirtuin 1 also contributes to telomere maintenance. Sirtuin 1 null mouse embryonic fibroblasts (Sirt1-/-MEFs) were shown to express a higher number of multitelomeric signals per chromosome (Palacios et al., 2010).

5.3.5.2 Signal-free ends

Signal-free ends are short telomeres that cannot be detected with the specific telomere QFISH staining (introduction figure 8, C). Signal-free ends has been reported to lead to chromosome fusions, constitute telomere dysfunction and limit cellular survival in the absence of telomerase (Hemann et al., 2001).

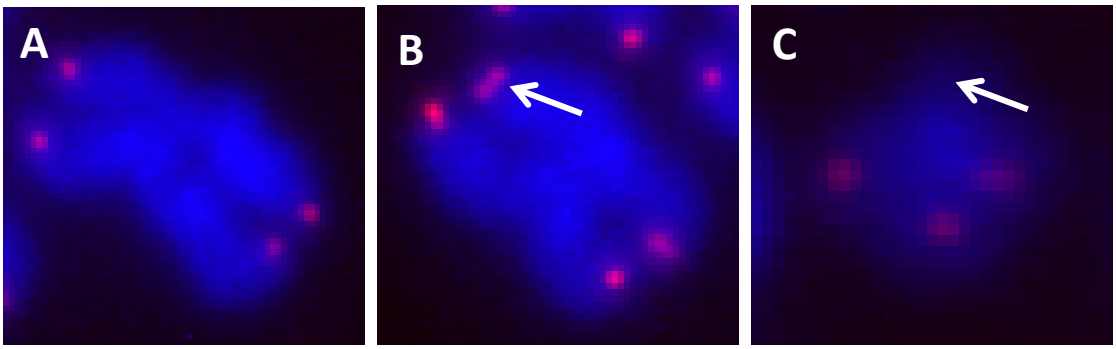

Introduction figure 8. Chromosome telomeres Q-FISH staining. A) Chromosome with normal signal of telomeres. **B)** Chromosome with an arm with multitelomeric signal (white arrow). **C)** Chromosome with an arm with signal free ends (white arrow). Images are examples extracted from the thesis data.

6. IMMUNE SYSTEM

The immune system consists of all the different biological structures and procedures that a host organism has as defense system to protect against disease. The system has to be able to distinguish all sort of different external pathogens, ranging from small viruses to big parasites and differentiate them from the organism's own tissues to function properly. Actually, immune system disorders can result in autoimmune and inflammatory diseases and cancer (O'Byrne et al., 2001). Conversely, pathogens can rapidly evolve to avoid detection and neutralization by the immune system; however, host defense mechanisms have also evolved to recognize and neutralize evolving pathogens.

Simple unicellular organisms like bacteria possess rudimentary immune systems in the form of enzymes to protect against bacteriophage virus infections. Other basic immune mechanisms, including phagocytosis, antimicrobial defensins and the complement system, evolved in ancient eukaryotes and remains nowadays in their descendants, such as in plants and in invertebrates. Jawed vertebrates, comprising humans, have developed even more sophisticated defense mechanisms (Beck et al., 1996), like the ability to adapt over time to recognize pathogens more efficiently and specifically.

This adaptive or acquired immunity generates immunological memory[8] after an initial response to a pathogen, leading to an enhanced response in subsequent encounters with that same pathogen. Therefore, in numerous species, the immune system can be classified into innate and the adaptive immune system (or humoral and cell-mediated immunity).

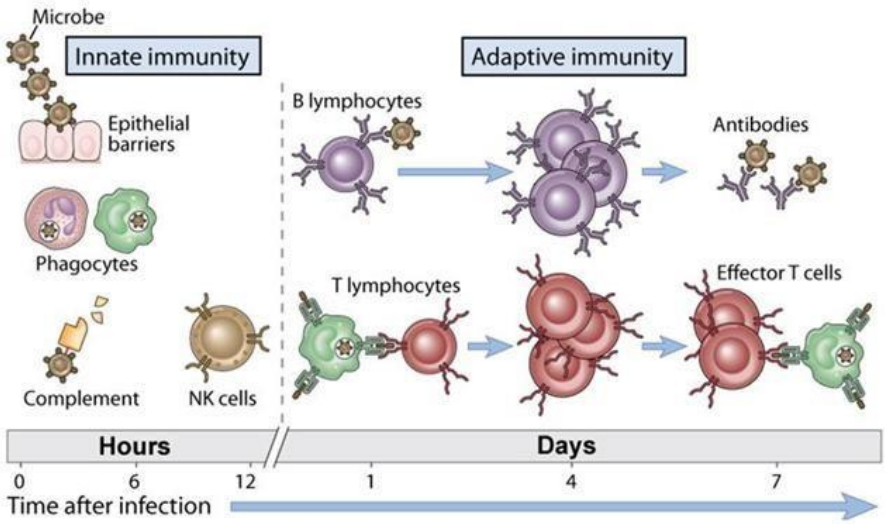

Introduction figure 9. Innate and adaptive immune response. Diagram showing the two types of immune response that the host has against pathogens. Innate immunity is the first barrier that the organism has against pathogens to resist the infection during the first hours. Afterwards, immune cells involved in the adaptive immunity generate a long-term response with antibodies specific for the antigens presented to the B cells. Image from Abbas et al., 2011.

[8] This process of acquired immunity memory is the basis of vaccination.

6.2 INNATE IMMUNE RESPONSE

During the initial phase of an infection, a rapid inflammatory response is generated by the innate immune system that blocks the spreading of the infectious agents. The innate immune system, also known as the non-specific immune system (Grasso et al., 2002), is a generic response that provides immediate defense against infections by other organisms and is an evolutionarily old defense strategy found in all classes of plant and animal life. Indeed, it is the dominant immune system of plants, fungi, insects, and primitive multicellular organisms (Janeway et al., 2001). However, unlike adaptive immune system, the system does not provide to the host long-lasting immunity (Alberts et al. 2002).

The innate immune system receptors are germline-encoded and have been evolutionally selected to recognize pathogen-derived compounds essential for pathogen survival or endogenous cellular molecules released in response to infection (Matzinger, 1994; Yang et al., 2010a; Erridge, 2010).

6.2.1 Toll like receptors (TLRs)

Also known as pattern recognition receptors (PRRs), innate immune receptors are found in the serum, on the cell surface, in endosomes, and in the cytoplasm (Medzhitov, 2007). The Toll-like receptors (TLRs) represent a particularly important group of PRRs (Gay et al., 2007), which trigger innate immune responses after recognition of a wide variety of pathogen-derived compounds. TLRs are expressed on the membranes of dendritic cells, macrophages, natural killer cells, T and B lymphocytes and also in non-immune cells such as epithelial cells, endothelial cells, fibroblasts and neurons (Delneste et al., 2007; Lafon et al., 2006).

In human cells, ten TLRs respond to a range of Pathogen-Associated Molecular Patterns (PAMPs), including lipopolysaccharide (TLR4), lipopeptides (TLR2 associated with TLR1 or TLR6), bacterial flagellin (TLR5), viral dsRNA (TLR3), viral or bacterial ssRNA (TLRs 7 and 8) and CpG-rich unmethylated DNA (TLR9), among others (Kumar et al., 2009). All these TLRs, recently reviewed (Botos et al., 2011), are located on cell surfaces or within endosomes and have important roles in the protection against pathogenic organisms all over the animal kingdom.

Despite the wide variety of ligands recognized by TLRs, a common structural framework is shared in their ligand-binding extracellular receptor domains (or ectodomains, ECD). All these ECDs adopt horseshoe-shaped structures and are built from tandem copies of leucine-rich repeat (LRR) motifs, which are the building blocks of TLRs. ECDs are typically 22–29 residues in length and contain hydrophobic residues spaced at distinctive intervals. Interestingly, LRR motifs are found in many proteins in animals, plants and microorganisms (Palsson-McDermott et al., 2007).

Classically, after ligand binding, two extracellular domains dimerize forming an "m"-shaped structure, docking the ligand molecule in the middle of two TLR molecules. This ligand-induced dimerization brings the transmembrane and cytoplasmic domains in close proximity and triggers a downstream signalling cascade.

Specifically TLR3 has been studied in this thesis, since it was found differently expressed between iPSC derived cells and their original cell type.

6.2.1.1 Toll-like receptor 3 (TLR3)

TLR3 recognizes dsRNA, produced by most viruses at some stage in their lifecycles, being a potent indicator of viral infection. TLR3 is located inside endosomes, contrarily to other cytoplasmic dsRNA receptors. Cells normally have short chains of dsRNA (25 bp or less), such as in miRNA and tRNA hairpins. This is the reason why TLR3 dimers cannot bind dsRNA of less than 40 bp, providing an essential mechanism for preventing self-reactive responses against the cell's own dsRNA.

Homodimerization of TLR3 is essentially required for ligand binding (wang et al., 2010), and an intact binding site is required for dsRNA binding and stable dimerization to activate the downstream signalling cascade. TLR3 ectodomains, which are made by 23 LRR, bind as dimers to 45 bp segments of dsRNA, the minimum length required for TLR3 binding and activation (Wang et al., 2010). Furthermore, binding is independent of base sequence and occurs only at pH 6.5 and below (Leonard et al., 2008). It has been identified the essential interacting residues in the complex. The dsRNA interacts at two sites on each TLR3-ECD, one near the N-terminus (comprising LRR-NT and LRRs 1–3), and one near the C-terminus (comprising LRRs 19–23) (Liu et al., 2008). Mutational analyses (Wang et al., 2010) have established that these three sites individually interact weakly with their binding partners but together form a high affinity receptor-ligand complex. Simultaneous interaction of all three sites at the same time is therefore required for stable and functional binging of TLR3/dsRNA. In addition, the two ECDs interact with each other at their LRR-CT motifs.

In the cell, two TLR3 ECDs interacting on the luminal side of an endosome bring the two TIR domains together on the cytoplasmic side, forming a dimeric scaffold on which adaptor molecules could bind and initiate a signalling cascade. When TLR3 dimerizes, it is recruited TICAM1 for the production of pro-inflammatory cytokines (Brikos et al., 2008). TICAM recruits poly-ubiquitinated RIP1, which interacts with TRAF6/TAK1 complex and leads to activation of NF-κB and induction of pro-inflammatory cytokines.

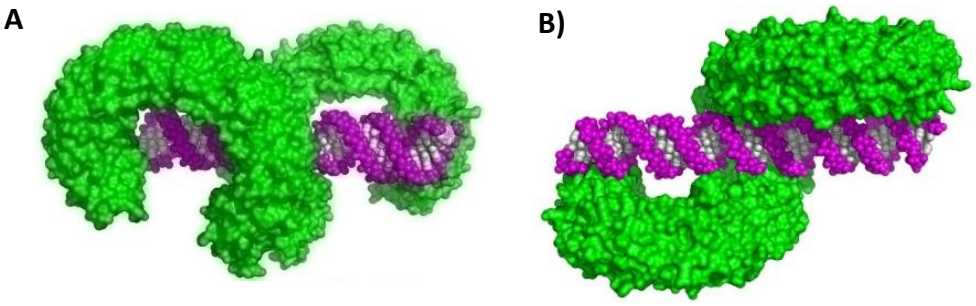

Introduction figure 10. Structure of the TLR3 dimer/dsRNA complex. A) Molecular surface of TLR3 dimer (green) with bound dsRNA. The interaction of the C-terminal capping motifs stabilizes the TLR3 dimer. **B)** Top view. Figure from Botos et al., 2011.

6.2 ADAPTIVE IMMUNE RESPONSE

In vertebrates, the initial innate immune response is followed by an adaptive immune response, in which highly specific B and T cell receptors recognize the pathogen antigens and generate antibodies against them leading to pathogen elimination (Janeway, Jr. et al., 2002). The adaptive immune system, also known as acquired immune system, is composed of highly specialized, systemic cells and processes that eliminate pathogens or prevent their growth.

Adaptive immunity provides long-lasting protection, since it creates immunological memory after an initial response to a specific pathogen, and leads to an enhanced response to subsequent encounters with that particular pathogen in a highly specific manner to destroy attacking pathogens and toxic molecules produced by them. If the system is unable to discriminate harmful from harmless foreign molecules; the effects of this may be fever, asthma or allergy.

The cells that carry out the adaptive immune response are white blood cells known as lymphocytes, classified in two different classes: B cells and T cells, for antibody responses and cell mediated immune response. B cells are activated to secrete antibodies, immunoglobulin proteins that travel through the bloodstream and bind to the foreign antigen to inactivate it, preventing the antigen to bind to the host (Alberts et al., 2002). T cells are distinguished from B cells and NK cells by the presence of a T cell receptor on the cell surface and can be classified into helper and cytotoxic T cells (Alberts et al., 2002). While in innate immunity pathogen recognition receptors are already encoded in the germline, in adaptive immunity antigen receptors consist of many structurally similar molecules with millions of different specific binding combinations created by rearrangements and mutations within the binding site regions of the variable domains of the B and T cell receptor (Jung et al., 2004; Schatz et al., 2005). Therefore, adaptive immune receptors are acquired during the lifetime of the organism.

6.2.1 Cytotoxic T lymphocytes (CTL)

Cytotoxic T lymphocytes (CTLs), also known as killer T cells, CD8+ T cells or cytolytic cells, are a type of white cells that kill infected cells, cancer cells or cells damaged in other ways. Most CTLs express T cell receptors (TCR) that recognize specific antigens, often from virus or cancer cells.

Pathogen antigens bind to class I major histocompatibility complex (MHC-I) molecules and are brought to the surface of the cell, where they can be recognized by the T cells. When the TCR is specific for an antigen, it binds to the complex of the class I MHC molecule and the antigen, the CD8+ CTL becomes activated and destroys it. CD8 and the MHC molecules high affinity binding keeps the CTL and the target cell bound closely together during antigen-specific activation.

6.3 IPSC IMMUNE RESPONSE

One of the main advantages of iPSC technology for clinical application has been thought to be the potential of autologous cell therapies to remove immune rejection eliminating the need for immune suppression drugs and their associated side effects. Then, iPSC derived from patient cells that are differentiated into a specific cell type are unlikely to provoke an immune response in the same individual, making immunosuppression therapy dispensable. However, taking into account the prevalence of naturally happening autoimmune diseases such as diabetes type I, multiple sclerosis or systemic lupus erythematosus, the idea of an immune alteration or reactivity of patient's own cells is not rare to contemplate, signifying that immunogenic privilege of autologous cells could have been underestimated.

6.3.1 Allogeneic iPSC immune alterations

Regarding rejection of transplanted allogeneic cells and organs, the main immune response involves the major histocompatibility complex-I (MHC-I), expressed on every nucleated cell in the body, whose function is to display foreign antigens to T cells. Humans have three main MHC class I genes, known as HLA-A, HLA-B and HLA-C. Proteins encoded from these genes are present on the surface of nearly all cells. On the surface, these proteins are bound and present protein fragments (peptides) exported from within the cell. Then, these peptides are displayed to the immune system by the MHC1 proteins. If the immune system recognizes the peptides as foreign, like viral or bacterial peptides, it responds by prompting the infected cell to self-destruct. Pick et al. already showed that during reprogramming, iPSC downregulated expression of human leukocyte antigen (HLA)-A/B/C and β2 microglobulin (β2M) (Pick *et al.*, 2012), the two components of MHC-I. Their results showed very low expression levels of MHC class I (MHC-I) proteins on the surface of hESC. During differentiation of ESC, MHC-I levels increased back, resulting in an increase in immunogenicity, through increasing expression of HLA (Boyd *et al*., 2010; Bonde *et al.*, 2008; Robertson *et al*., 2007; Drukker *et al*., 2002).

6.3.2 Syngeneic Models

Professor Fairchild was one of the former scientists who expressed concerns about potential immunogenicity of iPSCs derivatives in syngeneic models (Fairchild et al., 2010). Indeed, work by Zhao et al. in 2011 demonstrated that when injecting retrovirally reprogrammed iPSCs in syngeneic recipients, it was induced a T-cell-dependent immune response potent enough to almost completely prevent the formation of teratomas in mice (Zhao *et al*., 2011). This rejection was not observed after injection of syngeneic mouse embryonic stem cells (ESC). Interestingly, Episomal vectors reprogrammed iPSCs were capable of forming teratomas. However, authors also showed $CD4^+$ T cell infiltration in those teratomas produced with the non-integrative reprogramming method, with apparent necrosis within parts of the tumour, suggesting that the reprogramming process itself may impact on the potential immunogenicity of reprogrammed cells. Authors revealed as well that Zg16 and Hormad1 genes overexpression in iPSCs was directly contributing to the immunogenicity of iPSC derivatives (Zhao *et al.*, 2011).

In 2013 it was found that the injection of mouse iPSCs into syngeneic C57BL/6 mice produced teratomas and was not rejected (Thanasegaran et al., 2013). Likewise, iPSC derived cells were not rejected after syngeneic transplantation (Ghua *et al*., 2013). Also Araki R. et al. compared the immunogenicity of differentiated skin and bone marrow tissue derived from integration-free mouse iPSC generated by episomal vectors and ESC-derived tissue, and did not observe any differences between the two groups (Araki *et al*., 2013). However, cardiomyocytes derived from these same iPSCs were highly immunogenic.

In the same line, in another research using non-human primates, Morizane et al. found that autologous transplantation of the iPSC-derived cells generated a minimal immune response compared with allografts both in the nonhuman primate brains in the absence of immunosuppression (Morizane *et al*., 2013). They suggested thus that immunosuppression is not necessary for autologous transplantation of iPSC-derived neural cells into brain.

Liu et al. made a new turn on the topic when reported that human iPSCs derived neural progenitor cells (NPC) were more immunogenic when iPSCs came from skin fibroblasts (SF) than when iPSCs came from umbilical cord mesenchymal stem cells (UMCs) (Liu *et al.,* 2013), suggesting that low immunogenicity due to the lower cell commitment of UMCs could be retained after cell reprogramming and further differentiation. NPCs differentiated from UMC-iPSC retained low immunogenicity as the parental UMCs, because SFs as a more committed cell, generally carry a higher number of instabilities than UCMs and thus are more likely to become more immunogenic as reported.

Taken together all these publications seem to suggest that some but not all iPSCs derived cells could become immunogenic at different extents. Thus, estimating immunogenicity of iPSCs derived cells appears to be of great relevance in the field. Furthermore, it is possible that genetic and epigenetic alterations during reprogramming can somehow contribute to the immunogenicity of iPSCs derivatives. It is still an open question to know which kind of tissues differentiated from iPSC can be immunogenic, idea firstly proposed by Dr. Xu (Zhao *et al*., 2011), and reviewed recently (Cao *et al*., 2014).

Whether genetic alterations in pluripotent cells are meant to be immunogenic or not for transplantation potential is to be determined yet. It is likely that most iPSCs genomic aberrations acquired during reprogramming are going to be harmless and only a few types of abnormalities are actually hazardous. Thus it appears to be of great relevance to estimate the immunogenicity of clinical valuable cells, as well as the tissue specific propensity to become immunogenic in relationship with the number and type of cumulated defects.

In this thesis we wanted to compare an F1 population of original patient cells with their corresponding iPSC derived cells (F2), comprising iPSC derived fibroblasts, neural stem cells, cardiomyocytes and endoderm cells. We aim to compare F2 derived from iPSCs reprogrammed with 3 different methods: retroviral transduction, Episomal vectors and mRNA transfections.

OBJECTIVES AND HYPOTHESISE

Even though cell reprogramming is an established technique for production of induced pluripotent stem cells (iPSC), several challenges still need to be addressed before clinical application.

- The first objective is the replacement of the oncogene c-Myc by the cell cycle gene Cyclin D1 in the reprogramming cocktail, as a way to promote DNA repair through homologous recombination during the reprogramming process in order to reduce genetic instability and avoid the threat of cancer in iPSC.

- We hypothesise that 3F+Cyclin D1 made iPSC will have reduced genetic instability due to Cyclin D1 involvement in DNA repair mechanisms and the fact that it is not involved in as much pleiotropic and tumorigenic effects as c-Myc.

- The second objective is to characterise and identify alterations in the immune response of iPSC derived cells, by comparing with the original non-reprogrammed cells.

- We hypothesise that iPSC derived from patient cells that are differentiated into a specific cell type are unlikely to provoke an immune response in the same individual.

MATERIALS AND METHODS

Cell culture

Mouse C2C12 cells were obtained from ATCC (CRL-1772). Mouse Embryonic Fibroblasts were obtained from embryos of pregnant mice Wild Black6, C57 strain, at day 12.5 post coitum (extraction protocol approved by the university of Barcelona ethics committee). Human foreskin fibroblasts were obtained from ATCC (SCRC-1041). All three lines were cultured in DMEM (Gibco # 21969-035) supplemented with glutamate 1% (GlutaMAX 200mM, Gibco # 35050-038), penicillin-streptomycin 1% (10.000 U/ml) and Fetal Bovine Serum 10% (Gibco # 10270-106). In order to arrest MEFs to prepare feeder layer, cells were treated with Mytomicin C during 4h or irradiated with gamma irradiation. Mouse iPSC mESC (W4 and G4 mESC clones) were maintained on irradiated mouse embryonic fibroblasts (irMEFs) in G4 medium: knockout (KO)-DMEM (Gibco # 10829-018) supplemented with glutamate 1%, penicillin-streptomycin 1%, Fetal Bovine Serum 15%, non-essential aminoacids 1% (NEM-NEAA 100x Gibco), sodium pyruvate 1% (Gibco # 11360), 2-mercaptoethanol 0.2%, the cytokine *leukemia inhibitori factor* (LIF) 0,02% (Chemicon # ES61107, 1.000 U/ml) and 2mM valproic acid (Sigma-aldrich, 1069-66-5). Retrovirally made hiPSC were maintained on irradiated human foreskin fibroblasts (irHFFs) in hES medium consisting of knockout (KO)-DMEM, 1mM pen/strep, 1 mM Gluta-MAX, 1X nonessential amino acids (NEAA), 55 μM β-mercaptoethanol (β-ME) (Gibco, Carlsbad, CA), 10% Knockout (KO) serum replacement (Invitrogen, Carlsbad, CA), and 10 ng/ml FGF2 (R&D Systems Inc., Minneapolis, MN). For maintenance of undifferentiated colonies, differentiated cells were manually removed and undifferentiated cells were passaged once a week. Feeder-free clinical grade mRNA iPSC were cultured in Flex E8 culture medium (Life Technologies, A2858501) on Vitronectin (Life Technologies, A14700) coated plates. Essential 8 medium components: DMEM F-12, L-ascorbic acid, Selenium, Transferrin, $NaHCO_3$, Insulin, FGF2 and TGFβ1.

Six human skin fibroblast cell lines and their iPSC that have been previously published were analysed in this study. IPSC were then differentiated to fibroblasts by plating embryoid bodies on gelatine coated plates using DMEM/10% FBS for three to six weeks. Permissions to use the published iPSC lines were granted under normal guidelines from the authors of the relevant publications. Ethics and permission to obtain human fibroblasts and iPSC was obtained from the relevant institutes of the published articles.

Generation of human and mouse iPSC by viral infection

For human fibroblasts or mouse C2C12 reprogramming experiments, about 50,000 or 100,000 cells were seeded per well of a 6-well plate and infected with retroviral supernatants of a polycistronic retroviral vector containing *Oct4*, *Sox2*, *Klf4* and GFP as a reporter gene (pPMXS-OSKG). Then, either pMSCV - c-Myc or p-Babe puro Cyclin D1 was also used to infect for 3F+c-Myc or 3F+Cyclin D1 respectively. Retroviruses for the different factors were produced. Phoenix ecotropic packaging cell line was used to produce supernatant with virus to infect mouse cells, and phoenix amphotropic for human cells, using Polyethylenimine as transfection reagent according to the manufacturer's instructions. After 24 h, DMEM medium was replaced, cells were incubated at 32°C, and viral supernatant was harvested after 24 and 48 h. Infection consisted of a 45-min supernatant spinfection at 750 g in the presence of 1 mg/mL polybrene. Three rounds of infections on consecutive days were performed. Two days after beginning the last round of infection, cells were trypsinized and seeded onto feeder layers of irradiated MEFs or HFFs depending on whether cells were mouse or human. The medium was changed upon platting to G4 with LIF for mouse iPSC or hES with

FGF2 for human iPSC. Cultures were maintained at 37°C, 5% CO_2, changing medium every other day.

Synthetic mRNA reprogramming to iPSC

Clinical grade reprogramming method was done using Stemgent's microRNA-enhanced mRNA reprogramming kit (STEMGENT, #00-0071) protocol. Messenger RNA used for transfections are included in Stemgent kit, minus Cyclin D1 mRNA, that was used to replace c-Myc and was synthetized by in vitro transcription (IVT) using the MEGAscript Kit (Ambion, Ref#AM1334). DNA template for the mRNA IVT for Cyclin D1 was made by cloning Cyclin D1 ORF between the 3' and 5' untranslated regions (UTRs) of alpha-globin by splint ligation to increase the stability and translation efficiency of the transcript. Using Cyclin D1 template proceed to synthesize the messenger RNA by IVT. Cyclin D1 mRNA was functionally tested by counting the % EdU positive cells after 24h in low serum and transfecting HFFs with different amounts of mRNA (Supplementary figure 2, E). RNase and DNase free tubes and tips were used, and it was eliminated RNases in gloves and working surface with RNaseZap (Sigma, #R2020). For the cells transfection, briefly, HFFs were seeded on vitronectin-coated 24MW plate wells at six different densities: 7.5k, 10k, 12.5k, 15k, 17.5k and 20k. The next day, three densities with 50-70% confluency were selected. Transfections were done in cells cultured in Pluriton medium (Stemgent Ref#00-0070), adding 300ng B18R/ml to inhibit immune response to transfected material. Pluriton medium was conditioned 24h before on irHFFs the day before adding it to the target HFFs to be transfected. MicroRNA and mRNAs were transfected as indicated by the manufacturer's protocol (STEMGENT, #00-0071) using stemgent's transfection reagent. Messenger RNA cocktail is transfected at a proportion of 3:1:1:1 of the reprogramming genes: Oct4, Sox2, Klf4, Lin28 and c-Myc or Cyclin D1 (OSKLM or OSKLD). It was transfected 200ng of mRNA per well of a 24MW plate. MicroRNA to enhance reprogramming efficiency is transfected at day 0 and 4, and mRNA from day 1 to 12. At day 14-15 colonies were picked by mechanically scrapping them and were transferred to Vitronectin coated plates in Conditioned Pluriton mixed 1:1 with E8 medium. Rho kinase inhibitor (ROCKi, Y-27632, STEMCELL #72302) was added at 10μM final concentration during the first 24h after colony picking to prevent cell apoptosis. Medium was change to E8 (not feeder conditioned and with no Pluriton) 24h later and refreshed daily. Colonies were passaged by gentle dissociation with 0.5mM EDTA when they are 75-80% confluence.

In vitro differentiation

To differentiate mouse iPSC to cardiomyocytes, EBs were seed on gelatin and cultured in DMEM medium with 10% FCS and 100mM of Ascorbic Acid changed every second day for 2 weeks, until beating started. To differentiate mouse iPSC to fibroblast-like cells, EBs on gelatin and DMEM medium with 10% FCS changed every second day for 3-6 weeks.

Mouse and human iPSC general differentiation was carried out by plating embryoid body (EBs) on gelatin and the DMEM medium, with 20% FCS changed every second day for 2–3 weeks. Human iPSC in vitro guided differentiation toward endoderm, mesoderm, and ectoderm was done using PSC Neural Induction Medium kit (A1647801) for Neural Stem Cells coating the plates with Geltrex (Life Technologies, A1413201). Cardiomyocytes (CM) differentiation was done using PSC Cardiomyocyte Differentiation kit (A2921201) and CM were kept in culture until beating was stable. Definitive endoderm was differentiated from iPSC using PSC Definitive Endoderm

(DE) Induction kit (A27654SA). Motor Neurons were differentiated from Neural Stem Cells using the motor neuron induction medium: hES media supplemented with Sonic hedgehog 200ng/ml, 50 μM Retinoic Acid, 8ng/ml FGF2, 10ng/ml Activin A during 50 days. As an internal control for all the differentiation protocols, we differentiated in parallel a commercial Episomal made iPSC (Life Technologies, A18945).

Teratoma formation

Animal experiments were approved by the University of Barcelona ethics committee. Two million cells were subcutaneously injected at the flank of athymic FoxN1 nu/nu mice (ENVIGO). After 3-4 months teratomas were extirpated and fixed in paraformaldehyde 4% O/N. Next day teratomas were embedded in paraffin and sections were analyzed for Hematoxilin-Eosin staining to recognize germ layer structures and for KI-67 to assess the in vio tumorigenic potential of injected iPSC.

Immunofluorescence, immunocytochemistry and flow cytometry

Cells were grown on plastic cover slide chambers and fixed with 4% paraformaldehyde (PFA). After fixation and washing, cells were blocked with PBS containing 6% donkey serum, and 0.5% Triton X-100 for 30 min. Cells were then stained for appropriate markers described in the figures. Pluripotency markers: anti-Oct4 (Santa Cruz, sc-5279, 1:60), anti-Sox2 (CalBiochem, sc1002, 1:100) anti-SSEA3 (Abcam MC631, ab16286, 1:10), anti-SSEA4 (Biolegend, MC-813-70, 1:50) and anti-Tra-1-81 (Merck, MAB4381, 1:200). For generally differentiated cells cells it was performed an IF for endoderm marker anti-AFP (Dako, A0008, 1:400), mesoderm marker anti-αSMA (Sigma, A5228-100) and ectoderm marker anti-Tuj1 (Biolegend, MMS-435P-100, 1:500). Primary antibodies for guided differentiation into Cardiomyocyte markers: anti-Cardiac troponin T (Abcam, ab10214, 1:400) and anti-Gata4 (Santa Cruz, sc-9053, 1:200); Neuronal markers: anti-Nestin (Biolegend, 841801, 1:200), anti-MAP2 (R&D systems, MAB8304, 1:250); Motor Neurons markers: anti-OLIG2 (R&D systems, AF2418), HB9 (Hybridoma bank, 81.5c10-s, 1:100); endoderm cells were analyzed with anti-hCXCR4 PE conjugated (FAB173P); astrocyte markers: anti-S-100 (Dako, Z0311, 1:100), anti GFAP (Dako, Z0334, 1:200). Secondary antibodies used were all the Alexa Fluor Series from Invitrogen (diluted 1:200). Images were taken using a Leica SP5 confocal microscope. During confocal microscopic observation, all the images were taken using the same settings. It was performed a tile scan image gathering with an AF6000 Epifluorescence microscope for SCI spinal cord IF. TLR3, anti-human CD283 (TLR3)-PE conjugated, (eBioscience, 12-9039-80) at a 1:100 dilution. All flow cytometry analysis was performed on a FACS Canto II machine.

H2AX Double strand breaks (DSB) and Rad51immunofluorescence staining

Methanol:acetic fixed cells were stained for anti-gamma H2AX (Ser139) antibody (Novus, NB100-78356-0.025, 1:500) to determine the % of DNA double strand breaks (DSBs) and Rad51, NB100-148, Bionova, 1:300. Cells were blocked in PBS, 2% Donkey serum, 0.05%Triton-X100. Primary antibody was incubated o/n at 4ºC. Secondary antibody, goat anti-mouse A568 (A11031), was incubated 1:1000 for 2h at 37ºC. Quantification was performed using ImageJ by counting γH2AX and Rad51 positive foci in 200 nuclei per experiment. To stain the cell membrane, cells were incubated with WGA (wheat germ agglutinin A594, Thermo Fisher #W11262), 1:500 in PBS during 10min at 37ºC after fixation with PFA 4% before permeabilizing.

Alkaline phosphatase staining
Pluripotent stem cells present high levels of alkaline phosphatase enzyme. Alkaline Phosphatase Blue Membrane Substrate Solution (AB0300-1KT) was used to detect iPSC AP expression levels as a standard assay.

Western Blot
Protein extracts of cells collected by centrifugation, washed twice in PBS, lysed in 1x lysis buffer (50 nM Tris-HCl, 70 mM 2 mercaptoethanol, and 1% sodium dodecylsulfate (SDS) and the concentration of total protein was measured.. Lysates were then boiled for 5 min, and subjected to 12% polyacrylamide SDS gels or 4-12% SDS resolving gels (Invitogen). After electrophoresis, proteins were transferred to a nitrocellulose membrane using a submerged transfer apparatus (BioRad), filled with 25mM Tris Base, 200 mM glycine, and 20% methanol. After blocking with 5% non-fat dried milk in TBS-T (50 mM Tris- HCl (pH 8.0), 150mM NaCl, and 0,1% Tween 20) the membrane was incubated with the primary antibodies diluted in TBS-T and washed extensively. The membrane was washed 3 times with TBS-T and then incubated with the appropriate horseradish peroxidase linked secondary antibody (Amersham). The detection was performed with the Western Breeze Immunodetection Kit (Invitrogen). Membranes were blotted overnight at 4°C with anti-Oct4 (Santa Cruz Biotechnology, Inc, sc-5279, 1:100) and anti-Cyclin D1 (Santa Cruz, sc753, 1:500).

Kariotype analysis
In order to see chromosome G bands, methanol:acetic acid (3:1) fixed cells were stained with Wright: Sorensen buffer (1:3). Chromosomes were analysed and classified using Ikaros software.

Electrophysiology
It was determined the electrophysiology of sodium and potassium currents of iPSC derived Motor Neurons using the patch-clamp voltage recording method. In several cells, Na currents could be inhibited by tetrodotoxin (TTX). Motor neuron firing action potentials were also recorded.

Telomere length and cytogenetic analysis using telomere Q-FISH on metaphases
Cells were incubated with 0.1 μg/mL colcemide (Gibco) for 4 h at 37°C, , swollen in hypotonic buffer (Sodium citrate 0.03M) for 25-45min and then fixed in methanol:acetic acid (3:1). Cells were concentrated and 30ul were dropped onto slides falling from 10cm high. After washing, metaphase spreads were fixed in 4% formaldehyde in PBS, and FISH was performed as described previously (Samper *et al*., 2000; Tarsounas *et al*., 2003), using a telomere probe (Panagene, Cy3-TEL). For analysis of chromosomal aberrations, metaphases were analyzed by superimposing the telomere image on the DAPI image using TFL-telo software.

Single Nucleotide Polymorphism (SNP), Copy number variation (CNV) and Methylome array
Single nucleotide polymorphism and copy number variation was analyzed with Infinium Omni5.0-8 v1.3 Kit (20001112). Total 1ug DNA was hybridized to the bead chips o/n following manufacturer's instructions. Methylome analysis was performed using Infinium MethylationEPIC kit (WG-317-1001), which targets >830k methylated CpGs in promoter, gene body, and enhancer regions for genome wide methylation studies.

Real Time PCR
Total mRNA was isolated using Ambion RNA purification columns kit (#12183018), and 500ng was used to synthesize cDNA using the SensiFAST cDNA synthesis kit (Bioline, BIO65053). One µL of the reaction was used to quantify gene expression by quantitative PCR as previously described (Aasen *et al*., 2008). Primers sequences are listed in supplementary table 1. Relative quantification was determined according to the $\Delta\Delta C_T$ method.

NSC injection into rat spinal cord
Neural Stem Cells (NSC), 2·10^6, suspended in 10µl, were injected in between segments T8-9, using a stereotaxic arm with an attached Hamilton, at two levels: rostral (5µl) and caudal (5µl) separated by 2-3 mm, at a speed of 2µl/min. Right after injecting the cells, a complete transection was practiced in the middle of the two injection sites. After transection, rats were maintained alive until two months. After this time, rats were perfused and spinal cords were extirpated and embedded in sucrose for 6 days. In order to cut the tissue with a cryostat microtome, spinal cords were embedded in OCT and froze at -80ºC. Cords were entirely cut longitudinally in 10µm thick slices. Longitudinal cuts were stained by immunofluorescence for Tuj1 and GFAP to detect neurons and astrocytes respectively. All experiments performed were approved by the ethics committee responsible of the animal house facility.

MN injection into spinal cord in an SMA mouse model
Neural Stem Cells were differentiated into Motor Neurons (MN) to test engraftment and survival in a Spinal Muscle Atrophy (SMA) mouse model (Smn(2B/-)). MNs were injected in 15-17 days old SMA mice (n=7). Isoflurane was used to anesthetize. 40.000 MN Vybrant CFDA-tagged (green tracker) resuspended in 2ul of MN medium were injected with a Hamilton into the spinal cord at segment L1 to innervate L4-L5. Sham control SMA mice (n=6) were injected with MN medium.

Proteomic analysis for Global analysis
Protein solubilisation was performed with 1% sodium dodecyl sulfate (SDS) lysis buffer, and samples were quantified using BCA Reagent (Thermo Scientific) following the manufacturer's instructions. For global analysis, 50mg of proteins from each sample were digested and labelled with tandem mass tag (TMT 10-plex) isotopic label reagent set (Thermo Scientific, Rockford, IL, USA) following the manufacturer's instructions. Labelled peptides were separated by means of nanoliquid chromatography using a nanoLC ULTRA AS2 (Eksigent). For identification of TMT labelled peptides, higher energy collisional dissociation (HCD) with 40% fixed collision energy (CE) was the fragmentation method used. Data was processed using Proteome Discoverer 1.4.1.14 (Thermo Fisher Scientific). For database searching, raw mass spectrometry files were submitted to the in-house Homo sapiens UniProtKB/Swiss-Prot database using SEQUEST (Thermo FisherScientific). The method used for HLA typing was PCR-sequence specific oligonucleotide reverse (PCR-SSO) using bead arrays on a Luminex platform.

LPS and Poly(I:C) stimulation and IL6 detection
F2 cells were seeded in 24-w plate and once 80% confluent they were stimulated o/n with 100ng/ml lipopolysaccharides (LPS) and 1ug/ml Poly(I:C) to stimulate an innate immune response. The next day, supernatants were collected and analysed with an ilumina cytokine kit for IL6.

Illuminex cytokine detection array

Cytokine production determination was assessed by Luminex (Millipore, Billerica, MA, USA) at 48h culture point following the manufacturer's instructions. Briefly, supernatants were incubated for 2h with corresponding anticytokine magnetic beads, and then washed with 1x washing buffer and stained with detection antibodies (provided) for 1h. Strepatividin-PE was then added for 30 more minutes. During all incubation steps the plate was agitated at 650rpm. After washing, plate was agitated for 15 minutes at 650rpm and read in the xMAP Luminex reader (Waltham, MA, USA).

Lentiviral production

TLR3 Lentiviral Vector (human) (pLenti-GIII-UbC) (Abcam, LV335740) was used to overexpress TLR3 full length. Viral particles were produced with a 293T packaging cell line. NSC were infected once with viral supernatants. At day 3 after transduction with viral particles, infected NSC were selected with puromycin during 7 days to isolate transduced cells. Then overexpression of the transgene was checked by RT-PCR and FACS.

Apoptosis assay and CTL degranulation detection

All animal experiments were approved by the University of Barcelona ethics committee. Cells were in vivo injected isogenically into C3H mice. Four iPSC clones and four iPSC derived cardiomyocytes clones were injected in duplicate into the testis of mice. One week after injection, cells were reinjected again for boosting the priming of the Cytotoxic T lymphocytes (CTLs) against injected cells. One week after reinjection (final priming period of 14 days), CTLs were collected with an isolation by FICOLL gradient from mice smashed spleens. For T cell kill assay, CTLs were added on top of the cardiomyocyte line that was injected in the mouse from where the CTLs were isolated. Co-culture assay lasted 4h. CTLs degranulation in response to cytotoxic activation was determined by CD107a staining (Biolegend, FITC anti-mouse CD107a, #121605) and apoptosis of target cardiomyocytes was assessed by an Annexin V-FITC staining (Apoptosis detection kit, Biotools, Cat #B32115). CD107a antibody must be in the medium during the coculture because CD107a protein is rapidly endocyted following externalization. After coculture, CTLs were collected by pipetting up and down in the well. Rinse the dish with cold buffer. Check microscopically for any remaining cell, if necessary, rinse the dish again. Once CTLs have been removed, target cells were trypsinized and stained for annexin V. Staining percentage was analyzed by flow cytometry.

Differential Protein Annotation and Bioinformatics Analyses

Proteins identified in different amounts in each of the two experiments were analysed using the bioinformatics tool DAVID v6.7 (Database for Annotation, Visualization and Integrated Discovery; http://david.abcc.ncifcrf.gov/) in order to identify overrepresented biological pathways (*21, 22*). Similarly, differential proteins were analysed for protein-protein interaction networks using the online tool STRING v10 (*23*).

Statistical Analyses

All experiments were repited three times and unpaired two-tailed Student's t-test was calculated to determine significance. To determine differentially expressed quantified proteins between the groups (F1 versus F2) statistical analysis was carried out using SPSS for Windows (version 21.0, Chicago, IL, USA). Comparison between groups (F1 vs F2) was performed using Student's t-test. $p \leq 0.05$ was considered to be significant.

DETAILED PROTOCOLS

Transduction protocol using Phoenix cells

1. Defrost 1 vial ($5x10^6$ cells) of Phoenix (amphotropic or ecotropic to infect human or mouse cells respectively) in a 10cm plate.

2. After 48-72h,wash x2 PBS, tripsinize cells with trypsin 0.5%, count cell number and seed $4,5x10^6$cells/plate.

3. After 24h transfect 10 µg of retroviral vector with 30 µl of Lipofectamine 2000 in a volume of 3ml of Opti-MEM:

   1.5ml OptiM + 30 µl Lipo + 1.5ml OptiM + 10 µg plasmid.
   Mix gently and let 20min at R/T in dark.

4. Add the transfection complex to the Phoenix cells resuspended in 3ml DMEM 10% (no P/S), o/n (16h maximum).

5. 24h later refresh the medium (add 6ml of DMEM) and let plates and incubate @ 32ºC. The same day seed 200.000 target cells/well (6-w) for infecting.

6. Collect supernatant 24h later with a 10ml pipette and filter the virus using a 0.45µm filter on the tip of the pipette. Add another 6ml of DMEM 10% to the Phoenix. Add 1ml polybrene/µl virus.

7. 1st infection (morning): Add 2ml of filtered virus to each well of a 6-w plate. Centrifuge: 45min 700G @ 32ºC. Leave it for 1h in the incubator @ 32ºC then remove the virus containing supernatant and replace it with fresh DMEM 10%.

8. 2nd infection (night): After the day collect virus again and add 7ml of DMEM 10% to the Phoenix (because during the night it evaporates) and infect again with 0.5 µl polybrene/ml virus. Add 2ml of filtered virus to each well of a 6-w plate. Centrifuge: 45min 700G @ 32ºC. Leave it for 1h in the incubator @ 32ºC then remove the virus containing supernatant and replace it with fresh DMEM 10%.

9. 3rd infection (morning): the next day, collect virus and infect cells during the day with 1 µl polybrene/ml virus. Add 2ml of filtered virus to each well of a 6-w plate. Centrifuge: 45min 700G @ 32ºC. Leave it for 1h in the incubator @ 32ºC then remove the virus containing supernatant and replace it with fresh DMEM 10%.

10. 48-72h later, seed cells onto feeder layer (650.000 cells/well) with the corresponding medium (G4 for mouse cells, hES medium for human cells)

Immunofluorescence Protocol

1. Grow cells on coverslips or on chamber slides to about 40-50% confluence. Remove medium and wash with PBS.

2. Carefully aspirate PBS, and fully cover the cells in PFA (paraformaldehyde) 4% during 30' at RT. Aspirate fixative, and wash 3x with PBS for 5min each. Do not let cells dry out.

3. Block samples in blocking buffer (PBS + 6% donkey serum, 1% BSA, and 0,5% triton 100x if the antigen is intracellular). Block for 1h at RT.

4. Wash with PBS, and add primary antibody (1:1000 dilution in blocking buffer with 0,1% triton 100x if the antigen is intracellular). Cover the sample with the required amount (100-200µl). Place the samples in a container with moist paper towels covered in aluminum foil. Place a piece of parafilm over the slide to ensure even coverage, and prevent cells from drying out. Incubate overnight at 4°C.

5. Wash 5' 3x with PBS at RT. Add 200ul secondary antibody and incubate 2h at 37°C.

6. Wash 5' 3x with PBS at RT. Cover the coverslip with DAPI and incubate for 3'. Mount with anti-fade and let dry for 5'. Seal with nail polish, let dry, and store at 4°C.

Flow cytometry immunostaining (FACS) protocol

1. Spin tripsinizated cells in eppendorfs at 1500rpm 5'. Discard St.
2. Wash x1 DPBS. Spin 1500rpm 5'. Discard St.
3. PFA 4% fixation of cells at 4ºC 30' in the dark (200ul/tube).
4. Wash x1 DPBS. Spin 1500rpm 5'. Discard St.
5. Add 250ul/tube of permeabilization buffer (TBS + 1%BSA + 0.5% Triton 100x + 6%Horse serum). Incubate 15' at 4ºC. Spin 1500rpm 5'. Discard St.
6. Add 200ul/tube of dilution buffer (PBS + 6% Horse serum + 1%BSA + 0.1% Triton 100x) + 1ary Ab (1:200). Incubate at 4ºC 30'. Spin 1500rpm 5'. Discard St.
7. Wash x3 with washing buffer (TBS+1%BSA + 0.1% Triton 100x). Spin 1500rpm 5'. Discard St.
8. Add 200ul/tube of dilution buffer + 2ary Ab (1:400). Incubate at 4ºC 30' in the dark. Spin 1500rpm 5'. Discard St.
9. Wash x3 with washing buffer. Spin 1500rpm 5'. Discard St.
10. Resuspend stained cells in 250ul of DPBS.

Quantitative real time PCR (qPCR) protocol

1. Tripsinizate cells. Wash with PBS. Pellets can be stored at -80ºC for as long as 6 months before extracting RNA.

2. Extract RNA with Life Technologies an RNA extraction kit (#12183018A).

3. Quantificate RNA with Nanodrop.

4. Prepare cDNA (Bioline, BIO-65053). Calculate final concentration of 1µg-500 ng of RNA. Dilute sample with water up to 15µl, then add 4µl buffer + 1µl RT.

5. To do the planning of the Real time PCR consider every sample in duplicate or triplicate.

6. Total volume: 15µl: 6µl (1 µl cDNA+5 µl water) + 9µl (7.5 µl SybrGreen (Ecogen, BIO-94005) + 0.75 µl Forward primer 10 µM + 0.75 Reverse primer 10µM).

7. It was used a 7500 Applied Biosystems machine. Lo Rox settings:

   10' 95ºC
   X 40 cycles: 10'' 95ºC
   34'' 60ºC

8. Evaluate results by double delta Ct analysis (2^(-delta delta Ct)).

Western blot protein detection

1. Lysate extraction: Trypsinize the cells and wash them with PBS. Add lysis buffer (50ul/sample) + protease inh (x200) + phosphatase inh (x200).

2. Quantify using Qubit prot. (dilute 1:5 first to take 1ul to quantify). Boil at 100ºC during 10min. Centrifugue at 2000rpm 5min. Work out the ul necessary to load between 40-60ug. Add loading buffer (x4). First add 2-M 10% to the loading buffer.

3. Prepare the precast gel. Remove it from the box, remove the long White stick of the bottom and remove the plastic covering the wells. Put it in the running cage and add MES (x20) diluted in distillated water. Total 400ml (20ml+380ml). Load the samples in the gel.

4. Run the gel at 30mA during the first 10min (corresponding to 42V). Then you can increase up to 100V to finish to run it. Keep an eye on the loading buffer while the samples run. Open the precast gel separating the two plastic walls and sink four sponges, two filter papers and one nitrocellulose membrane in transfer buffer.

5. Stick one filter paper to the gel to transport it to bind the nitrocellulose membrane. Wrap the gel-membrane with the filter papers. On every side put two sponges. The side of the gel goes in the negative side (catode). Run the transference at 20V during 1h (1h to transfer small proteins and 2h for big proteins).

6. Wash the membrane with TBS-Tween and block for 1h in TBS-T 5%milk. Wash x3 TBS-T. Add 1^{ary} ab at the manufacturer's recommended dilution o/n 4ºC rocking. Wash x3 TBS-Tween. Add 2^{ary} ab at the manufacturer's recommended dilution 1h RT rocking. Wash x3 TBS-Tween.

7. Add ECL (1ml A + 1ml B) during 3-5min. Remove the leftover and put the membrane in the revealing cassete.

8. Open the revealing cassete in a dark room and put on top the nitrocellulose revealing radiography. Close the cassete to expose the signal during 2', 5', 10', 20' or 30' depending on the amount of signal visible. After the exposure submerge the radiography in the revelation liquid for 2'. Then wash it in the water container and submerge it in the fixation liquid for 7'. Let the radiography dry and label on top the protein ladder, the date, ab and dilution.

Alkaline Phosphatase staining

1. Remove cell culture media from cells.
2. Wash with cold PBS x1 (3ml per well of a 6-w).
3. Fix with PFA 4% 1'30'' on ice (1ml per well of a 6-w plate), rocking or moving around the plate to ensure good coverage and fixing.
4. Wash with cold PBS x1.
5. AP stain: 1ml reactive A +1ml reactive B (per well of a 6-w). Reagents from Sigma, AB0300-1KT, Alkaline Phosphatase Blue Membrane Substrate Solution.
6. Keep it away from light covering the plate with tin foil.
7. Leave it rocking at RT for 20'-40'. Check every 5'. Do not leave it for more than 1 or 2h maximum.
8. Wash with cold PBS x1. Fix cells again with PFA 4% for 2' at RT after developing the blue color.
9. Wash with cold PBS x1.
10. Count blue positive colonies. 90% blue colonies are considered fully reprogrammed iPSC.
11. Plates can be stored at 4ºC during 4 weeks adding PBS.

Immunohistochemistry (IHC) staining of frozen sections

1. To preserve tissue morphology and retain the antigenicity of the target molecules, fix the tissue by vascular perfusion with 50-70ml of formaldehyde. If it is not possible to fix by perfusion, dissected tissue may be fixed by immersion in a 10% formalin solution for 4 to 8 hours at room temperature. It is commonly accepted that the volume of fixative should be 50 times greater than the size of the immersed tissue. Avoid fixing the tissue for greater than 24 hours since tissue antigens may either be masked or destroyed. All rodent tissues are usually perfused-fixed with the exception of lung, spleen, and embryonic tissue, which are immersion fixed. For cryopreservation of tissues prior to fixation, snap freeze fresh tissue immediately in isopentane mixed with dry ice, and keep at -70°C. Do not allow frozen tissue to thaw before cutting.

2. After tissue has been properly fixed, embed the tissue in sucrose solution over 48h. Embed the tissue completely in OCT compound prior to cryostat sectioning and freeze at -20 to -80 °C.

3. Cut 5-15 µm thick tissue sections using a cryostat (temperature is between -15 and -23 °C). The section will curl if the specimen is too cold. If it is too warm, it will stick to the knife.

4. Thaw-mount the sections onto gelatin-coated histological slides. Slides are pre-coated with gelatin to enhance adhesion of the tissue. Dry the slides for 30 minutes on a slide warmer at 37 °C. Slides containing cryostat sections can be stored at -20 to -70 °C for up to 12 months.

5. Air dry the sections for 30 minutes at room temperature to prevent sections from falling off the slides during antibody incubations. Slides can be stored unfixed for several months at -70 °C. Frozen tissue samples saved for later analysis should be stored intact.

6. When staining cryostat sections stored in a freezer, thaw the slides at room temperature for 10-20 minutes. Then fix for 8 minutes at 2-8 °C for 20 minutes.

7. Rehydrate the slides in wash buffer for 10 minutes. Drain the excess wash buffer. Block non-specific staining between the primary antibodies and the tissue, by incubating in blocking buffer (PBS + 6% donkey serum and 0,5% triton if the antigen is intracellular) for 1h at RT.

8. Add primary antibodies diluted in Incubation Buffer according to manufacturer's instructions. Incubate overnight at 4°C to allow optimal specific

binding of antibodies to tissue targets and reduce non-specific background staining.

9. Wash slides 3 times for fifteen minutes each in wash buffer. Incubate with the secondary antibody diluted in Incubation Buffer according to the manufacturer's instructions for 60 minutes at room temperature. From this step forward samples should be protected from light.

10. Wash slides 3 times for 15'. Add DAPI solution to stain the nucleous, and incubate 2-5 minutes at room temperature. Wash with PBS. Mount with mounting media and visualize using a fluorescence microscope.

Mouse perfusion and fixation (PFA 4%)

1. Fill with 50ml PBS and PFA 4% two syringe pumps and place them in the perfusion pumper machine. Run the liquid first a little bit in case there are air bubbles.

2. Anesthetize the mice with ketamine/xilacine following manufacturer's advices.

3. Fix the mice face-up by pinning hands and feet with thick needles to a foam platform (with holes for dripping down the fluid to a recipient container).

4. Excise the skin on the belly area and open to find the heart, cutting the diaphragm. Cut out the ribs and breastbone to access comfortably the heart (work quickly at this stage since the heart has to be pumping when starting the perfusion).

5. Introduce the needle with the butterfly catheter through the left ventricle. Secure the butterfly catheter with a pin to the foam.

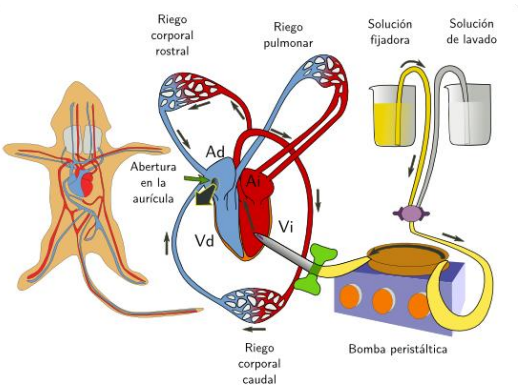

6. Start running PBS a few seconds and observe the heart filling up. Immediately make a cut in the right atrium (a gush of blood should pour out).

7. If PBS is running properly the mice will lift the head and the tail will get erect for a few seconds and drop again. Run the 50 ml of PBS through the mouse (liver should look yellowish and the heart pinkish).

8. Change to perfuse PFA 4% and let run at least 30 ml (tissues should become stiff). Stop the flow and un-pin the mouse. Excise the organs to be studied and immerse in 4% PFA for 48h.

Neural Stem Cells (NSC) induction from iPSC

(protocol based on PSC Neural Induction Kit, #A1647801, Life Technologies).

1. Pre-warm complete PSC Neural Induction Medium (#A1647801) to RT.

2. On day 0 of neural induction (about 24 hours after PSC splitting), PSCs should be at 15–25% confluency. Refresh the media adding 2,5 ml of pre-warmed complete PSC Neural Induction Medium into each well of 6-well plate. Return plates to the 37°C incubator with a humidified atmosphere of 5% CO2.

3. On day 2 of neural induction, morphology of cell colonies should be uniform. Mark all non-neural differentiated colonies, if any, and remove such unwanted colonies with a Pasteur glass pipette or pipette tip. Aspirate the spent medium and add 2,5 ml pre-warmed complete PSC Neural Induction Medium into each well of the 6-well plate. Return the plates into the incubator.

4. On day 4 of neural induction, cells will be reaching confluency. Any non-neural differentiated colonies should be marked and removed. Aspirate the spent medium from each well and replace it with 5 mL of pre-warmed complete PSC Neural Induction Medium per well. Return the plates into the incubator.

5. On day 6 of neural induction, cells should be at near maximal confluence. Remove any non-neural differentiated colonies and add 5 mL of pre-warmed complete PSC Neural Induction Medium into each well. Return the plates into the incubator. If the color of cells turns brownish with many floating cells during day 4 to 7 of neural induction, it indicates that the starting density of PSCs was too high. In this case, change the medium every day with 5 mL of PSC Neural Induction Medium per well.

6. On day 7 of neural induction, NSC (P0) are ready to be harvested and expanded. Cells must be passaged with Rock inhibitor in Geltrex coated plates (A1413201). Then induction medium can be diluted with Advanced DMEM/F12 as a NSC expansion medium.

Pluripotent Stem Cells (PSCs) differentiation into cardiomyocytes

(protocol based on PSC Cardiomyocyte Differentiation Kit, # A25042SA, Life Technologies).

1. Coat a 12-w plate with Geltrex at RT during 1h.

2. On day 0 (day of splitting), PSC should be at 70–85% confluence. Trypsinize iPSC with EDTA 0,5mM. Incubate 2' at 37ºC.

3. Aspirate the EDTA solution and resuspend the cells in an appropriate amount of Essential 8 Medium to obtain a split ratio (typically 1:8 to 1:12) in order to achieve 30–70% confluence within four days.

4. Move the plate in several quick back-and-forth and side-to-side motions to disperse the cells across the surface and place them gently in a 37°C incubator with a humidified atmosphere of 5% CO2. To promote cell survival add ROCK inhibitor (10 μM Y27632) at the time of splitting.

5. On day 1 (about 24 hours after PSC splitting), iPSC should be at 10–30% confluence. Refresh medium and return the plate to incubator. On days 2 and 3, as well refresh cells with Essential 8 Medium.

6. On day 4, the PSC culture should exhibit 30–70% confluence (ideal is 35–60%). Aspirate the spent medium and add 1ml of pre-warmed Cardiomyocyte Differentiation Medium A to each well of the 12-well plate.

7. On day 6, the cells will start to become opaque. Shedding of dead cells is normal. Aspirate the spent medium from each well and replace it with 1 ml of pre-warmed Cardiomyocyte Differentiation Medium B.

8. On day 8, the cells will continue to become more opaque. Aspirate the spent medium from each well and replace it with 1 ml of pre-warmed Cardiomyocyte Maintenance Medium per well.

9. On days 10 and 12, refresh cells with Cardiomyocyte Maintenance Medium. Contracting cardiomyocytes can appear as early as day 10.

10. On day 14, spontaneously contracting syncytium of troponin T cardiac type 2 (cTnT2) positive cardiomyocytes will be present and ready for use in various research applications. Differentiated cells can be further cultured to day 20 for harvesting.

PSC Definitive Endoderm (DE) Induction protocol

(protocol based on PSC Definitive Endoderm Induction Kit, # A3062601, Life Technologies).

1. Day 0: Plate iPSC. Trypsinize with EDTA 0.5mM 2' at 37ºC, previously washed with PBS.

2. Aspirate the EDTA solution and collect the cell clumps in an appropriate amount of Essential 8 Medium to obtain a split ratio clumps at ~1:10 split ratio (from 70% confluent culture) into Vitronectin coated plates. For extremely confluent hPSC cultures (i.e., >90%confluent), it will be necessary to seed clumps at a 1:15–1:30 split ratio as the optimum range for seeding density is 0.01× 106–0.04 × 106cells/cm2. Otherwise, the culture will be over-confluent post-plating and the cells will detach during induction.

3. Move the plates in several quick back-and-forth and side-to-side motions to disperse the cells across the surface and place them in a37°C incubator with a humidified atmosphere of 5% CO2. Add ROCK inhibitor (Y27632, 10 μM) at the time of splitting.

4. Day 1: Begin DE induction: Warm the DE Induction Medium A from life technologies kit (A27654SA) to RT. Shake the bottle several times to ensure even distribution of the components in the medium.

5. Assess the iPSC; if the cells are 15–30% confluent, proceed with induction. If the culture is at a higher confluency, the cells will start detaching.

6. Aspirate spent Essential 8 medium completely from the wells and add pre-warmed DE Induction Medium A. Incubate cells at 37°C for 24 hours.

7. Day 2: Warm the DE Induction Medium B to RT. Shake the bottle several times to ensure even distribution of the components in the medium.

8. Aspirate spent DE Induction Medium A completely from the well and add pre-warmed DE Induction Medium B. Incubate cells at 37°C for 24 hours.

9. Day 3: Characterize induced cells. After 24 hour incubation of cells in DE Induction Medium B, cells will be ready to be assessed for Definitive Endoderm characteristics or be further differentiated to downstream lineages.

Motor neuron (MN) induction

Based on: Jha BS, Rao M, Malik N. Motor neuron differentiation from pluripotent stem cells and other intermediate proliferative precursors that can be discriminated by lineage specific reporters. Stem Cell Rev. 2015 Feb; 11 (1): 194-204. Doi: 10.1007/s12015-014-9541-0.

NSC to MN progenitors:

1. Plate cells on Geltrex coated 6-w plates (1ml/w 1h at 37ºC or o/n at 4ºC). Passage 1:4 a fully confluent well of NSC.

2. When cells are 80% confluent transfer to hES media + SHH 200ng/ml, RA 50µM, FGF2 8ng/ml, Activin A 10ng/ml. Incubate for 2 days.

3. Coat a plate with ornithine-laminine: thaw laminin o/n at 4ºC and always keep it on ice. Dilute ornithine 1:5 in sterile water. Coat 1ml O/w 1h at 37ºC or o/n at 4º. Wash 2x with sterile water. Coat with 20µg/ml laminin 2h at 37ºC or o/n at 4ºC. Wash with PBS x1.

4. Cells should be 100% confluent, then plate 100,000 cells/cm2 (950,000 cells/well of a 6-w) onto Ornithine-laminin coated wells in hES + SHH 200ng/ml, RA 50µM, FGF2 8ng/ml.

5. Change medium every 48h. Every day add fresh RA (1µl of 100nM to 2ml medium). Cells can be frozen from day 10. Keep culturing cells until day 16. Cells at this stage should be OLIG2 positive.

6. Maturation of Motorneuron precursors (MNP): Transfer cells to hES medium + 10ng/ml BDNF and 10ng/ml GDNF. Culture cells for 3 weeks changing medium every 2-3 days. Cells should be HB9 positive.

Q-FISH measurement of telomere length.

Protocol extracted from Dra. María Blasco's laboratory in Centro Nacional de Investigaciones Oncológicas (CNIO).

1. Day 1: Metaphase obtention.

2. Add colcemid (KARYOMAX COLCEMID SOLUTION LIQUID 19ML, #15210-040, Life Technologies, S.A., 35,22 EUR) to the cells in culture (10ul for each ml of medium from stock 10ug/ml). Prepare one P10 plate if cells are not dividing fast (MEFs, HFFs…) and only one well of a 6-w plate if cells are dividing at a high rate (for example iPSC).

3. Leave cells in medium with colcemid between 2-4 hours. Exceptionally you can leave O/N to increase the number of metaphases in cells with low division rate.

4. After incubation, tripsinize cells. Centrifuge 8' at 800rpm. Aspirate medium, leaving 1ml of supernatant. Resuspend cells in that 1ml.

5. Add slowly and softly, while vortexing tubes at 1000rpm, 9ml of hypotonic solution (0,03M sodium citrate, Sigma S4641-500G, 44,8 EUR) pre-warmed at 37ºC. Leave tubes in the warm bath at 37ºC for 25'.

6. Add 3 drops of fresh fixer (methanol/acetic acid 3:1). Methanol quality for analysis, ACS and ISO. Put tape onto the tubes labeling.

7. Centrifuge 8' at 800rpm. Aspirate supernatant, leaving 1ml.

8. Add 2ml of fresh fixer drop by drop while vortexing tubes. Then add 7ml more slowly (faster than first 2ml). If there are many tubes, add first the 2ml to all tubes and then the rest.

9. Repite (Centrifuge, aspirate leaving 1ml and add fixer the same way). Store at -20ºC until metaphases preparation.

10. Centrifuge 8' at 800rpm. Aspirate supernatant leaving a specific amount of fixer depending on the size of the cells pellet (700ul – 200ul for big – little pellets). Resuspend cells.

11. Prepare slides, labeling them with pencil. Rinse the slide with 45% acetic (acetic diluted in H2O) by pouring 500ul on top of it. As an alternative, distillated H2O can also be used instead of acetic.

12. Drain acetic and drop 30ul of the cell suspension onto the slide (2-3 dropplets). Drops must fall from a distance of around 20-30cm on top of the slide. The more distance the better. By doing this, some cells are going to break when crushing

against the slide as they are fixed with a bigger cytoplasmic volume due to the hypotonic solution incubation.

13. Dry slides O/N at RT.

14. Day 2: Metaphase hybridations: Prepare acidified pepsin and incubate at 37ºC for 15' (for every glass box prepare: 200mg pepsin + 200ml H2O + 168ul of concentrate HCl).

15. Place slides in washing chambers to make easier all washing steps. Glass box: 200ml of PBS are required to cover slides.

16. Wash slides in PBS (with no Ca/Mg), rocking during 15' (60-70rpm).

17. Fix cells in PFA 4% for 2'. Rocking 60-70rpm. Wash 5' in PBS x3. Rocking 60-70rpm.

18. Digest with pepsin pre-warmed 10' at 37ºC. Wash 5' in PBS x2. Rocking 60-70rpm.

19. Fix cells in PFA 4% for 2'. Rocking 60-70rpm. Wash 5' in PBS x3. Rocking 60-70rpm.

20. Dehydrate putting slides in ethanol 70% -- 90% -- 100%, 5' each. Rocking 60-70rpm. Dry slides from 5' to 20'.

21. Prepare prove solution Cy3-TEL (Panagene, Cy3-OO-CCCTAACCCTAACCCTAA-Lys, 50nmole, 900 EUR).

Stock	**250ul (10 slides)**	**Final concentration**
1M Tris pH7.2	2,5ul	10mM Tris
Buffer MgCl2	21,4ul	
Formamide desionized	175ul	70%
Probe (25ug/ml)	5ul	0,5ug/ml
10% Blocking reagent	12,5ul	0,25%
H2O	33,6ul	

Buffer MgCl2: 25mM MgCl2, 9mM citric acid, 82mM Na2HPO4, adjust pH7.

22. Add a line of 25ul of the prove solution on top of every coverslide (one per each slide). Revert the slides on top of the coverslide and smash the slide against the coverslide. Push firmly to make the prove solution distribute all through the slide and the leftover fall out the edges.

23. Denaturalize at 80ºC in a heating plate for exactly 3'.

24. Incubate in a wet chamber 2h in the dark at RT.

25. Wash 15' x2 strongly rocking (use the vortex with a rectangular adapter at a speed of 150rpm). Place the glass box on top of the vortex. After 5' check that coverslides have fallen. The last 10' set the vortex at 100rpm.

26. Washing solution:

Stock	**For 400ml**	**Final concentration**
Formamide (standard)	280ml	70%
1M Tris Ph7.2	4ml	10mM Tris
BSA 10% in H2O	4ml	0,10%
H2O	112ml	

27. Wash 5' x3 with TBS-Tween (0,08%). Rocking 90rpm.

28. Dehidrate putting slides in etanol 70% -- 90% -- 100%, 5' each. Rocking 60-70rpm. Dry slides.

29. Cover with Vectashield (Mounting medium/DAPI, 3:1). Add a line of 25ul of the mounting/DAPI solution on top of every coverslide (one per each slide). Revert the slides on top of the coverslide and smash the slide against the coverslide. Push firmly to make the solution distribute all through the slide and the leftover fall out the edges.

30. Dry for 5' and seal the edges. Store at 4ºC in the dark.

31. Take images of the metaphases and analyze them with TFL-TELO software to identify telomere length intensity.

Lentivirus infection

1. Trypsinize target cells (Neural Stem Cells) gently with TryplE (#12563-029).

2. Resuspend the cells in fresh pre-warmed culture medium at concentration of $2 \cdot 10^5$ cell in a final volume of 200 µl into sterile conical tubes.

3. Add concentrated viral supernatants to the cells at a MOI of 5. A part from the TLR3 FL overexpression plasmid, include a transduction well with a negative control virus with an appropriate blank control viral construct. In this case, the negative control is an empty vector that has an Ubiquitin (UbC) promoter.

4. Also leave one well of uninfected cells as an additional standard control. Following the infection, incubate the cells at 37°C with 5% CO_2.

5. Gently mix and incubate cells for 50 minutes in the incubator at 37°C with 5% CO_2. Leave the lid of the tube loosen.

6. Seed infected cells in a Geltrex pre-coated (2h at 37ºC) 6-well plate. Incubate the cells at 37°C with 5% CO_2.

7. The next day remove virus containing medium and resuspend cell pellet with 2 ml of fresh complete culture media.

8. The following day, split the cells 1:3 or 1:5 (depending on the growth rate of your target cells) and continue incubating for 48 hours in complete media.

9. Infected cells can then be selected for stable expression using appropriate antibiotic selection at a minimum concentration, in this case with puromycin selection at a final concentration of 2,5µg/ml.

10. TLR3 expression can then be assayed by Western blot, FACS or RT-PCR.

Phenol:chloroform:isoamil acid DNA extraction

1. After an o/n proteinase K digestion at 4ºC, mix (1:1) the digested samples with Phenol + Chloroform + Isoamil Acid (IAA) (25:24:1). Example: 500µl + 500µl. If digested reaction is less, such as 50µl, add water until reaching 500µl.

2. Mix thoroughly manually during 15min (5min mixing, 5min pause and 5min mixing).

3. Centrifuge samples 15min at 14000 rpm at RT. Carefully take the upper layer phase, which contains the DNA, to a new eppendorf. Don't mix with the medium layer, which contains protein and would contaminate your samples.

4. Add 250µl Ammonium acetate (7.5M) to the extracted phase. Add cold EtOH (1:1). Example: 750µl + 750µl. To help precipitation add glycogen at 0.5µg/ml. Mix gently by inverting eppendorf 3-4 times.

5. Precipitate DNA: 1min liqN or 20min -80ºC or o/n -20ºC.

6. Centrifuge 20min at 13000rpm at 4ºC. Remove supernatant. No need to drain everything as we are cleaning with 70% EtOH. Add 1ml of 70% EtOH and centrifuge again 20min at 13000rpm at 4ºC.

7. Remove supernatant and drain as much as possible. Let the pellet dry at RT until no EtOH remains.

8. Resuspend DNA pellet in 30µl of DNase and RNase free water. Quantify genomic DNA samples.

Spinal Cord induced injury detailed procedures

1. Animals will be induced for deep anesthesia plane with 3% of isofluorane using the plexiglass chamber connected to the anesthesia workstation and keep with 1.5-2% isofluorane when is anesthesically induced (normally 1-2 minutes after 3% isofluorane induction). To check the anesthesia stage, the muscles should be relaxed, with no pedal retraction or palpebral and corneal reflexes.

2. The animals will be pre-medicated with subcutaneous morphine (2.5 mg/kg) and Baytril (enrofloxacine, 5 mg/kg, Bayer, Germany).

3. Shave the dorsal area between the neck and hindlimbs extending ~2 cm bilaterally from the spine and pulverized with clorhexidine solution covering the whole shaved area and paint the surgical area with betadine. It is recommended to use a separated surface for shaving the animals in order to avoid contamination in the surgical area.

4. Position the animals on heating pad (set up at 37ºC) mounted on Spinal Cord Unit with stretched anterior and posterior legs adjusting the mouth and nose in to the anesthesic mask keeping enough space for gas interchange

5. Set up the Anesthesia Workstation at 1,5% of isofluorane and maintain this flow during all surgery.

6. Introduce an intravenous cannula in the more visible and caudal venous in the tale. Compression of the tale and EtOH pulverization dilatants' the vessels. Connect the pre-filled cannula to the continuous 0.9% of NaCl perfusion, 2ml/hour. Maintain the caudal in during all surgical and transplantation procedure.

7. Put the eye drops (Lipolac; 1 drop to each eye) and keep the eyes closed.

8. Perform a longitudinal skin incision of approximately 2.5 cm with scalpel blade. Dissect the fat tissue without cutting it, keeping the fat pad under the skin.

9. Make an incision on the middle line of the muscles overlying the vertebral column exposing the T7-T10 vertebral segments.

10. Position the alm retractors to keep the incision widely open. It is very important to visualized the thoraco-dorsal arteria, located over the T6 segment and avoid to touch it for any hemorrage complication.

11. Detach the spinotrapezium muscle from bone on the spinal laminaes using the scalpel blades or detacher. Use the headband magnifier visor for fine visualization of the operation procedure.

12. Identify the T7 and T8 vertebral apophysis by anatomical criteria (both keeps transversal and parallel between each other).

13. Under the headband magnifier carefully lift the T9 spine backwards while introducing slowly a Rongeur of a very fine-pointed side-cutting bone. Cut out T9 and T8 vertebral apophysis leaving clean lateral spaces avoiding lateral compression of the cord. SCI by complete cross section at T8 will be performed by cutting the cord from the boton with an iridectomy scissors helped by a hook.

14. Cell transplantation: Immediately after injury (for acute stage intervention) 10 µl of cell suspension (containing 2 million cells) will be intrathecal administrated caudally to the injured area.

15. Cover the laminectomy areas with a piece of subcutaneous fat pad. Remove vertebrae clamps and retractors.

16. Carefully suture the deep and superficial muscle layers with reabsorvible Monosyn 4/0 and finally suture the skin.

17. Remove the superficial blood on the incision area with diluted H_2O_2.

18. Close the anesthesia flow and leave the animal to wake up on a heating pad.

19. Carefully empty the animal´s bladder manually pressing the bladder until is completely empty.

20. All animals will be subjected to post-surgery cares, passive and active rehabilitation protocols as was previously described (*Rodriguez-Jimnez, F.J., A. Alastrue-Agudo, S. Erceg, M. Stojkovic, and V. Moreno-Manzano. 2012. FM19G11 favors spinal cord injury regeneration and stem cell self-renewal by mitochondrial uncoupling and glucose metabolism induction. Stem Cells. 30:2221-2233*).

Trasplante de Motoneuronas derivadas de iPSCs en ratones Smn(2B/-)

1. Para este procedimiento se emplearán un modelo de ratones con atrofia muscular espinal, correspondiente a la cepa Smn(2B/-). En cada experimento se utilizará un número total de 6 animales. Estos ratones serán clasificados en dos grupos: grupo control (n=3 ratones) tratado con salino y grupo tratado con motoneuronas (n=3 ratones). Se realizarán hasta 10 experimentos independientes con 6 animales cada uno hasta llegar a un total de 60 animales. El procedimiento se aplicará en ratones de entre 10 y 15 días de edad. El experimento pretende comprobar si las motoneuronas humanas son capaces de extender sus axones para inervar los músculos de las patas traseras de los ratones para mejorar la supervivencia o movilidad.

2. Previamente al trasplante celular habrá que anestesiar a los ratones mediante ketamina-xilacina a una dosis de 50mg/kg y 5mg/kg respectivamente. Se dará analgesia pre-operatoria (Buprenorfina a una dosis de 0.1mg/kg, que tiene un efecto más rápido). Se llevará a cabo la monitorización durante la duración de la anestesia, puesto que puede ocurrir la muerte por sobredosis anestésico. Los ratones se colocarán sobre una manta calefactora durante toda la operación y hasta su recuperación.

3. Las motoneuronas a ser trasplantadas serán pretratadas in vitro con cell tracker (tinción fluorescente intracelular) para su posterior identificación una vez fijados los tejidos. 40.000 células resuspendidas en un volumen de 2ul se inyectarán en la médula espinal a nivel lumbar y/o cervical de cada ratón del grupo con tratamiento celular.

4. Para el grupo control se inyectarán 2µl de suero salino utilizando el mismo procedimiento que en los ratones del grupo tratado con células. Se emplea un volumen de 2µl dado que una alta densidad celular facilita una mayor supervivencia y capacidad de asentamiento celular post-inyección.

5. Se realizará la inyección usando una pipeta de precisión Hamilton con una punta de cristal modelada a partir de pipetas Pasteur de vidrio. La Hamilton será fijada mediante un aparato de estereotaxia sujeto a la mesa de operaciones.

6. Para realizar la inyección se utiliza una técnica que ya dominamos. Primero es necesario hacer una única incisión para dejar al descubierto la médula espinal a nivel lumbar y/o cervical. Para ello se practicará con un bisturí una pequeña incisión de 5 mm en la piel, cortando tejido conectivo y muscular hasta llegar al hueso. Entonces se practicará una laminectomía parcial, perforando en la vértebra el mínimo espacio necesario para permitir la inyección de las células en la médula. Se procederá a inyectar los 2µl de volumen de forma progresiva a lo largo de un tiempo de 2 minutos para no aumentar la presión medular de forma brusca.

7. Se cierra la incisión (2-3 puntos), suturando primero la capa muscular y luego la piel con una seda de 6-0 ambas. Nos aseguramos de que el ratón se recupera con éxito de la anestesia y comprobamos su estado al día siguiente.

8. Al final de la cirugía se administrará una dosis de meloxicam. Durante las primeras 72h después de la operación se supervisará el ratón y se administrará analgésicos diariamente (meloxicam a dosis: 2mg/kg). A partir de entonces se administrará también a aquellos ratones que presenten signos de dolor. Los animales permanecerán junto a la madre para que pueda continuar alimentándolos por lactancia materna. Para evitar el rechazo materno se rebozarán las crías en las virutas de la jaula antes de devolverlos con la madre.

9. Para evitar el rechazo de las motoneuronas por parte del sistema inmunitario de los ratones, estos se inmunosuprimirán mediante la administración de ciclosporina A por inyección subcutánea cada 48h en dosis de 20mg/kg.

10. A día 28 de vida de los ratones se sacrificarán 3 animales del grupo de inyectados con células y 3 del grupo inyectado con suero salino y se perfundirán previa anestesia con ketamina-xilacina a una dosis de 75 mg/kg y 7,5mg/kg respectivamente, y se procederá a la fijación de tejido neural para estudiar si las células se han injertado y sobrevivido.

11. Con el resto de animales se estudiará la mejora de la motilidad y la curva de supervivencia. Aunque es cierto que en la medida de lo posible debe evitarse la muerte natural como criterio de punto final, en este caso es imprescindible. Para determinar el porcentaje de supervivencia de ambos grupos se contabilizarán los días en que los ratones hayan perecido de forma natural. La esperanza de vida media de los ratones de este modelo de atrofia es de 26-30 días, por lo tanto entre 15-20 días después de la intervención. En este modelo de SMA nunca se ha reportado ningún caso que haya superado los 40 días.

12. Durante los últimos días de vida, si el animal presentara sufrimiento a causa de la enfermedad genética se administrará meloxicam a dosis: 2mg/kg. No obstante en este modelo de atrofia en ratones, no se observan manifestaciones fenotípicas de malestar severo como la caída de pelo, arqueamiento de la espalda, agresividad, automutilación o aspecto comatoso. Tampoco se produce pérdida de peso sino estancamiento de este. Además los ratones no son separados en ningún caso de la madre, que es quien se ocupa de alimentar-los, siendo raro el caso en que la madre se niega a alimentar a sus crías.

Willmann, R., et al., *Developing standard procedures for pre-clinical efficacy studies in mouse models of spinal muscular atrophy: report of the expert workshop "Pre-clinical testing for SMA", Zurich, March 29-30th 2010.* Neuromuscul Disord, 2011. **21**(1): p. 74-7

Cyclin D1 template and mRNA production protocol

We have extracted protocols from two articles:
-Loh et al., Curr Protoc Stem Cell Biol 2012, CHAPTER: Unit4A.5 (for ORF forward primer phosphorylation)
Simeonov KP, Uppal H. Direct reprogramming of human fibroblasts to hepatocyte-like cells by synthetic modified mRNAs. PLoS One. 2014 Jun 25;9(6):e100134. doi: 10.1371/journal.pone.0100134. eCollection 2014. (for splint ligation protocol).

Materials list:

-Falcon 15mL Conical Centrifuge Tubes (Falcon, #14-959-53A), x1 box.
-Falcon 50mL Conical Centrifuge Tubes (Falcon #14-432-22), x1 box.
-RNase-free 1,5ml eppendorf tubes (Thermo Fisher, #AM12400), x1 bag.
-RNase-free 0,3ml eppendorf tubes (Thermo Fisher, #AM12300), x1 bag.
-Six-well plates (Cornig, #CLS3516), x1 box.

-MEGAscript Kit, (Ambion, #AM1334), x1 kit.

-1.2µl ARCA (TriLinkBioTechnologies, #N-7003, stock: 100mM), x1 unit.

-1.5µl 5-Methyl-CTP (TriLinkBioTechnologies, #N-1014, stock: 100mM), x1 unit.

-1.5µl Pseudo-UTP (TriLinkBioTechnologies, #N-1019, stock: 100mM), x1 unit.

-Qiaquick PCR purification kit (Qiagen, #28104), x1 kit.
-Qiaquick Gel Extraction Kit, (Qiagen #28704), x1 kit.
-MicroRNA-enhanced mRNA reprogramming kit (STEMGENT, #00-0071), x1 kit.

-Pluriton basal media (Stemgent Ref#00-0070), x1 bottle.

-CTS E8 complete medium (Life Technologies # A26561-01), x6 bottles.
-Vitronectin (Life Technologies, #A14700), x5 ml

-Knock out serum replacement (LifeTechnologies, #10828028), x1 bottle.
-Dimetil sulfoxid (Sigma, #472301), x1 bottle.

Phosphorylate forward primer.

1. Reaction Mix (50µl total): 300pmol forward primer (3µl 100µM), 1µl (10U) PNK, 5µl 10X Buffer, 50nmol ATP (0,5µl 100µM stock), 40,5 µl MQ. Incubate 30 min 37ºC.

2. Order the 3'UTR oligo already phosphorylated.

3. ORF PCR. Reaction Mix (25µl total): 2x KAPA Mix: 12.5µl, 10µM Forward Primer: 0.75µl, 10µM Reverse Primer: 0.75µl, 3ng/µl Template DNA: 1µl, Water: 10µl. Note: Primers are ORF specific. PCR Setup:

1 cycle:
95ºC 5min
20 cycles:
98ºC 20sec
65ºC 15sec
72ºC 60sec
1 cycle:
72ºC 5min
4ºC hold

4. Run a gel (Speed E-Gel protocol on 1.2% gel, load ~100ng in 20µl per well) to make sure the amplicons are the correct length, may need to extract the correct band using CloneWell Gel.

5. Purify tubes with Qiaquick Purification Kit (if not doing gel band purification). Quantify with nanodrop each tube (yield ~55ng/µl in 50µl).

Template Splint Ligation protocol

1. Reaction Mix (50µl total): 10x Ligation Buffer: 5µl, 5µM 5'UTR: 2µl, 5µM 3'UTR: 2µl, 2µM 5'Splint: 2.5µl, 2µM 3'Splint: 2.5µl, ORF DNA from above (~50ng total maximum, corresponds to ~40nM, 1µl should be enough) and water: to 50µl. Note: Splints are ORF specific, but UTRs are not.

2. Add 1 unit of vortexed Ampligase and vortex mix thoroughly. Ligation Setup:

5 cycles:
95ºC 10sec
45ºC 1min
50ºC 1min
55ºC 1min
60ºC 1min

3. Purify with Qiaquick Purification Kit

4. Large Scale Template Tail PCR (we adapted this to the recommendations of our own high fidelity enzyme). Reaction Mix for 6 reactions (153µl total): 2x KAPA Mix: 76.3µl, 10µM Forward Template Primer: 4.6µl, 5µM Reverse Tail Template Primer: 9.2µl, DNA: 31µl from ligation and water: 32µl.

5. Template Tail PCR Setup is same as ORF PCR (except with 30 cycles instead of 20). Run some of the template PCR product next to the ORF PCR product on a 1.2% gel with Speed E-Gel protocol to see if there is a discreet band of correct length (slightly longer than ORF PCR product).

6. Template PCRs should be purified using traditional gel extraction to avoid loss of product. Open gel with a razorblade and excise bands with a new blade for each template. Gel purify using the Qiaquick Gel Extraction Kit. Re-purify with Qiaquick PCR purification kit (elute with water) since gel purification produces consistently bad 260/280 ratio. Adjust concentration to rounded number.

7. Sequence templates. Templates can now be directly used to template IVT.

In Vitro Transcription (IVT)

This protocol explains in detail how to synthetize by IVT the mRNA for transfections. MEGAscript Kit, Ambion, Ref #AM1334.

1. Using Cyclin D1 gene template, proceed to synthesize the messenger RNA by in vitro transcription (IVT). Use RNase and DNase free tubes and tips and eliminate RNases in gloves, working surface and with RNaseZap (Sigma, #R2020). In case the template is cloned inside a plasmid first it has to be digested and amplified by PCR.

2. Plasmid Digestion. Digest 5µg of plasmid each time, no more. Cut 10 µg preparing two digestions of 5µg. Prepare a mix with all the other components and add DNA in the end so it does not stick to the walls and out of reach for the restriction enzyme. Add 20-30U of enzyme (usually: 5-10 U/µl), 10µl 10X buffer and RNase-DNase free water to a final volume 100µl. Add 10U more of enzyme and digest all night at 37ºC.

3. Next day load 3µl in agarose gel to check digestion on gel. Check on gel again. If a 100% is not cut, add 10U more and digest 2h 37ºC. When 100% is cut, pool together both digestions and purify with Qiaquick PCR purification kit. Elute in 70µl: 40µl 1' sit, 1' spin and 30 µl 1'sit, 1'spin. The expected concentration is 100ng/µl.

4. Template preparation, PCR tailing (set reaction as described above in step 5 of template splint ligation protocol). Set the reaction on ice. Use 5-10 ng of cut plasmid as PCR template per tube. Then, put together all the PCR reaction in one tube. Run 1-2 µl on agarose gel to check there is only one band. Purify with Qiaquick PCR purification kit; elute in 30µl. Concentration should be around 200ng/µl

5. To start IVT, work in RNase free dedicated area. Clean surfaces, racks and pipettes with RNaseZap. Frequently during the process spray a bit of RNaseZap on a tissue and wipe surface, pipettes, etc. It is also recommended to wear surgical mask. Use only RNase free filter tips and tubes.

6. Place RNA Polymerase enzyme mix (supplied in Megascript kit) on ice. Vortex ribonucleotide solutions until thawed and store them on ice. Aliquot dNTPs mix to avoid freeze/thaw cycles.

7. Thaw buffer at 37ºC, vortex, and keep at RT. This is important to avoid precipitation. Aliquot enzyme mix to avoid freeze/thaw cycles.

8. Shake and spin down components of the kit before using.

9. Start with 0.5-1 µg DNA template. Reaction is set on PCR tubes at RT. Prepare mix in this order, mixing well after adding each component:

H_2O up to 20µl
2µl ATP (supplied in Megascript kit)
0.4µl GTP (supplied in Megascript kit)
1.2µl ARCA (TriLinkBioTechnologies Ref#N-7003, stock: 100mM)
1.5µl 5-Methyl-CTP (TriLinkBioTechnologies Ref#N-1014, stock: 100mM)
1.5µl Pseudo-UTP (TriLinkBioTechnologies Ref#N-1019, stock: 100mM)
2 µl 10x reaction buffer (supplied in Megascript kit)
0.5-1µg template DNA
2µl Enzyme Mix (supplied in Megascript kit)
Total volume 20 µl

10. Gently flick the tube or mix well with pipette. Quick spin. Incubate for 2-4h 37ºC in PCR machine (we usually prefer 4h).

11. DNase treatment: Add 1 µl Turbo DNase (supplied in Megascript kit). Mix well by pipetting + pulse spin. Incubate for 15' at 37ºC.

12. Transfer 20 µl of the IVT reaction to RNase free 1.5 ml centrifuge tube.

13. Precipitate RNA by adding 30µl Nuclease-free Water (supplied in Megascript kit) to the 20 µl reaction, mix and add 30µl LiCl Precipitation Solution (Megascript kit). Mix thoroughly.

14. Chill for at least 30' at -20ºC. Centrifuge at 4ºC for 15' at maximum speed to pellet the RNA. Carefully remove the supernatant and keep it in case RNA didn't precipitate.

15. Wash pellet with 0.5ml 70% EtOH RNase free. Centrifuge at 4ºC for 15' at maximum speed to pellet RNA. Carefully remove the supernatant (put it aside in case RNA did not precipitate).

16. Air-dry pellet at RT (at this stage the pellet might be visible white, or invisible if it becomes transparent).

17. mRNA dephosphorylation: add 42µl nuclease-free water + 5µl Alkaline Phosphatase Buffer + 3 µl Alkaline Phosphatase (1U/µl) (Promega, #M182A). Incubate 30' at 37ºC.

18. Precipitate with LiCl again (add 30µl LiCl).

19. Wash with 0.5ml EtOH 70%. Air-dry pellet at RT.

20. Resuspend in 50µl TE (put aside 1µl RNA to quantify and 1µl to run in a denaturing agarose gel). Quantify by Nanodrop.

21. Dilute it to a final concentration of 100ng/µl with RNase free TE (Ambion Ref# AM9861) or RNase free water.

22. Check RNA quality by gel: prepare a 1.2% agarose denaturing gel made of: MOPSx10 (final concentration: 20mM), non-contaminated agarose + formaldehyde (final concentration 2M). Formaldehyde should be added in a gas extracting hood. Electrophoresis equipment should be RNase free: used only for RNA gels and cleaned with RNaseZap.

23. Run 1µl (200-300ng) of RNA + 4µl of RNase-free water with 5µl of Gel Loading Buffer II (Ambion, Ref#AM8546G) for RNA + 1µl BrEt 0.1 mg/ml (dilute 1µl BrEt 10 mg/ml stock solution in 100µl gel loading buffer). Incubate RNA 5' at 70ºC.

24. Load ssRNA ladder (DNA ladder is double strand and runs different. Get Invitrogen ssRNA 2kb ladder).

25. Load RNA and run gel in 1XMOPS buffer at 70V for 45'.

26. If RNA is clean of RNases, it should be a single clear band. If it is degraded a smear will be observed in the lower part.

27. Storing mRNA and checking functionality: if there are no RNases in the samples, RNA can be kept even at 4ºC for a few days; however it is always recommended to be stored at -80ºC. If RNA has been frozen and thawed several times, run a gel to check integrity.

28. Check by Western Blot that the gene is still expressed 12-24h after transfecting your target cells. Depending on the protein turnover of your gene you may need to wait no more than 16h.

29. Antibiotics could inhibit transfection complex formation depending on transfection reagent used, and therefore it is recommended to exclude antibiotics from the complex formation step. Transfection complexes can be added to cells grown in complete culture medium containing low levels of antibiotics (0.1-1X final concentration of P/S).

Micro-RNA enhanced mRNA reprogramming protocol:

Non-integrative reprogramming method based on Stemgent's microRNA-enhanced mRNA reprogramming kit (STEMGENT, #00-0071) protocol, with the replacement of c-Myc mRNA by Cyclin D1. This protocol explains in detail the procedure to transfect target cells and defines how to pick, passage and freeze iPSC colonies when they appear after the transfection period.
Reprogramming timeline:

1. Aliquot reagents. Aliquot Pluriton basal media (Stemgent Ref#00-0070) and E8 complete medium (Life Technologies #A1517001) in 50ml tubes and store at -20ºC. The day before using it, aliquots should be thawed o/n at 4ºC. B18R and Pluriton supplement must be aliquot in sizes of 2.4µl and 1.6µl (for 6 and 4 ml of total medium respectively) to avoid freeze/thaw cycles. Aliquot Vitronectin (Life Technologies, #A14700) in sizes of 60-100µl to avoid freeze/thaw cycles. Aliquot messenger RNA cocktail at a proportion of 3:1:1:1:1 of the reprogramming genes: Oct4, Sox2, Klf4, Lin28 and Cyclin D1 (OSKLD) (all 100 ng/µl). Prepare aliquot size depending on the number of wells you want to transfect: 200ng of total mix (2µl) per well in 24MW plate. Aliquot MicroRNA. Prepare aliquot size depending on the number of wells you want to transfect: 0.7µl/well in 24MW plate.

2. Day -2: Plate a feeder layer of irradiated human foreskin fibroblasts (irHFFs) and leave it o/n with Pluriton to condition the medium (1vial of irHFFs into 2 wells of a 6MW plate in 2ml of medium each).

3. Day -1: Coat 24MW plate with 250µl/well of vitronectin diluted 1:100 in PBS for at least 1h at RT. Plate human foreskin fibroblasts (HFF) in FibroGRO™ Xeno-Free Human Fibroblast Expansion Medium (Millipore, Ref # SCM044) the vitronectin coated wells.

4. Seed cells at 6 different densities (7.5k, 10k, 12.5k, 15k, 17.5k and 20k per well) to decide the next day the three best ones to start the transfections with.

5. Transfecting cells (Day 0): If cells are looking healthy, select the three best densities, between 50-70% confluency, to start transfections.

6. Thaw one B18R aliquot on ice. Once thawed, keep the vial on ice at all times.

7. Collect the 4ml Pluriton conditioned medium and add 2.4µl of the B18R (0.6µl B18R/1ml Pluriton equivalent to 300ng B18R/ml). Add 1.6µl of Pluriton supplement to the 4ml conditioned Pluriton before adding to the cells.

8. Aspirate the target cells medium from each of the 3 wells to be transfected and add 666µl of the conditioned medium with B18R and supplement to each well. Keep the remaining 2ml at 4ºC as a backup. Incubate the cells for 2h at 37ºC, at 5% CO2 and appropriate oxygen tension, then proceed to transfect.

9. MicroRNA transfection (Day 0 and 4): Tube 1: (2.1µl of microRNA, 0.7µl/well) + 12.85µl transfection buffer. Tube 2: 12.55µl buffer + 2.4µl Stemgent transfection reagent.

10. Transfer the content of tube 2 into tube 1 and pipet gently 3 to 5 times to generate the transfection complex (total 30µl). Incubate the mix for 15' at RT.

11. Holding the plate at a 45 degrees angle, add 10µl/well into the medium in each well to be transfected. After adding the transfection complex to the wells, gently rock the plate from side-to-side and front-to-back to distribute the transfection complex evenly.

12. Messenger RNA-OSKD1- transfections (Day 1-11): Tube 1: (6µl of mRNA mix, 2µl/well) + 9µl buffer. Tube 2: 12.65µl buffer + 2.4µl of reagent stemgent.

13. Transfer the content of tube 2 into tube 1 and pipet gently 3 to 5 times to generate the transfection complex (total 30µl). Incubate the mix for 15' at RT.

14. Holding the plate at a 45 degrees angle, add 10µl/well into the medium in each well to be transfected. After adding the transfection complex to the wells, gently rock the plate from side-to-side and front-to-back to distribute the transfection complex evenly.

15. Colony picking: As an indication of reprogramming, cells must show signs of mesenchymal to epithelial transition (MET) around days 4-6. Keep transfecting until day 12. If cells don't display MET when reaching 100% confluence or if cellularity starts declining, transfections should be considered to stop for that particular density.

16. Colonies can start appearing as early as day 10.

17. At day 14-15 pick colonies, when they are big enough, by mechanically scrapping them. Transfer picked colonies into vitronectin-coated plates. Add to the cells condition Pluriton mixed 1:1 with E8 medium. Add Rho kinase inhibitor (ROCKi, Y-27632, STEMCELL #72302) at 10µM final concentration (10mM stock) during the first 24h after colony picking to prevent cell apoptosis.

18. Change to E8 medium[9] 24h later and onwards (without feeder layer conditioned medium and with no Pluriton). Maintain cells by daily medium exchange. Failure to replace medium daily can result in spontaneous differentiation.

Colony passaging

19. When colonies are ready, passage them by gentle dissociation with EDTA. Notice that colonies are ready to passage when they are around 75-80% confluent. However, if there are few big colonies (not properly disaggregated in the previous passage) it should be considered to passage earlier, as this could threaten the proper growth of iPSC.

20. Coat a 6-well plate with 1ml/well vitronectin (1:100 in PBS) for 1h at RT.

21. Remove culture medium and wash once with PBS. Add 1ml of 0.5mM EDTA and incubate for 2' at 37ºC in the incubator. Remove EDTA carefully not to detach the cells and then immediately resuspend cells in E8 supplemented with 10µM ROCK inhibitor by pipetting up and down three to four times (no more to avoid cell death). Do not centrifuge.

22. Remove vitronectin and wash the plate with PBS. Then distribute resuspended cells into the 6-w plate wells depending on the desired split ratio.

Cell freezing

23. Remove culture medium and wash once with PBS. Add 1ml of 0.5mM EDTA and incubate for 2' inside the incubator.

24. Remove EDTA carefully not to detach the cells and resuspend them in E8 supplemented with 10µM ROCK inhibitor by pipetting up and down three to four times.

25. Collect resuspended cells in a 15ml tube and centrifuge at 200g for 5' at RT. Discard supernatant.

26. Resuspend cells in 90% knock out serum replacement (KSR) + 10% DMSO, add 1ml/ freezing vial. Store first at -80ºC and 24h later transfer vials to liquid Nitrogen.

Cell thawing

[9] In the case of the failed reprogramming attempts for MEFs, in the conditioned G4 medium we also added VPA 0.5mM from day 1 to day 11 and siRNAs (Infb1, Stat2 and Eif2ak2) every other day (days 0, 2, 4, 6, 8, 10): Eif2ak2 siRNA (stock 20µM): add 0.5µl; Infb1 siRNA (stock 10µM): add 1µl; Stat2 siRNA (stock 10µM): add 1µl. These amounts were used for each well of a 6-w plate (0.5ul + 1ul + 1ul) for every 2ml.

27. Coat several wells (depending on the number of cells to be thaw) of a 6-well plate with 1ml/well vitronectin (1:100 in PBS) for 1h at RT.

28. Immerse the cryotube in a 37ºC water bath. Thaw quickly by gently swirling until only a small piece of frozen material is left. Spray the tube with 70% EtOH before entering it into the safety cabinet hood.

29. Transfer cells to a 15 ml tube and add 10ml of warm E8 medium + 10µM ROCKi drop wise and gently mix cells. Centrifuge the tube at 200g for 5' at RT. Discard supernatant. Gently resuspend cells into 6ml of warm E8 + 10µM ROCKi and plate cells on the three vitronectin coated wells.

-Loh et al., Curr Protoc Stem Cell Biol 2012, CHAPTER: Unit4A.5 (for ORF fwd primer phosphorylation).

-Kamen P. Simeonov, Hirdesh Uppal Regarding – DOI: 10.1371/journal.pone.0100134 (for the rest of splint ligation protocol).

-http://assets.stemgent.com/files/1369/original/AppNoteMicroRNA_GK_061314.pdf

Cytotoxic T lymphocytes CTL coculture with CM
(All animal experiments were approved by the University of Barcelona ethics committee).

1. Cells are in vivo injected isogenically into C3H mice. Four iPSC clones and four iPSC derived cardiomyocytes clones are injected subcutaneously in mice in duplicate. One week after injection, cells are reinjected again for boosting the priming of the Cytotoxic T lymphocytes (CTLs) against injected cells.

2. One week after reinjection (final priming period of 14 days), collect CTLs with an isolation by FICOLL (density of 1,077g/ml) gradient from mice smashed spleens. Briefly, spleens are smashed with two coverslips and cell lysate was resuspended in 5ml of RPMI-10 + 1%Pen/Strep medium and filtered through an autoclaved Nylon filter.

3. In a 15ml tube prepare 2,5ml of Ficoll + 1ml of FBS + 5ml of RPMI with cells (2,5ml Ficoll: 5ml RPMI with cells, 1:2 ratio). Do not mix phases.

4. Centrifuge at 500xg 30' at RT. Remove centrifuge brake. Collect the white layer interphase to a new tube with PBS. Be careful not to contaminate with the lower Ficoll phase. Cells in this interphase are mononuclear cells of which a 20-40% is expected to be activated T cells. Wash x3 with PBS, this time centrifuging at 200xg. Count the number of cells.

5. The day before extracting the CTLs, seed target cells, in our case the same cardiomyocyte (CM) lines that were injected into the mice from where the CTLs are isolated. Put 30.000 cells in a well of a 96-w plate.

6. For T cell kill assay, add 30.000 isolated CTLs on top of the cardiomyocyte seeded the day before. Co-culture assay of CTL: CM lasts 4h. CTLs degranulation in response to cytotoxic activation is determined by CD107a staining (Biolegend, FITC anti-mouse CD107a, #121605) and apoptosis of target cardiomyocytes was assessed by an Annexin V-FITC staining (Apoptosis detection kit, Biotools, Cat #B32115).

7. CD107a antibody must be in the medium during the co-culture because CD107a protein is rapidly endocyted following externalization. After co-culture, CTLs are collected by pipetting up and down in the well. Rinse the dish with cold buffer. Check under the microscope for any remaining cell, if necessary, rinse the dish again.

8. Once CTLs have been removed, target cells are trypsinized and stained for Annexin V for apoptosis assay. Briefly, trypsinize cells and wash in cold PBS. Then, add 30µl of binding buffer + (0.5µl/sample) of Annexin V-FITC conjugated to tripsinized cells and incubate 5' on ice in the dark. Then, add on top 120µl of binding buffer + PI (0,5µl/sample). Analyze by flow cytometry immediately. Cells considered viable are both Annexin V and PI negative, while cells that are in early apoptosis are Annexin V positive and PI negative, and cells that are in late apoptosis or already dead are both Annexin V and PI positive.

RESULTS

C-Myc can be replaced by Cyclin D1 to reprogram mouse C2C12 cells.

To test the pluripotency potential of Cyclin D1 to replace c-Myc oncogene in the reprogramming cocktail, we first transduced C2C12 mouse cell line. A retroviral delivery system to overexpress the reprogramming factors was used as described in the methodology. We infected C2C12 cells with three conditions: 3F (Oct4, Sox2 and Klf4), 3F+c-Myc and 3F+Cyclin D1. Oct4 and Cyclin D1 protein levels were checked by western blot to corroborate that the retroviral vector was being expressed (Supplementary Figure 1, B). Infected cells were seeded onto a feeder layer of MEFs in G4 media for a colony formation assay.

We isolated individual clones by mechanically picking emerging colonies with a cell scraper from a colony formation assay for 3F+c-Myc and for 3F+Cyclin D1. GFP reporter gene was also monitored to be expressed during the first days after the infection (Supplementary Figure 1, A) Once picked, clones were cultured adding VPA to the medium following *Teng et al.* protocol, as it was reported to enhance Oct4 promoter activity in myogenic cells such as C2C12 (Teng *et al.*, 2010). After 3 weeks of expansion, best 3 clones were chosen selecting by Alkaline Phosphatase staining, morphology and absence of GFP expression. These clones were expanded to passage 10. Then, clones were stained by immunofluorescence for pluripotency markers: Oct4, Sox2, SSEA3 and SSEA4 (Figure 1, A) to check their pluripotency at protein level; and also by real time PCR for pluripotency markers: Oct4, Sox2, Nanog, Rex1 and Utf1 (Figure 1, B). IPSC were then differentiated in vitro into the three germ layers and cells were stained with markers for mesoderm (Alfa Smooth Muscle Actinin, SMA), endoderm (alfa-1-Fetoprotein, AFP) and ectoderm (B-III-Tubulin, Tuj1) (Figure 1, C). We checked that at this point GFP was not expressed what indicates transgene expression is silenced (supplementary figure 1, D).

We also analyzed alkaline phosphatase expression (Supplementary Figure 1, C), as a recognized pluripotency marker. Alkaline phosphatase was also analyzed to study the reprogramming efficiency. For every condition 1000 cells were seeded on irradiated feeder cells to let them grow for two and three weeks before staining them for the stem cell marker alkaline phosphatase. Results show that the reprogramming process is being accelerated from three weeks required by 3F+c-Myc clones to only two weeks with 3F+Cyclin D1 (Figure 1, D), as shown by a higher alkaline phosphatase number of colonies in 3F+Cyclin D1 after two weeks (p-value = 0.0062). However, efficiency is not higher but similar to 3F+c-Myc after 3 weeks (day 21).

Cell stress genes decrease when reprogramming with Cyclin D1.

C-Myc pleiotropic effect activates several pathways simultaneously, originating replicative and oxidative stress to cells during the reprogramming process. In order to determine whether Cyclin D1 can reprogram cells causing less cell stress, we tested by qPCR the expression of several markers related with DNA damage response: ATM and 53BP1, NFkB related protein MnSOD, apoptosis inhibition related genes IAP2 and GADD45b and sirtuins 1, 3 and 6. We analyzed C2C12 RNA as negative control and mouse Embryonic Stem Cells RNA as a stem cell internal control. Three clones for every condition (3F+c-Myc and 3F+Cyclin D1) were compared at passage 1 and passage 5. Differences where mainly found during early passage 1, where iPSC clones reprogrammed with 3F+c-Myc expressed higher levels of IAP2 (p-value = 0.0184),

Gadd45b (p-value = 0.0342) and sirtuin1 (p-value < 0.0001) than clones reprogrammed with 3F+Cyclin D1 (Figure 1, E-G). The induction of GADD45b and IAP2 is associated with the inhibition of apoptosis, functioning as a protective mechanism against apoptosis, as a protective mechanism, suggesting that 3F+c-Myc iPSC clones might require to be assisted or protected from more stress and damage than Cyclin D1 clones. Interestingly, Sirt1 is upregulated in 3F+c-Myc clones during early passage 1, and is decreased in 3F+Cyclin D1 clones, meaning either Cyclin D1 protein is directly or indirectly interacting with Sirtuin 1 protein levels or 3F+Cyclin D1 clones might originate less genomic instability, avoiding the requirement of Sirtuin 1 function. The rest of the genes analyzed gave no significant differences between conditions (Supplementary Figure 1, E-I).

We wondered whether stress genes were also affected in human cell reprogramming, that's why we also retrovirally infected human foreskin fibroblasts (HFFs) for the same three conditions as for C2C12 cells previously described. After 2 weeks of being onto feeders, 3F reprogramming colony formation assay gave rise to 1 colony, but 3F+Cyclin D1 reprogramming gave rise to 28 colonies, a 40% of the number of colonies raised with 3F+c-Myc (71 colonies). GFP expression was used as a reporter of polycistronic retroviral vector expression (Supplementary figure 2, A). A polyclonal scrape of different colonies randomly picked was stained with Tra-1-81 and analyzed by FACS. 3F+c-Myc iPSC had 1,3% positive cells and 3F+Cyclin D1 had a 5,6% (Supplementary Figure 2, C), suggesting again an acceleration of the reprogramming process with 3F+Cyclin D1 reprogramming compared with 3F+c-Myc.

Three clones per condition were picked and passaged for the human reprogramming. After 5 passages hiPSC were stained for pluripotency markers Oct4 and Sox2 (Supplementary Figure 1, B). Then, the same cell stress markers were tested as in mouse at previously in early passage in human reprogramming cells. Sirtuin 1, at day 4 after infection, was found to be differently expressed between the two conditions (p=0.0215) as seen in mouse, but GADD45B and ATM2 levels were not different. However, human 3F+c-Myc colonies expressed higher levels of sirtuin 6 (p=0.0042) and 53BP1 (p=0.0185) compared to 3F+Cyclin D1 colonies (data not shown).

Sirtuin 1 is not essential when reprogramming MEFs with 3F+Cyclin D1.

It has been reported that Sirt1 has an essential role for proficient telomere elongation and for genomic stability in the reprogramming process of induced pluripotent stem cells (De Bonis *et al*., 2014). Correspondingly, we found that Sirtuin 1 is significantly upregulated in 3F+c-Myc clones (Figure 1, E). However, in 3F+Cyclin D1 clones, Sirtuin 1 is downregulated compared to the control C2C12 (p-value = 0,0096).

Thus, in order to determine whether Sirtuin 1 role can be bypassed by reprogramming with 3F+Cyclin D1, we reprogrammed Sirtuin 1 null MEFs with our condition. Wild type and Sirtuin 1 null mouse embryonic fibroblasts (*wt and Sirt1-/-* MEFs) were transduced with the conditions 3F, 3F+c-Myc and 3F+Cyclin D1. Afterwards, we performed an alkaline phosphatase staining of reprogramming cells seeded in 6 well plates: 10.000 cells/well onto feeders. Positive colonies were counted and numbers were graphed (Figure 1, H). Transduced wild type MEFs showed that 3F+c-Myc reprogramming was producing more number of colonies than 3F+Cyclin D1 reprogramming. But transduced Sirt1-/- MEFs showed that 3F+c-Myc number of

colonies was decreased (p-value = 0,01), suggesting that Sirtuin 1 is essential to rescue genetic alterations or instability accumulated on cells due to cell stress induced by c-Myc. It was previously found that knocking down Sirtuin 1 with siRNA produced a threefold reduction in the number of iPSC colonies when reprogramming with c-Myc (Lau *et al*., 2012). Here, after reprogramming sirtuin 1 null MEFs with c-Myc we have found a fourfold reduction (p-value = 0,01). On the other hand, in 3F+Cyclin D1 reprogramming, Sirtuin 1 was not essential at all, as in 3F+c-Myc reprogramming, as there was no difference between wild type and Sirtuin 1 null MEFs reprogramming (Figure 1, H). Thus, Sirtuin 1 seems to be not essential when reprogramming with 3F+Cyclin D1, contrarily to 3F+c-Myc reprogramming.

Cyclin D1 made mouse iPSC show a reduced % of DSB.

DNA double strand breaks (DSB) appear as a consequence of oxidative and replicative stress and can be repaired by homologous recombination (HR) or by the classical or alternative non-homologous end joining (NHEJ). Both replicative and oxidative stresses are induced during the reprogramming process. Furthermore, replication stress has been linked with genomic instability on mouse and human iPSC (Ruiz et al., 2015). Additionally, Myc expression causes an accumulation of reactive oxygen species (ROS), which generates DNA breaks (Khanna and Jackson 2001). Moreover, c-Myc expression suppresses the classical NHEJ pathway by binding to ku70 (Li et al., 2012) and in various cancer cell lines Myc also inhibits homologous recombination through regulation of RAD51 (Luoto et al., 2010). Furthermore all Myc protein family members contain the Box II domain that has been reported to interact and inhibit Ku70 (Li et al., 2012), protein necessary for non-homologous end joining (NHEJ) DSBs repair mechanism. On the other hand, it has been reported an unexpected non canonical function of Cyclin D1 in facilitating homologous recombination repair process by helping BRCA2 to recruit RAD51 to repair DSB in homologous recombination (Jirawatnotai et al., 2011; Chalermrujinanant et al., 2016). DSBs can be studied by detection of the standardly used biomarker: H2AX expression.

Therefore, we hypothesized that 3F+Cyclin D1 iPSC could present a lower number of DSBs than 3F+c-Myc iPSC. Results show that 3F+Cyclin D1 iPSC present a lower percentage of H2AX positive cells by immunofluorescence than 3F+c-Myc iPSC at passage 4 (Figure 1, I). The fact that c-Myc promotes replicative stress in the cell could explain why more DSB are found in 3F+c-Myc iPSC. Furthermore Cyclin D1 helps BRCA2 recuitment of Rad51 and therefore promotes the more precise repairing machinery of the homologous recombination process.

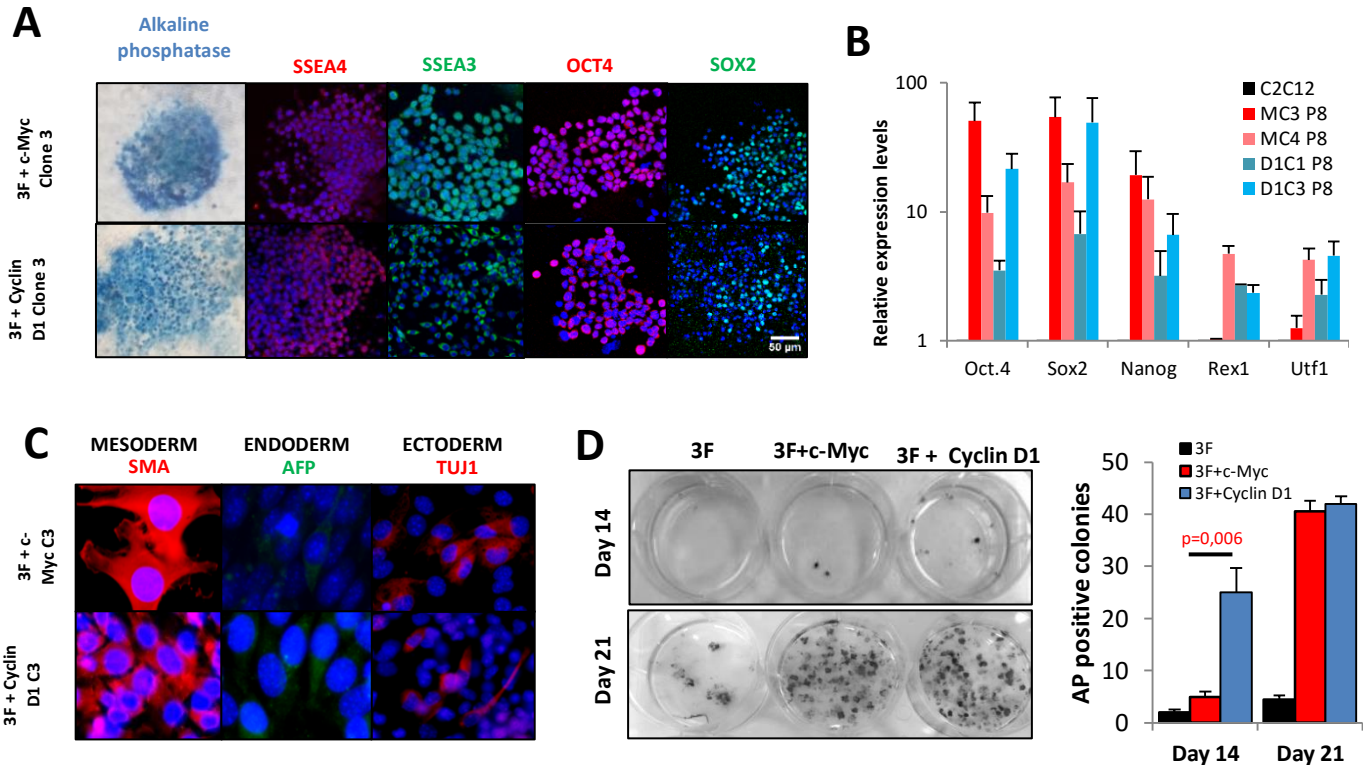
A
Alkaline phosphatase
SSEA4
SSEA3
OCT4
SOX2
3F + c-Myc Clone 3
3F + Cyclin D1 Clone 3
50 µm
B
Relative expression levels
100
10
1
C2C12
MC3 P8
MC4 P8
D1C1 P8
D1C3 P8
Oct.4
Sox2
Nanog
Rex1
Utf1
C
MESODERM
SMA
ENDODERM
AFP
ECTODERM
TUJ1
3F + c-Myc C3
3F + Cyclin D1 C3
D
3F
3F+c-Myc
3F + Cyclin D1
Day 14
Day 21
AP positive colonies
3F
3F+c-Myc
3F+Cyclin D1
p=0,006
Day 14
Day 21

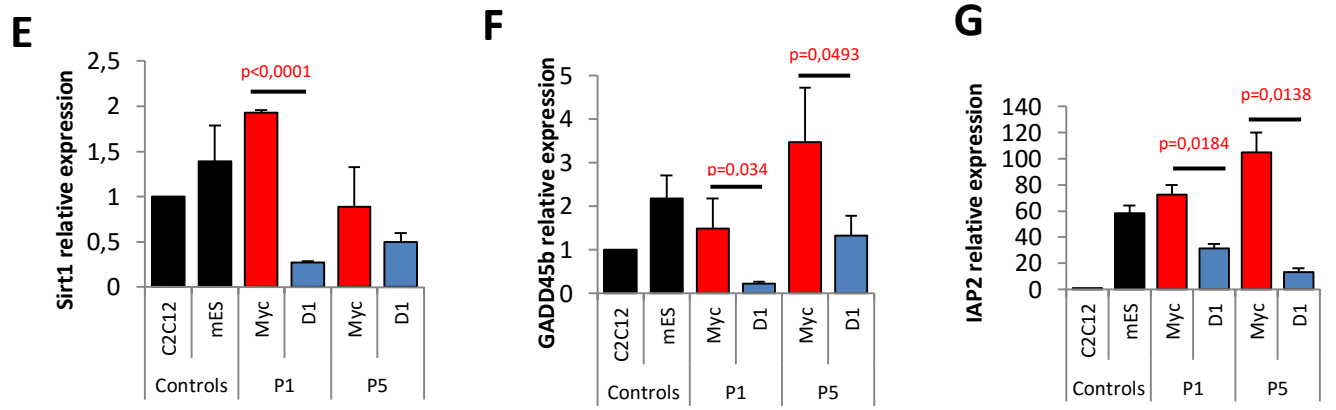
E
Sirt1 relative expression
p<0,0001
C2C12
mES
Myc
D1
Myc
D1
Controls
P1
P5
F
GADD45b relative expression
p=0,0493
p=0,034
C2C12
mES
Myc
D1
Myc
D1
Controls
P1
P5
G
IAP2 relative expression
p=0,0138
p=0,0184
C2C12
mES
Myc
D1
Myc
D1
Controls
P1
P5

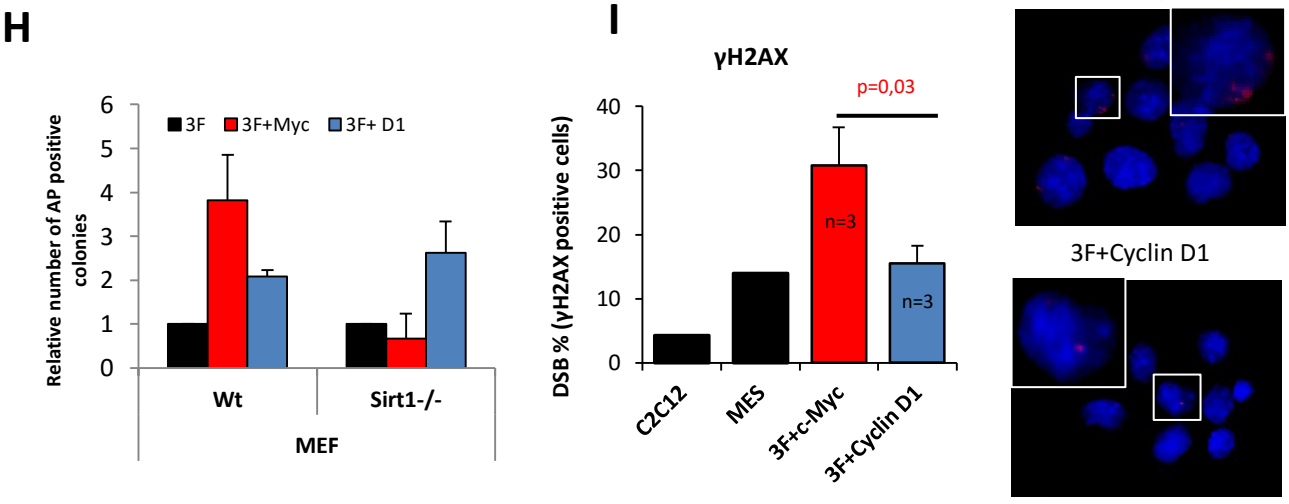
H
Relative number of AP positive colonies
3F
3F+Myc
3F+ D1
Wt
Sirt1-/-
MEF
I
γH2AX
DSB % (γH2AX positive cells)
p=0,03
n=3
n=3
C2C12
MES
3F+c-Myc
3F+Cyclin D1
3F+c-Myc
3F+Cyclin D1

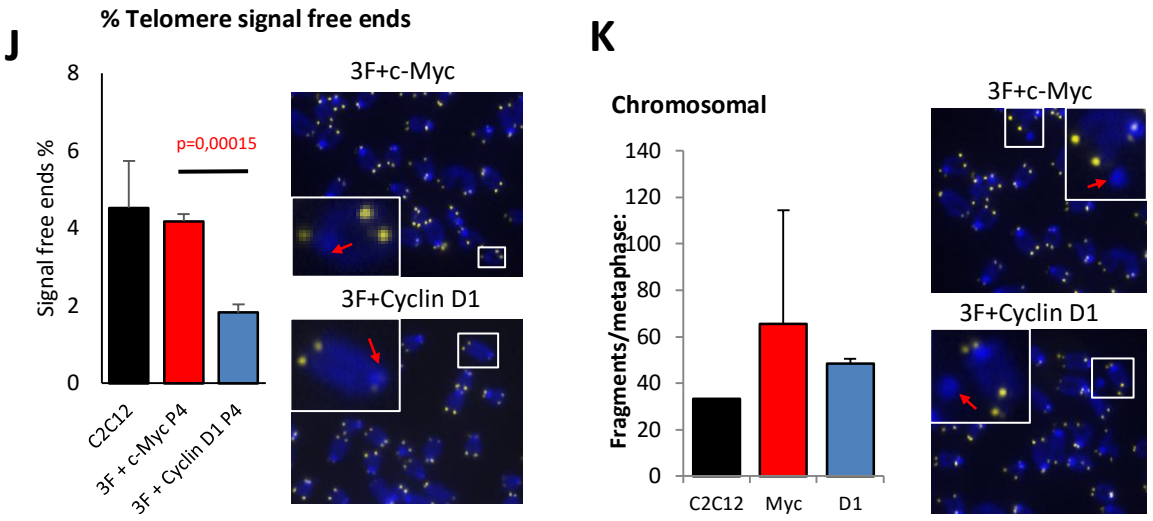

Figure 1. Cyclin D1 replaces c-Myc to reprogram mouse cells with reduced Sirt1 cell stress response and increased genetic instability.

A) Mouse iPSCs made with 3F+c-Myc and 3F+Cyclin D1 were characterized for their pluripotency. We analyzed alkaline phosphatase staining, Immunofluorescence staining of iPSCs colonies for Oct4 and SSEA3 and 4',6-diamidino-2-phenylindole (DAPI) for the nucleus and with RT-PCR **(B)** for mouse Oct4, Sox2, Nanog, Rex1 and Utf1. **C)** IPSCs were differentiated in vitro into: MESODERM stained with alfa smooth muscle actin (SMA); ENDODERM, stained with alfa 1 fetoprotein (AFP) and ECTODERM, stained with Tubulin 3 (TUJ1) and 4',6-diamidino-2-phenylindole (DAPI) for the nucleus. **D)** Alkaline phosphatase staining of reprogramming C2C12 cells in a colony formation assay in a 6-w plates, onto a feeder layer of MEFs treated with Mitomycin C. C2C12 were infected with 3F alone (Oct4, Sox2, Klf4), 3F+c-Myc or 3F+Cyclin D1, seeding 1,000 cells/well. Cells were stained after 14 and 21 days. Colonies were counted and graphed, showing how after 14 days 3F+Cyclin D1 infected cells start to form more alkaline phosphatase positive colonies than 3F+c-Myc infected cells (p-value=0,0062). After 21 days the number of colonies was not significantly different between conditions. The experiment was done in triplicate. **E)** Relative expression of the stress gene Sirtuin 1 at passage1 and 5 for both conditions (3F+c-Myc and 3F+Cyclin D1) comparing with C1C12 and mouse Embryonic Stem cells (mES). **F)** Relative expression of the NFkB target gene Gadd45b at passage1 and 5 for both conditions (3F+c-Myc and 3F+Cyclin D1) comparing with C1C12 and mES. **G)** Relative expression of the NFkB target gene IAP2 at passage1 and 5 for both conditions (3F+c-Myc and 3F+Cyclin D1) comparing with C1C12 and mES. **H)** Alkaline phosphatase staining of reprogramming Mouse Embryonic Fibroblasts (MEFs) in a colony formation assay (CFA). Wt and Sirt1-/- MEFs were transduced with the conditions 3F, 3F+c-Myc and 3F+Cyclin D1. Then, 10.000 cells/well were seeded onto feeders in a 6-well plate for a CFA. After 21 days, alkaline phosphatase staining was performed. Experiment was done in duplicate. **H)** Sirtuin 1 is not essential when reprogramming MEFs with 3F+Cyclin D1. It is compared the relative number of colonies positive for AP found for the three conditions. 3F+Cyclin D1 reprogramming has the same reprogramming efficiency in wt and in Sirt1-/- MEFs, sugesting that Cyclin D1 is rescuing cells undergoing reprogramming negative effects. On the other hand, 3F+c-Myc reprogramming shows a reduction in the number of positive alkaline phosphatase colonies, as if c-Myc was not able to rescue reprogramming negative effects or as if c-Myc itself is causing emerging colonies to enter apoptosis by the lack of recovery of reprogramming negative effects by sirtuin 1. **I)** DNA double strand breaks (DSB) analysis of mouse iPSCs compared with C2C12 and mouse embryonic stem cells (MES) through H2AX immunofluorescence staining showing less yH2AX signal in 3F+Cyclin D1 than in 3F+c-Myc iPSCs. Two representative images are given. **J)** Telomere length analysis by quantitative fluorescence *in situ* hybridization (Q-FISH), using a Cy3 labeled prove to detect CCCTAA palindromic repeats. Representative images of telomere Q-FISH in mouse cells are shown. 4',6-diamidino-2-phenylindole (DAPI) was used to stain the nucleus. Comparison between 3F+Myc and 3F+Cyclin D1 samples, for the % of signal free ends of iPSCs telomeres compared to control C2C12. 3F+Cyclin D1 clones show a lower % of signal free ends compared with 3F+c-Myc clones. Three clones per condition with 10 metaphases per clone were studied. **K)** Comparison between 3F+Myc and 3F+Cyclin D1 samples for the number of chromosomal free fragment found in the nucleus of iPSCs cells, compared to the control C2C12. All cells were arrested in metaphase to allow detection. 3F+Cyclin D1 clones decrease the number of fragments from a 70,2% found in 3F+c-Myc to a 53,4% found in 3F+Cyclin D1. Three clones per condition with 10 metaphases per clone were studied.

3F+Cyclin D1 mouse iPSC decrease % of signal-free ends and fragments/metaphase.

One of the main aims of this study is to discern whether 3F + Cyclin D1 reprogrammed iPSC acquire less genomic instability during the reprogramming process as compared to 3F+c-Myc. Therefore we established a collaboration with Dra María Blasco laboratory in Centro National de Investigaciones Oncológicas (CNIO) where I stayed and received training to analyse telomere analysis to determine which condition accumulates fewer abnormalities. We analyzed chromosome instability in 3F+c-Myc and 3F-Cyclin D1 clones, at passage 4 and 8. For controls we used non infected C2C12 and infected C2C12 cells 2 weeks after the infection with 3F, 3F+c-Myc and 3F+Cyclin D1.

First we decided to analyze the overall telomere length distribution by using the quantitative telomere FISH (Q-FISH) assay for the samples collected for the two conditions at different passages with controls. We then expressed the same data classifying it in % of long telomeres, % of short telomeres and % of signal-free ends. We could observe that 3F+Cyclin D1 clones compared to 3F+c-Myc clones presented a significant ($p=0.00015$) 50% reduction of "signal-free" ends (4,18% to 1,83%) (Figure 1, J). Signal-free ends on iPSC telomeres is associated with the appearance of extrachromosomal telomere circles or t-circles (Lustig *et al*., 2003), which have been associated with cancer. Multitelomeric signals (MTS) were analysed as well, in this case both conditions showed no difference (data not shown).

Next, we sought to test what was the number of chromosomal free fragments present in the nucleus of reprogrammed cells with both conditions. Chromosomal fragments have been reported as a sign of instability after irradiation-induced lesions (Pantelias, 1986). Interestingly, 3F+c-Myc clones' average showed a higher tendency (70.19%) of chromosomal fragments/metaphase than 3F + Cyclin D1 clones (53.4%). Therefore, Cyclin D1 clones showed a trend of lower rate of chromosomal instability (Figure 1, K).

Messenger RNA mouse reprogramming

We also attempted several times to reprogram mouse embryonic fibroblast (MEFs) with mRNA transfections of the reprogramming factors as reported by Warren in human cells (Warren et al., 2010). At the beginning, we attempted with mRNA synthetized with non-modified nucleotides, and immune response of transfected cells was avoided by siRNA transfection of INFb1, Stat2 and Eif2ak2 as previously reported (Angel et al., 2010). However, we only managed to obtain partially reprogrammed colonies that suddenly stopped growing (Annexes Figure 1).

Then, we also attempted with modified mRNA (pseudouridine instead of uridine and 5-methyl cytosine instead of cytosine) as had been reported to prevent the mRNA from generating an innate immune response in the transfected cells (Karikó et al., 2008). However, we did not succeed either, ending up with the same partially reprogrammed colonies. After several attempts changing the amount of mRNA transfected material, the type of nucleotides (non-modified and modified), cell densities and different MEF sources, we decided to focus on the human mRNA made iPSC rather than mouse.

Clinical grade reprogramming of human fibroblasts (HFF) into iPSC using synthetic messenger RNA.

Given that we have shown that Cyclin D1 represents a safer alternative to c-Myc for reprogramming, we wanted to develop a clinical grade procedure to reprogram human cells into iPSC using Cyclin D1. Therefore, messenger RNA (mRNA) transfection of the reprogramming factors (OSKLM or OSKLD, here called MH and DH iPSC) was used to eliminate the retroviral risk of insertional mutagenesis or transgene reactivation. Messenger RNA transfection reprogramming was first done in 2010 (Warren et al., 2010), and it was reported to increase reprogramming efficiency.

IPSC were cultured feeder-free to eliminate contamination with irradiated feeder cells; instead, reprogrammed cells were cultured in vitronectin coated plates. OSKM mRNA was obtained from a commercial reprogramming kit (Stemgent); however, Cyclin D1 mRNA template was constructed by splint ligation to add the alfa globin 5'UTR and 3'UTR to the Cyclin D1 coding sequence in order to stabilize it (Annexe Figure 1, C). Then, mRNA was synthetized by IVT as described in the methods. The in vitro synthesis of the mRNA and the development of this transfection protocol was performed by Dra. Ana Belén Álvarez.

HFFs were then reprogrammed by mRNA transfections during 12 days in a row, including a microRNA transfection at day 1 and 4 for reprogramming enhancement. At day 15 colonies appeared and were mechanically picked. Due to his key experience, Dr. Michael Edel picked the colonies and did the passaging of the clones during early passages. OSKLM reprogramming gave rise to 22 colonies, OSKLD gave 8 and OSKL gave no colonies (Supplementary figure 2, F). Clones were picked monoclonally and passaged until passage 10, then three clones per condition were characterized by RT-PCR and IF (Figure 2, A-B; Supplementary figure 2, D). Alkaline phosphatase (AP) staining was also performed to characterize iPSC pluripotency (Figure 2, A). Karyotype analysis showed normal chromosomal display with the presence of no aneuploidies or detectable deletion or translocation in any of the iPSC clones reprogrammed with neither c-Myc nor Cyclin D1 (Figure 2, A).

Human mRNA made iPSC with both c-Myc and Cyclin D1 (MH and DH iPSC) were able to give tissues from the three germ layers when generally differentiated after embryoid body (EB) formation. Generally differentiated cells were analyzed by RT-PCR and by IF staining for markers for the three germ layers: SMA, AFP1 and Tuj1 (Figure 2, C-D; Supplementary figure 3, A). In order to determine a more detailed in vitro pluripotency potential of DH iPSC, both MH and DH iPSC were differentiated into specific tissues from the three germ layers. Therefore, we performed a guided differentiation to Neural Stem Cells (NSC), Cardiomyocytes (CM) and Definitive Endoderm (ENDO) as described in the methods section. All these different cell types were analyzed for their specific markers by RT-PCR and IF (Figure 2, E-G; Supplementary figure 3, B-D). Videos of the beating cardiomyocytes are also given as support (Supplementary figure 3, E). Qualitatively no differences were found in their in vitro pluripotency potential, as both conditions were able to differentiate into all three germ layers cell types equally. As an internal control a commercial iPSC cell line reprogrammed with Episomal vectors containing c-Myc in the reprogramming cocktail was also differentiated into the mentioned cell types.

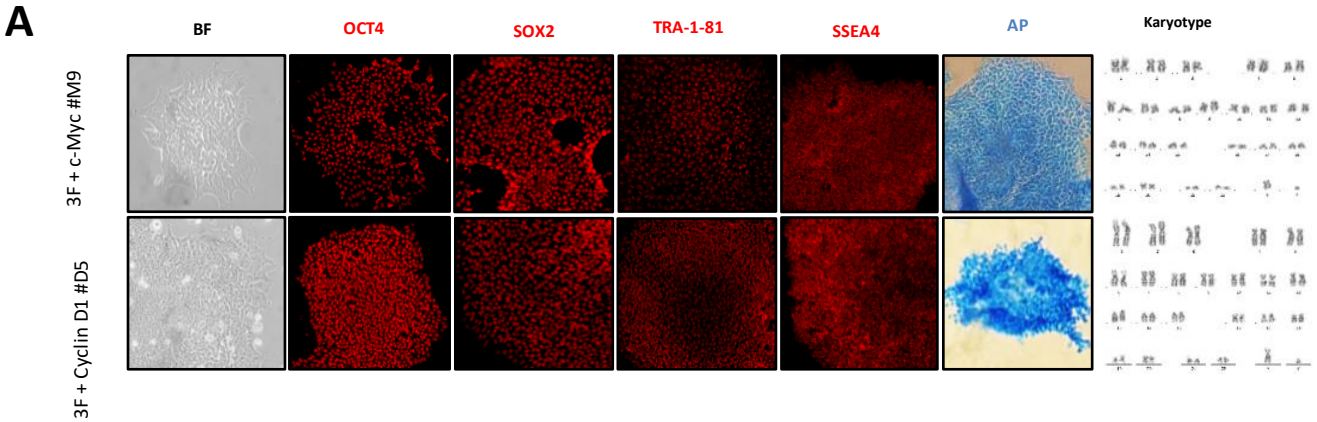
A
BF
OCT4
SOX2
TRA-1-81
SSEA4
AP
Karyotype
3F + c-Myc #M9
3F + Cyclin D1 #D5

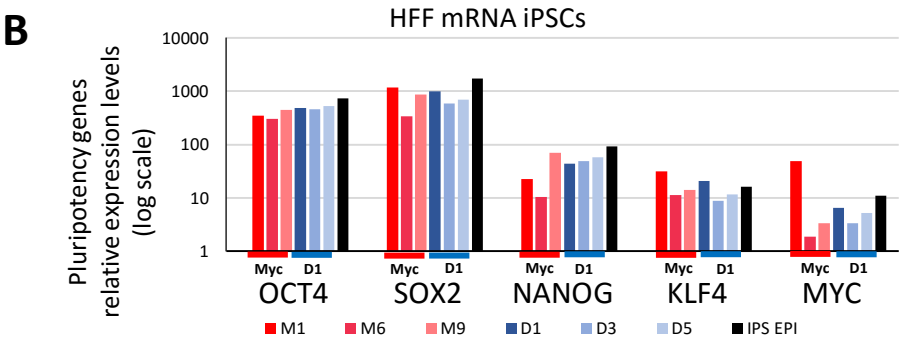
B
HFF mRNA iPSCs
Pluripotency genes
relative expression levels
(log scale)
10000
1000
100
10
1
Myc D1
OCT4
SOX2
NANOG
KLF4
MYC
M1 M6 M9 D1 D3 D5 IPS EPI

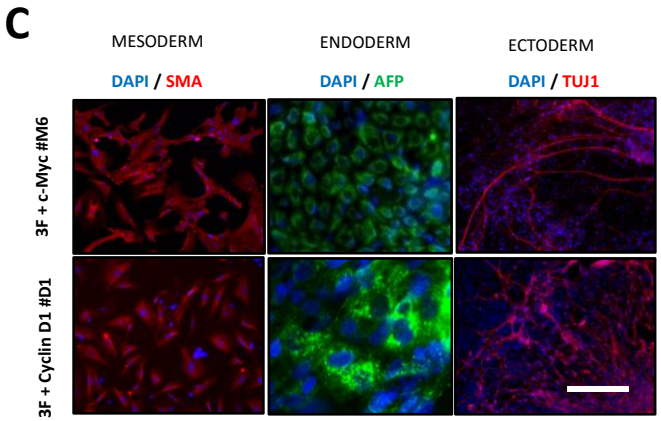
C
MESODERM
ENDODERM
ECTODERM
DAPI / SMA
DAPI / AFP
DAPI / TUJ1
3F + c-Myc #M6
3F + Cyclin D1 #D1

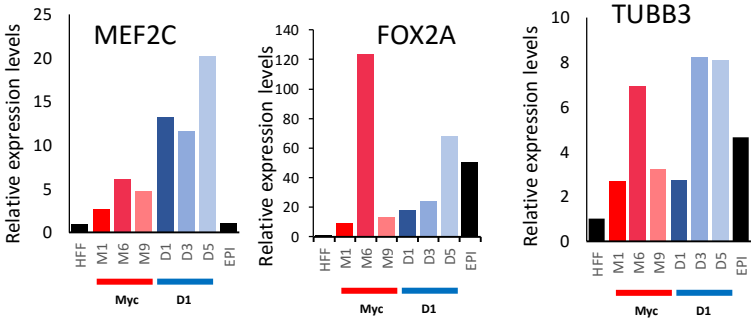
D
Relative expression levels
MEF2C
FOX2A
TUBB3
HFF M1 M6 M9 D1 D3 D5 EPI
Myc D1

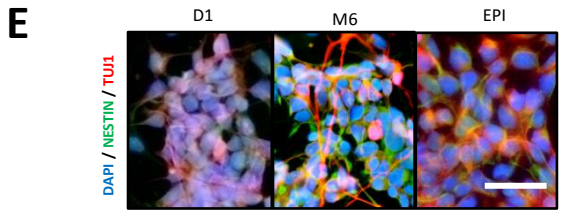
E
D1
M6
EPI
DAPI / NESTIN / TUJ1

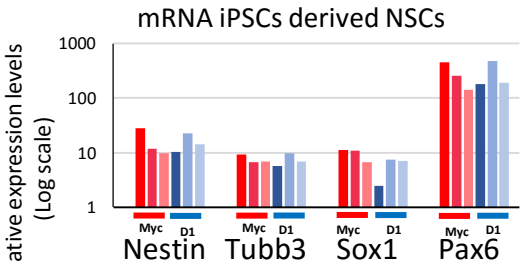
mRNA iPSCs derived NSCs
ative expression levels
(Log scale)
1000
100
10
1
Myc D1
Nestin
Tubb3
Sox1
Pax6

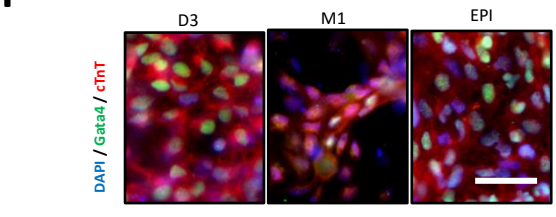
F
D3
M1
EPI
DAPI / Gata4 / cTnT

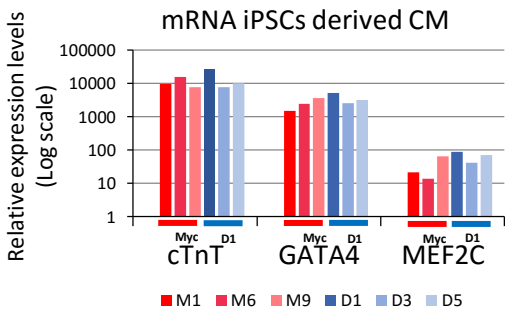
mRNA iPSCs derived CM
Relative expression levels
(Log scale)
100000
10000
1000
100
10
1
Myc D1
cTnT
GATA4
MEF2C
M1 M6 M9 D1 D3 D5

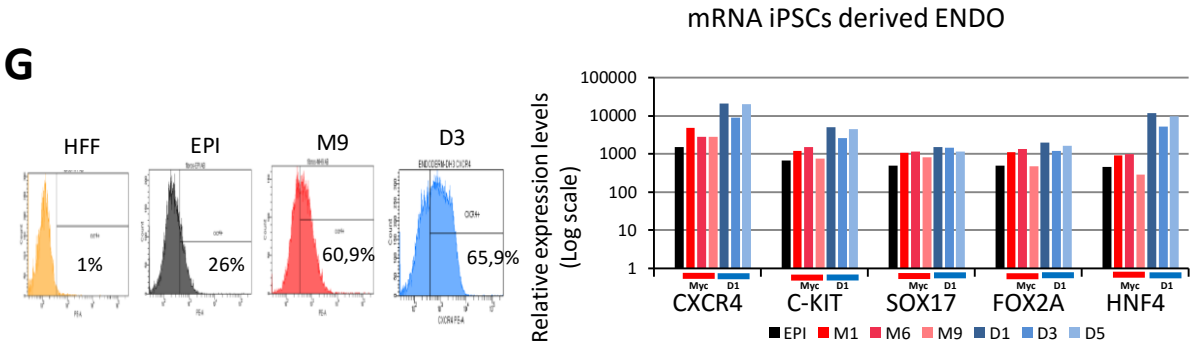

Figure 2. A new clinical grade method to generate human iPSCs replacing c-Myc with Cyclin D1.

A) Messenger RNA reprogrammed clones characterization: bright field (BF), immunofluorescence for pluripotency markers (OCT4, SOX2, TRA1-81, SSEA4) and alkaline phosphatase (AP). Karyotype of 20 metaphases per clone was also conducted; a representative image of normal karyotype is shown. One representative clone is shown for every condition (M9 and D5). Scale bars: 50µm. **B)** Real time PCR analysis of pluripotency markers OCT4, SOX2, NANOG, KLF4 and MYC. 3 clones per condition have been analyzed and compared with Episomal iPSCs. All values are relative expression levels to control HFFs and given in log scale. **C)** Immunofluorescence characterization of iPSCs general differentiation in vitro into MESODERM stained with alfa smooth muscle actin (SMA); ENDODERM, stained with alfa 1 fetoprotein (AFP) and ECTODERM, stained with Tubulin 3 (TUJ1). Scale bars: 20µm. **D)** Real time PCR analysis of generally differentiated. MEF2C, FOX2A and TUBB3 were analyzed to determine mesoderm, endoderm and ectoderm expression levels. **E)** Characterization of hiPSCs differentiated into Neural Stem Cells (NSC) by immunofluorescence (Nestin and Tuj1) and by qPCR (Nestin, Tubb3, Sox1 and Pax6). All values are relative expression levels to control HFFs and given in log scale. Scale bars: 10µm. **F)** Characterization of hiPSCs differentiated into Cardiomyocytes (CM) by immunofluorescence (Gata4 and cTnT) and by qPCR (cTnT, Gata4 and MEF2C). All values are relative expression levels to control HFFs and given in log scale. Scale bars: 10µm. **G)** Characterization of hiPSCs differentiated into Endoderm (ENDO) by flow cytometry (CXCR4 positive cells) and by qPCR (CXCR4, C-KIT, SOX17, FOX2A, HNF4). All values are relative expression levels to control HFFs and given in log scale.

In vivo differentiation of DH iPSC into teratomas reduce the % of KI67.

Athymic FoxN1 nu/nu mice were subcutaneously injected with both MH and DH iPSC to test and compare in vivo differentiation capacity. Teratomas were left to grow until a maximum volume of 2000mm^3 (Figure 3, A; Supplementary figure 4, A) and then were extirpated, fixed in paraformaldehyde and embedded in paraffin. Sections were made and stained for Hematoxylin/Eosin to determine three germ layer structures (Figure 3, B; Supplementary figure 4, B). Teratoma size was also affected by the reprogramming condition, two clones of DH iPSC gave rise to teratomas that stopped growing and stabilized their weigh. Despite this lack of growth, these clones also were able to form three germ layer structures in vivo.

IPSC tumorigenic threat in vivo was assessed by analyzing KI67% in the teratomas. KI67 staining is usually evaluated for determining tumor potentiality of neoplasms. After counting more than 200 cells from five randomly picked images from each teratoma, we found that MH iPSC injected gave rise to teratomas containing around 70% of KI67 positive cells in comparison with only 20% in DH teratomas (p=0.0097) (Figure 3, C; Supplementary figure 4, C). Even MH iPSC teratomas growth rate was higher in almost all three clones than DH iPSC teratomas. IPSC derived Neural stem cells were also analyzed in vitro for KI67% to compare MH and DH iPSC derived NSC

proliferative tumorigenic threat in vitro. Again, we saw significance between MH and DH clones (p=0.0311) (Figure 3, D).

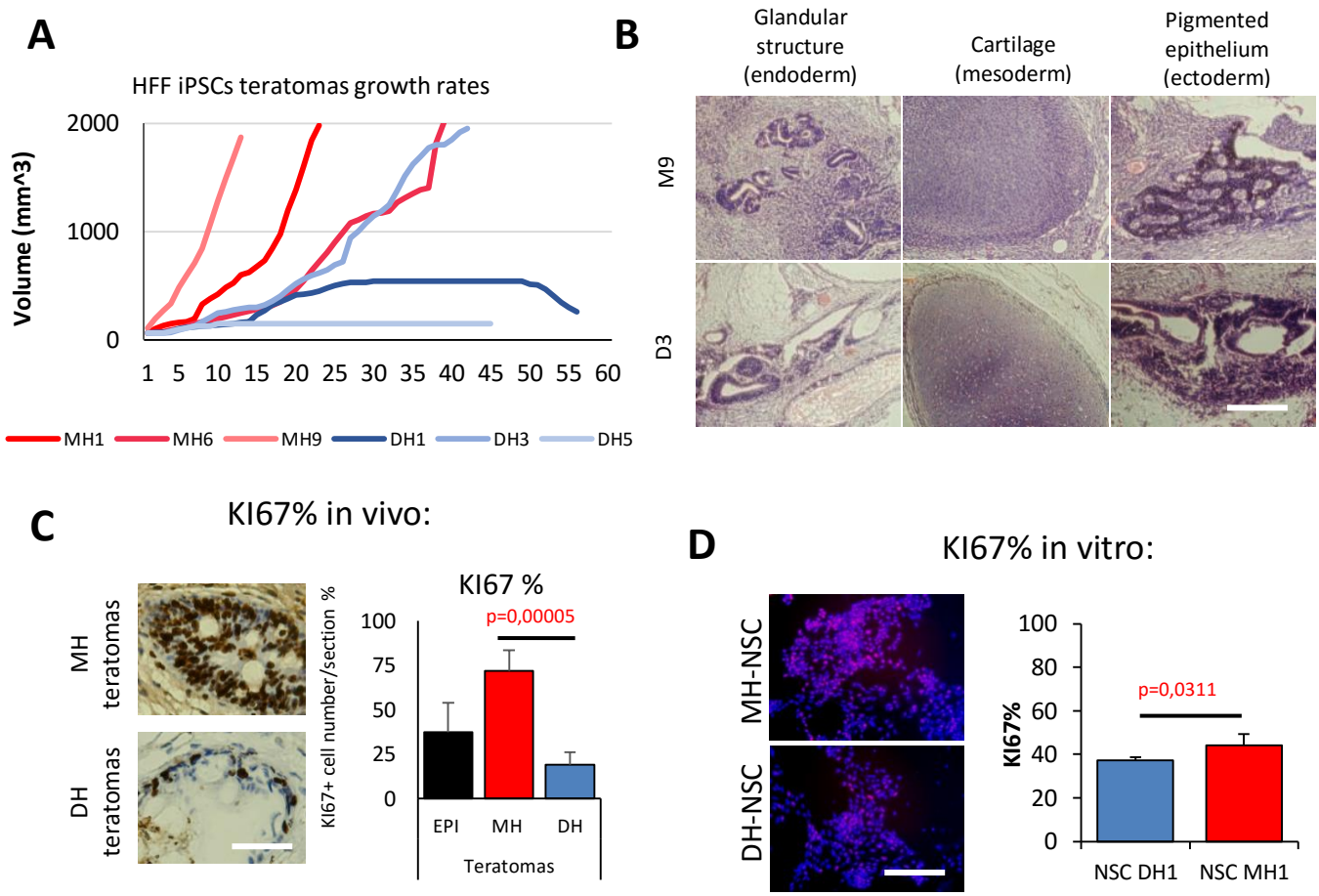

Figure 3. Cyclin D1 made iPSCs have a lower tumorigenic threat (KI67%) in vitro and in vivo compared to c-Myc made iPSCs.

A) In vivo pluripotency was tested with teratoma formation by injecting mRNA iPSCs from both conditions in athymic nude mice (Foxn1-/-) to examine the pluripotency potential into the three germ layers. Graph shows teratomas growth rates (volume in mm3) comparing c-Myc (M1, M6 and M9) and Cyclin D1 (D1, D3 and D5) iPSCs teratomas. **B)** Teratomas were fixed in PFA 4%, embedded in paraffin and stained for hematoxylin/eosin (H/E). Representative three-germ-layer structures are shown for every condition. Scale bars: 100µm. **C)** Cell proliferation rate (KI67%) assessment in teratomas comparing every condition. MH clones presented a higher KI67% compared to DH clones (p value=0,0097). Scale bars: 50µm.**D)** KI67% was determined in neural stem cells (NSC) in vitro comparing MH with DH NSC clones. After counting 1000 cells per condition, MH clones presented a higher KI67% compared to DH clones (p value= 0,0311). Scale bars: 100µm.

Cyclin D1 made human iPSC show a reduced % of DSB.

3F+Cyclin D1 mouse iPSC presented a lower number of DSBs than 3F+c-Myc iPSC. Therefore, we also analyzed the human clinical grade iPSC for DSB %. Results show that human DH iPSC also present a lower percentage of H2AX than MH iPSC at passage 10 (Figure 4, A-B).

Next, in order to corroborate that Cyclin D1 overexpression was promoting more DNA repair through homologous recombination, we assessed the levels of Rad51 in both conditions at passage 2, 10 and in NSC by counting the percentage of cells that their nucleus was positive for Rad51 (Figure 4, C-D). We have found that in early passage 2, MH clones display Rad51 in a major proportion in the cytoplasm than DH clones (Figure 4, B). It has been reported that homologous recombination is inhibited when Rad51 is retained in the cytoplasm as a consequence of AKT1 upregulation (Plo et al., 2008). Therefore, we conclude that MH clones at passage 2 present a lower rate of homologous recombination than DH clones.

Furthermore, Sirtuin 1 is recruited to the lesion site of DSBs and has been reported as necessary for initial DSB signaling event an DNA repair (Dobbin et al., 2013); correspondingly we found that sirt1 showed higher expression in MH than in DH iPSC as a consequence of the higher amount of DSBs. This increase in Sirt1 levels were only found during early passages (Figures 3, H), however, at passage 10, when Sirt1 levels had become already even, DSBs were still higher in MH iPSC. This could explain why Sirt1-/- MEFs couldn't be reprogrammed with c-Myc. IPSC derived CM and NSC showed no differences in Sirt1 levels between conditions (Supplementary figure 4, F).

As has been described in the introduction, c-Myc overexpression has been linked with promotion of alternative NHEJ repair mechanism. Thus, to check whether MH iPSC presented higher levels of alt-NHEJ than any other repairing type, we analyzed a battery of DNA damage response genes by RT-PCR: Rad51, Rad51B, Ku70, BRCA1, BRCA2, LIG3 and POLQ at different passages of iPSC made with Myc and Cyclin D1. Only LIG3 and RAD51B were found significantly different. The alternative NHEJ Ligase 3 (LIG3) levels (Figure 4, D) show that LIG3 is significantly more expressed in MH clones during early passage 3 than DH clones, supporting our idea. Rad51B was also found significantly differently ($p=0,024$) in passage 3 iPSC (Figure 4, G).

In order to find a possible footprint of the reprogramming process in any of the DNA damage repairing genes, we screened the methylation patterns by using the Infinium MethylationEPIC kit array. However, although we did not see differences globally between MH and DH clones, we checked for genes that are related with DNA repairing systems in iPSC (Figure 4, H). Interestingly differences ($\geq 20\%$) between MH and DH clones were found in several CpG sites of RAD51B gene, however they all were located inside the body of the gene instead of in the promoter. XRCC6 and RAD50 genes also had a significantly different methylation status between MH and DH clones. However, after analyzing these same genes by real time PCR, expression levels were not found differently regulated for this two genes, only RAD51B was found differently expressed at passage 3 iPSC (Figure 4, G).

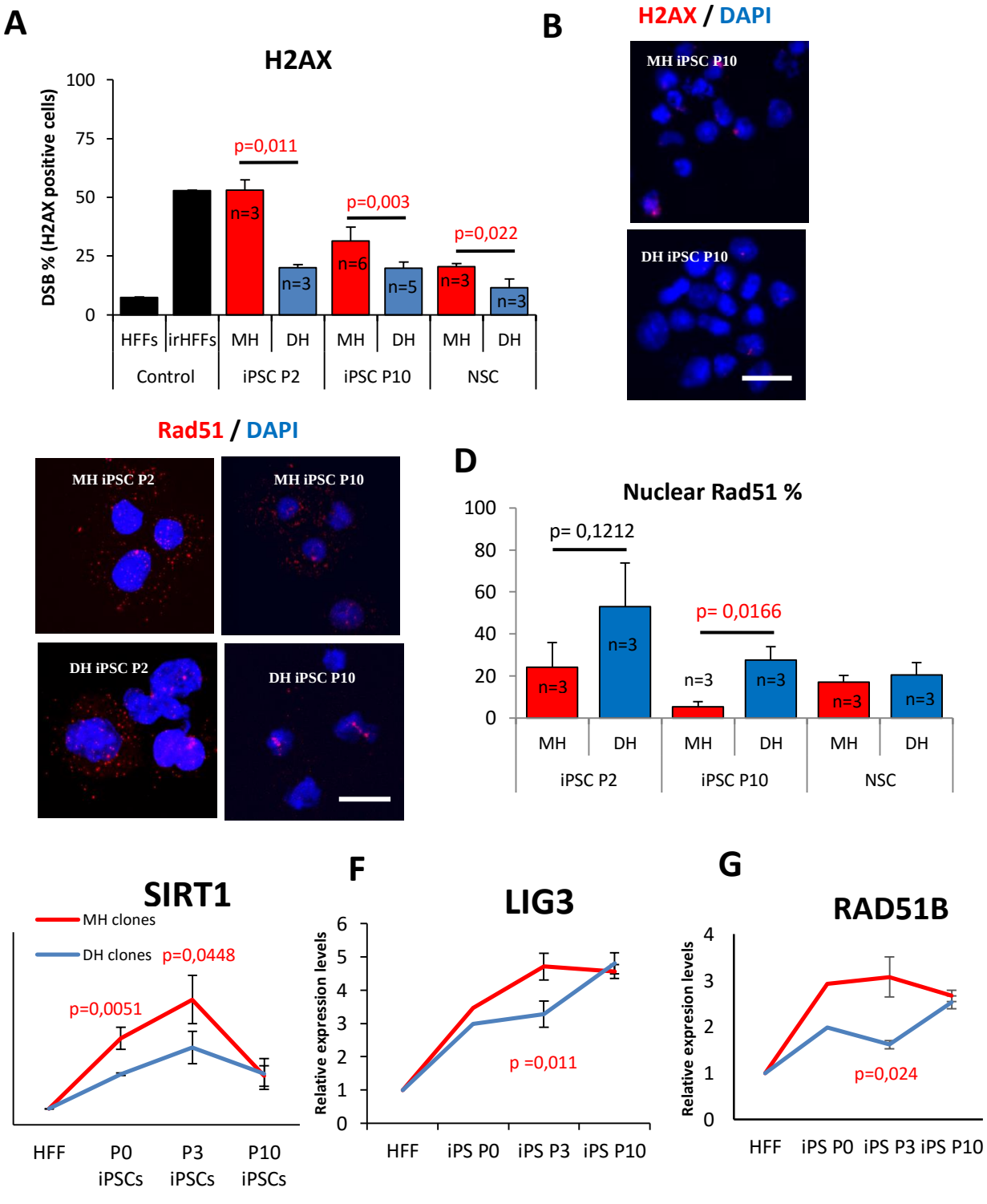
A
H2AX
DSB % (H2AX positive cells)
100
75
50
25
0
p=0,011
p=0,003
p=0,022
n=3
n=3
n=6
n=5
n=3
n=3
HFFs
irHFFs
MH
DH
MH
DH
MH
DH
Control
iPSC P2
iPSC P10
NSC
B
H2AX / DAPI
MH iPSC P10
DH iPSC P10
C
Rad51 / DAPI
MH iPSC P2
MH iPSC P10
DH iPSC P2
DH iPSC P10
D
Nuclear Rad51 %
100
80
60
40
20
0
p= 0,1212
p= 0,0166
n=3
n=3
n=3
n=3
n=3
n=3
MH
DH
MH
DH
MH
DH
iPSC P2
iPSC P10
NSC
E
SIRT1
Relative expression levels
12
8
4
0
MH clones
DH clones
p=0,0448
p=0,0051
HFF
P0 iPSCs
P3 iPSCs
P10 iPSCs
F
LIG3
Relative expression levels
6
5
4
3
2
1
0
p =0,011
HFF
iPS P0
iPS P3
iPS P10
G
RAD51B
Relative expresion levels
4
3
2
1
0
p=0,024
HFF
iPS P0
iPS P3
iPS P10
H
Differently methylated CpG sites of DNA repair genes in iPSC P10
Cyclin D1
c-Myc
1,0
0,8
0,6
0,4
0,2
0,0
Body 18,1%
TSS1500 9,7%
5'UTR 34,0%
TSS200 17,1%
Body 48,9%
Body 43,3%
Body 36,4%
Body 19,7%
Body 17,2%
Body 15,3%
Body 20,8%
Body 14,5%
Body 42,2%
Body 20,7%
CpG1
CpG2
CpG1
CpG1
CpG1
CpG2
CpG3
CpG4
CpG5
CpG6
CpG7
CpG8
CpG1
CpG2
BRCA1
RAD50
RAD51
RAD51B
XRCC6

Figure 4. Cyclin D1 iPSCs have lower DNA double strand breaks (DSB) and a higher Homologous Recombination rate through Rad51 recuitment compared to c-Myc iPSCs.

A) DNA double strand breaks (DSB) analysis of human iPSCs through H2AX immunofluorescence staining **(B)** showing less yH2AX signal in DH iPSCs and NSC than in MH. Scale bars: 20µm. **C)** Rad51 immunofluorescence staining: MH P2 iPSC present higher cytoplasmic retention of Rad51 than DH P2 iPSC. Scale bars: 10µm. **D)** Nuclear Rad51 protein % in MH and DH iPSC at passage 2, passage 10 and NSC. Passage 10 iPSC showed significant differences (p=0,0166) between conditions. **E)** Cell stress gene Sirtuin 1 is found significantly upregulated during early passages of MH iPSC compared with DH iPSC. However, after 10 passages Sirt1 levels equalize. **F-G)** RT-PCR analysis of ligase 3 (LIG3) and RAD51B in iPSC at passage 0, 3 and 10 compared with control HFFs. Three clones (n=3) per conditions were quantified. **H)** Methylation pattern of several CpG sites of the DNA repair genes: BRCA1, RAD50, RAD51, RAD51B and XRCC6, that were found differently methylated between MH and DH NSC. It is shown the position of the CpG on the gene (TSS1500, TSS200, 5'UTR and Body) and the % of diference between c-Myc and Cyclin D1.

Cyclin D1 made human iPSC show a decreased % of MTS per chromosome.

We wanted to investigate whether human iPSC reprogrammed with Cyclin D1 (DH iPSC) had an improved chromosomal stability as found in mouse iPSC. We thus repeated the telomere analysis through QFISH staining and determined the % of signal free ends and multitelomeric signals. In this case no differences were found in the % of signal-free ends between conditions. However, we show how MH iPSC and NSC carry a higher percentage of multitelomeric signal (MTS) per chromosome than DH iPSC and NSC (Figure 5, A and C). Therefore Cyclin D1 give raise to chromosomally more stable iPSC and NSC than MH. Number of free chromosome fragments was also analysed but no difference were seen between conditions for human iPSC (data not shown).

Telomere length was higher in MH than in DH NSC clones (Figure 5, B). Since the absence of telomere maintenance has been proposed to act as a tumor-suppressive mechanism (Serrano and Blasco, 2007), cells differentiated from DH iPSC might be less tumor prone.

Moreover, Sirt1 has been reported to be necessary for proficient telomere elongation and genomic stability of induced pluripotent stem cells (De Bonis et al., 2014). Sirt1 also contributes to telomere maintenance and augments global homologous recombination. Sirtuin 1 null mouse embryonic fibroblasts (Sirt1-/-MEFs) were shown to express higher multitelomeric signals per chromosome (Palacios et al., 2010).

Copy number variation (CNV), single nucleotide polymorphism (SNP) and methylome screening analysis.

In order to deepen more into other genetic instability differences between MH and DH iPSC, we did a screening for Copy number variation (CNV), single nucleotide polymorphism (SNP) and methylation patterns of iPSCs and iPSC derived cells. Thus, we established collaboration with Dr. Manel Esteller and Dr. Raul Delgado's laboratory from the Cancer epigenetics group in the *Institut d'Investigacions Biomèdiques de Bellvitge* (IDIBELL). We collected the samples and they carried out the array analysis to study SNP, CNV and a methylome analysis in our new condition made iPSC.

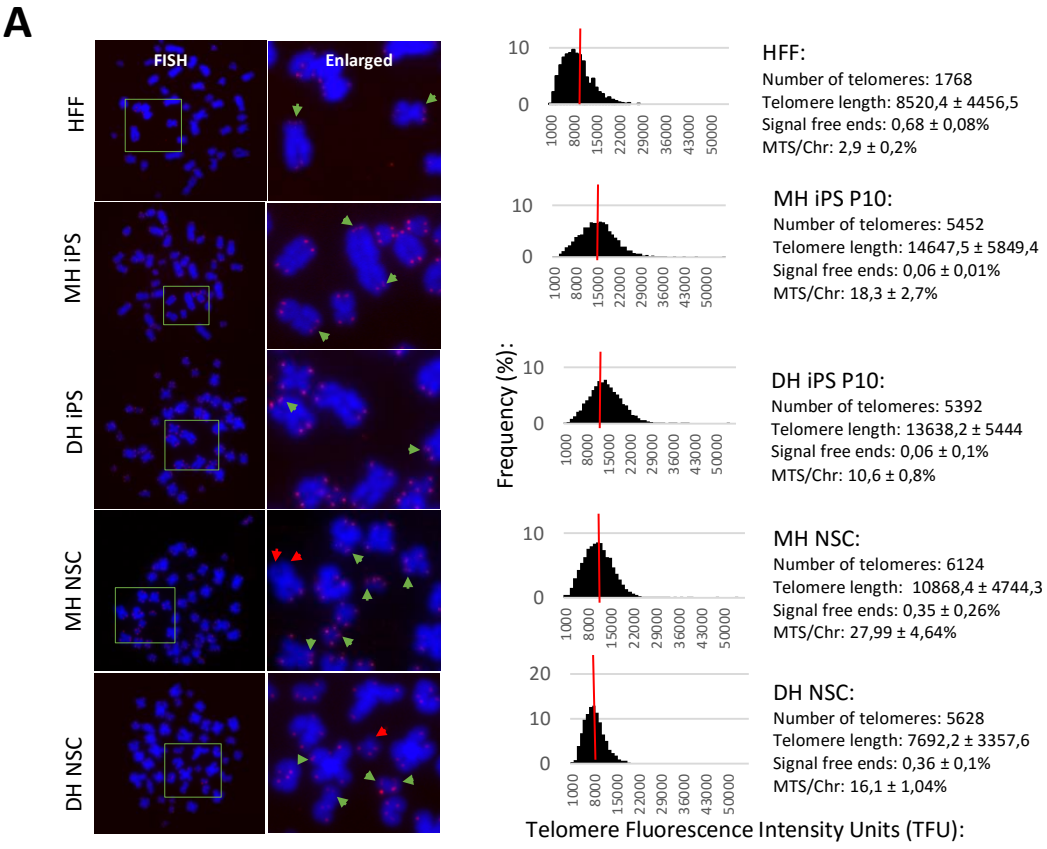
A
FISH
Enlarged
HFF
MH iPS
DH iPS
MH NSC
DH NSC
Frequency (%):
HFF:
Number of telomeres: 1768
Telomere length: 8520,4 ± 4456,5
Signal free ends: 0,68 ± 0,08%
MTS/Chr: 2,9 ± 0,2%
MH iPS P10:
Number of telomeres: 5452
Telomere length: 14647,5 ± 5849,4
Signal free ends: 0,06 ± 0,01%
MTS/Chr: 18,3 ± 2,7%
DH iPS P10:
Number of telomeres: 5392
Telomere length: 13638,2 ± 5444
Signal free ends: 0,06 ± 0,1%
MTS/Chr: 10,6 ± 0,8%
MH NSC:
Number of telomeres: 6124
Telomere length: 10868,4 ± 4744,3
Signal free ends: 0,35 ± 0,26%
MTS/Chr: 27,99 ± 4,64%
DH NSC:
Number of telomeres: 5628
Telomere length: 7692,2 ± 3357,6
Signal free ends: 0,36 ± 0,1%
MTS/Chr: 16,1 ± 1,04%
Telomere Fluorescence Intensity Units (TFU):

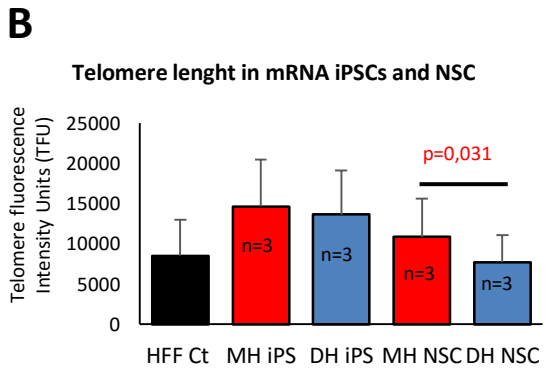
B
Telomere lenght in mRNA iPSCs and NSC
Telomere fluorescence Intensity Units (TFU)
p=0,031
n=3
HFF Ct
MH iPS
DH iPS
MH NSC
DH NSC

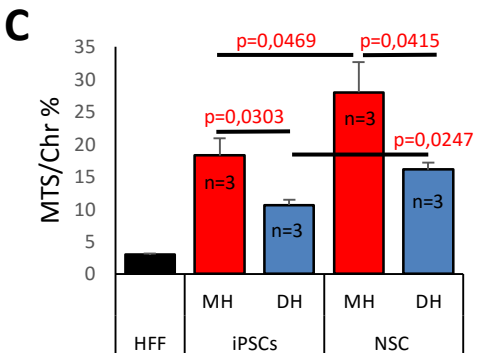
C
MTS/Chr %
p=0,0469
p=0,0415
p=0,0303
p=0,0247
n=3
HFF
MH
DH
iPSCs
NSC

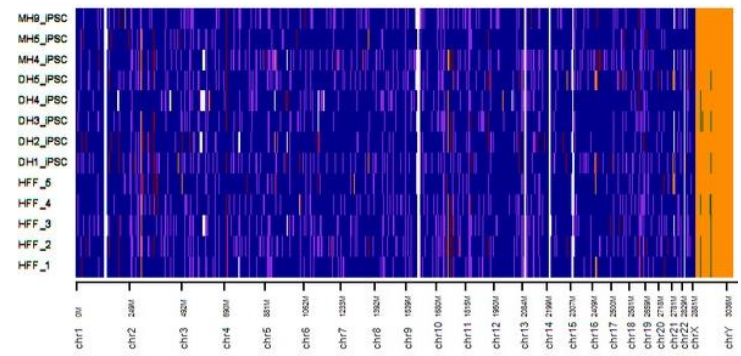
D
MH9_iPSC
MH5_iPSC
MH4_iPSC
DH5_iPSC
DH4_iPSC
DH3_iPSC
DH2_iPSC
DH1_iPSC
HFF_6
HFF_4
HFF_3
HFF_2
HFF_1

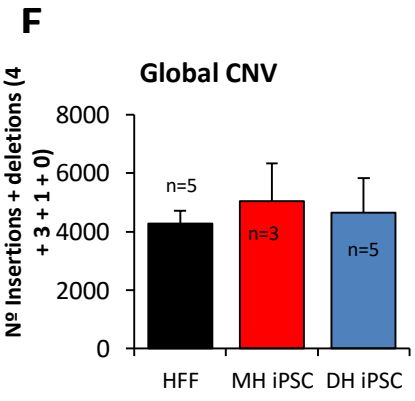
F
Global CNV
Nº Insertions + deletions (4 + 3 + 1 + 0)
n=5
n=3
HFF
MH iPSC
DH iPSC

Figure 5. Clinical grade human iPSCs replacing c-Myc with Cyclin D1 increase genetic stability.

A) Telomere length analysis by quantitative fluorescence *in situ* hybridization (Q-FISH), using a Cy3 labeled prove to detect CCCTAA palindromic repeats. Representative images of telomere Q-FISH in human cells are shown. Green squares are shown enlarged in the right column. Human foreskin fibroblasts (HFF) were reprogrammed into iPSC by weather MH or DH. IPSCs were passaged until passage 10, then cells were stained and analyzed for telomere length, signal free ends and multitelomeric signals per chromosome (MTS/Chr) %. IPSCs were differentiated into neural stem cells (NSC), then passaged 3 times and analyzed as in iPSCs. Three clones per condition with 10 metaphases per clone were studied. Blue: DAPI-stained chromosomes; red dots: telomeres; green arrows: multitelomeric signals (MTS); red arrows: signal free ends (SFE). **B)** Histograms showing frequency % of relative telomere lengths shown as telomere fluorescence units (TFUs). The medium telomere length (red bars on top of frequency graphs) is also shown as mean ± SE. Total numbers of telomeres analyzed per condition are shown. MTS/Chr% and signal free ends % values are also given. **C)** Graph presenting the % of MTS per chromosome in iPSCs and NSC made with both conditions. There's an increase in the % of MTS per chromosome in MH iPSCs and derived NSC compared with DH iPSCs and NSC as a result of cell stress. On the other hand, in mouse cells differences were not detected in multitelomeric signals but in the percentage of signal free ends (data not shown), that on the contrary was almost identical in human cells (data not shown). **D)** Copy Number Variation (CNV) was studied for passage 10 MH iPSCs (n=6 clones) and DH iPSCs (n=5 clones) with a human genome-wide array kit. Results are classified in function of the chromosome where they are located and the amount of copies of the segments analyzed. Garnet: 0-0,5 copies; yellow: 0,5-1,5 copies; green: 1,5-2,5 copies; blue: 2,5-3,5 copies; purple: 3,5-4,5 copies. **E)** Total number of CNV variation taking into account deletions of one or two copies (0 + 1) and insertions of one or two copies (3 + 4), averaging five samples for control HFFs, three for MH iPSC and five for DH iPSC.

It is well established that replicative stress increases SNPs incidence, therefore first we screened in our human clinical grade iPSC from both conditions the presence of SNPs in comparison with control HFFs using the Omnis 5.0 Illumina array. In order to decrease clonal variability and increase sample size, we expanded and characterize (annexes figure 2) more clones for both MH (final n=6 clones) and DH (final n=5 clones). We didn't find differences in SNP incidence between conditions (Figure 5, D), although there was a trend of SNP upregulation after MH reprogramming comparing with DH.

Chromosomal instability is characterized by chromosomal abnormalities and an altered gene expression signature. For example, c-Myc deregulation is directly linked with gene amplification. Hence, we assessed copy number variation (CNV) in our iPSC and NSC made with both conditions (Figure 5, E). CNVs were studied using the information gathered with a SNP array. When comparing conditions, we found a trend of decreased total amount of CNVs (both number of deletions and insertions) in DH clones. However, it wasn't significantly different neither due to huge standard deviation differences because of clonal variability. Now, we are analyzing more clones to reduce variability.

Furthermore, in order to compare if there was any differences at the genome methylation level between MH and DH iPSC we did a general methylome analysis between conditions. Correspondingly, analysis revealed no differences (data not shown, under analysis).

Global proteomic analysis of patient (F1) and iPSC-derived fibroblasts (F2).

There is a clear need in the field to better understand the immune response of cells derived from reprogrammed cells before we board on extensive clinical trials to treat human disease. Therefore, in order to address this second aim of the thesis, we performed a detailed assessment comparing six patient fibroblast cell lines (termed F1) reprogrammed into iPSC and subsequently differentiated back to fibroblast cells (termed F2).

Six human skin fibroblast cell lines (termed F1) that have previously been reprogrammed into iPSC, three by retroviral methods (Sanchez et al., 2012a; Sanchez et al., 2012b) and three by non-viral Episomal methods (Briggs et al., 2013), then differentiated back to fibroblasts (termed F2) (Figure 6, A) were analysed for their potential immune response. First, in collaboration with Dr. Rafael Oliva group and Dr. Josep Mª Estanyol from the Molecular Biology Unit in the Medicine Faculty, they performed a global proteomic analysis comparing F1 cell lines to their paired F2 and mapped the protein expression profile.

Overall, 1508 quantifiable proteins were detected with a confidence of 0.90 of which 87 proteins with significantly different expression levels between F1 and F2 cells. Categorising proteins based on function, we first demonstrated no difference in fibroblast markers CD90, Fibronectin and CD44 between F1 and F2 cells indicating that they are similar fibroblast cell populations for both viral and non-viral made iPSC-derived cells (Figure 6, B).

The main differences in protein expression in F2 cells are signal transduction, cell cycle and immune system proteins (Figure 6, C-E). Interestingly, the proteomic screen revealed many proteins that have been shown to interact with the toll-like receptor TLR3 and TLR4 pathway (Figure 6, F-G).

To verify the global proteomic analysis we performed flow cytometry analysis of the F1 and F2 populations and confirmed that the two fibroblast cell populations are similar for two fibroblast cell markers CD90, CD44 and negative for stem cell marker CD34 (Figure 6, I). This was the same for retrovirally made iPSC-derived cells or non-virally made iPSC-derived cells. Given that signal transduction proteins were the most represented differentially expressed proteins between F1 and F2 cells, we also verified that AKT signal transduction is overactivated in F2 cells compared to F1 cells by western blot analysis (Figure 6, H).

A

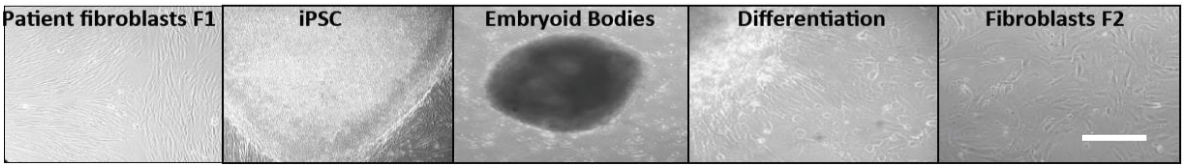

B

Proteins in hMSC, hHematopoietic and hFibroblasts cells

	Gene	Name	Access	P-value
hMSC	CD105	Endoglin	P17813	ni
	CD90	Thy-1 membrane glycoprotein	P04216	0,36
	CD44	CD44 antigen	P16070	0,40
	CD73/NT5E	5'-nucleotidase	P21589	0,72
	CD29/ITGB1	Integrin beta-1	P05556	0,61
hHematopoietic	CD45	Protein tyrosine-protein phosphatase	P08575	ni
	CD34	Hematopoietic progenitor cell antigen	P28906	ni
hFibroblasts	Fibronectin	Fibronectin	P02751	0,88

ni: protein not identified

C

Differential proteins involved in Immune Response (p≤0.05)

Accession	Description	F2:F1
According to Reactome (FDR 1%)		
P15151	Poliovirus receptor	1,57
Q8N8S7	Protein enabled homolog	1,50
Q14123	Calcium/calmodulin-dependent 3',5'-cyclic nucleotide phosphodiesterase 1C	1,43
O75369	Filamin-B	1,36
Q9Y2Z0	Suppressor of G2 allele of SKP1 homolog	1,35
P53992	Protein transport protein Sec24C	1,13
Q06124	Tyrosine-protein phosphatase non-receptor type 11	1,11
Q9UNM6	26S proteasome non-ATPase regulatory subunit 13	1,10
P67775	Serine/threonine-protein phosphatase 2A catalytic subunit alpha isoform	1,08
Q9BUF5	Tubulin beta-6 chain	1,06
O00231	26S proteasome non-ATPase regulatory subunit 11	1,04
P14314	Glucosidase 2 subunit beta	0,89
Q13409	Cytoplasmic dynein 1 intermediate chain 2	0,89
P31946	14-3-3 protein beta/alpha	0,87
P27361	Mitogen-activated protein kinase 3	0,86
P61769	Beta-2-microglobulin	0,78
Q9UBG0	C-type mannose receptor 2	0,72
According to Panther		
P02462	Collagen alpha-1(IV) chain	1,67
Q8TED1	Probable glutathione peroxidase 8	0,86
P61769	Beta-2-microglobulin	0,78
P08107	Heat shock 70 kDa protein 1A/1B	0,75
Q9UBG0	C-type mannose receptor 2	0,72
Q14155	Rho guanine nucleotide exchange factor 7	0,71
P07203	Glutathione peroxidase 1	0,66
P06703	Protein S100-A6	0,62

D

Differential proteins involved in Signal Tansduction (p≤0.05)

Accession	Description	F2:F1
P02462	Collagen alpha-1(IV) chain	1,67
P05121	Plasminogen activator inhibitor 1	1,62
Q14123	Calcium/calmodulin-dependent 3',5'-cyclic nucleotide phosphodiesterase 1C	1,43
Q06124	Tyrosine-protein phosphatase non-receptor type 11	1,11
Q9UNM6	26S proteasome non-ATPase regulatory subunit 13	1,10
P67775	Serine/threonine-protein phosphatase 2A catalytic subunit alpha isoform	1,08
Q9BUF5	Tubulin beta-6 chain	1,06
O00231	26S proteasome non-ATPase regulatory subunit 11	1,04
P31946	14-3-3 protein beta/alpha	0,87
P27348	14-3-3 protein theta	0,87
Q14247	Src substrate cortactin	0,87
Q9UBQ0	Vacuolar protein sorting-associated protein 29	0,86
P27361	Mitogen-activated protein kinase 3	0,86
P61586	Transforming protein RhoA	0,84
O14974	Protein phosphatase 1 regulatory subunit 12A	0,84
O60493	Sorting nexin-3	0,82
Q14155	Rho guanine nucleotide exchange factor 7	0,71

E

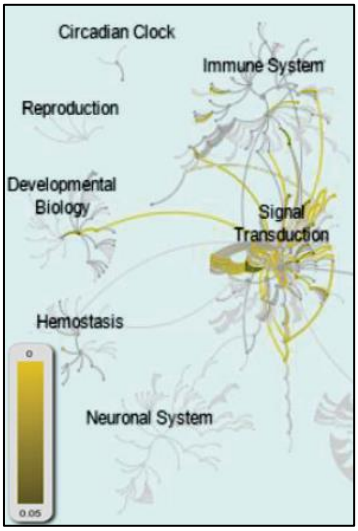

F

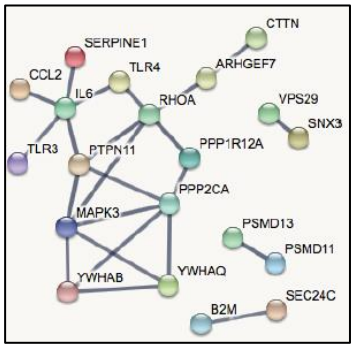

G

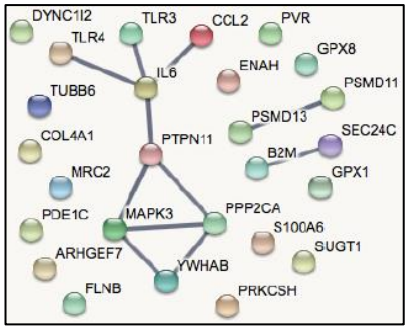

H

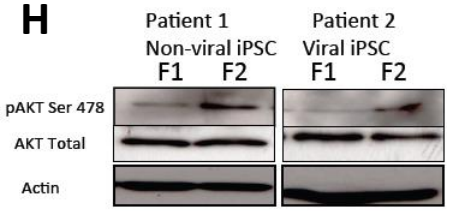

I

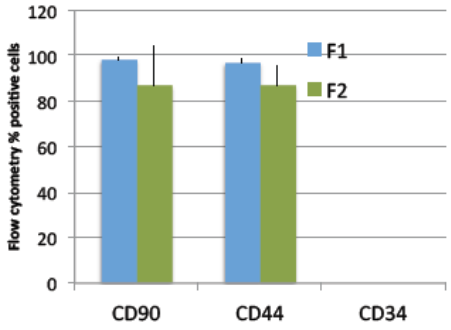

Figure 6: Global proteomic analysis of patient (F1) and iPSCs-derived fibroblasts (F2).

A) Panels left to right: photos representative of the patient fibroblasts, termed F1, iPSC clone, differentiation to embryoid bodies (EB) and iPSC-derived fibroblasts, termed F2, at two different passages (x100). Scale bars: 10µm. **B)** Table showing proteins characteristic of human mesenchymal stem cells (MSC), hematopoietic and fibroblasts that have either been identified or not in the F1 and F2 cells. The p-value indicates that there is no difference in the amount of these proteins between F1 and F2. **C)** Table showing the differential proteins between F1 and F2 involved in Immune Response according to Reactome and Panther. **D)** Table showing the differential proteins between F1 and F2 involved in Signal Transduction according to Reactome. **E)** Schematic of Pathways overrepresented (in yellow) of all proteins detected (Reactome). **F)** Interactions among the differential proteins involved in Signal Transduction and the TRL3, TRL4, IL6 and CCL2 proteins (highest confidence = minimum interaction score of 0.900). **G)** Interactions among the differential proteins involved in Immune System and the TRL3, TRL4, IL6 and CCL2 proteins (highest confidence = minimum interaction score of 0.900). **H)** Validation of proteomic screen. Western blot analysis of the PI3Kinase signal transduction pathway for total and phosphorylated AKT in F1 and F2 cells confirming overexpression of AKT signal transduction in F2 cells. **I)** Graph of flow cytometry for fibroblast markers CD90, CD44 and negative control marker CD34 (MSC marker) in F1 and F2 cells, demonstarting that the two populations of fibroblasts are similar.

Adaptive immune response of human iPSC-derived cells.

Analysis of HLA type by deep sequencing methods was performed to confirm HLA type for all cell types used (Figure 7, A). MHCI mRNA gene expression (HLA-A, B, C and B2M) for F1, iPSC and F2 cells by RT-PCR demonstrate that MHCI gene expression is down-regulated in iPSC, as previously published, but returns in F2 cells similar to F1 cells (Figure 7, B). We observed large variation between cell lines in MHCI gene expression, which has also been previously reported (Drukker et al., 2002). MHC1 protein expression was assessed by flow cytometry in all F1 and F2 cell lines and no difference in expression levels of MHCI was observed (Figure 7, C). Expression of MHC1 was the same for retrovirally made iPSC-derived cells (RV1-3) and non-virally made iPSC-derived cells (Epi1-3).

To mimic the possible *in vivo* functional response of MHCI expression to inflammation, MHC1 was stimulated with cytokine INF-gamma in F1 and F2 cells from both viral and non-viral made iPSC and MHC1 levels were measured by flow cytometry. Both F1 and F2 cells responded with an upregulation of MHCI expression in response to INF gamma and there was no difference indicating that the regulation of MHCI expression is not affected in iPSC derived cells (Figure 7, D). This suggests that MHCI expression is functionally normal in iPSC-derived cells.

To further analyse the adaptive immune response we assessed by ELISA the expression of immune cytokines secretion in F1 and F2 cells in response to bacterial and viral insult. We found that, after Poly(I:C) stimulation, IL15 and RANTES expression was down-regulated in F2 cells compared to F1 cells in both viral and non-viral made iPSC (Figure 7, E) suggesting there will be altered immunogenicity of transplanted iPSC-derived cells. However, due to huge variability among patient cells, standard deviation was too high to make differences significant. It was not the case for IL10, that was found upregulated in F2 after Poly(I:C) stimulation (Figure 7, E). Again, variability was too high to stablish significance.

A

	RV-1	RV-2	RV-3	Epi-1	Epi-2	Epi-3
HLA-A	A*03/A*23	A*25/A*33	A*01 A*03	A*01/A*30	A*23/A*30	A*02/A*03
HLA-B	B*08/B*44	B*14 B*18	B*15 B*18	B*08/B*14	B*53/B*58	B*07/B*35
HLA-C	C*04/C*07	C*08 C*12	C*07C*18	C*07/C*08	C*04/C*07	C*04/C*07
HLA-DR	DRB1*03/ DRB1*07	DRB1*07/ DRB1*15	DRB1*11	DRB1*03/D RB1*15	DRB1*15/ DRB1*16	DRB1*01
HLA-DQ	DQB1*02	DQB1*02/ DQB1*06	DQB1*03	DQB1*02/D QB1*06	DQB1*05/ DQB1*06	DQB1*03/ DQB1*05

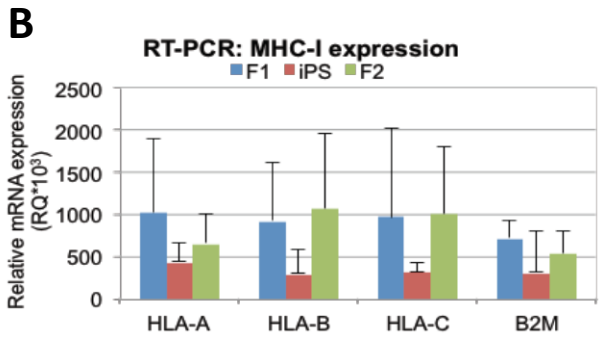

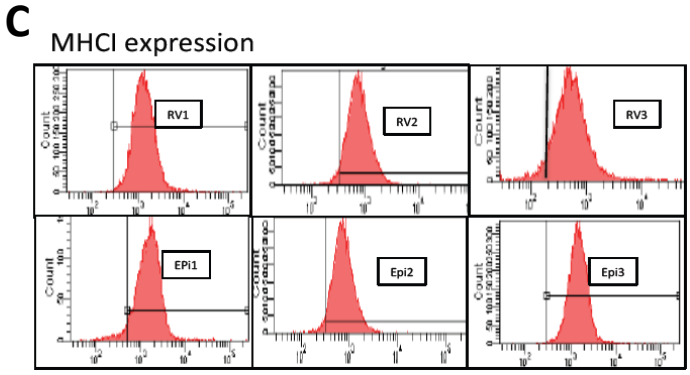

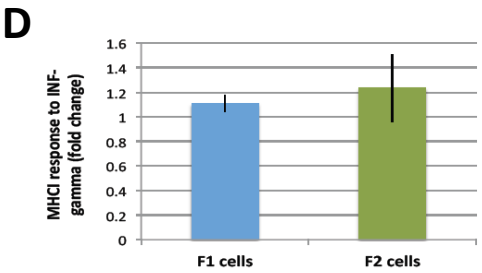

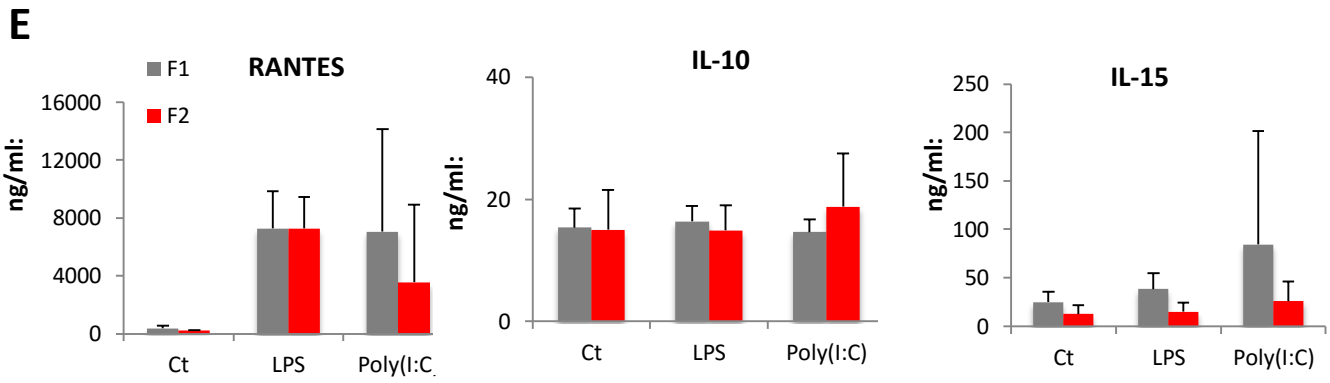

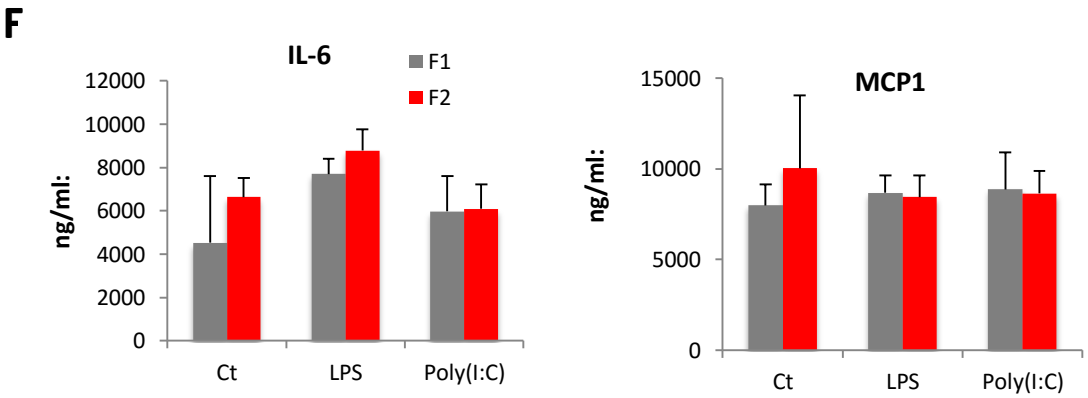

Figure 7: Adaptive immune response of human iPSC-derived cells.

A) Genotype of the HLA of the patient fibroblasts used in this study. **B)** RT-PCR data for HLA A, B, C and B2M (MHC-1 components) expression levels in patient fibroblasts, subsequent iPSC clones and iPSC-derived fibroblasts. **C)** Flow cytometry histograms of patient fibroblasts for MHC-I expression. **D)** Relative expression levels of MHC-I by flow cytometry for F1 cells and F2 cells stimulated with Interferon gamma. **E)** ELISA analysis graphs of expression levels of cytokines involved in the adaptive immune response: Rantes, IL15 and IL10. **F)** ELISA analysis graphs of expression levels of cytokines involved in inflammation and innate immune response of hiPSC-derived cells: MCP1 and IL6.

Inflammation and innate immune response in human iPSC-derived cells.

We next analysed the innate immune response by assessing the expression of 25 cytokines routinely assed by clinical immunologists by Elisa in viral or non-viral made iPSC derived cells, with or without viral ligand stimulation (Poly I:C) or bacterial ligand stimulation (LPS). We found no difference in expression of cytokines between viral and non-viral made F1 cells compared to F2 cells. Grouping viral made and non-viral made cells together, two main cytokines involved in inflammation, MCP1 and IL6, were found to be upregulated in iPSC-derived cells compared to F1 cells both without stimulation (Figure 7, F). However, in response to bacterial LPS and viral Poly (I:C), normal MCP1 and IL6 secretion was found for both F1 and F2 cells. Again, variability was too high to stablish significance.

Both IL6 and MCP1 are pro-inflammatory cytokines involved in the first steps of the innate immune response to recruit monocytes and neutrophils. Taken together the data indicates that higher levels of pro-inflammatory cytokines IL6 and MCP1 are being secreted by iPSC-derived cells (F2) at basal levels compared to F1 cells. However, F2 cells behave normally increasing IL6 and MCP1 secretion in response to bacterial or viral insult.

To investigate the mechanism underlaying the higher levels of pro-inflammatory cytokines being expressed in iPSC-derived cells, we hypothesised that the toll like receptor pathway is altered in F2 cells because it is the main pathway for cytokine secretion. Proteins associated with TLR3 had been found in the proteomic screen, prompting us to investigate toll-like receptor expression levels. By RT-PCR we show that TLR3 and TLR4 are more expressed in F2 than in F1 cells (Figure 8, A). This was confirmed by flow cytometry analysis for TLR3 protein expression, with 28.3% of F2 cells expressing TLR3 receptor compared to only 5.1% of F1 cells (Figure 8, B), a 5-fold higher number of cells with TLR3 receptor in iPSC derived cells. We then analysed our mouse C2C12 iPSC derived cells for TLR3 expression and found the same upregulation in F2 cells (Figure 8, C), confirming what we had observed in human iPSC-derived cells. No differences were found between MH and DH clones, thus data was grouped together. Data was taken from four iPSC clones differentiated into cardiomyocytes and compared with a control sample of mouse heart tissue from C3H mouse, the same mouse strain from where C2C12 cells were isolated. However, this time only TLR3 was found upregulated, as TLR4 showed the trend but was not significantly different (Figure 8, C).

Then, we also studied TLR3 and TLR4 in the clinical grade mRNA reprogrammed iPSC derived cells. No differences were found between MH and DH iPSC, thus data was grouped together. Interestingly, this time only CM (F2) and not NSC or generally differentiated cells, had upregulated levels of TLR3 in comparison with original HFFs (F1) (Figure 8, D).

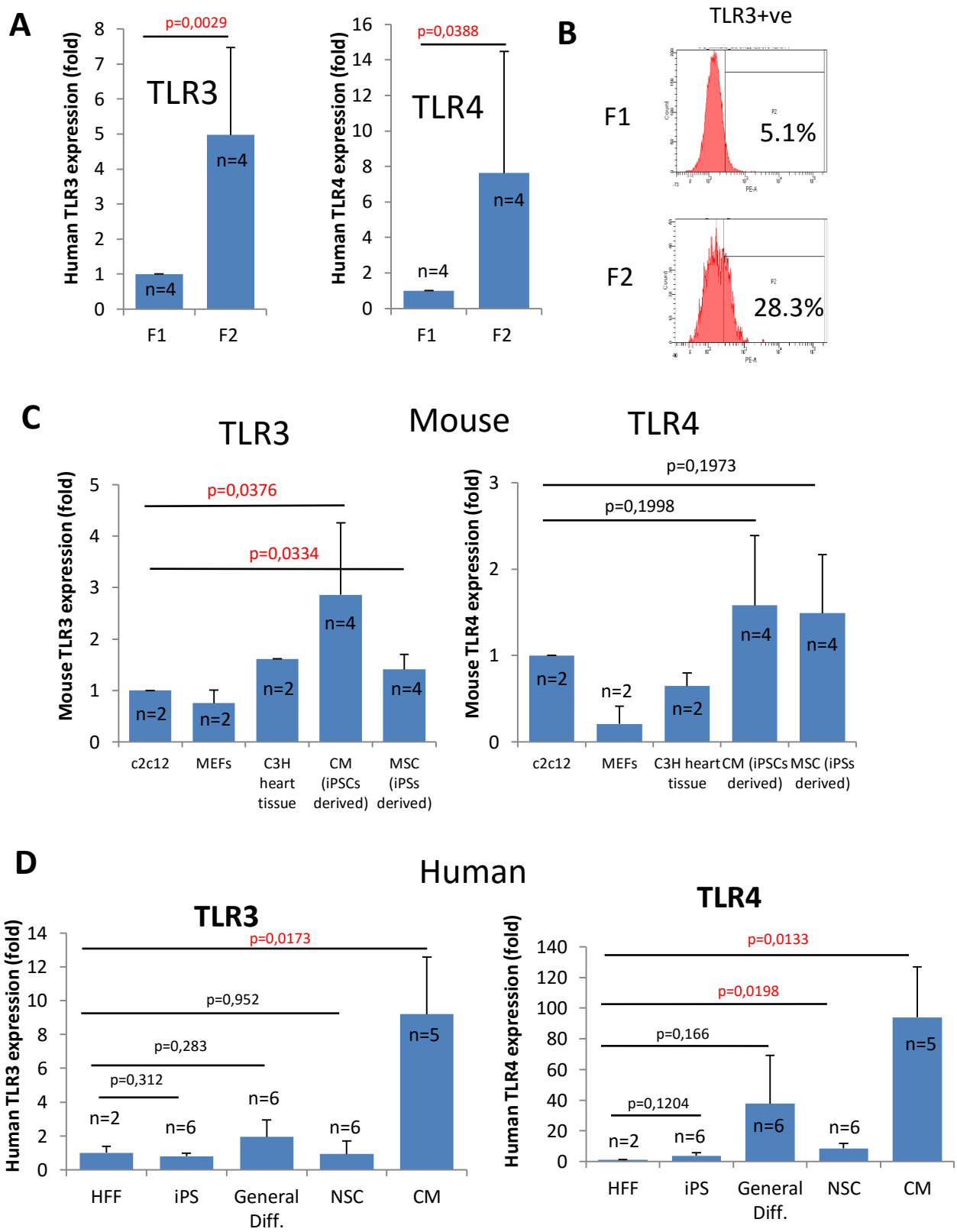

Figure 8: Mouse and human TLR3 and TLR4 in F1 and in iPSC-derived cells (F2).

A) Graph of RT-PCR analysis of TLR3 and TLR4 gene expression levels in the patient human F1 and F2 cells. **B)** Representative flow cytometry histograms of F1 and F2 cells stained for TLR3 receptor expression confirming that TLR3 is overexpressed in F2 cells (from 5,1% to 28,3%). **C)** Graphs summarising RT-PCR analysis TLR3 and TLR4 gene expression levels in mouse iPSC-derived fibroblast like cells and cardiomyocytes compared to physiological normal mouse embryonic fibroblasts (MEF), mouse C2C12 skeletal muscle cells and mouse heart tissue. **D)** Human mRNA made iPSCs and iPSCs differentiated NSC, CM and general differentiation analysis for TLR3 and TLR4.

Three CpG sites are hypomethylated in isoform B TSS of TLR3 in NSC.

In order to determine whether differences between F1 and F2 for TLR3 and TLR4 could be explained by an epigenetic mechanism, we used the methylome analysis done for the mRNA iPSC and their derived NSC in comparison with the original control HFFs. Furthermore, using the methylome analysis on the mRNA made iPSC is suitable to decrease variability issues associated with patient samples variation and to eliminate genetic background.

The methylome array analysis examined several CpG sites inside the sequence of TLR3 and TLR4. Results show no alteration at any CpG in the TLR4 promoter; however, we found hypomethylated CpGs inside the promoter of a short isoform of TLR3 (Figure 9, A). The array analyzed 4 CpG sites inside an alternative transcription start site (TSS) located in the promoter of this short TLR3 isoform B. These 4 CpG sites analyzed in the array were found hypomethylated in all iPSC clones (Figure 9, E). On the other hand, and most interestingly, in NSC we found that CpG site cg14827929 was highly hypomethylated and cg11273820 and cg00306510 were also hypomethylated in comparison with control HFFs (Figure 9, E). These CpG site are found inside the alternative TSS located inside the promoter of isoform B, a short isoform that differs from TLR3-FL at the protein level by lacking the first 8 leucine rich regions (LRRs) of the protein ectodomain responsible for the viral dsRNA recognition.

TLR3 isoform B is upregulated in iPSC derived cells.

To determine if the hypomethylation found in the TSS of the TLR3 isoform B promoter in NSC was affecting the expression of this isoform in iPSC derived cells, we analysed by qPCR several iPSC derived cell types: Neural Stem Cells, Cardiomyocytes and Endoderm cells differentiated from mRNA hiPSC. Specific primers were designed against the non-shared sequence of TLR3 isoform B transcript and it was compared with the TLR3 FL.

RT-PCR results show that compared to control HFFs isoform B, relative expression levels are significantly upregulated in all iPSC and iPSC differentiated cells (n=6 clones) (Figure 9, C). On the contrary, other F1 cell populations like mesenchymal stem cells (MSC) and umbilical cord blood (UCB) cells showed fewer or undetectable levels of isoform B TLR3 (Figure 9, D).

Patient F1 and F2 cells were also analysed for full length and short isoform (Figure 9, B) and although in almost all clones there was an increase in expression in F2 population, no significance was found due to high variation between patients.

A

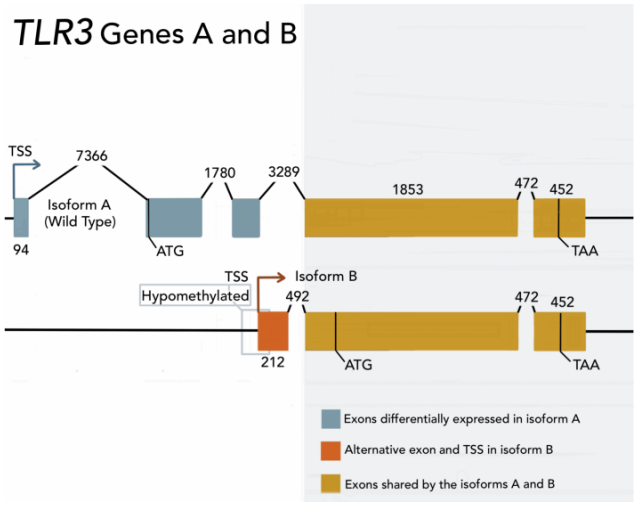

B

	TLR3 B	
	F1	F2
GUY	0,02658419	2,16777103
CHE	1,78783349	4,98541077
CRL1502	0,58326054	8,86249175
SP11	5,25872254	26,0229458
MSC	3,30056356	26,5697432
FB	17,2343189	13,2389094

C

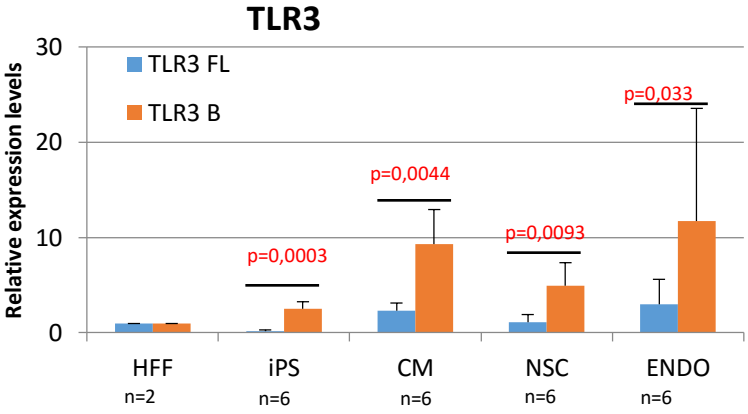

D

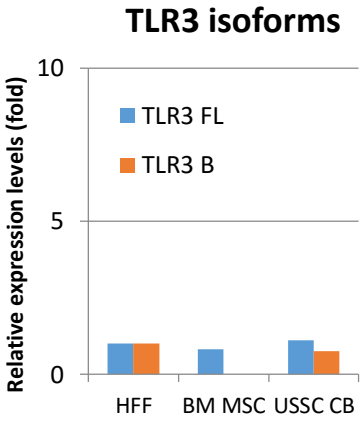

E

TargetID	CHR	MAPINFO	UCSC RefGene Name	UCSC RefGene Group	HFF_CTL	DH1_iPSC	DH3_iPSC	DH5_iPSC	MH1_iPSC	MH6_iPSC	MH9_iPSC	DH1_NSC	DH3_NSC	DH5_NSC	MH1_NSC	MH6_NSC	MH9_NSC
cg11273820	4	187002591	TLR3	Body	0,517	0,171	0,181	0,242	0,163	0,212	0,173	0,312	0,334	0,419	0,425	0,415	0,457
cg14827929	4	187002617	TLR3	Body	0,450	0,095	0,207	0,139	0,122	0,073	0,072	0,126	0,285	0,127	0,144	0,209	0,403
cg01414772	4	187002764	TLR3	Body	0,643	0,484	0,764	0,490	0,478	0,607	0,623	0,638	0,744	0,672	0,636	0,668	0,692
cg00306510	4	187003000	TLR3	Body	0,632	0,374	0,604	0,269	0,366	0,331	0,413	0,558	0,517	0,533	0,493	0,539	0,540

F

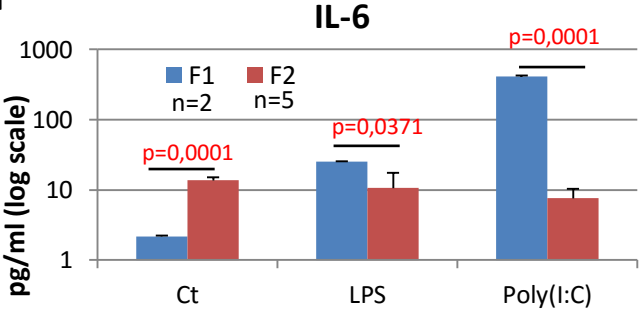

G

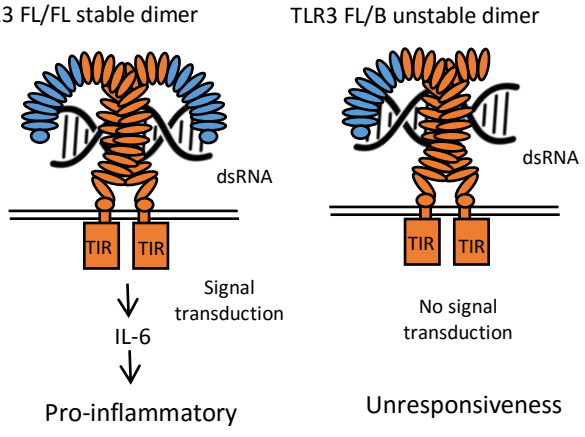

Figure 9: Human TLR3 isoform B generates F2 cells unresponsive to Poly(I:C), gaining anti-inflammatory properties producing less IL6.

A) Diagram of TLR3 gene exons and introns organization showing which exons are differentially expressed in full length isoform A and short isoform B. It is also shown the location of the alternative TSS found hypomethylated in NSC. Image kindly supplied by Dra. Jovita Mezquita. **B)** Raw RT-PCR expression levels of short TLR3 isoform in patient F1 and F2. Highlighted in red are the patient that presented an increase between F1 and F2. **C)** Relative expression levels of TLR3 full length (FL) and short isoform B determined by qPCR in mRNA made iPSCs and derived CM, NSC and Endoderm cells compared with control HFFs. **D)** Relative expression levels of TLR3 full length (FL) and short isoform B determined by qPCR in Bone marrow mesenchymal stem cells (BM MSC) and umbilical cord blood cells (USSC CB). **E)** Methylation state of 4 CpGs contained inside the alternative TSS that enables the transcription of the TLR3 short isoform B.**F)** Cytokine IL6 production (pg/ml expressed in log scale) comparing F1 (HFFs, n=2) and F2 cells (NSC, n=6 clones) without stimulation and after LPS and Poly(I:C) o/n stimulation. **G)** Graphical representation of the two hypothetical TLR3 dimerization options: full length with full length (FL/FL) or full length with isoform B (FL/B) interacting with viral dsRNA. In the first case, dimer structure is stable and active and transduces signal to produce a pro-inflammatory effect through IL6 production in case there's viral dsRNA. In the second case, an unstable dimer structure is nonfunctional and therefore unresponsive to dsRNA stimulation triggering an anti-inflammatory effect by the lack of signal transduction.

TLR3 short isoform confers unresponsiveness to viral stimulation

Functionally, homodimerization of TLR3 is essentially required for ligand binding (Wang et al., 2010b), and an intact binding site is required for dsRNA binding and a stable dimerization to activate the downstream signalling cascade to initiate pro-inflammatory response (Figure 9, G). Consistently, after LPS and Poly(I:C) stimulation in HFFs, IL-6 is secreted (Figure 9, F). However, we found that after LPS and Poly(I:C) stimulation of NSC, IL-6 was not upregulated (p value= 0,0371 and p= 0,0001 respectively) (Figure 9, F). Therefore, NSC were unresponsive to LPS and Poly(I:C) stimulation of TLR3. However nonstimulated F2 cells show higher level of IL6 secretion (p value= 0,0001) (Figure 9, F).

We hypothesize that his unresponsiveness can be explained taking into account that overexpression of the short B isoform found in all the different cell types differentiated from iPSC (Figure 9, C) was inhibiting TLR3 stimulation of the wild type TLR3-FL receptor, by competing with it in the dimerization process (Figure 9, G). Because an intact dimerization site is required for stabilization of the dsRNA/TLR3 dimer complex (Wang et al., 2010) the excess of isoform B might be competing with the FL-FL dimerization and therefore inhibiting the pathway signal transduction.

In vivo mouse model: immune response of transplanted syngeneic mouse iPSC and iPSC derived cells.

To determine the immunogenicity generated by mouse iPSC derived cardiomyocytes (CM) (characterized by RT-PCR in Figure 10, A), a T cell kill assay was performed to assess survival. Cells were injected in vivo into syngeneic C3H mice. To investigate if an adaptive immune response was generated, a priming period of 7 days was left from the injection time point until the collection of the cytotoxic T lymphocytes (CTLs). Four different iPSC derived cardiomyocytes lines were injected in duplicate into the testis of mice. All animal experiments were approved by the ethics committee.

Primed T cells degranulation activity was measured by flow cytometry by CD107a expression. The level of apoptosis of target iPSC and CM was determined by flow cytometry using Annexin V+PI. One week after cardiomyocytes injection, Cytotoxic T lymphocytes (CTLs) were isolated by FICOLL gradient from smashed spleens from mice. For T cell kill assay CTLs were added on top of the cardiomyocyte line that was injected in the mouse the CTLs were isolated from. Co-culture assay lasted 4h.

Interestingly, the data shows that when the primed T cells are placed on the iPSC-derived cardiomyocytes (CM) the level of CD107a or T cell activity, is reduced (Figure 10, C) and apoptosis is not increased neither (Figure 10, D). CD107a reduction suggests that iPSC derived CM might be secreting cytokines that could reduce T cell activity.

In conclusion, the data demonstrates that cell reprogramming process alters both the innate and adaptive immune response of iPSC-derived cells that provides an insight for future clinical applications of autologous human iPSC-derived cell transplantation.

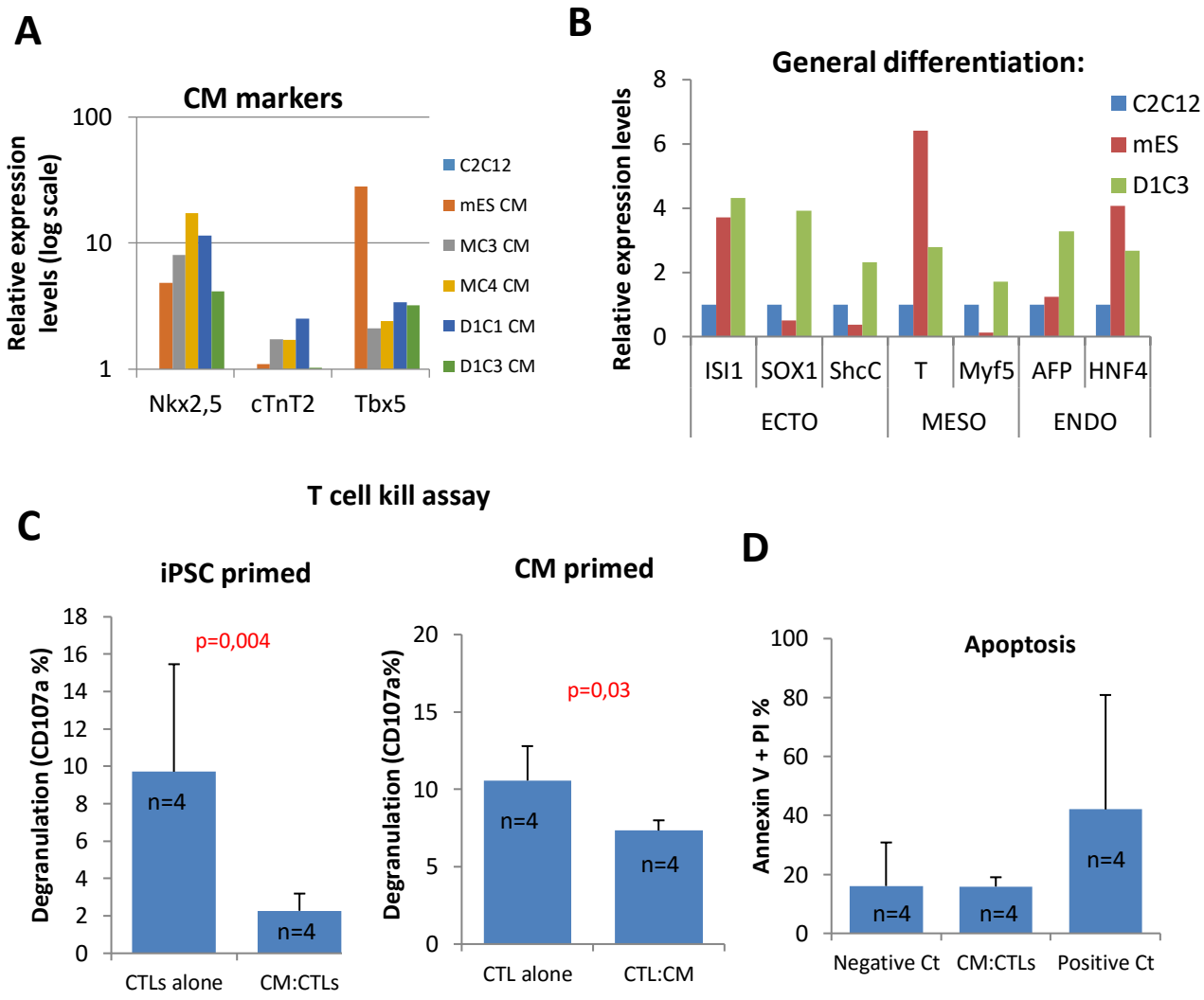

Figure 10: In vivo mouse model: immune response of syngenic mouse iPSC-derived cells.

A) RT-PCR characterization of C2C12 iPSCs derived Cardiomyocytes (CM) with cardiac markers: Nkx2.5, cTnT2 and Tbx5 for all 4 clones analysed compared with C2C12 negative control and mouse Embryonic Stem cells (mES) derived CM for positive control. **B)** RT-PCR characterization of C2C12 iPSCs generally differentiated clone D1C3. Markers for Ectoderm (ISI1, SOX1 and ShcC), Mesoderm (T and Myf5) and Endoderm (AFP and HNF4) were analysed. **C)** T cells CD107a% degranulation in response to mouse IPSCs and mouse iPSCs derived CM coculture with primed T cells in syngeneic C3H mice. In all cases a significant decrease in CD107a was reported when co-culturing cytotoxic T lymphocytes (CTLs) with either iPSCs or CM. demonstrating reduction in T cell activity when plated with cardiomyocytes and no change in apoptosis **(D)** of cardiomyocytes as seen by Annexin V+PI %. Negative control for apoptosis are CMs alone and positive control are CM treated with 10% DMSO.

Neural Stem Cells (NSC) engraft and survive in a Spinal Cord Injury (SCI) rat model.

Our laboratory is interested in finding a cellular therapy approach to study and treat spinal cord injury (SCI). Hence, we established collaboration with Dra Victoria Moreno from the Centro de Investigaciones Principe Felipe (CIPF) in Valencia where I stayed and received training to study our NSC using their SCI rat model. Therefore, we performed a practical test of the iPSC derived NSC by injecting them in a spinal cord injury (SCI) rat model in order to perform an in vivo functional assay to determine whether DH iPSC derived cells have an actual functional capability of survival and engraftment in vivo. We performed a spinal cord complete transection following published protocols (Lukovic et al., 2015).

In a similar experiment using the same model of spinal cord injury of complete transection, it was reported that HESCs derived oligodendrocytes progenitors and motor neurons progenitors improved motor recovery 4 months after transplantation (Erceg et al., 2010). In this experiment however, we only assessed survival two months after injection and identify NSC differentiation capabilities towards their natural derivatives in a spinal cord injured niche.

One clone of NSC differentiated from DH iPSC was chosen to test our new iPSC derived NSC capability of survival and engraftment in vivo. NSC tagged with cell tracker (Vybrant CFDA SE) were injected in this severe transection model into the spinal cord of four rats (Figure 11, A) as indicated in methods. To avoid rejection, cyclosporine was administrated through the water supply. At day 3 after injection one rat was sacrificed to see that cells were still alive and located near the injection site (Figure 11, B).

Lesion site is delimited by the lack of GFAP positive astrocytes because of the scaring process happening after cord transection. We show how after two months, at day 60, cells survived, engrafted and migrated to the lesion site, as shown by the green tracker in all three rats (Figure 11, B and supplementary figure 11, A). Also, in all rats cells migrated towards the caudal side of the spinal cord (Supplementary figure 5, B).

By studying colocalization of vibrant green marker with different antibodies we determined by immunofluorescence that NSC had differentiated 75,1% into mature neurons (MAP2-NSC colocalization), 1,9% immature neurons (Tuj1-NSC colocalization), 18,2% oligodendrocytes (OLIG2-NSC colocalization) and 5,2% mature astrocytes (S100-NSC colocalization) (Figure 5, C). These results reveal that Cyclin D1 made iPSC derived NSC exhibit an in vivo differentiation potential similar to what has been published likewise with c-Myc iPSC.

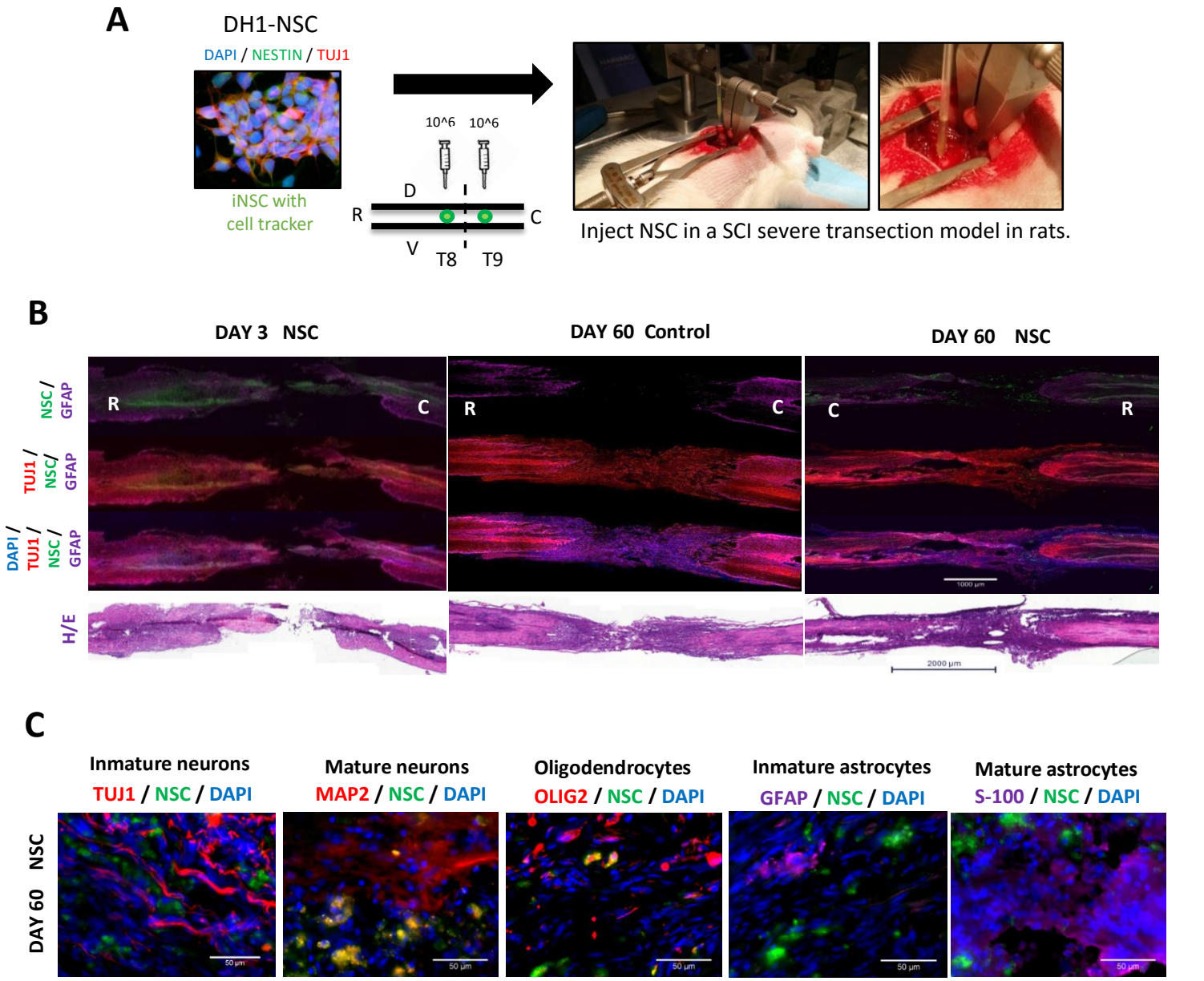

Figure 11. Clinical grade human iPSCs derived NSC engraft and migrate to the lesion site in a Spinal Cord Injury (SCI) rat model.

A) In a severe transection model in rats NSC were injected into the spinal cord in between segments T8-9, using a stereotaxic arm with an attached Hamilton. Cells, 2·10^6 in 10µl, were injected at two levels: rostral (5µl) and caudal (5µl) separated by 2-3 mm, at a speed of 2µl/min. **B)** Immunofluorescence of transection cuts of perfused spinal cords at day 3 after NSC injection, a control without cells at day 60 and a day 60 spinal cord after NSC injection and complete transection. Injected cells were tagged with cell tracker (Vybrant CFDA SE) to detect cells using a GFP detection wavelength. Tuj1 and GFAP were used to detect neurons and astrocytes respectively and DAPI to stain nuclei. A merge image is shown. Cells survived, engrafted and migrated as shown by the green tracker at day 3 and day 60. After injecting mRNA made iPSCs derived NSC in the spinal cord no neoplasm was formed. **C)** Colocalization study of vibrant green marker with different antibodies by immunofluorescence determines that NSC had differentiated 75,1% into mature neurons (MAP2), 1,9% immature neurons (Tuj1), 18,2% oligodendrocytes (OLIG2), 0% immature astrocytes (GFAP) and 5,2% mature astrocytes (S100).

DISCUSSION

Even though cell reprogramming is an established technique for production of induced pluripotent stem cells (iPSC), producing high quality patient specific iPSC suitable for cell therapy remains an important challenge, as there is a lack of clinical grade standard operating procedures. About half human iPSC exhibit genetic and epigenetic variations, thought to result from incomplete reprogramming, mutation in somatic cells and cellular stress during reprogramming (Koyanagi-Aoi *et al.,* 2013). Therefore, genetic instability are thought to be one of the potential barriers to clinical application of their derivative cells. A few months ago, the first iPSC clinical trial had to be stopped due to unexpected genetic instability found in the patient iPSC used in the trial, proving that genetic stability of iPSC is one major difficulty to elucidate before clinical application. Another of the major hurdles still to overcome is the tumorigenic threat associated with c-Myc pleiotropic effects. That's why we proposed an alternative reprogramming cocktail to solve this issue. Indeed, factor based genetic instability remains an important issue to address, which is the reason why we have assessed Cyclin D1 as a candidate to substitute c-Myc in the reprogramming cocktail. Glis1 was also reported to be able to substitute c-Myc (Maekawa *et al*., 2011); however, it also promoted multiple pro-reprogramming pathways, that were activated due to the upregulation of the transcription factors N-Myc, L-Myc, C-Myc, Nanog, ESRRB, FOXA2, GATA4, NKX2-5, as well as the other three reprogramming factors (Maekawa et al., 2011).

An important feat in the reprogramming process is to bypass the cell cycle arrest in adult differentiated cells. For example, inhibition of the p53 and p21 pathway as well as the expression of Lin28 increases iPSC generation predominantly by acceleration of the rate of cell division (Hanna et al., 2009). Therefore, accelerated kinetics of iPSC formation was directly proportional to the increase in cell proliferation (Hanna et al., 2009). C-Myc has been used classically for this purpose, as it is a transcription factor which regulates, among other functions, the expression of several genes involved in the control of cell proliferation like Cyclin D1. Then, we hypothesize that bypassing the cell cycle arrest by using Cyclin D1 would enable the replacement of c-Myc, removing all the other functions c-Myc has on the cell. Accordingly, we have found that without the acceleration of the cell cycle triggered by either c-Myc or Cyclin D1, 3F (Oct4, Sox2 and Klf4) alone showed a very low efficiency with retroviral methods and a null reprogramming efficiency with mRNA transfections due to the incapacity to bypass cell cycle arrest. Maintaing efficiency is a challenge to solve, especially when dealing with reprogramming patient cells.

It is unknown the minimum requirement tests for determining the clinically acceptable quality of iPSC. When assessing iPSC quality, the results of several tests are often qualitative, especially when dealing with epigenetic modifications, making it difficult to set thresholds for defining "normal" and "defective" cell lines. Another example is mutations; how many mutations and at what genes would classify iPSC defective? Since it is difficult to set the standards for quality of iPSC, these questions in turn raise another challenge, which is to what depth should the lines be analyzed, i.e. should we sequence the entire genome, epigenome and transcriptome of iPSC lines, and at what cost?

In order to replace c-Myc oncogene in the reprogramming cocktail, here we have used the cell cycle gene Cyclin D1 in combination with the other three factors, Oct4, Sox2 and Klf4 to reprogram somatic cells to pluripotency, showing a reduction in several genetic instability parameters.

In this study, we first tested reprogrammed mouse cells and assessed telomere length in the iPSC as a measure of genetic stability. Depending on the length, telomeres can be classified in long, short and signal-free ends (almost undetectable telomeres). Signal-free ends have been associated with chromosomal t-loops formation and are considered a sign of genetic instability. As we have observed, 3F+Cyclin D1 clones have half the percentage of signal free ends than 3F+c-Myc clones (Figure 1, J); demonstrating that 3F+Cyclin D1 mouse iPSC clones present a better quality telomere length. A comparison of chromosome instability between 3F+Cyclin D1 and 3F clones should have been assessed as control; however we were not able to grow iPSC clones from C2C12 with 3F transduction alone after picking them from the plate.

Another chromosomal stability analysis that has been conducted is the determination of the number of chromosome free fragments present in the nucleus of the cells. The contribution of an increase in the number of chromosomal fragments to iPSC stability is poorly understood. However, an increase in the number of fragments was reported to occur after irradiation-induced lesions (Pantelias, 1986). CHO cells in metaphase exposed to 5Gy X-ray irradiation led to an increase of chromosome fragments, suggesting that it must be a feature of instability rather than a helpful acquisition (Pantelias, 1986). Those results are in accordance with the fact that in mouse cells, 3F+c-Myc reprogramming increases the number of chromosomal fragments compared to 3F+Cyclin D1 (Figure 1, K), suggesting once more that c-Myc may be producing a higher stress in the cell than Cyclin D1.

To determine whether Cyclin D1 can reduce cell stress in the reprogramming process a battery of genes associated with cell stress and DNA damage were evaluated (Figure 1 and Supplementary Figure 1). ATM and p53 binding protein 1 (53BP1) are two DNA damage response genes. 53BP1 is a p53 binding protein that binds to the central DNA-binding domain of p53. It relocates to the sites of DNA strand breaks in response to DNA damage. The well-known tumor suppressor p53 plays a central role in the response of mammalian cells to genotoxic stress (Iwabuchi *et al.*, 1994). 53BP1 acts downstream of ATM in the DNA damage response pathway and is involved in tumor suppression in mice (Ward *et al*., 2003). Thus, defects in DNA damage recognition and repair mechanisms are associated with cancer predisposition, suggesting that cells might be more prone to tumorigenicity. On the other hand, ATM, the gene mutated in the disorder ataxia-telangiectasia, is a protein kinase that is a central mediator of responses to DNA double-strand breaks in cells (Kitagawa et al., 2005). But although ATM and 53BP1 were less expressed in 3F+Cyclin D1 clones in C2C12, the difference was not significant enough.

NFKB target genes such as inhibitor of apoptosis 2 (IAP2), manganese superoxide dismutase (MnSOD) and growth arrest DNA damage inducible gene 45 beta (GADD45b) were also evaluated. All they have protective effects against apoptosis. MnSOD for instance has been established to protect against oxidation induced apoptosis (Kasahara *et al.*, 2005). The inhibitors of apoptosis (IAPs) antagonize cell death and regulate the cell cycle; IAPs are a family of proteins that suppress apoptosis triggered by a variety of stimuli (LaCasse *et al.*, 1998; Hay, 2000). Induction of GADD45b by NF-kappaB downregulates pro-apoptotic JNK signaling (De Smaele *et al.*, 2001), functioning therefore as a protective mechanism as well. Interestingly, GADD45b and IAP2 genes transcripts levels are found upregulated in 3F+c-Myc clones compared to 3F+Cyclin D1 clones (Figure 1, F-G). Thus, induction of Gadd45b and IAP2

functioning as a protective mechanism may suggest that c-Myc clones might require to be assisted or protected from DNA damage induced apoptosis.

Finally, sirtuins 1, 3 and 6 levels were also analyzed, but only sirtuin 1 presented significant differences in expression (Figure 1, E). Sirtuins have been implicated in influencing a wide range of cellular processes like aging, transcription, apoptosis, inflammation and stress resistance. The role of Sirt1 in iPSC initially was thought to be important if not essential, as was reported to facilitate iPSC generation from mouse embryonic fibroblasts through deacetylation of p53, inhibition of p21 and enhancement of Nanog expression (Lau *et al*., 2012). But recently, Sirt1 has been actually described as necessary for proficient telomere elongation and genomic stability of induced pluripotent stem cells (De Bonis *et al.,* 2014). In Lau's paper it previously it was also found that knocking down sirtuin 1 with siRNA the number of iPSC colonies were three fold reduced. Here we've found that in MEFs null for sirtuin 1, the reduction is four fold when reprogramming with c-Myc (Figure 1, H).

It has to be taken into account that the oncogene c-Myc and Sirt1 form a positive feedback loop both contribute to amplify each other. Sirt1 expression is increased by c-Myc-dependent NAMPT activity and c-Myc function is enhanced by Sirt1 (Menssen et al., 2012). The fact that Sirt1 is not upregulated in 3F+Cyclin D1 clones as much as it is in 3F+c-Myc clones during early passage 1 (Figure 1, E), suggests that 3F+Cyclin D1 clones might originate less genomic instability, preventing sirtuin 1 from increasing their levels to repair any damage.

We wanted to understand whether Cyclin D1 could rescue iPSC from acquiring genomic instability during the reprogramming of MEFs lacking Sirtuin 1 (Sirt1-/-). Experiments performed show that 3F+Cyclin D1 can increase survival of cells during reprogramming to pluripotency. We propose that the absence of Sirtuin 1 does not prevent colonies from proliferating as if there were less alterations or instability than in 3F+c-Myc and colony cells were not stopped to proliferate. Then, Cyclin D1 in Sirt1-/- MEFs appears to be rescuing reprogramming comparing to c-Myc, suggesting that Cyclin D1 functions independent of Sirtuin 1 during reprogramming.

Human iPSC clinical grade reprogramming

The next step in the process of developing a clinical grade protocol was to find a proper reprogramming method that could reduce the threat of insertional mutagenesis and transgene reactivation associated with retroviral vectors.

It is widely accepted that reprogramming itself can induce both genetic and epigenetic defects in iPSCs (Doi et al.,2009; Kim et al., 2010; Polo et al., 2010; Lister et al., 2011). Even when using non-integrative virus-free methods as mRNA transfections (Gore et al., 2011) or episomal vectors (Taapken *et al*., 2011) approaches for reprogramming. The reprogramming method did not affect neither the frequency nor the type of genomic changes in hiPSCs (Taapken *et al.*, 2011). Nevertheless, the three main non-integrative methods for reprogramming adult cells to iPSC in a clinical grade way that have been proposed to be clinically acceptable are: synthetic mRNA transfections, Sendai virus and Episomal vectors.

Sendai virus has the advantages of wide host specificity and low pathogenicity, and the disadvantage of strong immunogenic response (Fusaki *et al*., 2009), triggering the applicability of this method to firstly require the development of less antigenic vectors. Episomal vectors consist of introducing episomal genes that are expressed and replicate when the host cell divides. Afterwards, the episomal vector is naturally gone when the iPSC multiply (Yu *et al*., 2009). Likewise, in the case of Sendai virus and episomal vectors, final clones have to be shown to be free of the original vector or virus. Still, it is always maintained the rare but potential chance of insertion of the Episomal vector DNA by homologous recombination. On the other hand, direct transfection of synthetic modified mRNA consists of the administration of mRNA modified to overcome innate antiviral immune responses. Although it is needed a daily transfection regimen to maintain a sustained expression, mRNA reprogramming allows a higher reprogramming efficiency (Warren *et al*., 2010).

A comparison of Episomal vectors, Sendai virus, mRNA transfection, Retrovirus and Lentiviral methods demonstrated that mRNA transfection was the one showing a lower number of aneuploidies (Schlaeger et al., 2015). It offers the finest option for future clinical applications as expression is transient over 48 hours and dose and timing can be controlled as requested. Thus, we decided to proceed with mRNA transfections method.

Messenger RNA made iPSC reprogrammed with c-Myc and Cyclin D1, here called MH and DH clones, gave a similar reprogramming efficiency percentage as with retroviral reprogramming (Supplementary figure 2, F), being Cyclin D1 half as efficient as c-Myc in the number of colonies. However and most importantly, we were not able to reprogram with 3F alone.

Furthermore, after general and guided differentiation no qualitative differences were seen in terms of their in vitro pluripotency potential (Figure 2, C-G). Later, when in vivo pluripotency potential was assessed, all clones from both conditions were able to form teratomas containing structures of tissues from the three germ layers (Figure 3, B).

Human iPSC tumorigenicity

One of the main concerns about reprogramming is the tumorigenic potential of iPSC. IPSC have been shown to have a higher tumorigenic potential than ES cells (Miura et al., 2009; Okita *et al.,* 2007), since they are made with the well-known oncogene c-Myc. C-Myc has been related with the activation of several pathways in the reprogramming process because of its pleiotropic effect, since it can cause permanent negative effects even with only transitory expression.

An interesting difference was found in the tumorigenic marker KI67, which was found to be highly expressed in MH iPSC teratomas in comparison with DH iPSC teratomas (Figure 3, C). Following the same trend we found that neural stem cells derived from MH iPSC had as well higher values of KI67 in vitro in comparison with DH derived NSC (Figure 3, D). Neoplastic risk after transplantation of iPSC differentiated cells has been concerning since the discovery of iPSC. Here, we show how DH iPSC and derived NSC present lower levels of KI67, decreasing thus the associated tumorigenic threat. We thought that one possible explanation was that some of the genes that are found

amplified in the CNV array assay might be involved in the tumorigenic growth. However, cluster analysis revealed no big differences regarding cancer related genes amplified. Another possibility was that the small differences found at the methylome level could explain the highly aggressive growth rate found in MH clones. Nevertheless, after looking for similarities with methylation patterns from online databases no matches were found.

Another evidence suggesting c-Myc iPSC higher tumorigenic risk, is that MH iPSC and NSC clones had longer telomeres than DH clones (Figure 5, B). Acquiring a certain telomere length is necessary for iPSC self-renewal capabilities; however long telomeres are also a hallmark of cancer. This is the reason why iPSC need to reach a balance between too short and too long telomeres. Nevertheless, telomere length in DH NSC are more similar to original HFFs than MH NSC, which are still too long for a differentiated cell type. This feature might also be relevant as cells that derive from iPSC should not retain any stem pluripotency property before they are transplanted into patients. Furthermore, in a recently published study after retrovirally made iPSC derived NSC injection into the spinal cord of injured rats, teratomas were formed (López-Serrano et al., 2016, Supplementary Figure 5, C). In this publication iPSC was made with c-Myc in the reprogramming cocktail.

DNA double strand breaks in human iPSC

DNA double strand breaks (DSBs) are a consequence of oxidative and replicative stress. DSBs repair mechanisms are homologous recombination (HR) and non-homologous end joining (NHEJ). C-Myc expression has been reported to accumulate reactive oxygen species (ROS), which in turn generate DNA breaks (Khanna and Jackson 2001). Furthermore, c-Myc suppresses NHEJ (Li et al., 2012) and HR in various cancer cell lines (Luoto et al., 2010); contrarily to Cyclin D1 that has been linked with facilitating homologous recombination repair process by helping BRCA2 to recruit RAD51 in repairing DNA DSBs in the HR process (Chalermrujinanant et al., 2016). The fact that we found a higher percentage and intensity of H2AX positive DSBs in MH than in DH iPSC and NSC supports the idea that DH iPSC render a better genetic stability through a less stressful reprogramming process.

NHEJ is the major pathway in mammalian cells for repairing DSBs (Hefferin et al., 2005; Burma et al., 2006). Mechanistically, c-Myc binds to Ku70 protein through the Myc Box II (MBII) domain and therefore directly disrupts the Ku/DNA-PKcs complex suppressing thus the DSBs repair leading to genetic instability (Li et al., 2012). All Myc protein family (C-Myc, L-Myc and N-Myc) have the Box II domain involved in the inhibition of DSB repair. L-Myc has been proposed as an alternative to c-Myc for its increase in reprogramming efficiency and reduced tumorigenic threat compared with c-Myc made iPSC (Nakagawa et al., 2010), however, Cyclin D1 is also a better choice since L-Myc Box II domain inhibits NHEJ repair (Li et al., 2012).

Furthermore, Rad51 is found retained in the cytoplasm in a higher proportion in MH clones than in DH clones. Since Rad51 cytoplasmic retention has been linked with inhibition of homologous recombination (Plo et al., 2008), this results supports our hypothesis that Cyclin D1 is promoting DNA repair by helping to recruit Rad51 to the site of the DNA break during reprogramming to iPSC.

Rad51 is a central protein in homologous recombination repair mechanism and is therefore of great relevance in terms of genomic stability. Their family members are homologous to the bacterial RecA, Archaeal RadA and yeast Rad51. Therefore, it is an evolutionary conserved protein in most eukaryotes. Here we have observed that both MH and DH clones presented cytoplasmic distribution of Rad51. However, DH clones had a lower signal than MH clones (Figure 4). Correspondingly, RAD51 overexpression has been reported as a negative prognostic marker for colorectal adenocarcinoma (Tennstedt et al., 2013), in a study that analyzed 1,213 biopsies from colorectal adenocarcinomas. Strong RAD51 expression was observed in 1% of colorectal carcinomas, moderate in 11%, weak in 34% and no expressed in 44%.

On the other hand, we have also found differences in RAD51B paralog in iPSC at passage 3. RAD51 paralogs are a family of five proteins (RAD51B, RAD51C, RAD51D, XRCC2 and XRCC3), that share at least 20% of sequence homology with RAD51. RAD51 paralogs are also important for homologous recombination (HR) since cells defective for them are sensitive to DNA-damaging agents like gamma radiation (Takata et al., 2001). Interestingly, RAD51B, has also been shown to be upregulated in MH clones at early passage 3, but not passage 10 (Figure 4, G). Consistently, it has been reported that expression of RAD51B paralog is de-regulated in several cancer cell types. For example, RAD51B expression is upregulated in gastric cancer tumours and correlates with a poor prognosis (Cheng et al., 2016); also overexpression of mutated versions of this gene have a high correlation with breast cancer predisposition (Golmard et al., 2013); as well as in chronic myelogenous leukemia (CML) cells (Albajar et al., 2011), where Rad51B protein levels were upregulated and Myc was found at high levels correlating with a resulting imatinib drug resistance. Likewise, BCR/ABL tyrosine kinase fusion protein, which enhances c-Myc expression, is directly interacting and phosphorylating both RAD51 and RAD51B, which could be influencing the repair efficiency of HR (Slupianek et al., 2009; Rieke et al., 2016). It had been hypothesize that BCR/ABL mediated tyrosine phosphorylation of Rad51B may affect the interaction between the paralogs to enhance the efficiency and/or diminish the fidelity of homologous recombination in CML (Rieke et al., 2016). All this information as well corroborates what we hypothesized that MH iPSC present a higher tumorigenic potential and have a higher propensity to generate genomic instabilities than DH iPSC.

Human ESC and iPSC have an altered cell cycle of 16-18h, with a short G1 phase with only 2,5h (Becker et al., 2006; Becker et al., 2007). Therefore, the cell has a short window of time to activate the repairing machinery for all damaged DNA DSBs acquired. The fact that LIG3 is significantly more expressed in MH clones during early passage 3 than DH clones (Figure 4, F), might link with the fact that c-Myc overexpression has been reported to promote the alternative NHEJ repairing mechanism rather than the classical NHEJ or Homologous Recombination.

Human iPSC telomere stability

Chromosome telomeres stability was also assessed with a QFISH analysis as in mouse cells. Multitelomeric signals (MTS) have been proposed to reflect increased breakage at chromosome termini and subsequent repair by homologous recombination mechanisms (Lydeard et al., 2007). Therefore multitelomeric signals are regarded as a type of genetic instability that are a result of telomere breakage during telomeres DNA

replication (Meeker et al., 2004; Muñoz et al., 2005; Blanco et al., 2007; Martinez et al., 2009; Sfeir et al., 2009; Tejera et al., 2010; Bosco et al., 2012).

Sirtuin 1 also contributes to telomere maintenance and augments global homologous recombination. Sirtuin 1 null mouse embryonic fibroblasts (Sirt1-/-MEFs) were shown to express a higher number of multitelomeric signals per chromosome (Palacios et al., 2010). Here we show how during the early passaging of MH iPSC Sirt1 levels are higher than DH iPSC (Figure 3, F). This fact, could be explained by the necessity of Myc made iPSC to restore all DNA damage caused by the stress c-Myc is driving on cells undergoing reprogramming, as shown by the increase in the MTS/Chr %.

While differences in signal free ends percentage were found in mouse iPSC between 3F + c-Myc and 3F + Cyclin D1, these differences were not found in human iPSC; however, differences were found in MTS/Chr percentage (Figure 5, A). This might be explained as fundamental differences exist between human and mouse telomere biology (Wright et al., 2000). The fact that c-Myc reprogramming increases the percentage of MTS/Chr supports our hypothesis that DH iPSC hold a greater chromosome stability than the classical MH iPSC.

BRCA2 and Rad51 are required for telomere length maintenance in MEFs (Badie et al., 2010). BRCA2 deletion and Rad51 inhibition led to telomere shortening and increased number of MTS in MEFs (Badie et al., 2010). Correspondingly, we see a decrease in Rad51 nuclear expression in MH clones, that might explain why we also see an increase in MTS in Myc made clones, since Rad51 was reported to be essential for facilitating telomere replication and capping and an alteration in normal levels could have affected.

Copy Number Variation in human iPSC

To advance iPSC technology we assessed CNV to see whether reprogramming with Cyclin D1 could lower the increase in CNV after reprogramming. Results showed that reprogramming increased CNV in both conditions; still MH presented a higher rate than DH iPSC clones, (Figure 5, D-E). However, no significance was found due to clonal variation. The fact that c-Myc containing cocktail has led to a higher trend of CNVs can be explained as it has been reported to be involved in gene amplification (Denis et al., 1991; Mai et al., 1994; Mai et al., 1996). It has been published that Myc overexpression elevates DHFR gene copy number within 3 weeks by 10 fold (Denis et al., 1991) or even just within 72h after overexpression (Mai et al., 1994; Mai et al., 1996). Indeed, every single cell expressing the conditional Myc gene had DHFR amplification (Mai et al., 1994). DHFR gene encodes for a protein that provides methotrexate (MTX) dug resistance; therefore also related with tumorigenic threat increase. Thus, Myc deregulates the normal “once per cycle” replication initiation, forcing several initiations of replication forks. Therefore, amplification of genes involved in DNA synthesis and cell-cycle progression provide a proliferative advantage to cells that harbour it (Kuschak et al., 2002).

C-Myc dysregulation is associated with illegitimate recombinations and long-range chromosomal rearrangements rather than single nucleotide polymorphism (Rockwood et al., 2002). Nevertheless in the case of mRNA reprogramming, c-Myc overexpression

lasted for 12 days on a row, which in turn might have been enough to cause CNVs differences found between MH and DH iPSC.

It was shown that reprogramming with protein transfections of the reprogramming factors led to lower increase in CNV in comparison with retroviral and lentivirally made iPSC (Park et al., 2014). Correspondingly, our result shows how the non-integrative method of mRNA transfection reprogramming does not present a significant increase in CNV between HFFs and iPSC.

Genomic alterations can also be selected during differentiation of PSC. For example, an abnormal subpopulation of ESC with multiple duplications in chromosome 20, after only 5 days, was selected in a cardiac differentiation experiment (Laurent *et al.*, 2011). Interestingly, multipotent adult stem cells also show frequent typical chromosomal abnormalities, like duplication of chromosome 19 in neural stem cells (NSC) or a deletion of chromosome 13 in mesenchymal stem cells (MSCs) (Ben-David *et al.*, 2011a).

CNV itself is not necessary a risky trait, as mounting number of papers show somatic mosaicism as a common feature of the human body, since there is already a considerable variation in the genomes of ordinary cells within our bodies (Chen et al., 2013; Lupski et al., 2013; Poduri et al., 2013; Biesecher et al., 2013). However, the more CNV a cell undergoes the more chances it is going to affect a relevant set of genes to promote transformation.

IPSC derived cells immune response

As the field grows and moves closer to clinical application the need to understand what will be the immune response of transplanted human iPSC-derived cells becomes paramount. Is autologous iPSC derive cells going to be a main source of cells for future cell therapies? Or maybe allogeneic iPSC derived cells HLA matched? Personalized againsts off the shelf cell sources needs to be devated over the next years.

The interaction of the human immune system with autologous reprogramed human cells remains an unexplored question. Four recent publications in animal studies (mice and non-human primates) indicate that there may be some immune response of autologous reprogramed cells (Liu et al., 2013; Zhao et al., 2011; Guha et al., 2013; Morizane et al., 2013). Data from human transplanted autologous reprogramed cells *in vivo* is limited and only one current clinical trial for iPSC-RPE cells exists with no immune response data available (Kamao et al., 2014; Alvarez et al., 2015). As the field grows and moves closer to clinical application the need to understand what will be the immune response of transplanted human iPSC-derived cells becomes paramount.

Patient cells that have been reprogrammed into iPSC and then differentiated to tissue specific cells can be considered artificial stem cells and many questions still exist about their function including genetic stability, ability to heal an injured tissue and their immune response. Artificially made stem cells provide a viable source of cells for cell replacement therapy. Therefore, they remain a prominent potential source of cells for the rapidly growing field of regenerative medicine.

Toll-like Receptor 3 (TLR3) short isoform overexpression in F2

Here, we have compared a population of patient cells (F1) with a population of iPSC derived cells (F2). Global proteomic analysis revealed that the two populations of fibroblast cells were mainly similar and no differences between viral made and episomal made iPSC was observed neither. However, there were differences in signal transduction and immune cell protein expression.

Central to the finding that iPSC-derived cells have altered immunogenicity is the sustained toll like receptor TLR3 expression. Double-stranded RNA (dsRNA), a frequent by-product of virus infection, is recognized by toll-like receptor 3 (TLR3) to mediate innate immune response to virus infection. The PI3K-Akt pathway plays an essential role in TLR3-mediated gene induction (Sarkar et al., 2004). We have found that both TLR3 and the Akt pathway is highly expressed in iPSC-derived cells and is most likely regulating expression of inflammatory cytokines IL6 and MCP1 as well as secondary adaptive immune system cytokines such as IL15 and RANTES. Increased levels of IL6 and MCP1 secretion by transplanted F2 cells (Figure 7, F) could cause recruitment of monocytes and neutrophils to further complicate a long-term inflammation response.

However, the down-regulation of IL15 and RANTES may result in a possible reduction of secondary T cell mediated response. This observation among others brings forward the interesting possibility that iPSC-derived cells may benefit from a suppressed immunogenic microenvironment favouring initial survival and subsequent engraftment and tissue regeneration. Interestingly, a recent study found that differentiation of human iPSC results in a loss of immunogenicity and leads to the induction of tolerance, despite expected antigen expression differences between iPSC-derived versus original somatic cells (De Almeida et al., 2014). In further agreement with this study it has also been demonstrated that neural progenitor cells from human induced pluripotent stem cells generated less autologous immune response (Huang et al., 2014).

Lee et al. found that the toll-like receptor 3 (TLR3) pathway enable efficient induction of pluripotency by viral or non-viral approaches (Lee et al., 2012b). Stimulation of TLR3 causes rapid and global changes in the expression of epigenetic modifiers to enhance chromatin remodelling and nuclear reprogramming. Furthermore, they conclude that activation of inflammatory pathways is required for efficient nuclear reprogramming in the induction of pluripotency (Lee et al., 2012b). Our finding suggests that this essential TLR3 pathway for achieving cell pluripotency is not re-set to the correct levels in iPSC-differentiated cells (F2) that then results in altered AKT signalling and cytokine secretion (Figure 6, H; Figure 7, E-F; Figure 9, E).

TLRs are expressed in the membrane of immune and non-immune cells (Delneste et al., 2007; Lafon et al., 2006). However, neurons also express TLRs, specifically TLR3 in order to have the ability to mount a strong inflammatory response by expressing inflammatory cytokines like TNF-α and IL-6 in absence of glia (Lafon et al., 2006). TLR3 recognizes dsRNA, produced by most viruses at some stage in their lifecycles, being a potent indicator of viral infection. Nevertheless, homodimerization of TLR3 is essentially required for ligand binding (wang et al., 2010b), and an intact binding site is required for dsRNA binding and stable dimerization to activate the downstream signalling cascade. TLR3 ectodomain, which is made by 23 LRR, bind as dimers to 45

bp segments of dsRNA, the minimum length required for TLR3 binding and activation (Wang et al., 2010b). The dsRNA interacts at two sites on each TLR3-ECD, one near the N-terminus (comprising LRR-NT and LRRs 1–3), and one near the C-terminus (comprising LRRs 19–23) (Liu et al., 2008). Mutational analyses (Wang et al., 2010b) have established that these three sites individually interact weakly with their binding partners but together form a high affinity receptor-ligand complex. Simultaneous interaction of all three sites at the same time is therefore required for stable and functional binging of TLR3/dsRNA. In the cell, two TLR3 ectodomains interacting on the luminal side of an endosome bring the two TIR domains together on the cytoplasmic side, forming a dimeric scaffold on which adaptor molecules could bind and initiate signalling cascade (Figure 10, F). When TLR3 dimerizes, it is recruited TICAM1 for the production of pro-inflammatory cytokines (Brikos et al., 2008).

TLR3 activation triggers a signal transduction that activates IL6 production. Therefore the fact that iPSC derived cells seem to express more TLR3 isoform B and the fact that this isoform blocks the correct function of the wild type full length isoform suggests that iPSC derived cells might be more prone to have anti-inflammatory properties (Figure 9, F) after being stimulated with pathogen associated molecular patterns (PAMPs), such as LPS and Poly(I:C) (Figure 9, E). Lack of IL6 cytokine excesive inflammatory response might be a positive property of iPSC derived cells. Nevertheless, there's no complete lack of IL6 secretion, since control basal levels of NSC without stimulation are higher than original HFFs. This small but stable level of IL6 secretion might be enough to maintain a desirable immune response in front of possible infections in transplanted iPSC derived cells inside patients.

Regarding the T cell kill assay, we have shown how after *in vivo* priming cytotoxic T lymphocytes (CTLs), not only there has not been an increase in CTLs cytotoxic degranulation, but a significant decrease (Figure 10, C). Interestingly after priming CTLs against iPSC, the decrease in CD107a degranulation marker was higher than when priming CTLs with CM, probably because of the decrease of MHC1 receptor expression reported in iPSC (Figure 8, B). Correspondingly, other studies showed that iPSC derived retinal pigmented epithelial cells (iPSC-RPE) have also been shown to inhibit T cell activation in vitro through TGF-β secretion (Sugita et al., 2015). Moreover, no increase in apoptosis was observed in CM co-cultured with primed CTLs against CMs, showing a lack of immunogenicity against syngeneic cells. Corneal Epithelial-like cells derived from hESC have been also reported to be less responsible for T cell proliferation and NK cell lysis in vitro (Wang et al., 2016). Moreover, in the paper, Wang et al. show that the immunological properties were not affected by interferon-γ. All these results indicated a low immunogenicity of ESC-CECs corroborating our findings.

The altered cytokine microenvironment of hiPSC-derived cells raises a number of issues to be considered for future cell transplantation. This may allow for hiPSC-derived cells to be used not only as an autologous cell therapy but also in a limited capacity as an allogeneic cell therapy. Recent work testing the allogeneic capacity of iPSC-derived cells in pig and rat models has revealed that this may not be the case and allogeneic iPSC-derived cells die *in vivo* at an early stage post transplantation (Sohn et al., 2015; Conradi et al., 2015).

Taken together the data demonstrate that the cell reprogramming process alters specific aspects of both the innate and adaptive immune response resulting in a reduction of immunogenicity, supporting similar findings recently described for human iPSC derived cells (de Almeida et al., 2014; Huang et al., 2014).

Cyclin D1 iPSC functional assay with NSC.

Keeping in mind that the final aim is the clinical application of iPSC derived cells, early this year, it has been published the first human clinical trial for iPSC transplantation therapies in the RIKEN institute, Japan (Mandai et al., 2017). It has consisted on iPSC derived retinal pigmented epithelial (RPE) cells transplantation in two age-related macular degeneration (AMD) patients. Therefore, an important challenge before iPSC can be used in the clinic is the survival and engraftment of iPSC derived cells in a hostile tissue environtment in vivo without evidence of pathology. Thus, in order to test engraftment of our new DH iPSC derived cells in vivo in an animal model, we explored injecting neural stem cells (NSC) into a Spinal cord injury (SCI) rat model. Hence, this functional assay of NSC injection resulted in a positive result of engraftment and survival. NSC not only survived 2 months after injection into rat spinal cords, but also migrated to the lesion site, which is delimited by the lack of astrocyte marker GFAP (Silver et al., 2004).

Hematoxylin eosin staining showed a recovery of the spinal cord tissue without any neoplasm. However, in order to determine whether this synaptic connection between the central nervous system (CNS) above and below the lesion is helping to recover the injury a longer period of time than two months and a larger number of animals would be required to be able to detect a significant quantifiable mobility improvement.

IPSCs can be differentiated to neural precursor cells, neural crest cells, neurons, oligodendrocytes, astrocytes, and even mesenchymal stromal cells. In SCI these can produce functional recovery by replacing lost cells and/or modulating the lesion microenvironment. Interestingly, after injecting DH iPSC clone DH1 derived NSC in the spinal cord of rats, no pathological neoplasm was formed; in contrast with our previous results where Retrovirally made iPSC (reprogrammed with c-Myc) derived Neural Stem Cells formed teratomas when injected into rat spinal cords in a similar model (López-Serrano et al., 2016). Remarkably, NSC differentiated in vivo into their derivatives: mature neurons (75,1%), oligodendrocytes (18,2%) and mature astrocytes (5,2%) (Figure 5, C).

CONCLUSIONS

- Cyclin D1 accelerates the reprogramming process by increasing pluripotency markers as shown by alkaline phosphatase in mouse and Tra-1-81 in human cells.

- Cyclin D1 decreases cell stress response genes during early reprogramming passages, such as IAP2, Gadd45b and Sirt1 in mouse cells and 53BP1, sirtuin 1 and Sirt6 in human cells. Furthermore Cyclin D1 rescued reprogramming in mouse Sirt1-/- MEFs compared to c-Myc, indicating it functions independent of Sirt1.

- Cyclin D1 made iPSC maintain the same pluripotency and differentiation potential in vitro and in vivo than c-Myc made iPSC.

- Cyclin D1 mouse made clones show a significant decrease in percentage of telomere signal-free ends and a trend of a lower number of chromosomal fragments in the nucleus. On the other hand, human DH iPSC show a decrease in % of multitelomeric signals per chromosome (MTS/Chr) in comparison with MH iPSC.

- Double strand breaks (DSBs) acquired during the reprogramming process and passaging until passage 10 and after differentiation to NSC are significantly lower when reprogramming with Cyclin D1 than with c-Myc.

- Cyclin D1 promotes DNA repair by enhancement of homologous recombination by helping to recruit Rad51, as has been recently reported (Chalermrujinanant et al., 2016). Here, MH clones show high levels of cytoplasmic Rad51 than DH clones; furthermore DH clones have higher nuclear Rad51.

- Gene copy number variation (CNV) is not significantly increased from HFFs to iPSC using synthetic mRNA transfections method.

- DH iPSC and NSC present significantly lower KI67 levels in vitro and in vivo compared with MH clones, demonstrating thus a lower tumorigenic threat of Cyclin D1 as a new component of the reprogramming cocktail as a substitute for c-Myc.

- In the in vivo spinal cord injury rat model, we demonstrated that DH iPSC derived NSC survive, engraft and differentiate into their derivatives 2 months after being injected into the spinal cord near the lesion site.

- Overall, results indicate that using Cyclin D1 for cell reprogramming is a better method to generate higher quality iPSC than using the classical c-Myc.

- Cell reprogramming process alters specific aspects of both the innate and adaptive immune response of iPSC-derived cells resulting in a reduction of immunogenicity, providing an insight for future clinical applications of autologous human iPSC-derived cell transplantation.

- We have described an upregulation of a short isoform (isoform B) of Toll-Like Receptor 3 (TLR3) in all iPSC derived cells as a consequence of the hypomethylated CpG sites found in the alternative transcription start site of the gene, not seen in normal endogenous cells.

- IPSC derived Neural Stem Cells remain unresponsive to Poly(I:C) stimulation and uncapable to secrete IL-6.

- We suggest that TLR3 short isoform B competes with the full length *wild type* isoform distabilitzing the essentially required dimerization process, for processing the signal transduction to create an inflammatory response.

- Lack of proinflammatory response may lead to beneficial consequences of future transplants of iPSC derived cells.

Future work/new directions:

- To increase the detection threshold of small CNV, we will perform a whole genome sequencing of the iPSC and NSC samples.

- Transfect an MMEJ reporter plasmid (pSV40-MMEJ), from Kostyrko et al., 2016, to iPSC to determine the actual levels of alternative NHEJ in both MH and DH iPSC.

- Apply for "La Marató" grant to perform a larger experiment in vivo with more rats to see whether NSC can help rescuing the mobility of rats in the long term. Then, rats would not be sacrificed until 3-4 months after injecting the cells to be able to detect functional recovery.

- After defining this protocol to obtain better quality iPSC, we want to focus on developing differentiation protocols into several cell types, such as motorneurons to assess an SMA mice model.

- Explore why after differentiating reprogrammed cells the epigenetic status of the alternative transcription start site for TLR3 remains hypomethylated. Try to remethylate this CpG with the CRISPR Cas9 technology.

- Increase the number of patients studied from 6 to larger cohorts to better define the TLR3 status in iPSC derived cells, to see whether it is a phenomena all across patients with very diverse genetic backgrounds. Furthermore, exploring other cell types derived from iPSCs a part from NSC, like CM or Endoderm, among others.

- Overexpress full length TLR3 with lentiviral vectors to overcompete with the short TLR3 isoform and show a recovery of response to LPS and Poly(I:C) stimulation.

- Analyze IL10 secretion levels of mouse iPSC derived cardiomyocytes as a measure of a possible explanation of the protective effect of CM over the CTLs.

BIBLIOGRAPHY

Aasen,T., Raya, A., Barrero, M.J., Garreta, E., Consiglio, A., Gonzalez, F., et al. (2008). Efficient and rapid generation of induced pluripotent stem cells from human keratinocytes. Nat. Biotechnol., 26, 1276-1284.

Abbas, Abul K.Lichtman, Andrew H. (2011) *Basic Immunology: Functions And Disorders Of The Immune System*. Philadelphia, Pa. : Saunders, 2011.

Adhikary S, Eilers M. (2005). Transcriptional regulation and transformation by Myc proteins. Nat Rev Mol Cell Biol. 2005 Aug;6(8):635-45.

Albajar M, Gómez-Casares MT, Llorca J, Mauleon I, Vaqué JP, Acosta JC, Bermúdez A, Donato N, Delgado MD, León J. (2011). MYC in chronic myeloid leukemia: induction of aberrant DNA synthesis and association with poor response to imatinib. Mol Cancer Res. 2011 May;9(5):564-76. doi: 10.1158/1541-7786.MCR-10-0356. Epub 2011 Apr 1.

Alvarez Palomo AB, S McLenachan, J Requena, C Menchon, C Barrot, F Chen, S Munne-Bosch and MJ Edel. (2013). Plant hormones increase efficiency of reprogramming mouse somatic cells to induced pluripotent stem cells and reduces tumorigenicity. Stem Cells Dev.

Alvarez Palomo AB, McLenachan S, Chen FK, Da Cruz L, Dilley RJ, Requena J, Lucas M, Lucas A, Drukker M, Edel MJ. (2015). Prospects for clinical use of reprogrammed cells for autologous treatment of macular degeneration. Fibrogenesis Tissue Repair. 2015 May 15;8:9. doi: 10.1186/s13069-015-0026-9. eCollection 2015.

Alberts, B., Johnson, A., Lewis, J., Raff, M., Roberts, K., & Walter, P. (2002). Molecular biology of the cell. Fourth Edition New York: Garland Science.

Albihn A, Johnsen JI, Henriksson MA. (2010) MYC in oncogenesis and as a target for cancer therapies. Adv Cancer Res. 2010;107:163-224. doi: 10.1016/S0065-230X(10)07006-5.

Allegrucci C, Wu YZ, Thurston A, Denning CN, Priddle H, Mummery CL, Ward-van Oostwaard D, Andrews PW, Stojkovic M, Smith N, Parkin T, Jones ME, Warren G, Yu L, Brena RM, Plass C, Young LE. (2007). Restriction landmark genome scanning identifies culture-induced DNA methylation instability in the human embryonic stem cell epigenome. Hum Mol Genet. 2007 May 15; 16(10):1253-68. Epub 2007 Apr 4.

Agami R, Bernards R. (2000). Distinct initiation and maintenance mechanisms cooperate to induce G1 cell cycle arrest in response to DNA damage. Cell. 2000 Jul 7;102(1):55-66.

Aggarwal P, et al. (2007). Nuclear accumulation of cyclin D1 during S phase inhibits Cul4-dependent Cdt1 proteolysis and triggers p53-dependent DNA rereplication. Genes Dev 21 (22): 2908-2922.

Amps K, Andrews PW, Anyfantis G, Armstrong L, Avery S, Baharvand H, Baker J, Baker D, Munoz MB, Beil S, Benvenisty N, Ben-Yosef D, Biancotti JC, Bosman A, Brena RM *et al*. and Zhou Q. (2011). Screening ethnically diverse human embryonic stem cells identifies a chromosome 20 minimal amplicon conferring growth advantage. Nat Biotechnol. 2011 Nov 27;29(12):1132-44. doi: 10.1038/nbt.2051.

Andrews A.J., Luger K. (2011). Nucleosome structure(s) and stability: variations on a theme, Annu. Rev. Biophys , 2011, vol. 40 (pg. 99-117).

Angel M, Yanik MF. Innate immune suppression enables frequent transfection with RNA encoding reprogramming proteins. (2010) PLoS One. 2010 Jul 23;5(7):e11756. doi: 10.1371/journal.pone.0011756.

Anguiano A, Tuchman SA, Acharya C, Salter K, Gasparetto C, Zhan F, Dhodapkar M, Nevins J, Barlogie B, Shaughnessy JD Jr, Potti A. (2009). Gene expression profiles of tumor biology provide a novel approach to prognosis and may guide the selection of therapeutic targets in multiple myeloma. J Clin Oncol. 2009 Sep 1;27(25):4197-203. doi: 10.1200/JCO.2008.19.1916. Epub 2009 Jul 27.

Aparicio T, Baer R, Gautier J. (2014). DNA double-strand break repair pathway choice and cancer. DNA Repair (Amst). 2014 Jul;19:169-75. doi: 10.1016/j.dnarep.2014.03.014. Epub 2014 Apr 18.

Araki R, Hoki Y, Uda M, Nakamura M, Jincho Y, Tamura C, Sunayama M, Ando S, Sugiura M, Yoshida MA, Kasama Y, Abe M. (2011). Crucial role of c-Myc in the generation of induced pluripotent stem cells. Stem Cells. 2011 Sep;29(9):1362-70. doi: 10.1002/stem.685.

Araki R, M Uda, Y Hoki, M Sunayama, M Nakamura, S Ando, M Sugiura, H Ideno, A Shimada, A Nifuji and M Abe. (2013). Negligible immunogenicity of terminally differentiated cells derived from induced pluripotent or embryonic stem cells. Nature. 2013 Feb 7;494(7435):100-4. doi: 10.1038/nature11807. Epub 2013 Jan 9.

Ashgar U., Witkiewicz A.K., Turner N.C., Knudsen E.S., (2015). The history and future of targeting cyclin-dependent kinases in cancer therapy. Nat Rev Drug Discov, 14(2):130-46.

Askew DS, Ihle JN, Cleveland JL. (1993). Activation of apoptosis associated with enforced Myc expression in myeloid progenitor cells is dominant to the suppression of apoptosis by interleukin-3 or erythropoietin. Blood 82: 2079–2087.

Atkin NB, Baker MC. (1982). Specific chromosome change, i(12p), in testicular tumours? Lancet. 1982 Dec 11;2(8311):1349.

Avilion AA, Nicolis SK, Pevny LH, Perez L, Vivian N, Lovell-Badge R. (2003). Multipotent cell lineages in early mouse development depend on SOX2 function. Genes Dev. 2003 Jan 1;17(1):126-40.

Badie S, Escandell JM, Bouwman P, Carlos AR, Thanasoula M, Gallardo MM, Suram A, Jaco I, Benitez J, Herbig U, Blasco MA, Jonkers J, Tarsounas M. (2010). BRCA2 acts as a RAD51 loader to facilitate telomere replication and capping. Nat Struct Mol Biol. 2010 Dec;17(12):1461-9. doi: 10.1038/nsmb.1943. Epub 2010 Nov 14.

Bai H, Chen K, Gao YX, Arzigian M, Xie YL, Malcosky C, Yang YG, Wu WS, Wang ZZ. (2012). Bcl-xL enhances single-cell survival and expansion of human embryonic stem

cells without affecting self-renewal. Stem Cell Res. 2012 Jan;8(1):26-37. doi: 10.1016/j.scr.2011.08.002.

Bailey JA, Eichler EE. (2006). Primate segmental duplications: crucibles of evolution, diversity and disease. Nat Rev Genet 7: 552-564.

Barlow JH, Faryabi RB, Callén E, Wong N, Malhowski A, Chen HT, Gutierrez-Cruz G, Sun HW, McKinnon P, Wright G, et al. (2013). Identification of early replicating fragile sites that contribute to genome instability. Cell 152: 620-632.

Bayani J, Selvarajah S, Maire G, Vukovic B, Al-Romaih K, Zielenska M, Squire JA. (2007). Genomic mechanisms and measurement of structural and numerical instability in cancer cells. Semin Cancer Biol. 2007 Feb;17(1):5-18. Epub 2006 Oct 26.

Beattie MS, Li Q, Bresnahan JC. (2000). Cell death and plasticity after experimental spinal cord injury. Prog Brain Res. 2000;128:9–21.

Beck G, Habicht GS. (1996). Immunity and the invertebrates. Sci Am. 1996 Nov;275(5):60-3, 66.

Becker KA, Ghule PN, Therrien JA, Lian JB, Stein JL, van Wijnen AJ, Stein GS. (2006). Self-renewal of human embryonic stem cells is supported by a shortened G1 cell cycle phase. J Cell Physiol. 2006 Dec;209(3):883-93.

Becker KA, Stein JL, Lian JB, van Wijnen AJ, Stein GS. (2007). Establishment of histone gene regulation and cell cycle checkpoint control in human embryonic stem cells. J Cell Physiol. 2007 Feb;210(2):517-26.

Beddington RS, Robertson EJ. (1989). An assessment of the developmental potential of embryonic stem cells in the midgestation mouse embryo. Development. 1989 Apr;105(4):733-7.

Beltran, E. et al. (2011). A cyclin-D1 interaction with BAX underlies its oncogenic role and potential as a therapeutic target in mantle cell lymphoma. Proc. Natl Acad. Sci. USA 108, 12461-12466.

Ben-David U. & Nissim Benvenisty. (2011a). The tumorigenicity of human embryonic and induced pluripotent stem cells. Nature Reviews Cancer 11, 268-277 (April 2011). doi:10.1038/nrc3034

Ben-David U, Mayshar Y, Benvenisty N. (2011b). Large-scale analysis reveals acquisition of lineage-specific chromosomal aberrations in human adult stem cells. Cell Stem Cell. 2011 Aug 5;9(2):97-102. doi: 10.1016/j.stem.2011.06.013.

Benzing C, Segschneider M, Leinhaas A, et al. (2006). Neural conversion of human embryonic stem cell colonies in the presence of fibroblast growth factor-2. Neuroreport. 2006;17:1675–1681.

Biesecker LG, Spinner NB. (2013). A genomic view of mosaicism and human disease. Nat Rev Genet. 2013 May;14(5):307-20. doi: 10.1038/nrg3424.

Blackburn EH. (2001) Switching and signaling at the telomere. Cell. 2001 Sep 21;106(6):661-73.

Blanco, R., Munoz, P., Flores, J.M., Klatt, P., and Blasco, M.A. (2007). Telomerase abrogation dramatically accelerates TRF2-induced epithelial carcinogenesis. Genes Dev. 21, 206–220.

Blight AR. (1992). Spinal cord injury models: Neurophysiology. J Neurotrauma. 1992;9:147–149. discussion 149–150.

Bock C, Kiskinis E, Verstappen G, Gu H, Boulting G, Smith ZD, Ziller M, Croft GF, Amoroso MW, Oakley DH, Gnirke A, Eggan K, Meissner A. (2011). Reference Maps of human ES and iPS cell variation enable high-throughput characterization of pluripotent cell lines. Cell. 2011 Feb 4;144(3):439-52. doi: 10.1016/j.cell.2010.12.032.

Bonde S, Chan KM, Zavazava N. (2008). ES-cell derived hematopoietic cells induce transplantation tolerance. PLoS One. 2008 Sep 15;3(9):e3212. doi: 10.1371/journal.pone.0003212.

Bosch-Presegué L, Vaquero A. (2014). Sirtuins in stress response: guardians of the genome. Oncogene. 2014 Jul 17;33(29):3764-75. doi: 10.1038/onc.2013.344. Epub 2013 Sep 2.

Bosco N, de Lange T. (2012). A TRF1-controlled common fragile site containing interstitial telomeric sequences. Chromosoma. 2012 Oct;121(5):465-74. doi: 10.1007/s00412-012-0377-6. Epub 2012 Jul 13.

Botos I, Segal DM, Davies DR. (2011). The structural biology of Toll-like receptors. Structure. 2011 Apr 13;19(4):447-59. doi: 10.1016/j.str.2011.02.004.

Bouchard C, Lee S, Laulus-Hock V, Loddenkemper C, Eilers M, Schmitt CA. (2007). FoxO transcription factors suppress Myc-driven lymphomagenesis via direct activation of Arf. Gene Dev 21: 2775–2787.

Boyd AS, Wood KJ. (2010). Characteristics of the early immune response following transplantation of mouse ES cell derived insulin-producing cell clusters. PLoS One. 2010 Jun 4;5(6):e10965. doi: 10.1371/journal.pone.0010965.

Boyer, L.A., Lee, T.I., Cole, M.F., Johnstone, S.E.,Levine, S.S., Zucker, J.P., Guenther, M.G., Kumar, R.M., Murray, H.L., Jenner, R.G., et al. (2005). Core transcriptional regulatory circuitry in human embryonic stem cells. Cell 122, 947-956.

Briggs JA, Sun J, Shepherd J, Ovchinnikov DA, Chung TL, Nayler SP, Kao LP, Morrow CA, Thakar NY, Soo SY, Peura T, Grimmond S, Wolvetang EJ. (2013). Integration-free induced pluripotent stem cells model genetic and neural developmental features of down syndrome etiology. Stem Cells. 2013 Mar;31(3):467-78. doi: 10.1002/stem.1297.

Brikos C, O'Neill LAJ. (2008). Signalling of toll-like receptors. In: S. Bauer GH, editor. Toll-like receptors (TLRs) and innate immunity. Berlin: Springer; 2008. pp. 21–50.

Bruno S, Darzynkiewicz Z. (1992). Cell cycle dependent expression and stability of the nuclear protein detected by Ki-67 antibody in HL-60 cells. Cell Prolif. 1992 Jan;25(1):31-40.

Bullwinkel J, Baron-Lühr B, Lüdemann A, Wohlenberg C, Gerdes J, Scholzen T. Ki-67 protein is associated with ribosomal RNA transcription in quiescent and proliferating cells. J Cell Physiol. 2006 Mar;206(3):624-35.

Burma S, Chen BP, Murphy M, Kurimasa A, Chen DJ. (2001). ATM phosphorylates histone H2AX in response to DNA double-strand breaks.J Biol Chem. 2001 Nov 9;276(45):42462-7. Epub 2001 Sep 24.

Burma S, Chen BP, Chen DJ. (2006). Role of non-homologous end joining (NHEJ) in maintaining genomic integrity. DNA Repair (Amst). 2006 Sep 8;5(9-10):1042-8. Epub 2006 Jul 5.

Cao J, Li X, Lu X, Zhang C, Yu H, Zhao T. (2014). Cells derived from iPSC can be immunogenic - yes or no? Protein Cell. 2014 Jan;5(1):1-3. doi: 10.1007/s13238-013-0003-2.

Carter NP. (2007). Methods and strategies for analyzing copy number variation using DNA microarrays. Nat Genet. 2007 Jul;39(7 Suppl):S16-21.

Casimiro MC, Crosariol M, Loro E, Ertel A, Yu Z, Dampier W, Saria EA, Papanikolaou A, Stanek TJ, Li Z, Wang C, Fortina P, Addya S, Tozeren A, Knudsen ES, Arnold A, Pestell RG. (2012). ChIP sequencing of cyclin D1 reveals a transcriptional role in chromosomal instability in mice. J Clin Invest. 2012 Mar;122(3):833-43. doi: 10.1172/JCI60256. Epub 2012 Feb 6.

Ceccaldi R, Liu JC, Amunugama R, Hajdu I, Primack B, Petalcorin MI, O'Connor KW, Konstantinopoulos PA, Elledge SJ, Boulton SJ, Yusufzai T, D'Andrea AD. (2015). Homologous-recombination-deficient tumours are dependent on Polθ-mediated repair. Nature. 2015 Feb 12;518(7538):258-62. doi: 10.1038/nature14184. Epub 2015 Feb 2.

Ceccaldi, R., Rondinelli, B., & D'Andrea, A. D. (2016). Repair Pathway Choices and Consequences at the Double-Strand Break. *Trends in Cell Biology*, *26*(1), 52–64.

Chalermrujinanant C, Michowski W, Sittithumcharee G, Esashi F, Jirawatnotai S. (2016). Cyclin D1 promotes BRCA2-Rad51 interaction by restricting cyclin A/B-dependent BRCA2 phosphorylation. Oncogene. 2016 Jun 2;35(22):2815-23. doi: 10.1038/onc.2015.354. Epub 2015 Sep 21.

Chen J, Liu J, Yang J, Chen Y, Chen J, Ni S, Song H, Zeng L, Ding K, Pei D. (2011). BMPs functionally replace Klf4 and support efficient reprogramming of mouse fibroblasts by Oct4 alone. Cell Res. 2011 Jan;21(1):205-12. doi: 10.1038/cr.2010.172.

Chen Q, Shi X, Rudolph C, Yu Y, Zhang D, Zhao X, Mai S, Wang G, Schlegelberger B, Shi Q. (2011). Recurrent trisomy and Robertsonian translocation of chromosome 14 in murine iPS cell lines. Chromosome Res 19: 857-868.

Chen K, Chmait RH, Vanderbilt D, Wu S, Randolph L. (2013). Chimerism in monochorionic dizygotic twins: case study and review. Am J Med Genet A. 2013 Jul;161A(7):1817-24. doi: 10.1002/ajmg.a.35957. Epub 2013 May 22.

Cheng SW, Davies KP, Yung E, Beltran RJ, Yu J, Kalpana GV. (1999). c-MYC interacts with INI1/hSNF5 and requires the SWI/SNF complex for transactivation function. Nat Genet. 1999 May;22(1):102-5.

Cheng Y, Yang B, Xi Y, Chen X. (2016). RAD51B as a potential biomarker for early detection and poor prognostic evaluation contributes to tumorigenesis of gastric cancer. Tumour Biol. 2016 Nov;37(11):14969-14978. Epub 2016 Sep 20.

Chernova OB, Chernov MV, Ishizaka Y, Agarwal ML, Stark GR. (1998). Myc abrogates p53-mediated cell cycle arrest in N-(phosphonacetyl)-L-aspartate-treated cells, permiting CAD gene amplification. Mol Biol 18: 536-545.

Chiang DY, Getz G, Jaffe DB, O'Kelly MJ, Zhao X, Carter SL, Russ C, Nusbaum C, Meyerson M, Lander ES. (2009). High-resolution mapping of copy-number alterations with massively parallel sequencing. Nat Methods. 2009 Jan;6(1):99-103. doi: 10.1038/nmeth.1276. Epub 2008 Nov 30.

Chin MH, Mason MJ, Xie W, Volinia S, Singer M, Peterson C, Ambartsumyan G, Aimiuwu O, Richter L, Zhang J, Khvorostov I, Ott V, Grunstein M, Lavon N, Benvenisty N, Croce CM, Clark AT, Baxter T, Pyle AD, Teitell MA, Pelegrini M, Plath K, Lowry WE. (2009). Induced pluripotent stem cells and embryonic stem cells are distinguished by gene expression signatures. Cell Stem Cell. 2009 Jul 2;5(1):111-23. doi: 10.1016/j.stem.2009.06.008.

Chng WJ, Huang GF, Chung TH, Ng SB, Gonzalez-Paz N, Troska-Price T, Mulligan G, Chesi M, Bergsagel PL, Fonseca R. (2011). Clinical and biological implications of MYC activation: a common difference between MGUS and newly diagnosed multiple myeloma. Leukemia. 2011 Jun;25(6):1026-35. doi: 10.1038/leu.2011.53. Epub 2011 Apr 5.

Choi Y.J., Anders L., (2014a). Signaling through cyclin D-dependent kinases. Oncogene, 33(15):1890-903.

Choi, Y. J. et al. (2014b). D-cyclins repress apoptosis in hematopoietic cells by controlling death receptor Fas and its ligand FasL. Dev. Cell 30, 255-267.

Choo A. M., Liu J., Lam C. K., Dvorak M., Tetzlaff W., Oxland T. R. (2007). Contusion, dislocation, and distraction: primary hemorrhage and membrane permeability in distinct mechanisms of spinal cord injury. J. Neurosurg. Spine 6, 255–266. 10.3171/spi.2007.6.3.255

Choo AB, Tan HL, Ang SN, Fong WJ, Chin A, Lo J, Zheng L, Hentze H, Philp RJ, Oh SK, Yap M. (2007). Selection against undifferentiated human embryonic stem cells by a cytotoxic antibody recognizing podocalyxin-like protein-1. Stem Cells. 2008 Jun;26(6):1454-63. doi: 10.1634/stemcells.2007-0576. Epub 2008 Mar 20.

Chuang TC, Moshir S, Garini Y, Chuang AY, Young IT, Vermolen B, van den Doel R, Mougey V, Perrin M, Braun M, et al. (2004). The three-dimensional organization of telomeres in the nucleus of mammalian cells. BMC Biol 2:12.

Connell-Crowley L, Harper JW, Goodrich DW. (1997). Cyclin D1/Cdk4 regulates retinoblastoma protein-mediated cell cycle arrest by site-specific phosphorylation. Mol Biol Cell. 1997 Feb;8(2):287-301.

Conradi L, Schmidt S, Neofytou E, Deuse T, Peters L, Eder A, Hua X, Hansen A, Robbins RC, Beygui RE, Reichenspurner H, Eschenhagen T, Schrepfer S. (2015). Immunobiology of fibrin-based engineered heart tissue. Stem Cells Transl Med. 2015 Jun;4(6):625-31. doi: 10.5966/sctm.2013-0202. Epub 2015 May 6.

Corti S, Nizzardo M, Simone C, Falcone M, Nardini M, Ronchi D, Donadoni C, Salani S, Riboldi G, Magri F, Menozzi G, Bonaglia C, Rizzo F, Bresolin N, Comi GP. (2012). Genetic correction of human induced pluripotent stem cells from patients with spinal muscular atrophy. Sci Transl Med. 2012 Dec 19;4(165):165ra162. doi: 10.1126/scitranslmed.3004108.

Cowan C. A., Klimanskaya I., McMahon J., Atienza J., Witmyer J., Zucker J. P., Wang S., Morton C. C., McMahon A. P., Powers D., Melton D. A. *(2004) Derivation of embryonic stem-cell lines from human blastocysts. N. Engl. J. Med. 350, 1353–1356*

Cowan C. A., Jocelyn Atienza, Douglas A. Melton, Kevin Eggan. (2005). Nuclear Reprogramming of Somatic Cells After Fusion with Human Embryonic Stem Cells. *Science 26 August 2005: Vol. 309 no. 5739 pp. 1369-1373. DOI:* 10.1126/science.1116447.

Cowling VH, Cole MD. (2006). Mechanism of transcriptional activation by the Myc oncoproteins. Semin Cancer Biol. 2006 Aug;16(4):242-52. Epub 2006 Aug 4.

Dang CV, Li F, Lee LA. (2005). Could Myc induction of mitocondrial biogenesis be linked to ROS production and genomic instability? Cell Cycle 4: 1465-1466.

Dang CV. (2010). Enigmatic MYC Conducts an Unfolding Systems Biology Symphony. Genes Cancer. 2010 Jun 1;1(6):526-531.

Darabi R., Robert W. Arpke, Stefan Irion, John T. Dimos, Marica Grskovic, Michael Kyba, Rita C.R. Perlingeiro. (2012). Human ES- and iPS-Derived Myogenic Progenitors Restore DYSTROPHIN and Improve Contractility upon Transplantation in Dystrophic Mice. Cell Stem Cell - 4 May 2012 (Vol. 10, Issue 5, pp. 610-619). DOI 10.1016/j.stem.2012.02.015.

Davies AA, Masson JY, McIlwraith MJ, Stasiak AZ, Stasiak A, Venkitaraman AR, West SC. (2001). Role of BRCA2 in control of the RAD51 recombination and DNA repair protein. Mol Cell. 2001 Feb;7(2):273-82.

Davies OR, Pellegrini L. (2007). Interaction with the BRCA2 C terminus protects RAD51-DNA filaments from disassembly by BRC repeats. Nat Struct Mol Biol. 2007 Jun;14(6):475-83.

Davis, A., & Chen, D. (2013). DNA double strand break repair via non-homologous end-joining. *Translational Cancer Research*, *2*(3), 130–43.

De Almeida PE, Meyer EH, Kooreman NG, Diecke S, Dey D, Sanchez-Freire V, Hu S, Ebert A, Odegaard J, Mordwinkin NM, Brouwer TP, Lo D, Montoro DT, Longaker MT, Negrin RS, Wu JC. (2014). Transplanted terminally differentiated induced pluripotent stem cells are accepted by immune mechanisms similar to self-tolerance. Nat Commun. 2014 May 30;5:3903. doi: 10.1038/ncomms4903.

De Bonis ML, Ortega S, Blasco MA. (2014). SIRT1 is necessary for proficient telomere elongation and genomic stability of induced pluripotent stem cells. Stem Cell Reports. 2014 Apr 17;2(5):690-706. doi: 10.1016/j.stemcr.2014.03.002. eCollection 2014.

Delneste Y, Beauvillain C, Jeannin P. (2007). Innate immunity: structure and function of TLRs. Med Sci (Paris). 2007 Jan;23(1):67-73.

Deng J, Shoemaker R, Xie B, Gore A, LeProust EM, Antosiewicz-Bourget J, Egli D, Maherali N, Park IH, Yu J, Daley GQ, Eggan K, Hochedlinger K, Thomson J, Wang W, Gao Y, Zhang K. (2009). Targeted bisulfite sequencing reveals changes in DNA methylation associated with nuclear reprogramming. Nat Biotechnol. 2009 Apr;27(4):353-60. doi: 10.1038/nbt.1530. Epub 2009 Mar 29.

Denis N, Kitzis A, Kruh J, Dautry F, Corcos D. (1991). Stimulation of methotrexate resistance and dihydrofolate reductase gene amplification by c-myc. Oncogene 6: 1453-1457.

Deumens R, Koopmans GC, Jaken RJ, et al. (2006). Stimulation of neurite outgrowth on neonatal cerebral astrocytes is enhanced in the presence of BDNF. Neurosci Lett. 2006;407:268–273.

Dietz V, Curt A. (2006). Neurological aspects of spinal-cord repair: Promises and challenges. Lancet Neurol. 2006;5:688–694.

Dimos JT, Rodolfa KT, Niakan KK, Weisenthal LM, Mitsumoto H, Chung W, Croft GF, Saphier G, Leibel R, Goland R, Wichterle H, Henderson CE, Eggan K. (2008). Induced pluripotent stem cells generated from patients with ALS can be differentiated into motor neurons. Science. 2008 Aug 29;321(5893):1218-21. Epub 2008 Jul 31. *DOI:* 10.1126/science.1158799.

Dobbin MM, Madabhushi R, Pan L, Chen Y, Kim D, Gao J, Ahanonu B, Pao PC, Qiu Y, Zhao Y, Tsai LH. (2013). SIRT1 collaborates with ATM and HDAC1 to maintain genomic stability in neurons. Nat Neurosci. 2013 Aug;16(8):1008-15. doi: 10.1038/nn.3460. Epub 2013 Jul 14.

Doi A, Park IH, Wen B, Murakami P, Aryee MJ, Irizarry R, Herb B, Ladd-Acosta C, Rho J, Loewer S, Miller J, Schlaeger T, Daley GQ, Feinberg AP. (2009). Differential methylation of tissue- and cancer-specific CpG island shores distinguishes human induced pluripotent stem cells, embryonic stem cells and fibroblasts. Nat Genet. 2009 Dec;41(12):1350-3. doi: 10.1038/ng.471. Epub 2009 Nov 1.

Draper J. S., Smith K., Gokhale P., Moore H. D., Maltby E., Johnson J., Meisner L., Zwaka T. P., Thomson J. A., Andrews P. W. *(2004).* Recurrent gain of chromosomes 17q and 12 in cultured human embryonic stem cells. Nat. Biotechnol. 22, 53–5.

Drukker M, Katz G, Urbach A, Schuldiner M, Markel G, Itskovitz-Eldor J, Reubinoff B, Mandelboim O, Benvenisty N. (2002). Characterization of the expression of MHC proteins in human embryonic stem cells. Proc Natl Acad Sci U S A. 2002 Jul 23;99(15):9864-9. Epub 2002 Jul 11.

Duyao MP, Buckler AJ, Sonenshein GE. (1990). Interaction of an NF-kappa B-like factor with a site upstream of the c-myc promoter. Proc Natl Acad Sci U S A. 1990 Jun;87(12):4727-31.

Eberhardy SR, Farnham PJ. (2001). C-Myc mediates activation of the cad promoter via a post-RNA polymerase II recruitment mechanism. J Biol Chem 276: 48562-48571.

Edel MJ, Menchon C, Menendez S, Consiglio A, Raya A, Izpisua Belmonte JC. (2010). Rem2 GTPase maintains survival of human embryonic stem cells as well as enhancing reprogramming by regulating p53 and cyclin D1. Genes Dev. 2010 Mar 15;24(6):561-73. doi: 10.1101/gad.1876710.

Eggers, J.P., Grandgenett, P.M., Lewallen, M.E., Tremayne, J., Singh, P.K., Swanson, B.J., Andersen, J.M., Caffrey, T.C., High, R.R., Ouellette, M., and Hollingsworth, M.A. (2011). Cyclin-dependent kinase 5 is amplified and overexpressed in pancreatic cancer and activated by mutant K-Ras. *Clinical Cancer Research*, 17(19): 6140-6150.

Eilers M, Eisenman RN. Myc's broad reach. Genes Dev. (2008). Oct 15;22(20):2755-66. doi: 10.1101/gad.1712408.

Elliott AM, Elliott KA, Kammesheidt A. (2010). High resolution array-CGH characterization of human stem cells using a stem cell focused microarray. Mol Biotechnol. 2010 Nov;46(3):234-42. doi: 10.1007/s12033-010-9294-1.

Erceg S, Lainez S, Ronaghi M, et al. (2008). Differentiation of human embryonic stem cells to regional specific neural precursors in chemically defined medium conditions. Plos One. 2008;3:e2122.

Erceg S, Ronaghi M, Oria M, Roselló MG, Aragó MA, Lopez MG, Radojevic I, Moreno-Manzano V, Rodríguez-Jiménez FJ, Bhattacharya SS, Cordoba J, Stojkovic M. (2010). Transplanted oligodendrocytes and motoneuron progenitors generated from human embryonic stem cells promote locomotor recovery after spinal cord transection. Stem Cells. 2010 Sep;28(9):1541-9. doi: 10.1002/stem.489.

Erridge C. (2010). Endogenous ligands of TLR2 and TLR4: agonists or assistants? J Leukoc Biol. 2010 Jun;87(6):989-99. doi: 10.1189/jlb.1209775. Epub 2010 Feb 23.

Esashi, F., Christ, N., Gannon, J., Liu, Y., Hunt, T., Jasin, M., & West, S. C. (2005). CDK-dependent phosphorylation of BRCA2 as a regulatory mechanism for recombinational repair. *Nature*, *434*(7033), 598–604.

Esteban, M.A., Wang, T., Qin, B., Yang, J., Qin, D., Cai, J., et al. (2009). Vitamin C enhances the generation of mouse and human induced pluripotent stem cells. Cell Stem Cell.

Evan GI, Wyllie AH, Gilbert CS, Littlewood TD, Land H, Brooks M *et al*. (1992). Induction of apoptosis in fibroblasts by c-Myc protein. Cell 69: 119–128.

Evan IG, Vousden KH. (2001). Proliferation, cell cycle and apoptosis in cancer. *Nature*. 411:342-348.

Evans MJ, Kaufman MH. (1981). Establishment in culture of pluripotential cells from mouse embryos. Nature. 1981 Jul 9;292(5819):154-6.

Fairchild PJ. (2010). The challenge of immunogenicity in the quest for induced pluripotency. Nat Rev Immunol. 2010 Dec;10(12):868-75. doi: 10.1038/nri2878.

Feber A, Clark J, Goodwin G, Dodson AR, Smith PH, Fletcher A, Edwards S, Flohr P, Falconer A, Roe T, Kovacs G, Dennis N, Fisher C, Wooster R, Huddart R, Foster CS, Cooper CS. (2004). Amplification and overexpression of E2F3 in human bladder cancer. Oncogene 2004, 23:1627-1630.

Feber A, Guilhamon P, Lechner M, Fenton T, Wilson GA, Thirlwell C, Morris TJ, Flanagan AM, Teschendorff AE, Kelly JD, Beck S. (2014). Using high-density DNA methylation arrays to profile copy number alterations. Genome Biol. 2014 Feb 3;15(2):R30. doi: 10.1186/gb-2014-15-2-r30.

Felsher DW, Bishop JM. (1999). Transient excess of Myc activity can elicit genomic instability and tumorigenesis. Proc Natl Acad Sci 96: 3940-3944.

Feng B, Jiang J, Kraus P, Ng JH, Heng JC, Chan YS, Yaw LP, Zhang W, Loh YH, Han J, Vega VB, Cacheux-Rataboul V, Lim B, Lufkin T, Ng HH. (2009). Reprogramming of fibroblasts into induced pluripotent stem cells with orphan nuclear receptor Esrrb. Nat Cell Biol. 2009 Feb;11(2):197-203. doi: 10.1038/ncb1827. Epub 2009 Jan 11.

Ferguson-Smith AC. (2011). Genomic imprinting: the emergence of an epigenetic paradigm. Nat Rev Genet. 2011 Jul 18;12(8):565-75. doi: 10.1038/nrg3032.

Fernandez PC, Frank SR, Wang L, Schroeder M, Liu S, Greene J, Cocito A, Amati B. (2003). Genomic targets of the human c-Myc protein. Genes Dev. 2003 May 1;17(9):1115-29. Epub 2003 Apr 14.

Fong H, Hohenstein KA, Donovan PJ. (2008). Regulation of self-renewal and pluripotency by Sox2 in human embryonic stem cells. Stem Cells. 2008 Aug;26(8):1931-8. doi: 10.1634/stemcells.2007-1002. Epub 2008 Apr 3.

Fong, C.Y., Peh, G.S., Gauthaman, K. and Bongso, A. (2009). Separation of SSEA-4 and TRA-1-60 labelled undifferentiated human embryonic stem cells from a heterogeneous

cell population using magnetic-activated cell sorting (MACS) and fluorescence-activating cell sorting (FACS). Stem Cell Rev. 5, 72-80.

Franco S, Murphy MM, Li G, Borjeson T, Boboila C, Alt FW. (2008). DNA-PKcs and Artemis function in the end-joining phase of immunoglobulin heavy chain class switch recombination. J Exp Med. 2008 Mar 17;205(3):557-64. doi: 10.1084/jem.20080044. Epub 2008 Mar 3.

Frit P, Barboule N, Yuan Y, Gomez D, Calsou P. (2014). Alternative end-joining pathway(s): bricolage at DNA breaks. *DNA* Repair (Amst). 2014 May;17:81-97. doi: 10.1016/j.dnarep.2014.02.007. Epub 2014 Mar 6.

Fu M, et al. (2005). Cyclin D1 represses p300 transactivation through a cyclin-dependent kinase-independent mechanism. J Biol Chem 280 (33): 29728-29742.

Fusaki N, Ban H, Nishiyama A, Saeki K, Hasegawa M. (2009). Efficient induction of transgene-free human pluripotent stem cells using a vector based on Sendai virus, an RNA virus that does not integrate into the host genome. Proc Jpn Acad Ser B Phys Biol Sci. 2009;85(8):348-62.

Fukasawa K, Choi T, Kuriyama R, Rulong S, Vande Woude GF. (1996). Abnormal centrosome amplification in the absence of p53. Science 271: 1744-1747.

Gadji M, Vallente R, Klewes L, Righolt C, Wark L, Kongruttanachok N, Knecht H, Mai S. (2011). Nuclear remodelling as a mechanism for genomic instability in cancer. Adv Cancer Res 112: 77-126.

Gadji M, Adebayo Awe J, Rodrigues P, Kumar R, Houston DS Klewes L, Dièye TN, Rego EM, Passetto RF, et al. (2012). Profiling three-dimensional nuclear telomeric architecture of myelodysplastic syndromes and acute myeloid leukemia defines patient subgroups. Clin Cancer Res 18: 3293-3304.

Gan, L. et al. (2009). Cyclin D1 promotes anchorage-independent cell survival by inhibiting FOXO-mediated anoikis. Cell Death Differ. 16, 1408-1417.

Ganesan S. (2011). MYC, PARP1, and chemoresistance: BIN there, done that? Sci Signal. 2011 Mar 29;4(166):pe15. doi: 10.1126/scisignal.2001946.

García-Díaz M, Bebenek K, Sabariegos R, Domínguez O, Rodríguez J, Kirchhoff T, García-Palomero E, Picher AJ, Juárez R, Ruiz JF, Kunkel TA, Blanco L. (2002). DNA polymerase lambda, a novel DNA repair enzyme in human cells. J Biol Chem. 2002 Apr 12;277(15):13184-91. Epub 2002 Jan 30.

Gay NJ, Gangloff M. (2007). Structure and function of Toll receptors and their ligands. Annu Rev Biochem. 2007;76:141-65.

George RE, Kenyon RM, McGuckin AG, Malcolm AJ, Pearson AD, Lunec J. (1996). Investigation of co-amplification of the candidate genes ornithine decarboxylase, ribonucleotide reductase, syndecan-1 and a DEAD box gene, DDX1, with N-myc in

neuroblastoma. United Kingdom Children's Cancer Study Group. Oncogene 12: 1583-1587.

Gerrard L, Rodgers L, Cui W. (2005). Differentiation of human embryonic stem cells to neural lineages in adherent culture by blocking bone morphogenetic protein signaling. Stem Cells. 2005;23:1234–1241.

Ghule, P.N. et al. (2010). Reprogramming the pluripotent cell cycle: restoration of an abbreviated G1 phase in human induced pluripotent stem (iPS) cells. J. Cell. Physiol. 13 Oct 2010 (doi: 10.1002/jcp.22440).

Giorgetti A., Nuria Montserrat, Trond Aasen, Federico Gonzalez, Ignacio Rodríguez-Pizà, Rita Vassena, Angel Raya, Stéphanie Boué, Maria Jose Barrero, Begoña Aran Corbella, Marta Torrabadella, Anna Veiga, Juan Carlos Izpisua Belmonte. (2009). Generation of induced pluripotent stem cells from human cord blood using *OCT4* and *SOX2*. Cell Stem Cell. 2009 October 2; 5(4): 353–357. doi: 10.1016/j.stem.2009.09.008.

Giorgetti A, N Montserrat, I Rodriguez-Piza, C Azqueta, A Veiga and JC Izpisua Belmonte. (2010). Generation of induced pluripotent stem cells from human cord blood cells with only two factors: Oct4 and Sox2. Nat Protoc 5:811-820.

Goncalves Dos Santos Silva A, Sarkar R, Harizanova J, Guffei A, Mowat M, Garini Y, Mai S. (2008). Centromeres in cell división, evolution nuclear organization and disease. J Cell Biochem 104: 2040-2058.

Golmard L, Caux-Moncoutier V, Davy G, Al Ageeli E, Poirot B, Tirapo C, Michaux D, Barbaroux C, d'Enghien CD, Nicolas A, Castéra L, Sastre-Garau X, Stern MH, Houdayer C, Stoppa-Lyonnet D. (2013). Germline mutation in the RAD51B gene confers predisposition to breast cancer. BMC Cancer. 2013 Oct 19;13:484. doi: 10.1186/1471-2407-13-484.

Gore A, Li Z, Fung HL, Young JE, Agarwal S, Antosiewicz-Bourget J, Canto I, Giorgetti A, Israel MA, Kiskinis E, Lee JH, Loh YH, Manos PD, Montserrat N,Panopoulos AD, Ruiz S, Wilbert ML, Yu J, Kirkness EF, Izpisua Belmonte JC, Rossi DJ, Thomson JA, Eggan K, Daley GQ, Goldstein LS, Zhang K. (2011). Somatic coding mutations in human induced pluripotent stem cells. Nature. 2011 Mar 3;471(7336):63-7. doi: 10.1038/nature09805.

Grad I, Hibaoui Y, Jaconi M, Chicha L, Bergström-Tengzelius R, Sailani MR, Pelte MF, Dahoun S, Mitsiadis TA, Töhönen V, Bouillaguet S, Antonarakis SE, Kere J, Zucchelli M, Hovatta O, Feki A. (2011). NANOG priming before full reprogramming may generate germ cell tumours. Eur Cell Mater. 2011 Nov 9;22:258-74; discussio 274. DOI: 10.5167/uzh-63252.

Grasso, P.; Gangolli, S.; Gaunt, Ian (2002). Essentials of Pathology for Toxicologists. CRC Press. ISBN 978-0-415-25795-4. Retrieved 30 August 2011.

Guenther MG, Frampton GM, Soldner F, Hockemeyer D, Mitalipova M, Jaenisch R, Young RA. (2010). Chromatin structure and gene expression programs of human embryonic

and induced pluripotent stem cells. Cell Stem Cell. 2010 Aug 6;7(2):249-57. doi: 10.1016/j.stem.2010.06.015.

Guha P, JW Morgan, G Mostoslavsky, NP Rodrigues and AS Boyd. (2013). Lack of immune response to differentiated cells derived from syngeneic induced pluripotent stem cells. Cell Stem Cell 12:407-412.

Gurdon J. B. (1962). The Developmental Capacity of Nuclei taken from Intestinal Epithelium Cells of Feeding Tadpoles *J Embryol Exp Morphol December 1962 10:622-640*.

Grossman SD, Rosenberg LJ, Wrathall JR. (2001). Relationship of altered glutamate receptor subunit mRNA expression to acute cell loss after spinal cord contusion. Exp Neurol. 2001;168:283–289.

Groth A., Rocha W., Verreault A., AlmouzniG. (2007). Chromatin challenges during DNA replication and repair, Cell, 2007, vol. 128 (pg. 721-733).

Guffei A, Lichtensztejn Z, Goncalves Dos Santos Silva A, Louis SF, Caporali A, Mai S. (2007). C-Myc-dependent formation of Robertsonian translocation chromosomes in mouse cells. Neoplasia 9: 578-588.

Habib O, Habib G, Choi HW, Hong KS, Do JT, Moon SH, Chung HM. (2013). An improved method for the derivation of high quality iPSCs in the absence of c-Myc. Exp Cell Res. 2013 Dec 10;319(20):3190-200. doi: 10.1016/j.yexcr.2013.09.014. Epub 2013 Oct 2.

Hammerman PS, Hayes DN, Wilkerson MD, Schultz N, Bose R, Chu A, Collisson EA, Cope L, Creighton CJ, Getz G, Herman JG, Johnson BE, Kucherlapati R, Ladanyi M, Maher CA, Robertson G, Sander C, Shen R, Sinha R, Sivachenko A, Thomas RK, Travis WD, Tsao MS, Weinstein JN, Wigle DA, Baylin SB, Govindan R, Meyerson M. (2012). Comprehensive genomic characterization of squamous cell lung cancers. *Nature* 2012, 489:519-525.

Han J., Ping Yuan, Henry Yang, Jinqiu Zhang, Boon Seng Soh, Pin Li, Siew Lan Lim, Suying Cao, Junliang Tay, Yuriy L. Orlov, Thomas Lufkin, Huck-Hui Ng, Wai-Leong Tam, Bing Lim. (2010). Tbx3 improves the germ-line competency of induced pluripotent stem cells. Nature. 2010 February 25; 463(7284): 1096–1100. Published online 2010 February 7. doi: 10.1038/nature08735.

Hanna J., Wernig M., et al. and Jaenisch R. (2007). Treatment of sickle cell anemia mouse model with iPS cells generated from autologous skin. Science 318, 1920. Doi: 10.1126/science.1152092.

Hanna J, Saha K, Pando B, van Zon J, Lengner CJ, Creyghton MP, van Oudenaarden A, Jaenisch R. (2009). Direct cell reprogramming is a stochastic process amenable to acceleration. Nature. 2009 Dec 3;462(7273):595-601. doi: 10.1038/nature08592. Epub 2009 Nov 8.

Harel NY, Strittmatter SM. (2006). Can regenerating axons recapitulate developmental guidance during recovery from spinal cord injury? Nat Rev Neurosci. 2006;7:603–616.

Hawkins RD, Hon GC, Lee LK, Ngo Q, Lister R, Pelizzola M, Edsall LE, Kuan S, Luu Y, Klugman S, Antosiewicz-Bourget J, Ye Z, Espinoza C, Agarwahl S, Shen L, Ruotti V, Wang W, Stewart R, Thomson JA, Ecker JR, Ren B. (2010). Distinct epigenomic landscapes of pluripotent and lineage-committed human cells. Cell Stem Cell. 2010 May 7;6(5):479-91. doi: 10.1016/j.stem.2010.03.018.

Hay BA. (2000). Understanding IAP function and regulation: a view from Drosophila. Cell Death Differ. 2000 Nov;7(11):1045-56.

He TC, Sparks AB, Rago C, Hermeking H, Zawel L, da Costa LT, Morin PJ, Vogelstein B, Kinzler KW. (1998). Identification of c-MYC as a target of the APC pathway. Science. 1998 Sep 4;281(5382):1509-12.

Hefferin ML, Tomkinson AE. (2005). Mechanism of DNA double-strand break repair by non-homologous end joining. DNA Repair (Amst). 2005 Jun 8;4(6):639-48. Epub 2005 Jan 23.

Hemann MT, Strong MA, Hao LY, Greider CW. (2001). The shortest telomere, not average telomere length, is critical for cell viability and chromosome stability. Cell. 2001 Oct 5;107(1):67-77.

Heo, L., Joo, C., Kim, Y.K., Ha, M., Yoon, M.J., Cho, J., *et al*. (2009). TUT4 in concert with Lin28 suppresses microRNA biogénesis through pre-microRNA uridylation. Cell, 138, 696-708.

Hessmann E, Schneider G, Ellenrieder V, Siveke JT. (2015). MYC in pancreatic cancer: novel mechanistic insights and their translation into therapeutic strategies. Oncogene. 2016 Mar 31;35(13):1609-18. doi: 10.1038/onc.2015.216. Epub 2015 Jun 29.

Hoeijmakers JH. (2009). DNA damage, aging, and cancer. N Engl J Med. 2009 Oct 8;361(15):1475-85. doi: 10.1056/NEJMra0804615.

Holcomb IN, Young JM, Coleman IM, Salari K, Grove DI, Hsu L, True LD, Roudier MP, Morrissey CM, Higano CS, Nelson PS, Vessella RL, Trask BJ. (2009). Comparative analyses of chromosome alterations in soft-tissue metastases within and across patients with castration-resistant prostate cancer. *Cancer Res* 2009, 69:7793-7802.

Holloman, W. K. (2011). Unraveling the mechanism of BRCA2 in homologous recombination. *Nature Publishing Group*, *18*(7), 748–754.

Hu, W., Liu, Y. & Yan, J. (2014). Microarray meta-analysis of RNA-binding protein functions in alternative polyadenylation. *PLoS One* **9**, e90774, doi:10.1371/journal.pone.0090774 (2014).

Huang K, Liu P, Li X, Chen S, Wang L, Qin L, Su Z, Huang W, Liu J, Jia B, Liu J, Cai J, Pei D, Pan G. (2014). Neural progenitor cells from human induced pluripotent stem

cells generated less autogenous immune response. Sci China Life Sci. 2014 Feb;57(2):162-70. doi: 10.1007/s11427-013-4598-6. Epub 2014 Jan 17.

Huang G, Ye S, Zhou X, Liu D, Ying QL. (2015). Molecular basis of embryonic stem cell self-renewal: from signaling pathways to pluripotency network. Cell Mol Life Sci. 2015 May;72(9):1741-57. doi: 10.1007/s00018-015-1833-2. Epub 2015 Jan 17.

Huangfu D, Osafune K, Maehr R, Guo W, Eijkelenboom A, Chen S, Muhlestein W, Melton DA. (2008). Induction of pluripotent stem cells from primary human fibroblasts with only Oct4 and Sox2. Nat Biotechnol. 2008 Nov;26(11):1269-75. doi: 10.1038/nbt.1502. Epub 2008 Oct 12.

Hulf T, Bellosta P, Furrer M, Steiger D, Svensson D, Barbour A, Gallant P. (2005). Whole-genome analysis reveals a strong positional bias of conserved dMyc-dependent E-boxes. Mol Cell Biol 25: 3401-3410.

Hussain SP, Amstad P, He P, Robles A, Lupold S, Kaneko I, Ichimiya M, Sengupta S, Mechanic L, Okamura S, Hofseth LJ, Moake M, Nagashima M, Forrester KS, and Harris CC. (2004). p53-induced upregulation of MnSOD and GPx but not catalase increases oxidative stress and apoptosis. Cancer Res 64: 2350–2356, 2004.

Hussein SM, Batada NN, Vuoristo S, Ching RW, Autio R, Närvä E, Ng S, Sourour M, Hämäläinen R, Olsson C, Lundin K, Mikkola M, Trokovic R, Peitz M, Brüstle O, Bazett-Jones DP, Alitalo K, Lahesmaa R, Nagy A, Otonkoski T. (2011). Copy number variation and selection during reprogramming to pluripotency. Nature. 2011 Mar 3;471(7336):58-62. doi: 10.1038/nature09871.

Hydbring P, Malumbres M, Sicinski P. (2016). Non-canonical functions of cell cycle cyclins and cyclin-dependent kinases. Nat Rev Mol Cell Biol. 2016 May;17(5):280-92. doi: 10.1038/nrm.2016.27. Epub 2016 Apr 1.

Itsykson P, Ilouz N, Turetsky T, et al. (2005). Derivation of neural precursors from human embryonic stem cells in the presence of noggin. Mol Cell Neurosci. 2005;30:24–36.

Iwabuchi K, Bartel PL, Li B, Marraccino R, Fields S. (1994). Two cellular proteins that bind to wild-type but not mutant p53. Proc Natl Acad Sci U S A. 1994 Jun 21;91(13):6098-102.

Jaenisch R, Young R. (2008). Stem cells, the molecular circuitry of pluripotency and nuclear reprogramming. Cell. 2008 Feb 22;132(4):567-82. doi: 10.1016/j.cell.2008.01.015.

Janeway, Charles; Paul Travers; Mark Walport; Mark Shlomchik (2001). Immunobiology; Fifth Edition.

Janeway CA Jr, Medzhitov R. (2002). Innate immune recognition. Annu Rev Immunol. 2002;20:197-216. Epub 2001 Oct 4.

Jeong J, Juhn K, Lee H, Kim SH, Min BH, Lee KM, Cho MH, Park GH, Lee KH. (2007). SIRT1 promotes DNA repair activity and deacetylation of Ku70. Exp Mol Med. 2007 Feb 28;39(1):8-13.

Ji, Z. & Tian, B. (2009). Reprogramming of 3' untranslated regions of mRNAs by alternative polyadenylation in generation of pluripotent stem cells from different cell types. *PLoS One* **4**, e8419, doi:10.1371/journal.pone.0008419 (2009).

Ji, J. and Zheng, P.S. (2010). Expression of Sox2 in human cervical carcinogenesis. Hum. Pathol. 41, 1438-1447.

Ji H, Wu G, Zhan X, Nolan A, Koh C, De Marzo A, Doan HM, Fan J, Cheadle C, Fallahi M, Cleveland JL, Dang CV, Zeller KI. (2011). Cell-type independent MYC target genes reveal a primordial signature involved in biomass accumulation. PLoS One. 2011;6(10):e26057. doi: 10.1371/journal.pone.0026057. Epub 2011 Oct 19.

Ji J, Ng SH, Sharma V, Neculai D, Hussein S, Sam M, Trinh Q, Church GM, McPherson JD, Nagy A, Batada NN. (2012). Elevated coding mutation rate during the reprogramming of human somatic cells into induced pluripotent stem cells. Stem Cells. 2012 Mar;30(3):435-40. doi: 10.1002/stem.1011.

Jiang M, Lv L, Ji H, Yang X, Zhu W, Cai L, Gu X, Chai C, Huang S, Sun J, Dong Q. (2011) Induction of pluripotent stem cells transplantation therapy for ischemic stroke. Mol Cell Biochem. (2011). Aug;354(1-2):67-75. doi: 10.1007/s11010-011-0806-5. Epub 2011 Apr 5.

Jirawatnotai S, Hu Y, Michowski W, Elias JE, Becks L, Bienvenu F, Zagozdzon A, Goswami T, Wang YE, Clark AB, Kunkel TA, van Harn T, Xia B, Correll M, Quackenbush J, Livingston DM, Gygi SP, Sicinski P. (2011). A function for cyclin D1 in DNA repair uncovered by protein interactome analyses in human cancers. Nature. 2011 Jun 8;474(7350):230-4. doi: 10.1038/nature10155.

Jirawatnotai, S., & Sittithumcharee, G. (2016). Paradoxical roles of cyclin D1 in DNA stability. *DNA Repair*, *42*(May), 56–62.

Jung D, Alt FW. (2004). Unraveling V(D)J recombination; insights into gene regulation. Cell. 2004 Jan 23;116(2):299-311.

Kamao H, Mandai M, Okamoto S, Sakai N, Suga A, Sugita S, Kiryu J, Takahashi M. (2014). Characterization of human induced pluripotent stem cell-derived retinal pigment epithelium cell sheets aiming for clinical application. Stem Cell Reports. 2014 Jan 23;2(2):205-18. doi: 10.1016/j.stemcr.2013.12.007. eCollection 2014.

Karikó K, Muramatsu H, Welsh FA, Ludwig J, Kato H, Akira S, Weissman D. (2008). Incorporation of pseudouridine into mRNA yields superior nonimmunogenic vector with increased translational capacity and biological stability. Department of Neurosurgery, University of Pennsylvania, Room 371 Stemmler Hall, 36th & Hamilton Walk, Philadelphia, Pennsylvania 19104-6087, USA. kariko@mail.med.upenn.edu. Mol Ther. 2008 Nov;16(11):1833-40. doi: 10.1038/mt.2008.200. Epub 2008 Sep 16.

Kasahara E, Lin LR, Ho YS, Reddy VN. (2005). SOD2 protects against oxidation-induced apoptosis in mouse retinal pigment epithelium: implications for age-related macular degeneration. Invest Ophthalmol Vis Sci. 2005 Sep;46(9):3426-34.

Kawamura T., Suzuki, J., Wang, Y.V., Mendez, S., Morera, L.B., Raya, A., Wahl, G.M., and Belmonte, J.C. (2009). Linking the p53 tumour suppressor pathway to somatic cell reprogramming. Nature 460, 1140-1144.

Kawate S, Fukusato T, Ohwada S, Watanuki A, Morishita Y. (1999). Amplification of c-myc in hepatocellular carcinoma: correlation with clinicopathologic features, proliferative activity and p53 overexpression. Oncology. 1999;57(2):157-63.

Kelly K, Cochran BH, Stiles CD, Leder P. (1983). Cell-specific regulation of the c-myc gene by lymphocyte mitogens and platelet-derived growth factor. Cell. 1983 Dec;35(3 Pt 2):603-10.

Kent, T., Chandramouly, G., McDevitt, S. M., Ozdemir, A. Y., & Pomerantz, R. T. (2015). Mechanism of microhomology-mediated end-joining promoted by human DNA polymerase theta. *Nat Struct Mol Biol*, *22*(3), 230–237.

Keirstead HS, Nistor G, Bernal G, et al. (2005). Human embryonic stem cell-derived oligodendrocyte progenitor cell transplants remyelinate and restore locomotion after spinal cord injury. J Neurosci. 2005;25:4694–4705.

Khanna KK, Jackson SP. (2001). DNA double-strand breaks: Signaling, repair, and the cancer connection. Nat Genet 27: 247-254.

Kim J. B., Boris Greber, Marcos J. Araúzo-Bravo, Johann Meyer, Kook In Park, Holm Zaehres & Hans R. Schöler. (2009). Direct reprogramming of human neural stem cells by *OCT4***.** *Nature* 461, 649-653 (1 October 2009) | doi:10.1038/nature08436.

Kim K., A. Doi, B. Wen, K. Ng, R. Zhao, P. Cahan, J. Kim, M. J. Aryee, H. Ji, L. I. R. Ehrlich, A. Yabuuchi, A. Takeuchi, K. C. Cunniff, H. Hongguang, S. Mckinney-Freeman, O. Naveiras, T. J. Yoon, R. A. Irizarry, N. Jung, J. Seita, J. Hanna, P. Murakami, R. Jaenisch, R. Weissleder, S. H. Orkin et al. (2010). Epigenetic memory in induced pluripotent stem cells Nature 467, 285–290 (16 September 2010) doi: 10.1038/nature09342.

Kitagawa R, Kastan MB. (2005). The ATM-dependent DNA damage signaling pathway. Cold Spring Harb Symp Quant Biol. 2005;70:99-109.

Kiuru M, JL Boyer, TP O'Connor and RG Crystal. (2009). Genetic control of wayward pluripotent stem cells and their progeny after transplantation. Cell Stem Cell 4:289-300.

Kolodner RD. (1995). Mismatch repair: mechanisms and relationship to cancer susceptibility. Trends Biochem Sci. 1995 Oct;20(10):397-401.

Kostyrko K, Mermod N. (2016). Assays for DNA double-strand break repair by microhomology-based end-joining repair mechanisms. Nucleic Acids Res. 2016 Apr 7;44(6):e56. doi: 10.1093/nar/gkv1349.

Koyanagi-Aoi, M., Ohnuki, M., Takahashi, K., Okita, K., Noma, H., Sawamura, Y., Teramoto, I., Narita, M., Sato, Y., Ichisaka, T., Amano, N., Watanabe, A., Morizane,

A., Yamada, Y., Sato, T., Takahashi, J. & Yamanaka, S. (2013). Differentiation-defective phenotypes revealed by large-scale analyses of human pluripotent stem cells. *Proc Natl Acad Sci U S A* **110**, 20569-20574, doi:10.1073/pnas.1319061110 (2013).

Kumar H, Kawai T, Akira S. (2009). Pathogen recognition in the innate immune response. Biochem J. 2009 Apr 28;420(1):1-16. doi: 10.1042/BJ20090272.

Kuo, T.C., Chavarria-Smith, J.E., Huang, D., and Schlissel, M.S. (2011). Forced expression of cyclin-dependent kinase 6 confers resistance of pro-B acute lymphocytic leukemia to Gleevec treatment. *Molecular Cell Biology*, 31(13): 2566-2576

Kuschak TI, Taylor C, McMillan-Ward E, Israels S, Henderson DW, Mushinski JF, Wright JA, Mai S. (1999). The ribonucleotide reductase R2 gene is a non-transcribed target of c-Myc-induced genomic instability. Gene 238: 351-365.

Kuschak TI, Kuschak BC, Taylor CL, Wright JA, Wiener F, Mai S. (2002). C-Myc initiates illegitimate replication of the ribonucleotide reductase R2 gene. Oncogene 21: 909-920.

LaCasse EC, Baird S, Korneluk RG, MacKenzie AE. (1998). The inhibitors of apoptosis (IAPs) and their emerging role in cancer. Oncogene. 1998 Dec 24;17(25):3247-59.

Lafon M, Megret F, Lafage M, Prehaud C. (2006). The innate immune facet of brain: human neurons express TLR-3 and sense viral dsRNA. J Mol Neurosci. 2006;29(3):185-94.

Lahne H.U., Kloster M.M., Lefdal S., Blomhoff H.K., Naderi S., (2006). Degradation of cyclin D3 independent of Thr-283 phosphorylation

LaPlaca M. C., Simon C. M., Prado G. R., Cullen D. K. (2007). CNS injury biomechanics and experimental models. Prog. Brain Res. 161, 13–26. 10.1016/S0079-6123(06)61002-9.

Lau Lee Yin , Qian Peng , Sze Wan Fong, Andy C. H. Chen, Kai Fai Lee, Ernest H. Y. Ng, Andras Nagy, William S. B. Yeung. (2012). Sirtuin 1 Facilitates Generation of Induced Pluripotent Stem Cells from Mouse Embryonic Fibroblasts through the miR-34a and p53 Pathways. Published: September 21, 2012. DOI: 10.1371/journal.pone.0045633.

Laurent LC, Ulitsky I, Slavin I, Tran H, Schork A, Morey R, Lynch C, Harness JV, Lee S, Barrero MJ, Ku S, Martynova M, Semechkin R, Galat V, Gottesfeld J, Izpisua Belmonte JC, Murry C, Keirstead HS, Park HS, Schmidt U, Laslett AL, Muller FJ, Nievergelt CM, Shamir R, Loring JF. (2011). Dynamic changes in the copy number of pluripotency and cell proliferation genes in human ESCs and iPSCs during reprogramming and time in culture. Cell Stem Cell. 2011 Jan 7;8(1):106-18. doi: 10.1016/j.stem.2010.12.003.

Lavialle C, Modjtahedi N, Lamonerie T, Frebourg T, Landin RM, Fossar N, Lhomond G, Cassingena R, Brison O. (1989). The human breast carcinoma cell line SW 613-S: an experimental system to study tumor heterogeneity in relation to c-myc amplification, growth factor production and other markers. Anticancer Res. 1989 Sep-Oct;9(5):1265-79.

Lee H, Shamy GA, Elkabetz Y, et al. (2007). Directed differentiation and transplantation of human embryonic stem cell-derived motoneurons. Stem Cells. 2007;25:1931–1939.

Lee J, Sayed N, Hunter A, Au KF, Wong WH, Mocarski ES, Pera RR, Yakubov E, Cooke JP. (2012a). Activation of innate immunity is required for efficient nuclear reprogramming. Cell. 2012 Oct 26;151(3):547-58. doi: 10.1016/j.cell.2012.09.034.

Lee , P. Y., Chien, Y., Chiou, G. Y., Lin, C. H., Chiou, C. H. & Tarng, D. C. (2012b) Induced pluripotent stem cells without c-Myc attenuate acute kidney injury via downregulating the signaling of oxidative stress and inflammation in ischemia-reperfusion rats. *Cell Transplant* **21**, 2569-2585, doi:10.3727/096368912X636902 (2012b).

Lefort N, Feyeux M, Bas C, Féraud O, Bennaceur-Griscelli A, Tachdjian G, Peschanski M, Perrier AL. (2008). Human embryonic stem cells reveal recurrent genomic instability at 20q11.21. Nat Biotechnol. 2008 Dec;26(12):1364-6. doi: 10.1038/nbt.1509. Epub 2008 Nov 23.

Lengauer C, Kinzler KW, Vogelstein B. (1997). Genetic instability in colorectal cancers. Nature. 1997 Apr 10;386(6625):623-7.

Leonard JN, Ghirlando R, Askins J, Bell JK, Margulies DH, Davies DR, Segal DM. (2008). The TLR3 signaling complex forms by cooperative receptor dimerization. Proc Natl Acad Sci U S A. 2008 Jan 8;105(1):258-63. doi: 10.1073/pnas.0710779105. Epub 2008 Jan 2.

Li Y, McClintick J, Zhong L, Edenberg HJ, Yoder MC, Chan RJ. (2005a). Murine embryonic stem cell differentiation is promoted by SOCS-3 and inhibited by the zinc finger transcription factor Klf4. Blood. 2005 Jan 15;105(2):635-7. Epub 2004 Sep 9.

Li XJ, Du ZW, Zarnowska ED, et al. (2005b). Specification of motoneurons from human embryonic stem cells. Nat Biotechnol. 2005;23:215–221.

Li B., Carey M., Workman J.L. (2007). The role of chromatin during transcription. Cell, 2007, vol. 128 (pg. 707-719).

Li R, Liang J, Ni S, Zhou T, Qing X, Li H, He W, Chen J, Li F, Zhuang Q, Qin B, Xu J, Li W, Yang J, Gan Y, Qin D, Feng S, Song H, Yang D, Zhang B, Zeng L, Lai L, Esteban MA, Pei D. (2010). A mesenchymal-to-epithelial transition initiates and is required for the nuclear reprogramming of mouse fibroblasts. Cell Stem Cell. 2010 Jul 2;7(1):51-63. doi: 10.1016/j.stem.2010.04.014. Epub 2010 Jun 17.

Li Z, Owonikoko T, Ramalingam SS, Doetsch PW, Xiao Z, Khuri F, Curran W, Deng X. (2012). C-Myc suppression of DNA double-strand break repair. Neoplasia 14: 1190-1202.

Lieber MR. (2010). The mechanism of double-strand DNA break repair by the nonhomologous DNA end-joining pathway. Annu Rev Biochem. 2010;79:181-211. doi: 10.1146/annurev.biochem. 052308.093131.

Lim DS, Kim ST, Xu B, Maser RS, Lin J, Petrini JH, Kastan MB. (2000). ATM phosphorylates p95/nbs1 in an S-phase checkpoint pathway. Nature. 2000;404:613–617.

Lister R, Pelizzola M, Kida YS, Hawkins RD, Nery JR, Hon G, Antosiewicz-Bourget J, O'Malley R, Castanon R, Klugman S, Downes M, Yu R, Stewart R, Ren B, Thomson JA, Evans RM, Ecker JR. (2011). Hotspots of aberrant epigenomic reprogramming in human induced pluripotent stem cells. Nature. 2011 Mar 3;471(7336):68-73. doi: 10.1038/nature09798. Epub 2011 Feb 2.

Little CD, Nau MM, Carney DN, Gazdar AF, Minna JD. (1983). Amplification and expression of the c-myc oncogene in human lung cancer cell lines. Nature. 1983 Nov 10-16;306(5939):194-6.

Liu L, Botos I, Wang Y, Leonard JN, Shiloach J, Segal DM, Davies DR. (2008). Structural basis of toll-like receptor 3 signaling with double-stranded RNA. Science. 2008 Apr 18;320(5874):379-81. doi: 10.1126/science.1155406.

Liu P, Chen S, Li X, Qin L, Huang K, Wang L, Huang W, Li S, Jia B, Zhong M, Pan G, Cai J, Pei D. (2013). Low immunogenicity of neural progenitor cells differentiated from induced pluripotent stem cells derived from less immunogenic somatic cells. PLoS One. 2013 Jul 26;8(7):e69617. doi: 10.1371/journal.pone.0069617.

Loh, Y.H., Agarwal, S., Park, I.H., Urbach, A., Huo, H., Heffner, G.C., et al. (2009). Generation of induced pluripotent stem cells from human blood. Blood (Advanced online publication).

Lombardi L, Newcomb EW, Dalla-Favera R. (1987). Pathogenesis of Burkitt lymphoma: expression of an activated c-myc oncogene causes the tumorigenic conversion of EBV-infected human B lymphoblasts. Cell. 1987 Apr 24;49(2):161-70.

López-Serrano C, Torres-Espín A, Hernández J, Alvarez-Palomo AB, Requena J, Gasull X, Edel MJ, Navarro X. (2016). Effects of the spinal cord injury environment on the differentiation capacity of human neural stem cells derived from induced pluripotent stem cells. Cell Transplant. 2016 Apr 5.

Louis SF, Vermolen BJ, Garini Y, Young IT, Guffei A, Lichtensztejn Z, Kuttler F, Chuang TC, Moshir S, Mougey V, et al. (2005). C-Myc induces chromosome rearrangements through telomere and chromosome remodelling in the interphase nucleus. Proc Natl Acad Sci 102: 9613-9618.

Ludwig TE, Levenstein ME, Jones JM, et al. (2006). Derivation of human embryonic stem cells in defined conditions. Nat Biotechnol. 2006;24:185–187.

Luger K., Mader A.W., Richmond R.K., Sargent D.F., Richmond T.J. (1997). Crystal structure of the nucleosome core particle at 2.8 A resolution, Nature, 1997, vol. 389 (pg. 251-260).

Lujan E., Marius Wernig. (2010). An imprinted signature helps isolate ESC-equivalent iPSCs. *Cell Research* **20**:974–976. doi: 10.1038/cr.2010.117; published online 10 August 2010

Lukovic D, Moreno-Manzano V, Lopez-Mocholi E, Rodriguez-Jiménez FJ, Jendelova P, Sykova E, Oria M, Stojkovic M, Erceg S. (2015). Complete rat spinal cord transection as a faithful model of spinal cord injury for translational cell transplantation. Sci Rep. 2015 Apr 10;5:9640. doi: 10.1038/srep09640.

Lund RJ, Närvä E, Lahesmaa R. (2012). Genetic and epigenetic stability of human pluripotent stem cells. Nat Rev Genet. 2012 Oct;13(10):732-44. doi: 10.1038/nrg3271. Epub 2012 Sep 11.

Luoto KR, Meng AX, Wasylishen AR, Zhao H, Coackley CL, Penn LZ, Bristow RG. (2010). Tumor cell kill by c-Myc depletion: Role of Myc regulated genes that control DNA double-strand break repair. Cancer Res 70: 8748-8759.

Lupski JR. (2013). Genetics. Genome mosaicism--one human, multiple genomes. Science. 2013 Jul 26;341(6144):358-9. doi: 10.1126/science.1239503.

Lustig AJ (2003) Clues to catastrophic telomere loss in mammals from yeast telomere rapid deletion. *Nat Rev* **4**:916–923.

Lydeard JR, Jain S, Yamaguchi M, Haber JE. (2007). Break-induced replication and telomerase-independent telomere maintenance require Pol32. Nature. 2007 Aug 16;448(7155):820-3. Epub 2007 Aug 1.

Maekawa M, Yamaguchi K, Nakamura T, Shibukawa R, Kodanaka I, Ichisaka T, Kawamura Y, Mochizuki H, Goshima N, Yamanaka S. (2011). Direct reprogramming of somatic cells is promoted by maternal transcription factor Glis1. Nature. 2011 Jun 8;474(7350):225-9. doi: 10.1038/nature10106.

Mahajan KN, Nick McElhinny SA, Mitchell BS, et al. (2002). Association of DNA polymerase mu (pol mu) with Ku and ligase IV: role for pol mu in end-joining double-strand break repair. Mol Cell Biol. 2002;22:5194–202.

Mai S. (1994). Overexpression of c-myc precedes amplification of the gene encoding dihydrofolate reductase. Gene 148: 253-260.

Mai S, Hanley-Hyde J, Fluri M. (1996). c-Myc overexpression associated DHFR gene amplification in hamster, rat, mouse and human cell lines. Oncogene 12: 277-288.

Mai S, Garini Y. (2005). Oncogenic remodelling of the three-dimensional organization of the interphase nucleus: c-Myc induces telomeric aggregates whose formation precedes chromosomal rearrangements. Cell Cycle 4: 1327-1331.

Mai S, Garini Y. (2006). The significance of telomeric aggregates in the interphase nuclei of tumor cells. J Cell Biochem 97: 904-915.

Maitra A, Arking DE, Shivapurkar N, Ikeda M, Stastny V, Kassauei K, Sui G, Cutler DJ, Liu Y, Brimble SN, Noaksson K, Hyllner J, Schulz TC, Zeng X, Freed WJ, Crook J, Abraham S, Colman A, Sartipy P, Matsui S, Carpenter M, Gazdar AF, Rao M,

Chakravarti A. (2005). Genomic alterations in cultured human embryonic stem cells. Nat Genet. 2005 Oct;37(10):1099-103.

Mandai M, Watanabe A, Kurimoto Y, Hirami Y, Morinaga C, Daimon T, Fujihara M, Akimaru H, Sakai N, Shibata Y, Terada M, Nomiya Y, Tanishima S, Nakamura M, Kamao H, Sugita S, Onishi A, Ito T, Fujita K, Kawamata S, Go MJ, Shinohara C, Hata KI, Sawada M, Yamamoto M, Ohta S, Ohara Y, Yoshida K, Kuwahara J, Kitano Y, Amano N, Umekage M, Kitaoka F, Tanaka A, Okada C, Takasu N, Ogawa S, Yamanaka S, Takahashi M. (2017). Autologous Induced Stem-Cell-Derived Retinal Cells for Macular Degeneration. N Engl J Med. 2017 Mar 16;376(11):1038-1046. doi: 10.1056/NEJMoa1608368.

Marchetto Maria C.N., Cassiano Carromeu, Allan Acab, Diana Yu, Gene W. Yeo, Yangling Mu, Gong Chen, Fred H. Gage, Alysson R. Muotri. (2010). A Model for Neural Development and Treatment of Rett Syndrome Using Human Induced Pluripotent Stem Cells. Cell - 12 November 2010 (Vol. 143, Issue 4, pp. 527-539). Doi:10.1016/j.cell.2010.10.016.

Marcu KB, Patel AJ, Yang Y. (1997). Differential regulation of the c-MYC P1 and P2 promoters in the absence of functional tumor suppressors: implications for mechanisms of deregulated MYC transcription. Curr Top Microbiol Immunol. 1997;224:47-56.

Margolin AA, Palomero T, Sumazin P, Califano A, Ferrando AA, Stolovitzky G. (2009). ChIP-on-chip significance analysis reveals large-scale binding and regulation by human transcription factor oncogenes. Proc Natl Acad Sci U S A. 2009 Jan 6;106(1):244-9. doi: 10.1073/pnas.0806445106. Epub 2008 Dec 31.

Martin GR. (1981). Isolation of a pluripotent cell line from early mouse embryos cultured in medium conditioned by teratocarcinoma stem cells. Proc Natl Acad Sci U S A. 1981 Dec;78(12):7634-8.

Martinez P, Thanasoula M, Muñoz P, Liao C, Tejera A, McNees C, Flores JM, Fernandez-Capetillo O, Tarsounas M, Blasco MA. (2009). Increased telomere fragility and fusions resulting from TRF1 deficiency lead to degenerative pathologies and increased cancer in mice. Genes Dev. 2009 Sep 1;23(17):2060-75. doi: 10.1101/gad.543509. Epub 2009 Aug 13.

Martins-Taylor K, Nisler BS, Taapken SM, Compton T, Crandall L, Montgomery KD, Lalande M, Xu RH. (2011). Recurrent copy number variations in human induced pluripotent stem cells. Nat Biotechnol. 2011 Jun 7;29(6):488-91. doi: 10.1038/nbt.1890.

Martins-Taylor K, Xu RH. (2012). Concise review: Genomic stability of human induced pluripotent stem cells. Stem Cells. 2012 Jan;30(1):22-7. doi: 10.1002/stem.705.

Masuda, S., Wu, J., Hishida, T., Pandian, G. N., Sugiyama, H. & Izpisua Belmonte, J. C. (2013). Chemically induced pluripotent stem cells (CiPSC): a transgene-free approach. *J Mol Cell Biol* **5**, 354-355, doi:10.1093/jmcb/mjt034 (2013).

Mateos-Gomez, P. A., Gong, F., Nair, N., Miller, K. M., Lazzerini-Denchi, E., & Sfeir, A. (2015). Mammalian polymerase θ promotes alternative NHEJ and suppresses recombination. *Nature*, *518*(7538), 254–7.

Matzinger P. (1994). Tolerance, danger, and the extended family. Annu Rev Immunol. 1994;12:991-1045.

Mayshar Y, Ben-David U, Lavon N, Biancotti JC, Yakir B, Clark AT, Plath K, Lowry WE, Benvenisty N. (2010). Identification and classification of chromosomal aberrations in human induced pluripotent stem cells. Cell Stem Cell. 2010 Oct 8;7(4):521-31. doi: 10.1016/j.stem.2010.07.017.

Medzhitov R. (2007). Recognition of microorganisms and activation of the immune response. Nature. 2007 Oct 18;449(7164):819-26.

Meeker AK, Hicks JL, Iacobuzio-Donahue CA, Montgomery EA, Westra WH, Chan TY, Ronnett BM, De Marzo AM. (2004). Telomere length abnormalities occur early in the initiation of epithelial carcinogenesis. Clin Cancer Res. 2004 May 15;10(10):3317-26.

Meissner A. (2010). Epigenetic modifications in pluripotent and differentiated cells. Nat Biotechnol. 2010 Oct;28(10):1079-88. doi: 10.1038/nbt.1684.

Menssen, A., Hydbring, P., Kapelle, K., Vervoorts, J., Diebold, J., Lüscher, B., … Hermeking, H. (2012). The c-MYC oncoprotein, the NAMPT enzyme, the SIRT1-inhibitor DBC1, and the SIRT1 deacetylase form a positive feedback loop. *Proceedings of the National Academy of Sciences of the United States of America*, *109*(4), E187-96.

McCarroll SA, Altshuler DM. (2007). Copy-number variation and association studies of human disease. Nat Genet. 2007 Jul;39(7 Suppl):S37-42.

McLenachan S., Cristina Menchón, Angel Raya, Antonella Consiglio, and Michael J. Edel. (2012). Cyclin A_1 Is Essential for Setting the Pluripotent State and Reducing Tumorigenicity of Induced Pluripotent Stem Cells. Stem Cells and Development. October 10, 2012, 21(15): 2891-2899. doi:10.1089/scd.2012.0190.

Millar C.B. (2013). Organizing the genome with H2A histone variants, Biochem. J., 2013, vol. 449 (pg. 567-579).

Miltenberger RJ, Sukow KA, Farnham PJ. (1995). An E-box-mediated increase in cad transcription at the G1/S-phase boundary is suppressed by inhibitory c-Myc mutants. Mol Cell Biol 15: 2527-2535.

Miura K, Y Okada, T Aoi, A Okada, K Takahashi, K Okita, M Nakagawa, M Koyanagi, K Tanabe, M Ohnuki, D Ogawa, E Ikeda, H Okano and S Yamanaka. (2009). Variation in the safety of induced pluripotent stem cell lines. Nature biotechnology 27:743-745.

Modrich P. (1997). Strand-specific mismatch repair in mammalian cells. J Biol Chem. 1997 Oct 3;272(40):24727-30.

Montserrat N, E Nivet, I Sancho-Martinez, T Hishida, S Kumar, L Miquel, C Cortina, Y Hishida, Y Xia, CR Esteban and JC Izpisua Belmonte. (2013). Reprogramming of human fibroblasts to pluripotency with lineage specifiers. Cell Stem Cell 13:341-350.

Moon AF, Gosavi RA, Kunkel TA, Pedersen LC, Bebenek K. (2015). Creative template-dependent synthesis by human polymerase mu. Proc Natl Acad Sci U S A. 2015 Aug 18;112(33):E4530-6. doi: 10.1073/pnas.1505798112. Epub 2015 Aug 3.

Moriguchi, H., Chung, R.T., and Sato, C. (2010). Tumorigenicity of human induced pluripotent stem cells depends on the balance of gene expression between p21 and p53. Hepatology 51, 1088-1089.

Morizane A, D Doi and J Takahashi. (2013). Neural induction with a dopaminergic phenotype from human pluripotent stem cells through a feeder-free floating aggregation culture. Methods Mol Biol 1018:11-19.

Muñoz P, Blanco R, Flores JM, Blasco MA. (2005). XPF nuclease-dependent telomere loss and increased DNA damage in mice overexpressing TRF2 result in premature aging and cancer. Nat Genet. 2005 Oct;37(10):1063-71. Epub 2005 Sep 4.

Muvarak N, Kelley S, Robert C, Baer MR, Perrotti D, Gambacorti-Passerini C, Civin C, Scheibner K, Rassool FV. (2015). c-MYC Generates Repair Errors via Increased Transcription of Alternative-NHEJ Factors, LIG3 and PARP1, in Tyrosine Kinase-Activated Leukemias. Mol Cancer Res. 2015 Apr;13(4):699-712. doi: 10.1158/1541-7786.MCR-14-0422. Epub 2015 Mar 31.

Nag S, Qin J, Srivenugopal KS, Wang M, Zhang R. (2013). The MDM2-p53 pathway revisited. J Biomed Res. 2013 Jul;27(4):254-71. doi: 10.7555/JBR.27.20130030. Epub 2013 Jun 6.

Nakagawa M, Takizawa N, Narita M, Ichisaka T, Yamanaka S. (2010). Promotion of direct reprogramming by transformation-deficient Myc. Proc Natl Acad Sci U S A. 2010 Aug 10;107(32):14152-7. doi: 10.1073/pnas.1009374107. Epub 2010 Jul 26.

Närvä E, Autio R, Rahkonen N, Kong L, Harrison N, Kitsberg D, Borghese L, Itskovitz-Eldor J, Rasool O, Dvorak P, Hovatta O, Otonkoski T, Tuuri T, Cui W, Brüstle O, Baker D, Maltby E, Moore HD, Benvenisty N, Andrews PW, Yli-Harja O, Lahesmaa R. (2010). High-resolution DNA analysis of human embryonic stem cell lines reveals culture-induced copy number changes and loss of heterozygosity. Nat Biotechnol. 2010 Apr;28(4):371-7. doi: 10.1038/nbt.1615

Nazor KL, Altun G, Lynch C, Tran H, Harness JV, Slavin I, Garitaonandia I, Müller FJ, Wang YC, Boscolo FS, Fakunle E, Dumevska B, Lee S, Park HS, Olee T, D'Lima DD, Semechkin R, Parast MM, Galat V, Laslett AL, Schmidt U, Keirstead HS, Loring JF, Laurent LC. (2012). Recurrent variations in DNA methylation in human pluripotent stem cells and their differentiated derivatives. Cell Stem Cell. 2012 May 4;10(5):620-34. doi: 10.1016/j.stem.2012.02.013.

Nelsen CJ, et al., (2005). Short term cyclin D1 overexpression induced centrosome amplification, mitotic spindle abnormalities, and aneuploidy. J Biol Chem 280: 768-776.

Nesbit CE, Tersak JM, Prochownik EV. (1999). MYC oncogenes and human neoplastic disease. Oncogene 18: 3004-3016.

Nguyen DQ, Webber C, Ponting CP. (2006). Bias of selection on human copy-number variants. PLoS Genet 2: e20.

Niehrs C, Acebron SP. (2012). Mitotic and mitogenic Wnt signalling. EMBO J. 2012 Jun 13;31(12):2705-13. doi: 10.1038/emboj.2012.124. Epub 2012 May 22.

Nishino K, Toyoda M, Yamazaki-Inoue M, Fukawatase Y, Chikazawa E, Sakaguchi H, Akutsu H, Umezawa A. (2011). DNA methylation dynamics in human induced pluripotent stem cells over time. PLoS Genet. 2011 May;7(5):e1002085. doi: 10.1371/journal.pgen.1002085. Epub 2011 May 26.

Niwa H, Miyazaki J, Smith AG. (2000). Quantitative expression of Oct-3/4 defines differentiation, dedifferentiation or self-renewal of ES cells. Nat Genet. 2000 Apr;24(4):372-6.

Niwa H. (2007). How is pluripotency determined and maintained? Development. 2007 Feb;134(4):635-46. Epub 2007 Jan 10.

Oberley LW, Lindgren LA, Baker SA, and Stevens RH. (1976). Superoxide lon as the cause of the oxygen effect. Radiat Res 68: 320–328, 1976.

O'Byrne KJ, Dalgleish AG. (2001). Chronic immune activation and inflammation as the cause of malignancy. Br J Cancer. 2001 Aug 17;85(4):473-83.

O'Donovan PJ, Livingston DM. (2010). BRCA1 and BRCA2: breast/ovarian cancer susceptibility gene products and participants in DNA double-strand break repair. Carcinogenesis. 2010 Jun;31(6):961-7. doi: 10.1093/carcin/bgq069. Epub 2010 Apr 16.

Ogawa Y, Sawamoto K, Miyata T, Miyao S, Watanabe M, Nakamura M, et al. (2002). Transplantation of in vitro-expanded fetal neural progenitor cells results in neurogenesis and functional recovery after spinal cord contusion injury in adult rats. Journal of neuroscience research. 2002;69:925–33.

Okita K, T Ichisaka and S Yamanaka. (2007). Generation of germline-competent induced pluripotent stem cells. Nature 448:313-317.

Olshavsky N.A., Groh E.M., Comstock C.E., Morey L.M., Wang Y., Revelo M.P., Burd C., Meller J., Knudsen K.E., (2008). Cyclin D3 action in androgen receptor regulation and prostate cancer. Oncogene, 27(22):3111-21.

Orian A, van Steensel B, Delrow J, Bussemaker HJ, Li L, Sawado T, Williams E, Loo LW, Cowley SM, Yost C, et al. (2003). Genomic binding by the Drosophila Myc, Max, Mad/Mnt transcription factor network. Genes Dev 17: 1101-1114.

Pagliuca FW, Millman JR, Gürtler M, Segel M, Van Dervort A, Ryu JH, Peterson QP, Greiner D, Melton DA. (2014). Generation of functional human pancreatic β cells in vitro. Cell. 2014 Oct 9;159(2):428-39. doi: 10.1016/j.cell.2014.09.040.

Palacios JA, Herranz D, De Bonis ML, Velasco S, Serrano M, Blasco MA. (2010). SIRT1 contributes to telomere maintenance and augments global homologous recombination. J Cell Biol. 2010 Dec 27;191(7):1299-313. doi: 10.1083/jcb.201005160.

Palm W, de Lange T. (2008). How shelterin protects mammalian telomeres. Annu Rev Genet. 2008; 42:301-34. doi: 10.1146/annurev.genet.41.110306.130350.

Palsson-McDermott EM, O'Neill LA. (2007). Building an immune system from nine domains. Biochem Soc Trans. 2007 Dec;35(Pt 6):1437-44.

Pantelias GE. (1986). Radiation-induced cytogenetic damage in relation to changes in interphase chromosome conformation. Radiat Res. 1986 Mar;105(3):341-50.

Park H, Kim D, Kim CH, Mills RE, Chang MY, Iskow RC, Ko S, Moon JI, Choi HW, Man Yoo PS, Do JT, Han MJ, Lee EG, Jung JK, Zhang C, Lanza R, Kim KS. (2014). Increased genomic integrity of an improved protein-based mouse induced pluripotent stem cell method compared with current viral-induced strategies. Stem Cells Transl Med. 2014 May;3(5):599-609. doi: 10.5966/sctm.2013-0149. Epub 2014 Apr 24.

Pera MF, Tam PP. (2010). Extrinsic regulation of pluripotent stem cells. Nature. 2010 Jun 10;465(7299):713-20. doi: 10.1038/nature09228.

Peterson S. E. and Jeanne F. Loring. (2013). Genomic Instability in Pluripotent Stem Cells: Implications for Clinical Applications. Published on December 20, 2013, doi: 10.1074/jbc.R113.516419.

Peterson SE, Westra JW, Rehen SK, Young H, Bushman DM, Paczkowski CM, Yung YC, Lynch CL, Tran HT, Nickey KS, Wang YC, Laurent LC, Loring JF, Carpenter MK, Chun J. (2011). Normal human pluripotent stem cell lines exhibit pervasive mosaic aneuploidy. PLoS One. 2011;6(8):e23018. doi: 10.1371/journal.pone.0023018. Epub 2011 Aug 16.

Piedrahita JA. (2011). The role of imprinted genes in fetal growth abnormalities. Birth Defects Res A Clin Mol Teratol. 2011 Aug;91(8):682-92. doi: 10.1002/bdra.20795. Epub 2011 Jun 6.

Pick M, Ronen D, Yanuka O, Benvenisty N. (2012). Reprogramming of the MHC-I and its regulation by NFκB in human-induced pluripotent stem cells. Stem Cells. 2012 Dec;30(12):2700-8. doi: 10.1002/stem.1242.

Plo I, Laulier C, Gauthier L, Lebrun F, Calvo F, Lopez BS. (2008). AKT1 inhibits homologous recombination by inducing cytoplasmic retention of BRCA1 and RAD51. Cancer Res. 2008 Nov 15;68(22):9404-12. doi: 10.1158/0008-5472.CAN-08-0861.

Poduri A, Evrony GD, Cai X, Walsh CA. (2013). Somatic mutation, genomic variation, and neurological disease. Science. 2013 Jul 5;341(6141):1237758. doi: 10.1126/science.1237758.

Polo JM, Liu S, Figueroa ME, Kulalert W, Eminli S, Tan KY, Apostolou E, Stadtfeld M, Li Y, Shioda T, Natesan S, Wagers AJ, Melnick A, Evans T, Hochedlinger K. (2010). Cell type of origin influences the molecular and functional properties of mouse induced pluripotent stem cells. Nat Biotechnol. 2010 Aug;28(8):848-55. doi: 10.1038/nbt.1667. Epub 2010 Jul 19.

Pusch, O, G Bernaschek, M Eilers, and M Hengstschläger. (1997). "Activation of c-Myc Uncouples DNA Replication from Activation of G1-Cyclin-Dependent Kinases." *Oncogene* 15 (6): 649–56. doi:10.1038/sj.onc.1201236.

Pyndiah, S., Tanida, S., Ahmed, K. M., Cassimere, E. K., Choe, C., & Sakamuro, D. (2011). c-MYC suppresses BIN1 to release poly(ADP-ribose) polymerase 1: a mechanism by which cancer cells acquire cisplatin resistance. *Science Signaling*, *4*(166), ra19.

Rahl PB, Lin CY, Seila AC, Flynn RA, McCuine S, Burge CB, Sharp PA, Young RA. (2010). c-Myc regulates transcriptional pause release. Cell. 2010 Apr 30;141(3):432-45. doi: 10.1016/j.cell.2010.03.030.

Rajagopalan H, Nowak MA, Vogelstein B, Lengauer C. (2003). The significance of unstable chromosomes in colorectal cancer. Nat Rev Cancer. 2003 Sep;3(9):695-701. doi: 10.1038/nrc1165.

Renan MJ. (1989). Does NF-kappa B relieve the transcription block in c-myc? Cancer Lett. 1989 Sep 15;47(1-2):1-9.

Rieke DT, Ochsenreither S, Klinghammer K, Seiwert TY, Klauschen F, Tinhofer I, Keilholz U. (2016). Methylation of RAD51B, XRCC3 and other homologous recombination genes is associated with expression of immune checkpoints and an inflammatory signature in squamous cell carcinoma of the head and neck, lung and cervix. Oncotarget. 2016 Nov 15;7(46):75379-75393. doi: 10.18632/oncotarget.12211.

Robertson NJ, Brook FA, Gardner RL, Cobbold SP, Waldmann H, Fairchild PJ. (2007). Embryonic stem cell-derived tissues are immunogenic but their inherent immune privilege promotes the induction of tolerance. Proc Natl Acad Sci U S A. 2007 Dec 26;104(52):20920-5. Epub 2007 Dec 18.

Rockwood LD, Torrey TA, Kim JS, Coleman AE, Kovalchuk AL, Xiang S, Ried T, Morse HCIII, Janz S. (2002). Genomic instability in mouse Burkitt lymphoma is dominated by illegitimate genetic recombination, not point mutation. Oncogene 21: 7235-7240.

Rodriguez E, Houldsworth J, Reuter VE, Meltzer P, Zhang J, Trent JM, Bosl GJ, Chaganti RS. (1993). Molecular cytogenetic analysis of i(12p)-negative human male germ cell tumors. Genes Chromosomes Cancer. 1993 Dec;8(4):230-6.

Rogakou E.P., Pilch D.R., Orr A.H., Ivanova V.S., Bonner W.M. (1998). DNA double-stranded breaks induce histone H2AX phosphorylation on serine 139, J. Biol. Chem., 1998, vol. 273 (pg. 5858-5868).

Rounbehler RJ, Li W, Hall MA, Yang C, Fallahi M, Cleaveland JL. (2009). Targeting ornithine decarboxylase impairs development of MYCN-amplified neuroblastoma. Cancer Res 69: 547-553.

Rowland, B.D., Bernards, R., and Peeper, D.S. (2005). The KLF4 tumour suppressor is a transcriptional repressor of p53 that acts as a context-dependent oncogene. Nat. Cell Biol. 7, 1074-1082.

Rudolph, B, R Saffrich, J Zwicker, B Henglein, R Müller, W Ansorge, and M Eilers. (1996). "Activation of Cyclin-Dependent Kinases by Myc Mediates Induction of Cyclin A, but Not Apoptosis." *The EMBO Journal* 15 (12): 3065–76.

Ruff, P., Donnianni, R. A., Glancy, E., Oh, J., Symington, L. S., Ruff, P., Symington, L. S. (2016). RPA Stabilization of Single-Stranded DNA Is Critical for Break-Induced Replication. *CellReports*, *17*(12), 3359–3368.

Ruiz S, Lopez-Contreras AJ, Gabut M, Marion RM, Gutierrez-Martinez P, Bua S, Ramirez O, Olalde I, Rodrigo-Perez S, Li H, Marques-Bonet T, Serrano M, Blasco MA, Batada NN, Fernandez-Capetillo O. (2015) Limiting replication stress during somatic cell reprogramming reduces genomic instability in induced pluripotent stem cells. Nat Commun. 2015 Aug 21;6:8036. doi: 10.1038/ncomms9036.

Sánchez-Danés A, Richaud-Patin Y, Carballo-Carbajal I, Jiménez-Delgado S, Caig C, Mora S, Di Guglielmo C, Ezquerra M, Patel B, Giralt A, Canals JM, Memo M, Alberch J, López-Barneo J, Vila M, Cuervo AM, Tolosa E, Consiglio A, Raya A. (2012a). Disease-specific phenotypes in dopamine neurons from human iPS-based models of genetic and sporadic Parkinson's disease. EMBO Mol Med. 2012 May;4(5):380-95. doi: 10.1002/emmm.201200215. Epub 2012 Mar 8.

Sánchez-Danés A, Consiglio A, Richaud Y, Rodríguez-Pizà I, Dehay B, Edel M, Bové J, Memo M, Vila M, Raya A, Izpisua Belmonte JC. (2012b). Efficient generation of A9 midbrain dopaminergic neurons by lentiviral delivery of LMX1A in human embryonic stem cells and induced pluripotent stem cells. Hum Gene Ther. 2012 Jan;23(1):56-69. doi: 10.1089/hum.2011.054. Epub 2011 Nov 17.

Samper E, Goytisolo FA, Slijepcevic P, van Buul PP, Blasco MA. (2000). Mammalian Ku86 protein prevents telomeric fusions independently of the length of TTAGGG repeats and the G-strand overhang. EMBO Rep. 2000;1:244–252.

Sarkar SN, Peters KL, Elco CP, Sakamoto S, Pal S, Sen GC. (2004). Novel roles of TLR3 tyrosine phosphorylation and PI3 kinase in double-stranded RNA signaling. Nat Struct Mol Biol. 2004 Nov;11(11):1060-7. Epub 2004 Oct 24.

Serrano, M & Blasco, M.A. (2007). Cancer and ageing: convergent and divergent mechanisms. Nature Reviews Molecular Cell Biology 8, 715-722 (September 2007) doi:10.1038/nrm2242

Shaffer AL, Wright G, Yang L, Powell J, Ngo V, Lamy L, Lam LT, Davis RE, Staudt LM. (2006). A library of gene expression signatures to illuminate normal and pathological lymphoid biology. Immunol Rev. 2006 Apr;210:67-85.

Schatz DG, Spanopoulou E. (2005). Biochemistry of V(D)J recombination. Curr Top Microbiol Immunol. 2005;290:49-85.

Schlaeger TM, Daheron L, Brickler TR, Entwisle S, Chan K, Cianci A, DeVine A, Ettenger A, Fitzgerald K, Godfrey M, Gupta D, McPherson J, Malwadkar P, Gupta M, Bell B, Doi A, Jung N, Li X, Lynes MS, Brookes E, Cherry AB, Demirbas D, Tsankov AM, Zon LI, Rubin LL, Feinberg AP, Meissner A, Cowan CA, Daley GQ. (2015). A comparison of non-integrating reprogramming methods. Nat Biotechnol. 2015 Jan;33(1):58-63. doi: 10.1038/nbt.3070. Epub 2014 Dec 1.

Scholzen T, Gerdes J. (2000). The Ki-67 protein: from the known and the unknown. J Cell Physiol. 2000 Mar;182(3):311-22.

Schreiber, V., Dantzer, F., Ame, J.-C., & de Murcia, G. (2006). Poly(ADP-ribose): novel functions for an old molecule. *Nature Reviews. Molecular Cell Biology*, *7*(7), 517–28.

Schuldiner, M., Itskovitz-Eldor, J. and Benvenisty, N. (2003). Selective ablation of human embryonic stem cells expressing a "suicide" gene. Stem Cells 21, 257-265.

Schwartz, G.K. and Dickson, M.A. (2009). Cell cycle, CDKs and cancer: a changing paradigm. *Nature Reviews Cancer*, 9(3): 153-66

Serrano, M & Blasco, M.A. (2007). Cancer and ageing: convergent and divergent mechanisms. Nature Reviews Molecular Cell Biology 8, 715-722 (September 2007) | doi:10.1038/nrm2242.

Sfeir A, Kosiyatrakul ST, Hockemeyer D, MacRae SL, Karlseder J, Schildkraut CL, de Lange T. (2009). Mammalian telomeres resemble fragile sites and require TRF1 for efficient replication. Cell. 2009 Jul 10;138(1):90-103. doi: 10.1016/j.cell.2009.06.021.

Shao L, et al. (2008). Identification of chromosomal abnormalities in subtelomeric regions by microarray analysis: a study of 5,380 cases. Am J Med Genet A 146A: 2242-2251.

She X, et al. (2004). The structure and evolution of centromeric transition regions within the human genome. Nature 430: 857-864.

Shen-Ong GL, Keath EJ, Piccoli SP, Cole MD. (1982). Novel myc oncogene RNA from abortive immunoglobulin-gene recombination in mouse plasmacytomas. Cell. 1982 Dec;31(2 Pt 1):443-52.

Shi Y, Glynn JM, Guilbert WJ, Cotter TG, Bissonnette RP, Green DR. (1992). Role for c-Myc in activation-induced apoptotic cell death in T cell hybridomas. Science 257: 212–214.

Shi, Y., Desponts, C., Do, J.T., Hahm, H.S., Scholer, H.R., and Ding, S. (2008) Induction of pluripotent stem cells from mouse embryonic fibroblasts by Oct4 and Klf4 with small-molecule compounds. Cell Stem Cell, 3, 568-574.

Silva AG, Graves HA, Guffei A, Ricca TI, Mortara RA, Jasiulionis MG, Mai S. (2010). Telomere-centromere-driven genomic instability contributes to karyotype evolution in a mouse mocel of melanoma. Neoplasia 12: 11-19.

Silver J, Miller JH. (2004). Regeneration beyond the glial scar. Nat Rev Neurosci. 2004 Feb;5(2):146-56.

Skotheim RI, Monni O, Mousses S, Fossa SD, Kallioniemi OP, Lothe RA, Kallioniemi A. (2002). New insights into testicular germ cell tumorigenesis from gene expression profiling. Cancer Res. 2002 Apr 15;62(8):2359-64.

Slack GW, Gascoyne RD. (2011). MYC and aggressive B-cell lymphomas. Adv Anat Pathol. 2011 May;18(3):219-28. doi: 10.1097/PAP.0b013e3182169948.

Slupianek A, Jozwiakowski SK, Gurdek E, Skorski T. (2009). BCR/ABL kinase interacts with and phosphorylates the RAD51 paralog, RAD51B. Leukemia. 2009 Dec;23(12):2308-10. doi: 10.1038/leu.2009.164. Epub 2009 Aug 6.

Sodir NM, Evan GI. (2009). Nursing some sense out of Myc. *Journal of Biology*. 2009;8(8):77. doi:10.1186/jbiol181.

Sohn EH, Jiao C, Kaalberg E, Cranston C, Mullins RF, Stone EM, Tucker BA. (2015). Allogenic iPSC-derived RPE cell transplants induce immune response in pigs: a pilot study. Sci Rep. 2015 Jul 3;5:11791. doi: 10.1038/srep11791.

Solomon JM, Pasupuleti R, Xu L, McDonagh T, Curtis R, DiStefano PS, Huber LJ. (2006). Inhibition of SIRT1 catalytic activity increases p53 acetylation but does not alter cell survival following DNA damage. Mol Cell Biol. 2006 Jan;26(1):28-38.

Solovei I, Kreysing M, Lanctot C, Kosem S, Peichl , Cremer T, Guck J, Joffe B. (2009). Nuclear architecture of rod photoreceptor cells adapts to vision in mammalian evolution. Cell 137: 356-368.

Spits C, Mateizel I, Geens M, Mertzanidou A, Staessen C, Vandeskelde Y, Van der Elst J, Liebaers I, Sermon K. (2008). Recurrent chromosomal abnormalities in human embryonic stem cells. Nat Biotechnol. 2008 Dec;26(12):1361-3. doi: 10.1038/nbt.1510. Epub 2008 Nov 23.

Stadtfeld, M., Nagaya, M., Utikal, J., Weir, G. & Hochedlinger, K. (2008). Induced pluripotent stem cells generated without viral integration. *Science* **322**, 945-949, doi:10.1126/science.1162494 (2008)

Stadtfeld, M., Apostolou, E., Akutsu, H., et al. (2010). Aberrant silencing of imprinted genes on chromosome 12qF1 in mouse induced pluripotent stem cells. Nature 2010; 465:175-181.

Steinemann D, Göhring G, Schlegelberger B. (2013). Genetic instability of modified stem cells - a first step towards malignant transformation? Am J Stem Cells. 2013 Mar 8;2(1):39-51.

Sugita S, Kamao H, Iwasaki Y, Okamoto S, Hashiguchi T, Iseki K, Hayashi N, Mandai M, Takahashi M. (2015). Inhibition of T-cell activation by retinal pigment epithelial cells derived from induced pluripotent stem cells. Invest Ophthalmol Vis Sci. 2015 Jan 20;56(2):1051-62. doi: 10.1167/iovs.14-15619.

Sun, N., Panetta, N.J., Gupta, D.M., Wilson, K.D., Lee, A., Jia, F., et al. (2009). Feeder-free derivation of induced pluripotent stem cells from adult human adipose stem cells. Proc. Natl. Acad. Sci. U.S.A., 103, 15720-15725.

Swarnalatha M, Singh AK, Kumar V. (2012). The epigenetic control of E-box and Myc-dependent chromatin modifications regulate the licensing of lamin B2 origin during cell cycle. Nucleic Acids Res 40: 9021-9035.

Taapken SM, Nisler BS, Newton MA, Sampsell-Barron TL, Leonhard KA, McIntire EM, Montgomery KD. (2011). Karotypic abnormalities in human induced pluripotent stem cells and embryonic stem cells. Nat Biotechnol. 2011 Apr;29(4):313-4. doi: 10.1038/nbt.1835.

Talbert P.B., Henikoff S. (2010). Histone variants–ancient wrap artists of the epigenome, Nat. Rev. Mol. Cell Biol., 2010, vol. 11(pg. 264-275).

Takahashi K, Yamanaka S. (2006). Induction of pluripotent stem cells from mouse embryonic and adult fibroblast cultures by defined factors. Cell. 2006 Aug 25;126(4):663-76. Epub 2006 Aug 10.

Takahashi K., Koji Tanabe, Mari Ohnuki, Megumi Narita, Tomoko Ichisaka, Kiichiro Tomoda, Shinya Yamanaka. (2007). Induction of Pluripotent Stem Cells from Adult Human Fibroblasts by Defined Factors**.** Cell - 30 November 2007 (Vol. 131, Issue 5, pp. 861-872)**.** Doi: 10.1013/j.cell.2007.11.019.

Takata M, Sasaki MS, Tachiiri S, Fukushima T, Sonoda E, Schild D, Thompson LH, Takeda S. (2001). Chromosome instability and defective recombinational repair in knockout mutants of the five Rad51 paralogs. Mol Cell Biol. 2001 Apr;21(8):2858-66.

Tarsounas M, Davies D, West SC. (2003). BRCA2-dependent and independent formation of RAD51 nuclear foci. Oncogene. 2003;22:1115–1123.

Tejera AM, Stagno d'Alcontres M, Thanasoula M, Marion RM, Martinez P, Liao C, Flores JM, Tarsounas M, Blasco MA. (2010). TPP1 is required for TERT recruitment, telomere elongation during nuclear reprogramming, and normal skin development in mice. Dev Cell. 2010;18:775–789. doi: 10.1016/j.devcel.2010.03.011.

Teng HF, Kuo YL, Loo MR, Li CL, Chu TW, Suo H, Liu HS, Lin KH, Chen SL. (2010). Valproic acid enhances Oct4 promoter activity in myogenic cells. J Cell Biochem. 2010 Jul 1;110(4):995-1004. doi: 10.1002/jcb.22613.

Tennstedt P, Fresow R, Simon R, Marx A, Terracciano L, Petersen C, Sauter G, Dikomey E, Borgmann K. (2013). RAD51 overexpression is a negative prognostic marker for colorectal adenocarcinoma. Int J Cancer. 2013 May 1;132(9):2118-26. doi: 10.1002/ijc.27907. Epub 2012 Nov 5.

Tetzlaff W., Okon E. B., Karimi-Abdolrezaee S., Hill C. E., Sparling J. S., Plemel J. R., et al. . (2011). A systematic review of cellular transplantation therapies for spinal cord injury. J. Neurotrauma 28, 1611–1682. 10.1089/neu.2009.1177.

Thanasegaran S, Cheng Z, Ito S, Nishio N, Isobe K. (2013). No immunogenicity of IPS cells in syngeneic host studied by in vivo injection and 3D scaffold experiments. Biomed Res Int. 2013;2013:378207. doi: 10.1155/2013/378207. Epub 2013 Apr 18.

Thomson JA, Itskovitz-Eldor J, Shapiro SS, Waknitz MA, Swiergiel JJ, Marshall VS, Jones JM. (1998). Embryonic stem cell lines derived from human blastocysts. Science. 1998 Nov 6;282(5391):1145-7.

Tian, Y. et al. (2010). microRNA-10b promotes migration and invasion through KLF4 in human esophageal cancer cell lines. J. Biol. Chem. 285, 7986-7994.

Tobias C. A., Shumsky J. S., Shibata M., Tuszynski M. H., Fischer I., Tessler A., et al. . (2003). Delayed grafting of BDNF and NT-3 producing fibroblasts into the injured spinal cord stimulates sprouting, partially rescues axotomized red nucleus neurons from loss and atrophy, and provides limited regeneration. Exp. Neurol. 184, 97–113. 10.1016/S0014-4886(03)00394-7.

Truong LN, Li Y, Shi LZ, Hwang PY, He J, Wang H, Razavian N, Berns MW, Wu X. (2013). Microhomology-mediated End Joining and Homologous Recombination share the initial end resection step to repair DNA double-strand breaks in mammalian cells. Proc Natl Acad Sci U S A. 2013 May 7;110(19):7720-5. doi: 10.1073/pnas.1213431110. Epub 2013 Apr 22.

Tsan MF. (2001). Superoxide dismutase and pulmonary oxygen toxicity: lessons from transgenic and knockout mice (Review). Int J Mol Med 7: 13–19, 2001

Ulndreaj A., Chio J. C. T., Ahuja C. S., Fehlings M. G. (2016). Modulating the immune response in spinal cord injury. Expert Rev. Neurother. 16, 1127–1129. 10.1080/14737175.2016.1207532.

Vafa O, Wade M, Kern S, Beeche M, Pandita TK, Hampton GM, Wahl GM. (2002). C-Myc can induce DNA damage increase reactive oxygen species, and mitigate p53 function: A mechanism for oncogene-induced genetic instability. Mol Cell 9: 1031-1044.

Van Remmen H, Ikeno Y, Hamilton M, Pahlavani M, Wolf N, Thorpe SR, Alderson NL, Baynes JW, Epstein CJ, HuangTT, Nelson J, Strong R, and Richardson A. (2003). Life-long reduction in MnSOD activity results in increased DNA damage and higher incidence of cancer but does not accelerate aging. Physiol Genomics 16: 29–37, 2003.

Varlakhanova NV, Cotterman RF, deVries WN, Morgan J, Donahue LR, Murray S, Knowles BB, Knoepfler PS. (2010). Myc maintains embryonic stem cell pluripotency

and self-renewal. Differentiation. 2010 Jul;80(1):9-19. doi: 10.1016/j.diff.2010.05.001. Epub 2010 May 27.

Vawda R., Wilcox J., Fehlings M. (2012). Current stem cell treatments for spinal cord injury. Indian J. Orthop. 46, 10–18. 10.4103/0019-5413.91629.

Vermeulen, K., Bockstaele, D.R.V. and Berneman, Z.N. (2003). The cell cycle: a review of regulation, deregulation and therapeutic targets in cancer. *Cell Proliferation*, 36: 131-149

Vermolen BJ, Garini Y, Mai S, Mougey V, Fest T, Chuang TC, Chuang AY, Wark L, Young IT. (2005). Characterizing the three-dimensional organization of telomeres. Cytometry A 67: 144-150.

Wang N, Trend B, Bronson DL, Fraley EE. (1980). Nonrandom abnormalities in chromosome 1 in human testicular cancers. Cancer Res. 1980 Mar;40(3):796-802.

Wang, Y., et al. (2010a). Oct-4B isoform is differentially expressed in breast cancer cells: hypermethylation of regulatory elements of Oct-4A suggests an alternative promoter and transcriptional start site for Oct-4B transcription. Biosci. Rep. 31, 109-115.

Wang Y, Liu L, Davies DR, Segal DM. (2010b). Dimerization of Toll-like receptor 3 (TLR3) is required for ligand binding. J Biol Chem. 2010 Nov 19;285(47):36836-41. doi: 10.1074/jbc.M110.167973. Epub 2010 Sep 22.

Wang Z, Zhou Q, Duan H, Wang Y, Dong M, Shi W. (2016). Immunological Properties of Corneal Epithelial-Like Cells Derived from Human Embryonic Stem Cells. PLoS One. 2016 Mar 15;11(3):e0150731. doi: 10.1371/journal.pone.0150731. eCollection 2016.

Ward Irene M. , Kay Minn, Jan van Deursen, and Junjie Chen. (2003). p53 Binding Protein 53BP1 Is Required for DNA Damage Responses and Tumor Suppression in Mice**.** Mol Cell Biol. 2003 Apr; 23(7): 2556–2563. doi: 10.1128/MCB.23.7.2556-2563.2003

Warren, L., Manos, P. D., Ahfeldt, T., Loh, Y. H., Li, H., Lau, F., Ebina, W., Mandal, P. K., Smith, Z. D., Meissner, A., Daley, G. Q., Brack, A. S., Collins, J. J., Cowan, C., Schlaeger, T. M. & Rossi, D. J. (2010). Highly efficient reprogramming to pluripotency and directed differentiation of human cells with synthetic modified mRNA. *Cell Stem Cell* **7**, 618-630, doi:10.1016/j.stem.2010.08.012 (2010).

Wasylishen AR, Penn LZ. (2010). Myc: the beauty and the beast. Genes Cancer. 2010 Jun;1(6):532-41. doi: 10.1177/1947601910378024.

Waxman S. G. (1989). Demyelination in spinal cord injury. J. Neurol. Sci. 91, 1–14. 10.1016/0022-510X(89)90072-5.

Werbowetski-Ogilvie TE, Bossé M, Stewart M, Schnerch A, Ramos-Mejia V, Rouleau A, Wynder T, Smith MJ, Dingwall S, Carter T, Williams C, Harris C, Dolling J, Wynder C, Boreham D, Bhatia M. (2009). Characterization of human embryonic stem cells with features of neoplastic progression. Nat Biotechnol. 2009 Jan;27(1):91-7. doi: 10.1038/nbt.1516. Epub 2009 Jan 4

West M.H., Bonner W.M. (1980). Histone 2A, a heteromorphous family of eight protein species. Biochemistry, 1980, vol. 19 (pg. 3238-3245).

Wilmut I., A. E. Schnieke, J. McWhir, A. J. Kind & K. H. S. Campbell. (1997). Viable offspring derived from fetal and adult mammalian cells. Nature 385, 810 - 813 (27 February 1997); doi:10.1038/385810a0.

Wright WE, Shay JW. (2000). Telomere dynamics in cancer progression and prevention: fundamental differences in human and mouse telomere biology. Nat Med. 2000 Aug;6(8):849-51.

Woltjen, K., Michael, I. P., Mohseni, P., Desai, R., Mileikovsky, M., Hamalainen, R., Cowling, R., Wang, W., Liu, P., Gertsenstein, M., Kaji, K., Sung, H. K. & Nagy, A. (2009). PiggyBac transposition reprograms fibroblasts to induced pluripotent stem cells. *Nature* **458**, 766-770 (2009).

Wu X, Ranganathan V, Weisman DS, Heine WF, Ciccone DN, O'Neill TB, Crick KE, Pierce KA, Lane WS, Rathbun G, et al. (2000). ATM phosphorylation of Nijmegen breakage syndrome protein is required in a DNA damage response. Nature. 2000;405:477–482.

Wu H, Kim KJ, Mehta K, Paxia S, Sundstrom A, Anantharaman T, Kuraishy AI, Doan T, Ghosh J, Pyle AD, Clark A, Lowry W, Fan G, Baxter T, Mishra B, Sun Y, Teitell MA. (2008). Copy number variant analysis of human embryonic stem cells. Stem Cells. 2008 Jun;26(6):1484-9. doi: 10.1634/stemcells.2007-0993. Epub 2008 Mar 27.

Yamanaka S. (2008). Pluripotency and nuclear reprogramming. Philos Trans R Soc Lond B Biol Sci. 2008 Jun 27;363(1500):2079-87. doi: 10.1098/rstb.2008.2261.

Yang D, Tewary P, de la Rosa G, Wei F, Oppenheim JJ. (2010a). The alarmin functions of high-mobility group proteins. Biochim Biophys Acta. 2010 Jan-Feb;1799(1-2):157-63. doi: 10.1016/j.bbagrm.2009.11.002.

Yang J., Anouk L. van Oosten, Thorold W. Theunissen, Ge Guo, Jose C.R. Silva, Austin Smith. (2010b). Stat3 Activation Is Limiting for Reprogramming to Ground State Pluripotency. Cell Stem Cell, 2010 September 3; 7(3): 319–328. doi: 10.1016/j.stem.2010.06.022.

Yatsenko SA, et al. (2009). Molecular mechanisms for subtelomeric rearrangements associated with the 9q34.3 microdeletion syndrome. Hum Mol Genet.

Ye, L., Chang, J.C., Lin, C., Sun, X., Yu, J., and Kan, Y.W. (2009). Induced pluripotent stem cells offer new approach to therapy in thalassemia and sickle cell anemia and option in prenatal diagnosis in genetic diseses. Proc. Natl. Acad. Sci. U.S.A., 106, 9826-9830.

Ying Q.-L., Jason Wray, Jennifer Nichols, Laura Batlle-Morera, Bradley Doble, James Woodgett, Philip Cohen & Austin Smith. (2008). The ground state of embryonic stem cell self-renewal. *Nature* **453**, 519-523 (22 May 2008) | doi:10.1038/nature06968.

Yoshida, Y., Takahashi, K., Okita, K., Ichisaka, T., and Yamanaka, S. (2009). Hypoxia enhances the generation of induced pluripotent stem cells. Cell Stem Cell, 5, 237-241.

Yoshioka, N., Gros, E., Li, H. R., Kumar, S., Deacon, D. C., Maron, C., Muotri, A. R., Chi, N. C., Fu, X. D., Yu, B. D. & Dowdy, S. F. (2013). Efficient generation of human iPSC by a synthetic self-replicative RNA. *Cell Stem Cell* **13**, 246-254, doi:10.1016/j.stem.2013.06.001, 2013.

Yu, J., Vodyanik, M. A., Smuga-Otto, K., Antosiewicz-Bourget, J., Frane, J. L., Tian, S., Nie, J., Jonsdottir, G. A., Ruotti, V., Stewart, R., Slukvin, II & Thomson, J. A. (2007). Induced pluripotent stem cell lines derived from human somatic cells. *Science* **318**, 1917-1920, 2007.

Yu J, Thomson JA. (2008). Pluripotent stem cell lines. Genes Dev. 2008 Aug 1;22(15):1987-97. doi: 10.1101/gad.1689808.

Yu J, Hu K, Smuga-Otto K, Tian S, Stewart R, Slukvin II, Thomson JA. (2009). Human induced pluripotent stem cells free of vector and transgene sequences. Science. 2009 May 8;324(5928):797-801. doi: 10.1126/science.1172482. Epub 2009 Mar 26.

Yuan H, Corbi N, Basilico C, Dailey L. (1995). Developmental-specific activity of the FGF-4 enhancer requires the synergistic action of Sox2 and Oct-3. Genes Dev. 1995 Nov 1;9(21):2635-45.

Yuan Z, Zhang X, Sengupta N, Lane WS, Seto E. (2007). SIRT1 regulates the function of the Nijmegen breakage syndrome protein. Mol Cell. 2007 Jul 6;27(1):149-62.

Yuan T, Liao W, Feng NH, Lou YL, Niu X, Zhang AJ, Wang Y, Deng ZF. (2013). Human induced pluripotent stem cell-derived neural stem cells survive, migrate, differentiate, and improve neurological function in a rat model of middle cerebral artery occlusion. Stem Cell Res Ther. 2013 Jun 14;4(3):73.

Zhang, W., Geiman, D.E., Shields, J.M., Dang, D.T., Mahatan, C.S., Kaestner, K.H., Biggs, J.R., Kraft, A.S., and Yang, V.W. (2000). The gut-enriched Kruppel-like factor (kruppel-like factor 4) mediatesthe transactivating effect of p53 on the p21WAF1/Cip1 promoter. J. Biol. Chem. 275, 18391-18398.

Zhang Z, Gao Y, Gordon A, Wang ZZ, Qian Z, Wu WS. (2011). Efficient generation of fully reprogrammed human iPS cells via polycistronic retroviral vector and a new cocktail of chemical compounds. Epub 2011 Oct 26. PLoS One. 2011;6(10):e26592. doi: 10.1371/journal.pone.0026592.

Zhang ZN, Chung SK, Xu Z, Xu Y. (2014). Oct4 maintains the pluripotency of human embryonic stem cells by inactivating p53 through Sirt1-mediated deacetylation. Stem Cells. 2014 Jan;32(1):157-65. doi: 10.1002/stem.1532.

Zhao Y, Chaiswing L, Velez JM, Batinic-Haberle I, Colburn NH, Oberley TD, and St Clair DK. (2005). p53 translocation to mitochondria precedes its nuclear translocation and

targets mitochondrial oxidative defense protein-manganese superoxide dismutase. Cancer Res 65: 3745–3750, 2005.

Zhao S, Weng YC, Yuan SS, Lin YT, Hsu HC, Lin SC, Gerbino E, Song MH, Zdzienicka MZ, Gatti RA, et al. (2000). Functional link between ataxia-telangiectasia and Nijmegen breakage syndrome gene products. Nature. 2000;405:473–477.

Zhao T, Zhang ZN, Rong Z, Xu Y. (2011). Immunogenicity of induced pluripotent stem cells. Nature. 2011 May 13;474(7350):212-5. doi: 10.1038/nature10135

Zhou, H., Wu, S., Joo, J. Y., Zhu, S., Han, D. W., Lin, T., Trauger, S., Bien, G., Yao, S., Zhu, Y., Siuzdak, G., Scholer, H. R., Duan, L. & Ding, S. (2009). Generation of induced pluripotent stem cells using recombinant proteins. *Cell Stem Cell* **4**, 381-384, doi:10.1016/j.stem.2009.04.005, 2009.

Zindy, F., Eischen, C.M., Randle, D.H., Kamijo, T., Cleveland, J.L., Sherr, C.J., and Roussel, M.F., (1998). Myc signaling via the ARF tumor supressor regulates p53-dependent apoptosis and immortalization. Genes Dev. 12, 2424-2433.

Zlatanova J., Bishop T.C., Victor J.M., Jackson V., van Holde K. (2009). The nucleosome family: dynamic and growing, Structure, 2009, vol. 17 (pg. 160-171).

Zou X, Lin Y, Rudchenko S, Calame K. (1997). Positive and negative regulation of c-Myc transcription. Curr Top Microbiol Immunol. 1997;224:57-66.

Online links:

WHO, World Health Organization webpage Spinal Cord Injury, April, 2017.
http://www.who.int/mediacentre/factsheets/fs384/en/

APPENDICES

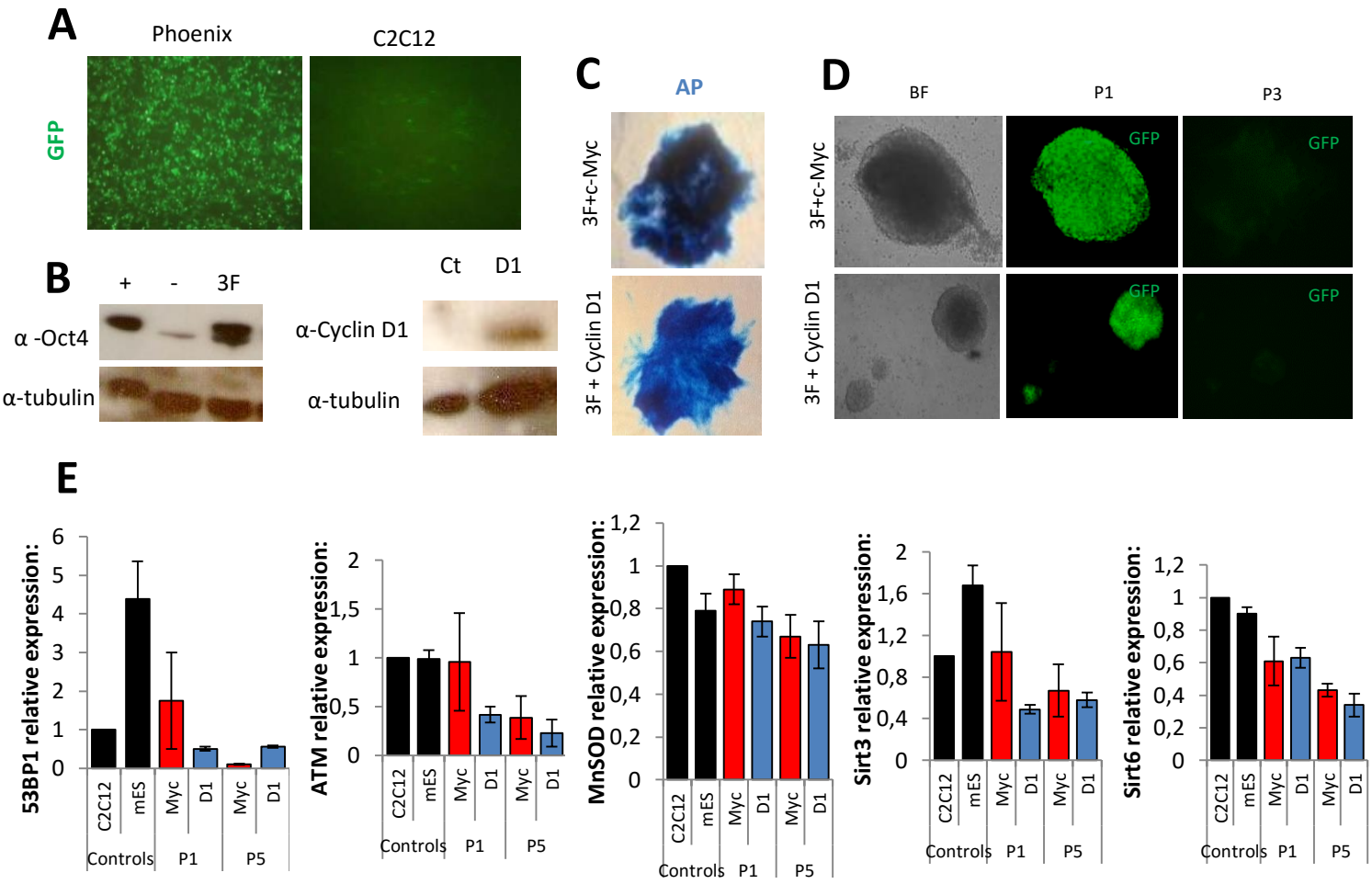

Suplementary figure 1. Mouse C2C12 iPSCs reprogramming and cell stress genes.

A) GFP reporter gene expression after transduction of reprogramming factors in Ecotropic Phoenix virus producing cells and infected mouse C2C12. **B)** Oct4 and Cyclin D1 protein expression level was checked by western blot to corroborate that the transgene was functionally producing protein. **C)** Alkaline phosphatase was shown positive for colonies picked after reprogramming C2C12 with 3F+c-Myc and 3F+Cyclin D1. **D)** C2C12 infected cells starting to form colonies both for 3F + c-Myc and 3F + Cyclin D1. Reporter GFP expression was detected at passage 1 meaning the transgene was on. At passage 3, the transgene was silenced as GFP expression was off. **E-I)** Other cell stress genes levels were checked by real time PCR at passage 1 and 5 and compared with control C2C12 and mouse Embryonic Stem cells levels**:** p53 binding protein 1 (53BP1), The protein kinase *ataxia*-telangiectasia mutated (ATM) implicated in the regulation of oxidative stress, Manganese superoxide dismutase (MnSOD) also implicated in oxidative stress and Sirtuin 3 (Sirt3) and Sirtuin 6 (Sirt6). No significant differences were found.

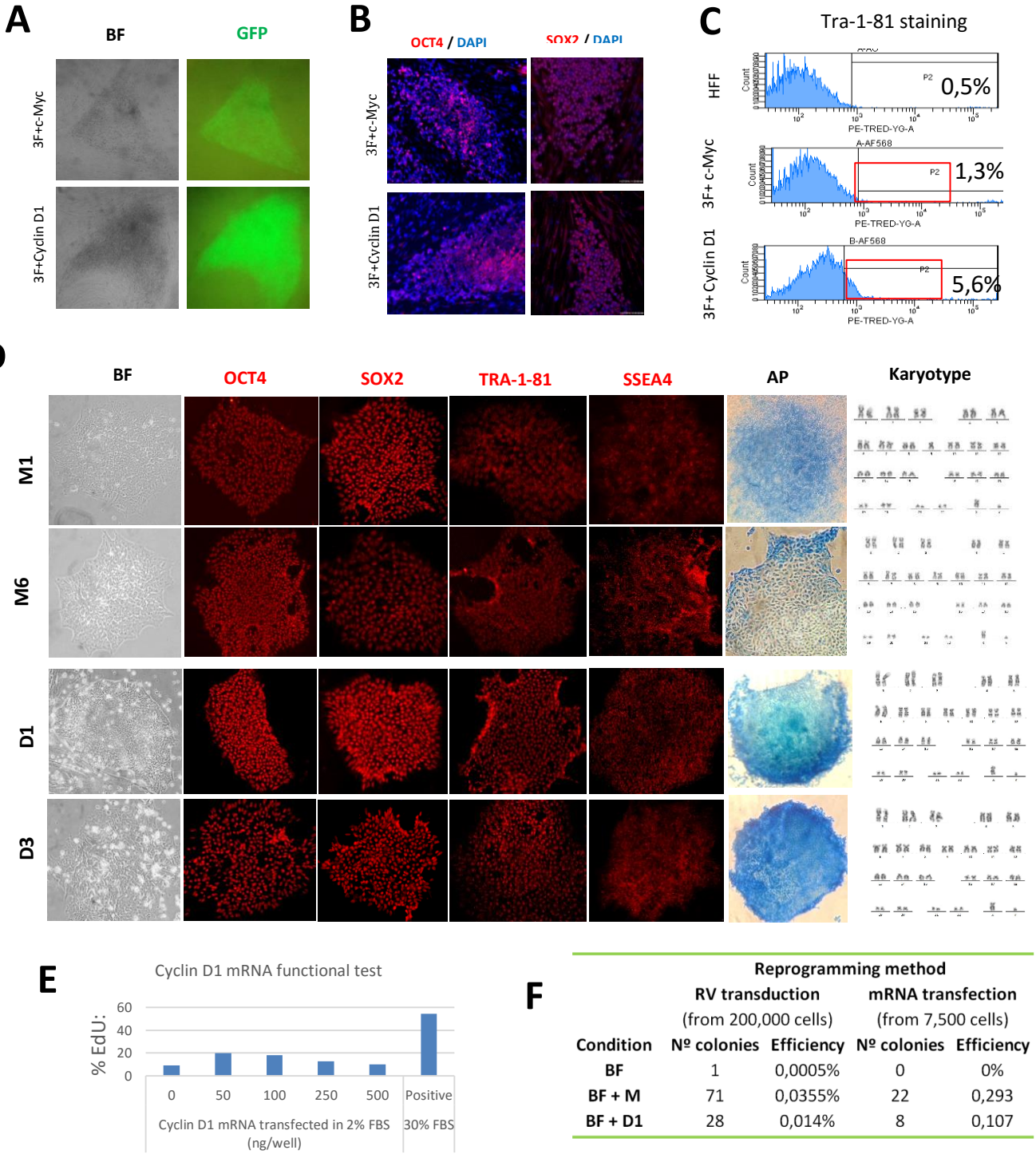

F

	Reprogramming method			
	RV transduction (from 200,000 cells)		mRNA transfection (from 7,500 cells)	
Condition	**Nº colonies**	**Efficiency**	**Nº colonies**	**Efficiency**
BF	1	0,0005%	0	0%
BF + M	71	0,0355%	22	0,293
BF + D1	28	0,014%	8	0,107

Supplementary figure 2. Cyclin D1 and c-Myc HFF iPSCs characterization. Retroviral transduction and mRNA transfection were used as reprogramming methods.

A) GFP reporter gene expression after transduction of reprogramming factors in human foreskin fibroblasts (HFFs) iPSCs colonies reprogrammed retrovirally with 3F + c-Myc and 3F + Cyclin D1. **B)** Immunofluorescence images showing a positive expression of Oct4 and Sox2 in human iPSCs at passage 5 made both with 3F+c-Myc and 3F+Cyclin D1. Nuclei were stained with DAPI. **C)** FACS analysis of Tra-1-81 staining of retrovirally infected HFFs cells with 3F + c-Myc (1,3%) and 3F + Cyclin D1 (5,6%) compared to a non-infected control (0,5%). A polyclonal scrape of randomly picked colonies was stained two weeks after the cells were cultured onto a feeder layer of irHFFs in hES medium. **D)** Messenger RNA reprogrammed clones characterization: bright field (BF), immunofluorescence for pluripotency markers (OCT4, SOX2, TRA1-81, SSEA4) and alkaline phosphatase (AP). Karyotype of 20 metaphases per clone was also conducted; a representative image of normal karyotype is shown. Four clones are shown, two for c-Myc (M1 and M6) and two for Cyclin D1 (D1 and D3). **E)** Cyclin D1 mRNA functional test. Graph shows the % of EdU positive HFFs after transfection of different concentrations of mRNA (0, 50, 100, 250 and 500ng/well). Cells were transfected in 2% FBS. As positive control cells were cultured in 30% FBS. **F)** Reprogramming efficiency and nº of colonies of HFFs reprogrammed with retroviral transduction and mRNA transfections comparing conditions: base factors (BF: OSKL), BF+c-Myc and BF+Cyclin D1.

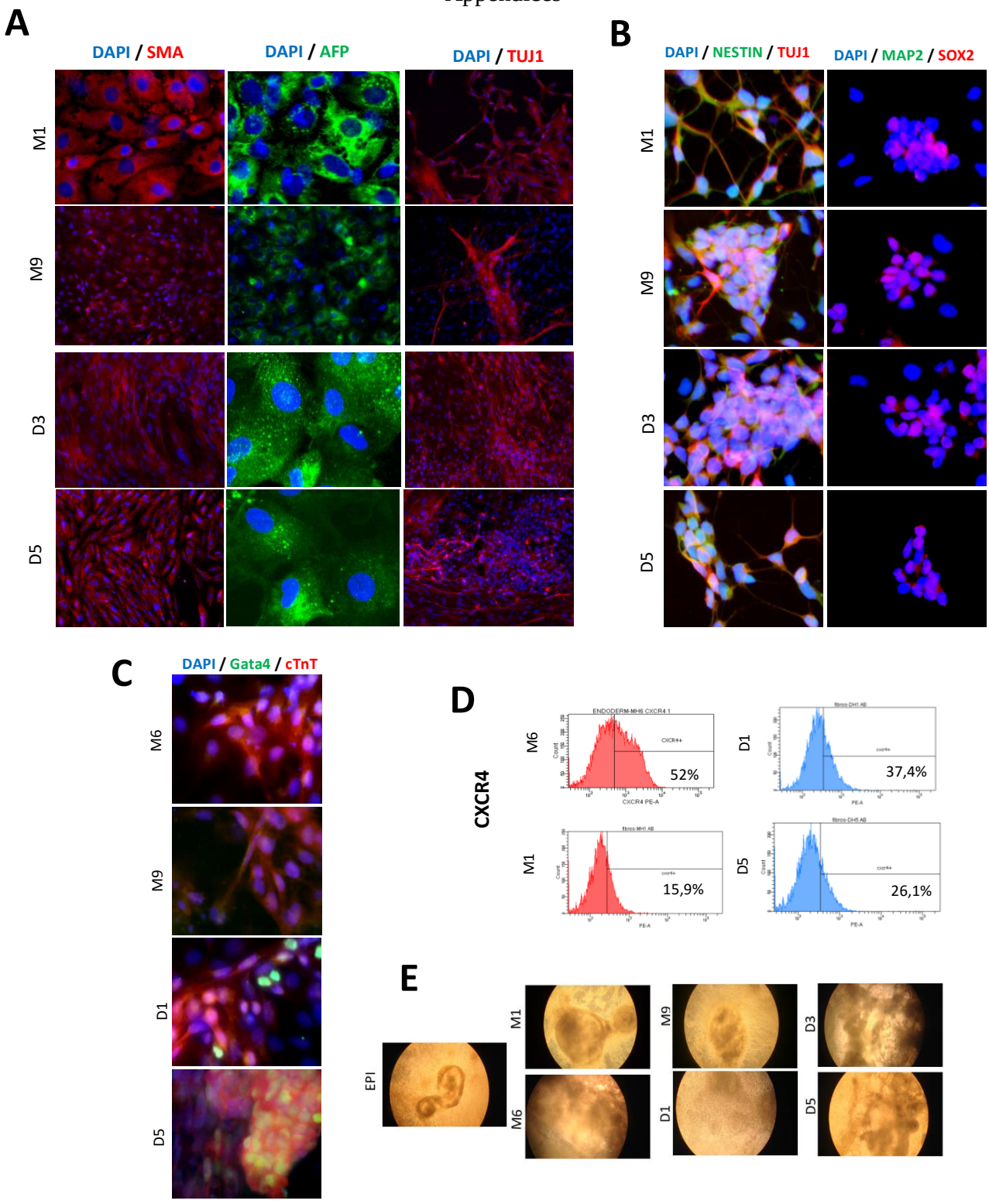

Supplementary figure 3. Cyclin D1 and c-Myc mRNA iPSCs derived Neural Stem Cells (NSC) and Cardiomyocytes (CM) characterization and videos for beating CM.

A) Immunofluorescence of generally differentiated iPSCs stained for endoderm (SMA), mesoderm (AFP) and ectoderm (Tuj1). Four clones are shown, two for c-Myc (M1 and M9) and two for Cyclin D1 (D3 and D5). Nuclei were stained with DAPI. **B)** Immunofluorescence of guided differentiation of iPSCs into Neural Stem Cells (NSC), stained for NESTIN, TUJ1, MAP2 and SOX2. Four clones are shown, two for c-Myc (M1 and M9) and two for Cyclin D1 (D3 and D5). Nuclei were stained with DAPI. **C)** Immunofluorescence of guided differentiation of iPSCs into Cardiomyocytes (CM), stained for GATA4 and cTnT. Four clones are shown, two for c-Myc (M6 and M9) and two for Cyclin D1 (D1 and D5). Nuclei were stained with DAPI. **D)** Flow cytometry analysis histograms of guided differentiation of iPSCs into definitive endoderm. Cells were stained for CXCR4. Four clones are shown, two for c-Myc (M6 and M9) and two for Cyclin D1 (D3 and D5). **E)** Videos of all clones (M1, M6, M9, D1, D3 and D5) differentiated into beating CM. As positive control Episomal iPSCs were also differentiated into CM.

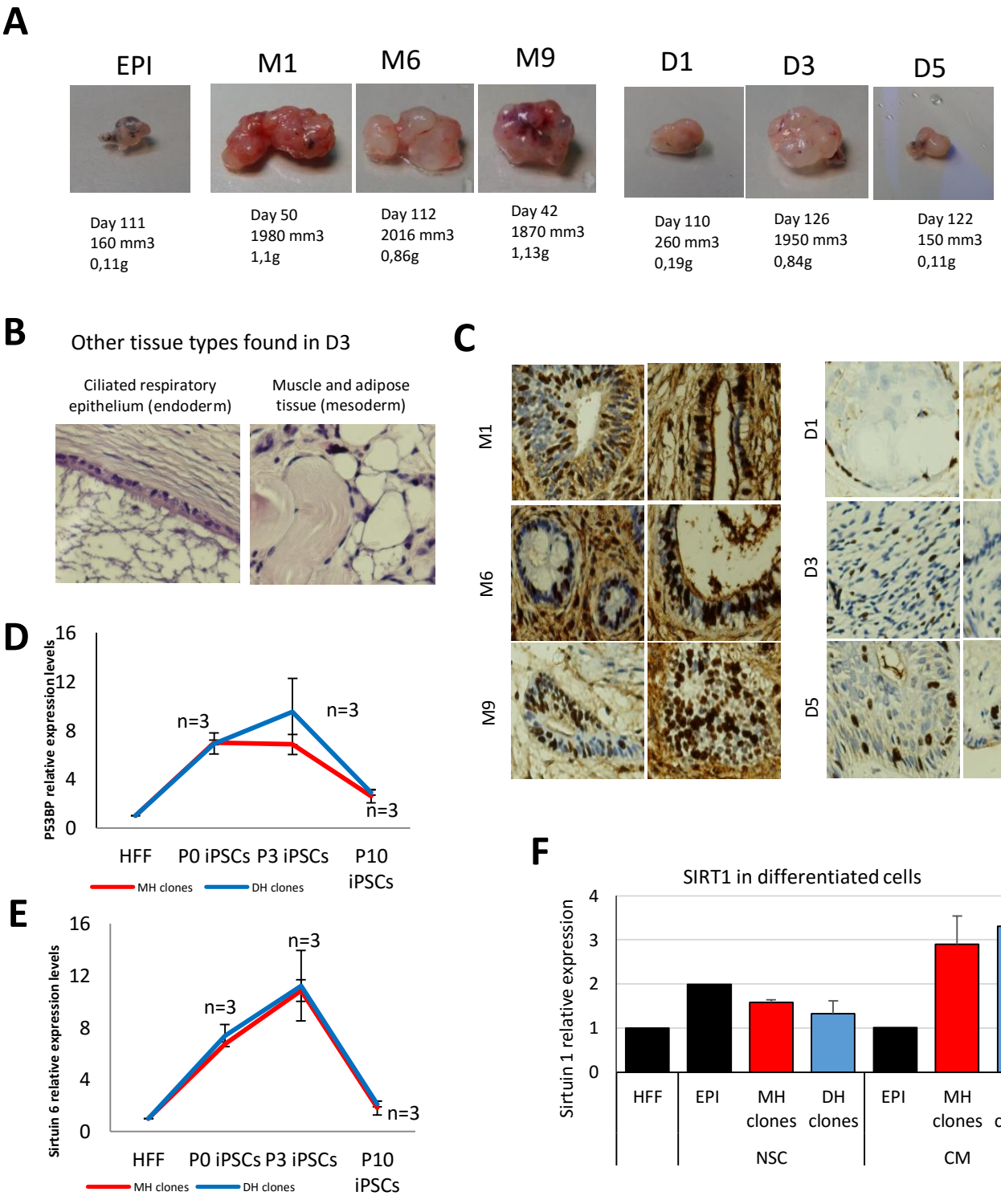

Supplementary figure 4. In vivo pluripotency differentiation potential assessment to teratomas and cell proliferation rate (KI67%).

A) Teratomas of mRNA made iPSCs injected in athymic nude mice (Foxn1-/-) to test the in vivo pluripotency potential into the three germ layers. **B)** Other examples of different tissues found in Cyclin D1 teratoma (D3): ciliated respiratory epithelium (endoderm) and muscle and adipose tissue (mesoderm). **C)** Immunohistochemistry staining of KI67 for each teratoma to assess proliferation. Five different fields were picked randomly for counting the % of positive cells per each teratoma. Two images per clone are shown. **D-E)** Other cell stress genes levels were checked by RT-PCR at passage 0, 3 and 10 and compared with control HFFs. P53 binding protein 1 (53BP1) *and Sirtuin 6 (Sirt6).* **F)** Sirtuin 1 levels by qPCR in iPSCs differentiated cells. After iPSCs differentiation into neural stem cells (NSC) and Cardiomyocytes (CM) Sirtuin 1 levels are not different between conditions.

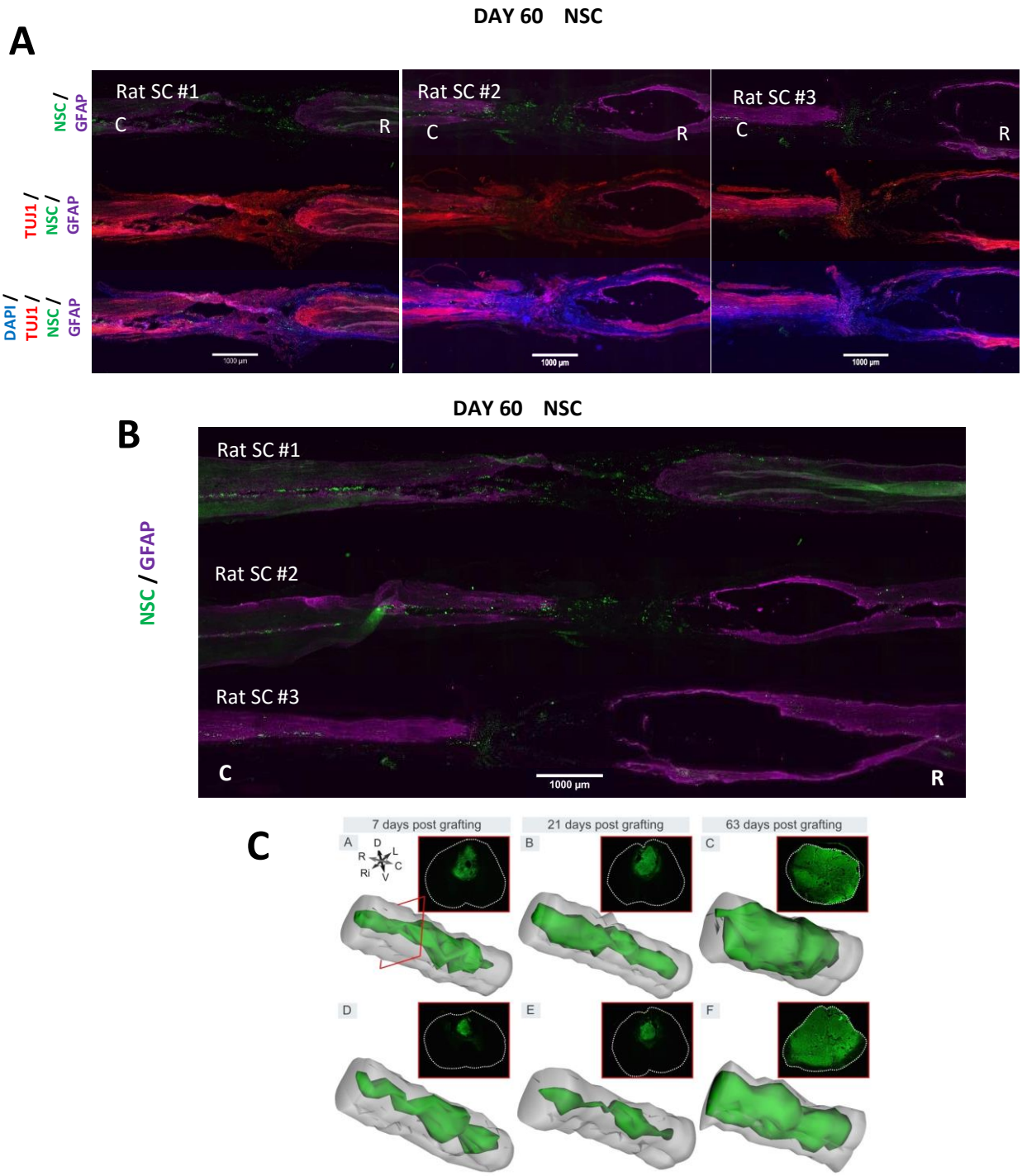

Supplementary figure 5. Clinical grade human iPSCs derived NSC engraft and migrate to the lesion site in a Spinal Cord Injury (SCI) rat model.

A) Immunofluorescence of transection cuts of perfused spinal cords at day 60 after NSC injection of three rats (SC #1, 2 and 3). Injected cells were tagged with cell tracker (Vybrant CFDA SE) to detect cells using a GFP detection wavelength. Tuj1 and GFAP were used to detect neurons and astrocytes respectively and DAPI to stain nuclei. A merge image is shown. Cells survived, engrafted and migrated as shown by the green tracker at day 3 and day 60. After injecting mRNA made iPSCs derived NSC in the spinal cord no neoplasm was formed. **B)** NSC tracking show migration preferences towards the lesion site and the caudal side of the spinal cord. **C)** Image extracted from López-Serrano et al., 2016. Retrovirally made iPSCs derived NSC were injected into the spinal cord. Grafted cell survival and localization in the injured spinal cord. The amount of grafted cells along 1 cm of the injured spinal cord was studied at 7, 21, and 63 dpt by immunolabeling with human marker SC121. The grafted cells occupied the main part of the spinal cord at 63 dpt, filling an area that was significantly increased compared to the area at 7 and 21 days (G, H). ***$p < 0.001$. Acute and subacute transplanted groups: at 7 dpt (n = 3), 21 dpt (n = 4), and 63 dpt (n = 6). Thus, retrovirally made iPSCs derived NSC gave raise to a tumour mass in the spinal cord.

ANNEXES

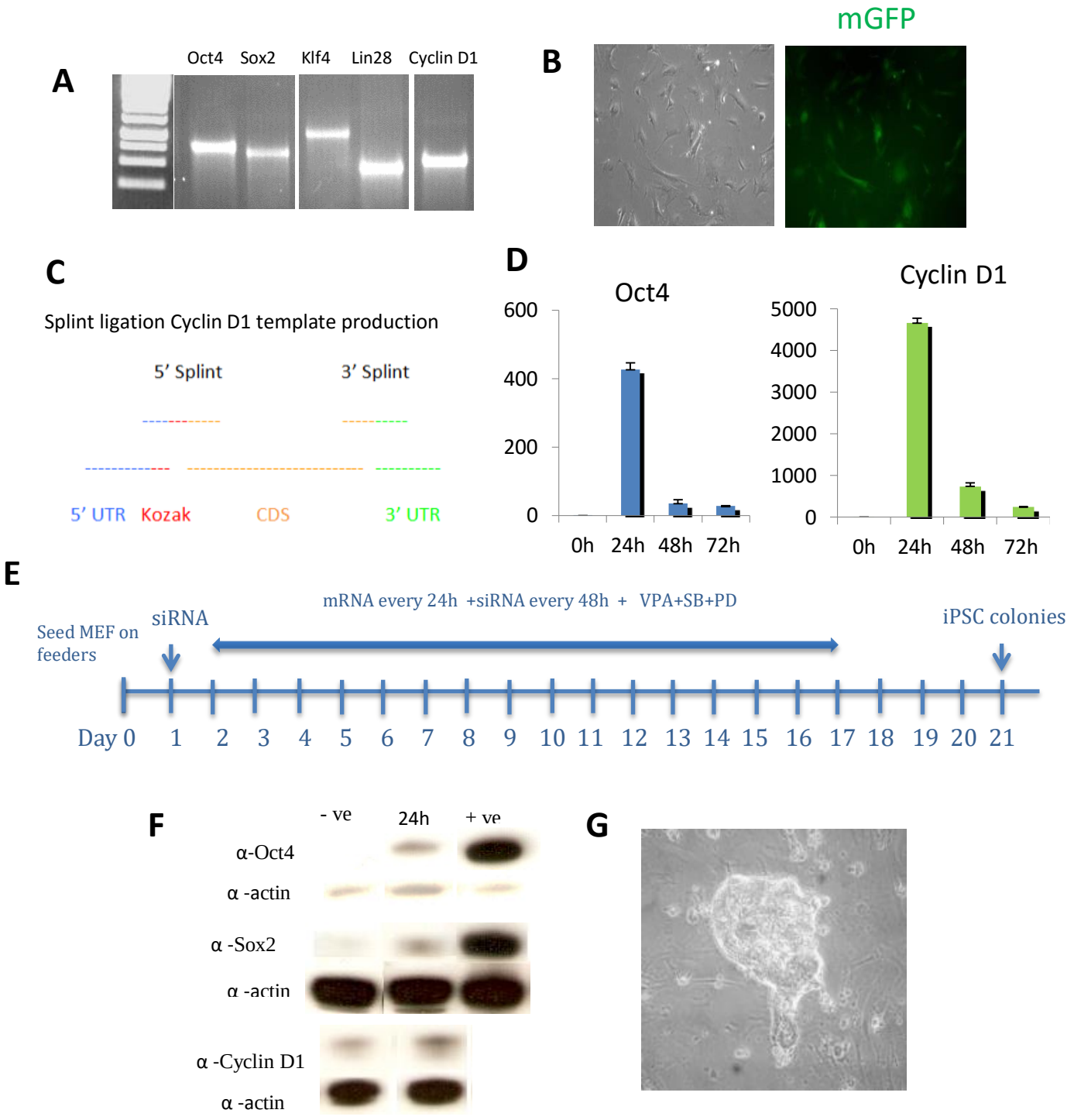

Annexes Figure 1. Messenger RNA transfection protocol.

A) Synthetic messenger RNA degradation is checked by agarose gel. Oct4, Sox2, Klf4, Lin28 and Cyclin D1 are shown. **B)** GFP expression after mRNA transfection of a transcript coding for the green fluorescent protein. Every reprogramming experiment was done in parallel with a mGFP transfected HFFs control. **C)** Diagram showing Cyclin D1 mRNA template production. ORF was cloned with a 5' and 3' UTR by splint ligation. **D)** Messenger RNA levels in the cell obtained by RT-PCR 24, 48 and 72h after transfect mouse fibroblasts with 200ng of Cyclin D1 and Oct4 compared with an untransfected control (0h). **E)** Schematic timeline of the mRNA transfection protocol. Different ng and different densities were tested, transfecting every 24h during 14-17 days. To increase reprogramming efficiency we added VPA, and SB431542, and PD0325901 (Zhang et al., 2011). To avoid immune response cells were pre-treated from day 1 onwards with siRNA against IFNb1, Stat2, Eif2ak2 (Angel et al., 2010). **F)** Protein expression levels determined by Western Blot of lysates from MEFs 24h after transfecting 200ng of mRNA coding for Oct4, Sox2 and Cyclin D1. Actin was used as loading control. Positive control are untransfected mouse embryonic stem cells. **G)** Partially reprogrammed iPSC colonies obtained from mRNA transfected MEFs. Scale bars, 100µm.

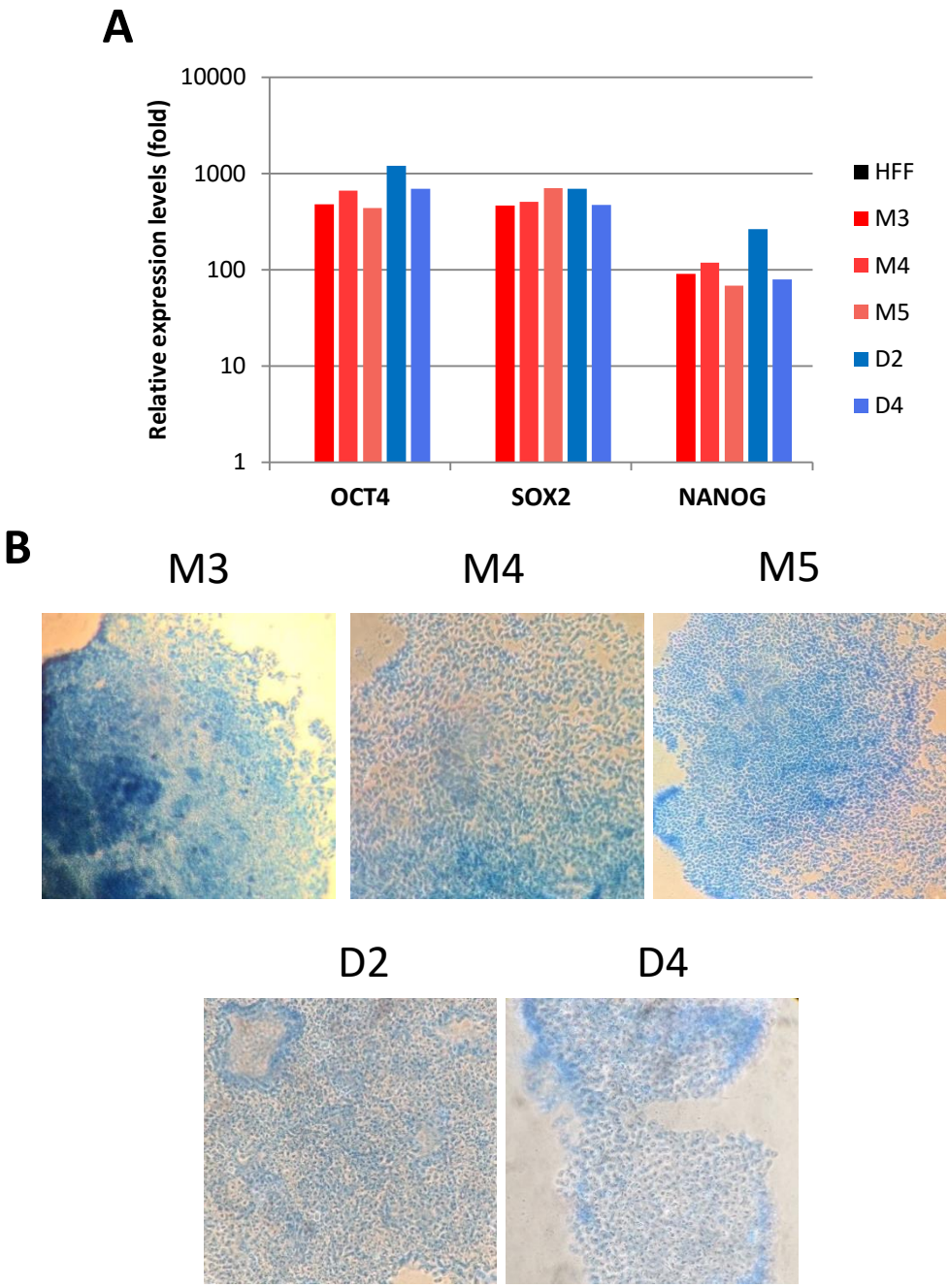

Annexes Figure 2. Characterization of pluripotency of the extra clones.

A) RT-PCR analysis of pluripotency markers Oct4, Sox2 and Nanog for M3, M4, M5, D2 and D4 clones compared with control HFFs. **B)** Alkaline Phosphatase staining of M3, M4, M5, D2 and D4 clones.

Annexe Table 1. RT-PCR forward and reverse primers used for human and mouse qPCR.

HUMAN GENES	FORWARD PRIMER	REVERSE PRIMER
hGAPDH	GCACCGTCAAGGCTGAGAAC	AGGGATCTCGCTCCTGGAA
hOCT4	GGAGGAAGCTGACAACAATGAAA	GGCCTGCACGAGGGTTT
hSOX2	TGCGAGCGCTGCACAT	TCATGAGCGTCTTGGTTTTCC
hNANOG	ACAACTGGCCGAAGAATAGCA	GGTTCCCAGTCGGGTTCAC
hKLF4	ACGATCGTGGCCCCGGAAAAGGACC	CAACAACCGAAAATGCACCAGCCCCAG
hC-Myc	GCGTCCTGGGAAGGGAGATCCGGAGC	TTGAGGGGCATCGTCGCGGGAGGCTG
hMEF2C	CTGGCAACAGCAACACCTACA	GCTAGTGCAAGCTCCCAACTG
hFOX2A	CTGAAGCCGGAACACCACTAC	CGAGGACATGAGGTTGTTGATG
hTUBB3	GGCCAAGTTCTGGGAAGTCA	CGAGTCGCCCACGTAGTTG
hNestin	CAGGAGAAACAGGGCCTACA	TGGGAGCAAAGATCCAAGAC
hSox1	TACAGCCCCATCTCCAACTC	GCTCCGACTTCACCAGAGAG
hPax6	GCTTCACCATGGCAAATAACC	GGCAGCATGCAGGAGTATGA
hcTNT	GGCAGCGGAAGAGGATGCTGAA	GAGGCACCAAGTTGGGCATGAAC
hGata4	AGGCCTCTTGCAATGCGGA	CTGGTGGTGGCGTTGCTGG
hCXCR4	TGTTGTCTGAACCCCATCCT	CTGTGAGCAGGTCCAG
hc-KIT	TTCTCTGCGTTCTGCTCCTAC	CCCACGCGGACTATTAAGTC
hSox17	TGGCGCAGCAGAATCCA	CCACGACTTGCCCAGCAT
hHNF4	CTGCAGGCTCAAGAAATGCTT	CTGCAGGCTCAAGAAATGCTT
hChat	AACGAGGACGAGCGTTTG	TCAATCATGTCCAGCGAGTC
hHoxB4	GTCGTCTACCCCTGGATGC	TTCCTTCTCCAGCTCCAAGA
hNkx6.1	ATTCGTTGGGGATGACAGAG	CCGAGTCCTGCTTCTTCTTG
hPeripherin	AGACCATTGAGACCCGGAAT	GGCCTAGGGCAGAGTCAAG
hHLA A	TCCTTGGAGCTGTGATCGCT	AAGGGCAGGAACAACTCTTG
hHLA B	TCCTAGCAGTTGTGGTCATC	TCAAGCTGTGAGAGACACAT
hHLA C	TCCTGGTTGTCCTAGCTGTC	CAGGCTTTACAAGTGATGAG
hB2M	TGACTTTGTCACAGCCCAAGATA	AATCCAAATGCGGCATCTTC
hTLR3	CCTGGTTTGTTAATTGGATTAACGA	TGAGGTGGAGTGTTGCAAAGG
hTLR4	CCAGTGAGGATGATGCCAGAAT	GCCATGGCTGGATCAGAGT
hTLR3 isoform B	AAGACACAACCAGGAACTGCC	GCTTCTCTGACCTTCCAGTCC
h53BP1	GTCAGGTCATTGAGCAGTTACCTC	TCCTCCACAGCAGGAGCAG
hATM	CCGTGATGACCTGAGACAAG	AACACCACTTCGCTGAGAGAG
hIAP2	ATGCTTTTGCTGTGATGGTG	TGAACT TGACGGATGAACTCC
hMnSOD	TGGCCAAGGGAGATGTTACA	TGATATGACCACCACCATTGAAC
hGADD45b	TCGGATTTTGCAATTTCTCC	GACTCGTACACCCCCACTGT
hSIRT1	TGGGTACCGAGATAACCTTCT	TGTTCGAGGATCTGTGCCAA
hSIRT3	GCATTCCAGACTTCAGATCGC	GTGGCAGAGGCAAAGGTTCC
hSIRT6	GCAGTCTTCCAGTGTGGTGT	AAGGTGGTGTCGAACTTGGG
hLIG3	GAAGAGCTGGAAGATAATGAGAAGG	AGTGGTTGTCAACTTAGCCTGG
hPOLQ	CAGCCCTTATAGTGGAAGAAGC	GCACATGGATTCCATTGCACTC
hRad51	CAATGCAGATGCAGCTTGAA	CCTTGGCTTCACTAATTCCCT
hRad51B	TTTCCCCACTGGAGCTTATG	CTTCGTCCAAAGCAGAAAGG
hBRCA1	ACAGCTGTGTGGTGCTTCTGTG	CATTGTCCTCTGTCCAGGCATC

hBRCA2	CTTGCCCCTTTCGTCTATTTG	TACGGCCCTGAAGTACAGTCTT
hKu70	ATGGCAACTCCAGAGCAGGTG	AGTGCTTGGTGAGGGCTTCCA
D1 ORF	GAACACCAGCTCCTGTGCTGCG	TCAGATGTCCACGTCCCGCAC
Xu-F1	TTGGACCCTCGTACAGAAGCTAATACG (Mandal et al., 2013)	
Xu-T120	T(120)CCTACTCAGGCTTTATTCAAGACCA (Mandal et al., 2013)	
5' splint D1	CGCAGCACAGGAGCTGGTGTTCCATGGTGGCTCTTATATTTCTT	
3' splint D1	CCCGCAGAAGGCAGCTCAGATGTCCACGTCCC	
5' UTR	TTGGACCCTCGTACAGAAGCTAATACGACTCACTATAGGGAAATAAGAGAGAAAAG AAGAGTAAGAAGAAATATAAGAGCCACCATG (Mandal et al., 2013)	
3' UTR	GCTGCCTTCTGCGGGGCTTGCCTTCTGGCCATGCCCTTCTTCTCTCCCTTGCACCTGTA CCTCTTGGTCTTTGAATAAAGCCTGAGTAGGAAGTGAGGGTCTAGAACTAGTGTCGA CGC (Mandal et al., 2013)	
MOUSE GENES	FORWARD PRIMER	REVERSE PRIMER
mGAPDH	CATGGCCTTCCGTGTTCCTA	CCTGCTTCACCACCTTCTTGAT
mOCT4	TAGGTGAGCCGTCTTTCCAC	GCTTAGCCAGGTTCGAGGAT
mSOX2	TGCGAGCGCTGCACAT	TCATGAGCGTCTTGGTTTTCC
mNANOG	AAACCAGTGGTTGAAGACTAGCAA	GGTGCTGAGCCCTTCTGAATC
mRex1	ACGAGTGGCAGTTTCTTCTTGGGA	TATGACTCACTTCCAGGGGGCACT
mUtf1	GGATGTCCCGGTGACTACGTCTG	GGCGGATCTGGTTATCGAAGGGT
mNkx 2.5	GACAGGTACCGCTGTTGCTT	AGCCTACGGTGACCCTGAC
mTbx5	TGACTGGCCTTAATCCCAAA	ACAAGTTGTCGCATCCAGTG
mcTnT2	GGAGGAGTACGAGGAGGAA	CTCCTTGGCCTTCTCTCTC
mTLR3	GAAGCAGGCGTCCTTGGACTT	TGTGCTGAATTCCGAGATCCA
mTLR4	CAGTGGTCAGTGTGATTGTGG	TTCCTGGATGATGTTGGCAGC
m53BP1	GTTACCTCAGCCAAACAGGACAAGCA	CCCTTCCTTCTCCTCCTCTAACTC
mATM	TGCACATACAAGGTGGTTCCC	CCACTCGAGAACACCGCTTC
mIAP2	GCTCAGAATCAAAGGCCAAG	CACCAGGCTCCTACTGAAGC
mMnSOD	TTAACGCGCAGATCATGCA	GGTGGCGTTGAGATTGTTCA
mGADD45b	TCCTGGTCACGAACTGTCAT	GATGTTTGGAGTGGGTCTCA
mSIRT1	CTTGCACTTCAAGGGACCAA	GTATACCCACCACATCTGAG
mSIRT3	GCTGCTTCTGCGGCTCTATAC	GAAGGACCTTCGACAGACCGT
mSIRT6	GACCTGATGCTCGCTGATG	GGTACCCAGGGTGACAGACA